Morphostratigraphy of marginal coastal environments

Claire Alexandra Barrett-Mold

University College London

PhD

I, Claire Alexandra Barrett-Mold confirm that the work presented in this thesis is my own. Where information has been derived from other sources, I confirm that this has been indicated in the thesis.

Abstract

This study is concerned with deciphering the evidence for recent variability in external coastal climate and estuary process forcing preserved within the machair/salt marsh deposits of the Loughros More estuary, Donegal, northwest Ireland. Late-Holocene coastal dynamics have contributed to the development of a complex suite of inter-estuary dune, strand, machair, saline and freshwater marsh sedimentary environments. These sedimentary environments occupy a vulnerable position within the tidal frame (MHW ±2m), and exhibit significant morphological change over more recent (10 to 1000 year) timescales as a result of sediment reworking and recycling within the context of the wider estuarine environment. A greater understanding of the functioning of these relatively naturally behaving systems (unmodified by human impacts) is important not only to increase the knowledge of this relatively unstudied region but also to provide supporting evidence for future studies of the currently unclear relative sea-level record of this region. From a coastal conservation perspective, it is important to understand how aeolian, estuarine-marine and fluvial processes drive habitat transitions and shifts in the associated species assemblages, and the sensitivity of these marginal coastal and estuarine sedimentary environments to future climate variability and change.

The Loughros More system provides an excellent case study within which to establish the main internal system controls and external driving factors influencing the formation and morphological evolution of low-lying marginal coastal/estuarine habitats in this region. To this end, contemporary morphological and ecological environments are examined with respect to their geomorphology; sedimentary make-up; historical landform changes and ecological characteristics. A stratigraphic approach is taken to examine the temporal (downcore) and spatial (intra-/ inter-site) variations and trends in the sedimentary sequences of estuarine margin deposits. Stratigraphies are presented for 5 cores and downcore sedimentological, geochemical, and ecological variations analysed. Chronological support is provided via ^{210}Pb, ^{137}Cs and optically stimulated luminescence (OSL) dating. Scanning XRF is used to provide exceptionally high-resolution sampling of down-core geochemistry. Results describe depositional transitions from tidal flat to high intertidal vegetated environments, where saltmarsh, maritime grassland and machair characteristics are evident. Complexity is also present throughout the stratigraphies, and here the study demonstrates the potential of high resolution scanning XRF (including time-series and multivariate analyses) in determining correlations and trends in these sedimentary sequences and associated forcing. Variations in regional storminess are determined to be the main external driving factor controlling the deposition of distinctive light and dark sediment layers within the stratigraphy across the study area.

Contents

List of Figures

List of tables

1. Introduction

1.1. Coastal depositional environments

Coastal sedimentary environments occur globally where there is a sufficient sediment supply, adequate accommodation space for the deposition of sediment, and favourable climatic and tidal conditions for the delivery and accretion of sediment, and in many cases for the establishment of vegetation cover (Carter, 1991; Duffy and Devoy, 1999; Łabuz, 2005; Short and Hesp, 1982). Depositional coasts encompass a wide range of sedimentary systems including, estuaries, deltaic systems, barrier island systems, strandplain coasts, reef coasts, glacial and paraglacial coastal systems; each of which may contain numerous distinct environments and a variety of morphological features (Davis and Fitzgerald, 2004). When comparing these systems globally, latitude exerts an overarching control on the environment present; for example, within the tropical latitudes mangrove swamps can have a significant impact on coastal system processes due to their extent and dense network of aerial roots (Mazda *et al*, 2006). In contrast, temperate estuarine and deltaic coastal sedimentary systems are typically comprised of the unvegetated intertidal, e.g. sandflats, mudflats, beaches; the vegetated intertidal, e.g. saltmarsh; and the vegetated supratidal, e.g. sand dunes and machair. However, clear definition of these units is often difficult due to temporal variability, for example the formation of embryo dunes in the summer months and their destruction in the stormier winter months (Hesp, 2002), and/or gradational changes obscuring precise boundaries between features (USACE, 2002).

Coastal classification systems have been devised by many authors (e.g. Boyd *et al.*, 1992; Curray, 1964; Davis and Hayes, 1984; Inman and Nordstrom, 1971; and Shepard, 1976). These include purely morphological descriptive schemes as well as those that relate to the physical processes important to the morphology (Komar, 1998). Davis and Hayes (1984) use wave height and tidal range to define the relative importance of these processes and thereby classify stretches of coast. Under this scheme coasts may be “tide-dominated”, “wave-dominated” or “mixed energy” (Figure 1.1). This method of classification has then often been combined with other criteria. For example, Boyd *et al.* (1992) propose a classification of sedimentary coastal environments based upon the dominant processes and relative power of wave, tide and fluvial forces (Figure 1.2A). They also add a relative time axis in order to define an evolutionary coastal classification (Figure 1.2B).

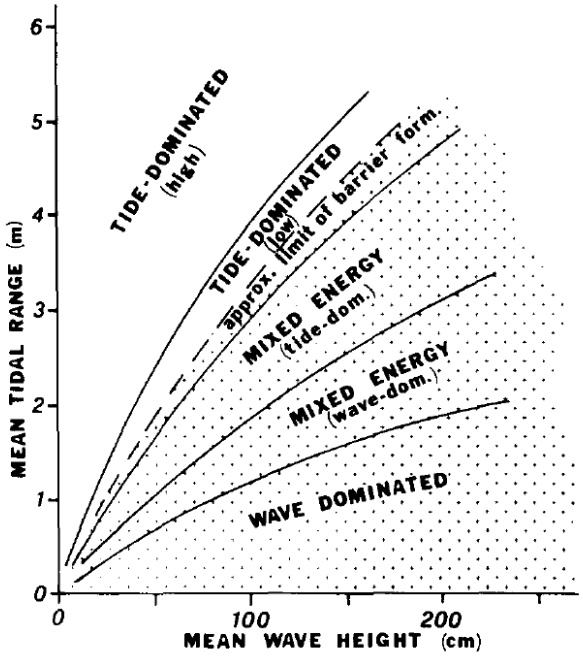

Figure 1.1 Relative influences of tide and wave height on coastal morphology (Davis and Hayes, 1984).

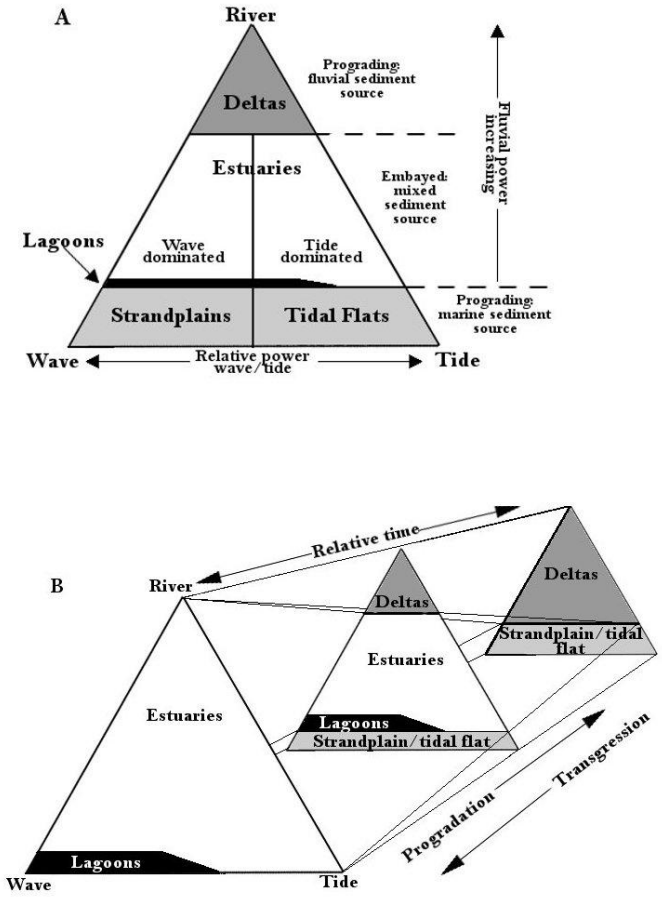

Figure 1.2 Boyd et al.'s (1992) ternary process-based classification (A) and evolutionary classification (B) for coastal sedimentary environments.

1.2. Paraglacial coastal systems

1.2.1. Spatial and temporal context

Mercier (2008a) describes two meanings of the paraglacial concept; firstly, the definition of "non-glacial processes that are directly conditioned by glaciations"; and secondly, "a period is defined as "paraglacial" when paraglacial processes occur". Mercier (2008a) states that as the paraglacial concept has meaning in spatial, systematic and temporal contexts it can therefore be used to describe a distinctive "paraglacial geomorphology".

Paraglacial coasts are defined by Forbes and Syvitski (1994) as "those on or adjacent to formerly ice-covered terrain, where glacially excavated landforms or glaciogenic sediments have a recognisable influence on the character and evolution of the coast and nearshore deposits". Consequently these systems are confined to higher latitude regions adjacent to major glaciation centres of the last ice age; for example north-west Europe, New Zealand and Canada (Figure 1.3). However, Chao *et al* (2002) believe that similar defining features and processes can be recognised in mid latitude coastal regions that have been exposed to high intensity periglacial processes such as the north-west coast of Spain.

High latitude and high altitude regions were widely affected by the glaciations of the Pleistocene period and the paraglacial coastal systems present today were initiated and formed after the end of the Last Glacial Maximum (Mercier, 2008a). With glacier ice retreat, the exposed landscape was highly susceptible to rapid change due to high erosion rates and reworking of glaciogenic sediments (Ballantyne, 2002a). Much of this remobilised sediment was transported and deposited towards the coast either as progradational features, such as gravel fans and barriers, or offshore on the continental shelf. The continued supply of this sediment to the coast and its reworking are still the dominant control on the sediment budget of paraglacial coasts implying that the transition period from paraglacial to non-glacial may be several tens of thousands of years (Ballantyne, 2002b). It is also stated by Mercier (2008b) that the spatial limits of the paraglacial system is inherently dependant on the time scale over which the system is viewed and that the response to climatic forcing may occur over varying timescales from an immediate reaction to several millennia.

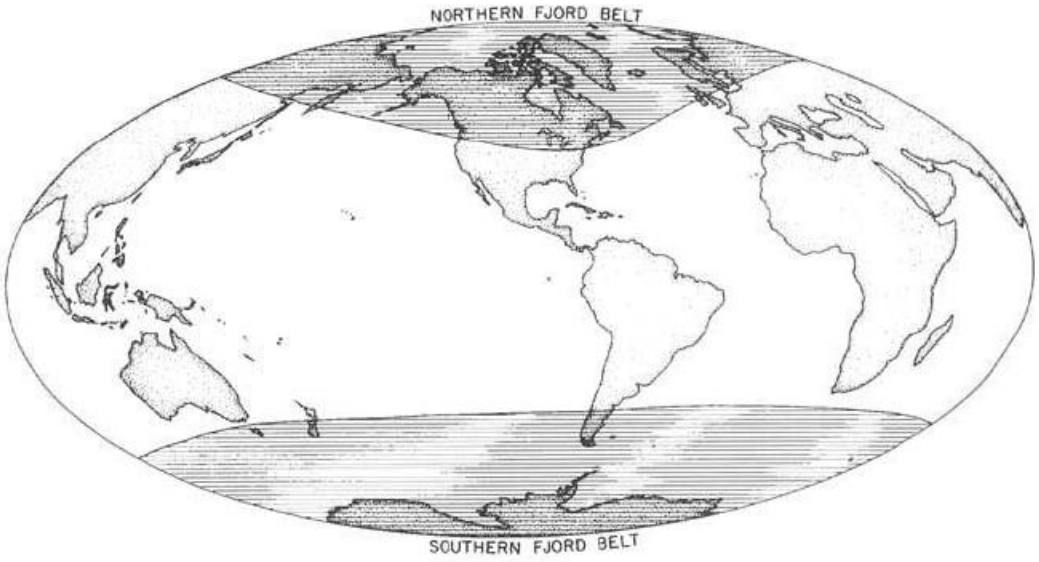

Figure 1.3 Global distribution of paraglacial coasts (Forbes and Syvitski, 1999)

1.2.2. Paraglacial coastal morphodynamics - barrier coasts

Ballantyne (2002a) recognises 3 distinct types of paraglacial coast: fjords and other glacially over-deepened basins; paraglacial barrier coastlines including drumlin coasts; and active outwash coasts. Of these systems paraglacial barrier chains are least common (Fitzgerald and van Heteren, 1999), yet may display the greatest variation in size, dynamics and morphological features present. One of the major controls on variation is the glacial history of an area as this will have a direct influence on the coastal topography and the nature of the sediment source (Ballantyne, 2002a; Fitzgerald and van Heteren, 1999). For example, in western Ireland one of the most distinctive features of the paraglacial coastline is the presence of drumlin-fed barriers, such as those found in Clew Bay. In glaciated terrain, drumlins are often the major source of beach sediment and are often associated with rapid shoreline change, particularly when combined with high rates of sea-level rise (Carter *et al*., 1990).

Paraglacial barrier coasts are characterised by the presence of beaches, baymouth bars, spits and barrier islands fed by the reworking of sediments of glaciogenic origin (Ballantyne, 2002a). They display high regional and local variability which is a factor of the inherent glacial topography and relative sea level change determining the availability of accommodation space and sediment supply (Fitzgerald and van Heteren, 1999). Forbes *et al*. (1995) recognise a distinctive morphodynamic behaviour characteristic of paraglacial barrier coasts which involves long periods of slow evolution punctuated by short episodes of rapid reorganisation. This morphodynamic readjustment occurs on a spatial scale of 1 to 10km and over a decadal timescale (i.e. 10 – 100 years). This type of mesoscale morphological adjustment has also been noted by Cooper *et al*. (2007) in sedimentary depositional systems on the north-west coast of

Ireland. Here they propose the formation and reworking of ebb tidal deltas as the driving force behind cyclic coastal change between two morphological states. Neither of the morphological states is stable in the long-term; this leads to a periodical switching between states (Forbes *et al*., 1995), maintaining stability in the system as a whole on a decadal timescale. This self-adjustment behaviour means that while external forces, e.g. storm events, sea-level rise and climate change, are important factors affecting coastal morphology they are not always necessary to affect or drive coastal change.

Fitzgerald and van Heteren (1999) propose a classification of paraglacial barrier systems based upon two key elements; the degree of compartmentalisation of the coastal system; and the wave and tidal energy classification of Hayes (1979). They consider all types of barrier to have evolved from spits and subsequently developed into other landforms (Ballantyne, 2002a). The classification identifies 6 types of paraglacial coastal barrier system (Table 1.1). Fitzgerald and van Heteren (1999) recognise barrier coastlines to be either "isolated" (ratio of barriers to intervening headlands ≤ 0.25) or "clustered" (ratio of barriers to intervening headlands ≥ 0.25). Clustered barrier coastlines can then be subdivided based upon the geomorphology of the segmentation of the coastline and the relative dominance of wave and tidal energy. It is suggested that this scheme may also be used in conjunction with existing classification schemes to define individual barriers. Fitzgerald and van Heteren (1999) recognise that scale is an important factor and should be taken into account when applying this classification as a barrier system classified as one type may, on a larger scale, form part of a system of another type. Although this classification scheme is based upon the paraglacial barrier coastlines of New England, USA, its authors have applied it to other regions of the world and have identified examples of all four main types.

Table 1.1 Fitzgerald and van Heteren's (1999) classification of paraglacial coastal barrier systems (after Ballantyne, 2002a).

Type	Description	Characteristics
1	Isolated	Highly compartmentalised coastline with numerous bedrock embayments. Limited, isolated sediment supply with a low long-term net input. Evolution involves a cyclic repetition of spit accretion, detachment and renewed accretion.
2	Clustered headland-separated	Barriers often formed across embayments of a submerged, irregular, bedrock dominated landscape. Short, narrow barriers. Sediment derived from various local on and offshore sources. Barriers often have a limited lifespan with landward barrier rollover or destruction and reformation longshore.
3a	Wave-dominated mainland-segmented	Smooth shorelines without significant internal compartmentalisation. Long sand dominated baymouth or welded barriers. Updrift moraines are the main sediment source.
3b	Mixed-energy mainland-segmented	Generally associated with tidal inlets and are sand dominated. Short barriers <4km attached to anchor points. Many barriers characterised by long-term retrogradational behaviour.
4a	Wave-dominated inlet-segmented	Abundant sediment supply results in burial of glacial palaeotopographic features. Long barriers supplied by updrift outwash deposits. Cyclic morphological changes related to storm overwash and breaching.
4b	Mixed-energy inlet-segmented	One example in New England. Tidal inlets and estuaries segment 4 sand barriers between 2 and 10km in length. Inherent topography controls barrier anchors. Sediment from onshore reworking of relict fluvial deposits and longshore transport of new fluvial sediments.

1.2.3. Sediment budgets

The presence and supply of glaciogenic sediments is a defining feature of paraglacial coasts (Forbes and Syvitski, 1994) and is characterised by two distinct sediment delivery methods: the direct release of glaciogenic sediments to the nearshore and the increased input of sediment from glacial rivers (Ballantyne, 2002a). Patterns of sediment delivery may vary over time depending on the location of deposits relative to the coastline and on relative sea level changes controlling the availability of these deposits (Forbes and Syvitski, 1994). Many of the sedimentary systems of the north east Atlantic are made up of quartzose sands which are of

Mid-Late Devensian to early Holocene in age. These sediments are derived from a variety of glacial and periglacial deposits, exposed flood plains and the former seas beds during times of lower sea level (Gilbertson *et al*., 1999). The supply of this sediment to the coast is a major influencing factor on coastal evolution (Ballantyne, 2002a) as it forms the largest component of the post-glacial sediment budget. For example, along the present day west coast of Donegal, north west Ireland, there are no other significant inputs to the coastal sediment budget; therefore reworking and cycling of these glacial and periglacial sediments is the major control on the sedimentary coastal landscape (Burningham and Cooper, 2003).

1.3. Marginal coastal systems

Marginal coastal systems are those that occur between the high intertidal and low supratidal. This is a narrow zone subject to the influence of a combination of wave, tidal, and in many estuarine environments, fluvial processes (Boggs, 1987). Accommodation space for these environments is framed by hinterland, coastal and nearshore topography/structure, within which vertical and lateral limits are imposed by tidal range.

Marginal marine areas are typically regions of high organic productivity and relatively high environmental variability (Gupta, 2002). They are characterised by intermittent to near constant sub-aerial exposure and are subject to a variety of energy levels through wave and tidal forcing (Boggs, 1987). Within the context of north-west Europe, high wave energies and strong wind climate create high stress environments where the associated ecology has adopted specific adaptations and specialisations to deal with the varying physio-chemical conditions.

1.3.1. System controls

The coastal morphodynamics of an area are defined by processes acting upon that particular section of coast. Due to the complex nature of coastal regimes and their variability, both temporally and spatially, the underlying controls are often difficult to infer (Allen, 1997). Factors influencing coastal shoreline morphology include, wave and tide regime, inherent geology and geological setting, tidal prism, sediment availability, influence of river inputs, bathymetry, climate and influence of storms (USACE, 2002). The variability in coastal shoreline position and morphology may be the response to a single factor or a combination of factors; however, the overarching factors forcing coastal change are sediment erosion transport and associated accretion (Anfuso *et al*, 2007), which are in turn defined by the relative importance of wave, tide and fluvial regimes (Burningham, 2008). On sedimentary coasts changes to these factors via, for example, alterations to the sediment supply, sea level and climate will influence the overall system dynamics.

Sediment supply

Coastal sediment cells are defined as a length of coastline within which the cycle of sediment erosion, transportation and deposition is self contained. Sediment eroded from the local coastline or delivered to the coast via rivers constitutes a positive input into the sediment budget of the coastal sediment cell, and may be worked into a variety of accretional coastal landforms (Komar, 1998). The sediment budget of a coastal cell is central to the magnitude, rates and patterns of geomorphological change within it (Pacheco *et al.*, 2008). For example, in their analysis of the Dungeness gravel barrier complex, southeast UK, Plater *et al*. (2009) recognised the sediment budget and the availability of accommodation space for the deposition of new sediment as the major factor in controlling the nature of barrier transgressional response to sea-level rise.

Sea level

The effect of any change in sea level on sedimentary coastal systems is to alter geomorphological configurations and their associated sediment dynamics (Pethick, 2001). In low lying coastal sedimentary systems the effect of a rise in sea level will be to inundate much of the surface area of the environment (Phillips, 2009). The natural response of many sedimentary coastal landforms to sea level rise is a landward roll-over transgression; this entails a migration upwards and landwards to maintain the position in the tidal frame (Pethick, 2001; Komar, 1998). If this response is not possible, for example due to geological constraint or human impact, the coastal landform will be lost via erosion or inundation.

Tides and waves

The five types of shoreline identified by Davis and Hayes (1984) (Figure 1.1) may occur over a wide range of tidal ranges and wave heights. However, at the lower end of the scale only a small change to the wave and/or tidal parameter may result in the formation of a characteristically different coastal morphology (USACE, 2002).

The effect a tide and associated incident waves have on coastal environments is controlled by shoreline geometry, bathymetry and geostrophic effect, i.e. the Coriolis Effect (Coughenhour *et al*, 2009). However, they can be seen to have three major impacts on the coastal zone. Firstly, the periodic exposure of different parts of the intertidal to wave energy and the exposure of significant areas of unvegetated sediment which becomes available for aeolian transportation. Secondly, the erosion and transportation of sediment by tidal currents, together with the formation of ebb and flood deltas. Thirdly, the filling and draining of tidal inlets, allowing the mixing of fresh and marine waters (USACE, 2002). The tidal effect on sediment deposition can lead to the production of “tidal rhythmites” and “tidalites” in some coastal sediment sequences. Tidal rhythmites are millimetre scale vertical laminations formed as a result of spring-neap tidal cycles whereas tidalites are sediments deposited under the action of tidal currents in the

intertidal and subtidal zones but do not necessarily preserve tidal periods (Coughenour *et al*, 2009). In these sequences coarser material is deposited in periods of tidal current flow and finer material during the period of slack water as the tide changes. Within tidal rhythmites variation in the thickness of these coarser laminations occur due to the varying energies associated with the spring-neap cycle. Such cycles have been identified in several depositional coastal environments including tidal flat (e.g. Allen and Duffy, 1998) and saltmarshes (e.g. Stupples, 2002). In addition to the identification of monthly spring-neap cycles (29.53 days), some multi-year astronomically controlled cycles can affect tidal sediment deposition. The lunar nodal cycle (18.6 years) exerts a control on the tidal amplitude and consequently the strength of the tidal current (Mazumder and Arima, 2005, Oost *et al*, 1993). Fossil and historic sediment sequences preserving the lunar nodal cycle signal are not common due the requirement for several decades of uninterrupted sedimentation (De Boer and Alexandre, 2012). However the effects of the cycle on present day coastal process can be seen; for example, an increase in the tidal amplitude due to the lunar nodal cycle combined with independent increases in storminess and/or mean sea-level can lead to increased coastal flooding (Eliot, 2012). Tidal cycles are only one process that may cause the creation of laminations or layering effects in depositional sequences; for example climate and sea-level change can result in visually similar deposits.

Climate

The climate of a region plays an important role in determining the wave and wind characteristics and consequently the frequency and magnitude of storm events. Therefore, climate has a significant influence over the morphodynamics of many coastal systems. In the northern hemisphere the North Atlantic Oscillation (NAO) is the primary mode of inter-annual atmospheric variation and climate variability across the north Atlantic region (Baldini *et al*, 2010; Burningham and French, 2012). This is associated with changes in the surface westerlies across the north Atlantic and into Europe as well as wind speeds, wave heights and directional components (Hurrell, 1995; Thomas *et al*, 2012). The changes in atmospheric circulation associated with the NAO are expressed in changes in sea-level pressure across the mid-Atlantic (Hurrell, 1995). It should be noted that the Arctic Oscillation (AO) is also seen to influence surface air temperature and sea-level pressure within this region (Thompson and Wallace, 1998). As the NAO is most active during the winter months it is standard practice to use a NAO winter index to assess changes. Positive phases of the NAO are associated with stronger than average westerly winds over the North Atlantic. This is due to extreme low pressures over the Ireland region and high pressures across the Azores (Dawson *et al*, 2002).

Wind has a significant influence over coastal geomorphology. Wind erosion, transportation and subsequent deposition of sediment are major contributors to coastal sediment dynamics (USACE, 2002). For example the formation of coastal dunes is dependent on aeolian sediment movement associated with a strong wind climate. Variations in the magnitude, direction and

frequency of the wind acting upon an area of coastline can also have a significant effect on coastal processes. For example a strong onshore wind can result in increased wave heights and therefore greater rates of erosion and overwash of coastal landforms.

Storm waves and storm induced currents are the dominant method of removal of beach sand; they may produce significant changes to coastal morphology over very short time periods, for example, breaching barriers, relocation of tidal channels, dune scarping, extensive overwash depositions (Thomas *et al*, 2012). The antecedent morphology of a system can also affect how the system responds to a storm event; for example Houser *et al*. (2008) describe how foredune height and extent relative to storm tide elevation are primary controls on how a barrier island responds to extreme storms. The NAO winter index has frequently been used in coastal studies as a proxy for storminess and associated episodes of erosion or deposition in the North East Atlantic coastal regions (Dawson *et al*, 2004; Clarke and Rendell, 2006; Burningham and French, 2012). However, its relationship to storminess is complex and although it can be strongly correlated to wind direction its association with wind speeds is less certain and varies significantly depending on the winter period defined (Burningham and French, 2012).

1.3.2. Signature environments

Along paraglacial coastlines signature environments of marginal coastal systems include saltmarsh, dunes, machair and tidal flats. These sedimentary environments are all located within the high intertidal to low supra-tidal vertical frame. Morphodynamics and sedimentary evolution are variably controlled by coastal energy regime (wind, waves and tides), sea-level change, sediment availability and accommodation space.

Saltmarshes

Saltmarshes are present throughout Europe especially on sheltered marine and estuarine, meso- or macro-tidal coasts (Figure 1.4); and occur within a narrow elevation range equivalent to neap to spring high water level (Boorman, 2003; Chmura *et al.,* 2001). They are described by Allen (1997) as high-intertidal vegetated platforms that are repeatedly flooded and are drained by tidal creeks which join, widen and deepen seaward. Boorman (2003) states four conditions required for the formation and growth of a saltmarsh:

1. A relatively stable area of sediment covered by the tide for a shorter period than it is exposed;
2. A supply of suitable sediment during the period of tidal cover;
3. Sufficiently low water velocities for sediment settling;
4. A supply of seed or propagules for the establishment of vegetation cover.

Saltmarshes are commonly divided into the pioneer marsh, covered by all tides except lowest neaps; lower marsh, covered by most tides; middle marsh, only covered by spring tides; high

marsh, only covered by highest spring tides; and transition zone, only occasionally covered during extreme tide surge events (Boorman, 2003; Davis and Fitzgerald, 2004). The proportion of estuary covered by marsh varies widely and is ultimately a function of tidal prism and wave energy. However the proportion of an estuary covered by vegetation tends to be an indication of the maturity of the system and the degree to which the estuary has been infilled with sediment (Davis and Fitzgerald, 2004).

Figure 1.4 Distribution of saltmarshes in Europe (Boorman, 2003)

In addition to the classification of saltmarshes based upon their maturity, i.e. low and high marsh, Allen (2000) describes 7 saltmarsh types based upon geomorphological features (Figure 1.5). The main discriminating feature of this classification is the degree of exposure of the marsh and hence the energy level of processes the marsh is subjected to. The classifications range from open coast (Figure 1.5a), which tend to be sandy, to marshes within estuaries (Figure 1.5e and f), which tend to be muddy if they are fed by a major river (Allen, 2000). Allen (2000) describes the ria/loch-head classification as a special case, which mainly only occurs in Brittany and the west coast of Ireland; these marshes are mainly muddy and may occur in waters with significantly reduced salinity where the resulting vegetation can be distinct from the other saltmarsh settings.

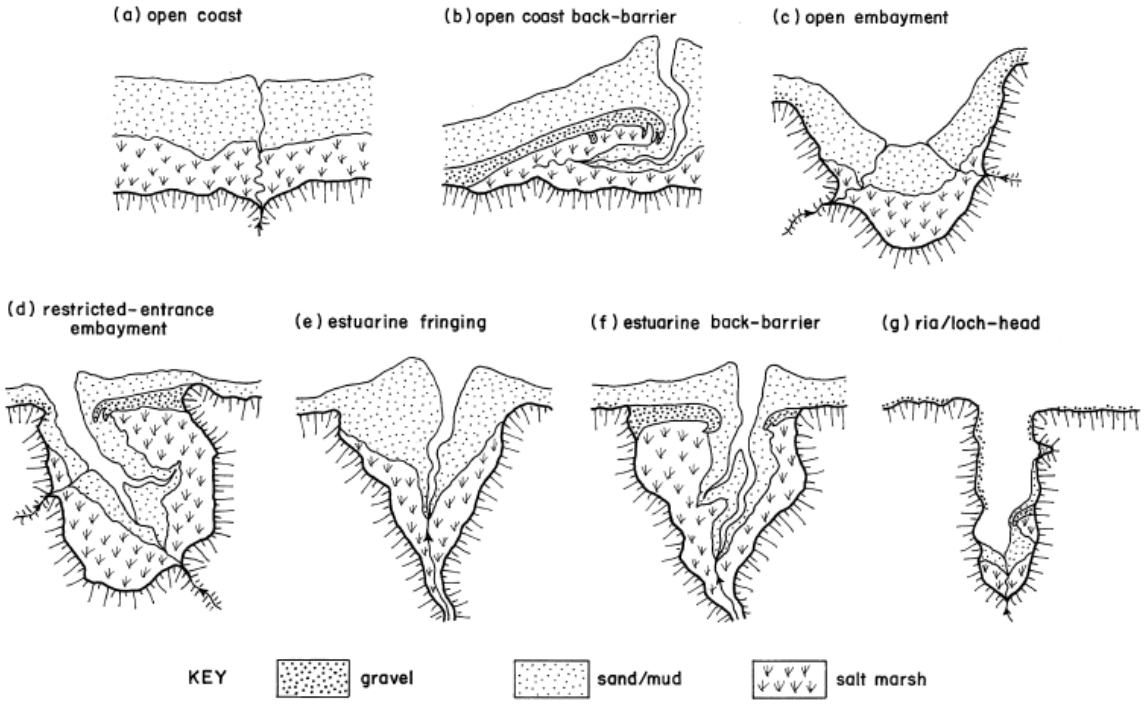

Figure 1.5 Geomorphological classifications of saltmarshes (Allen 2000).

Saltmarsh dynamics

Several interconnected factors are thought to be major drivers of vertical accretion, geomorphological and stratigraphical change within saltmarshes. These include sea level, tidal regime and range, wave climate, sediment supply, storm activity, vegetation composition and compaction (Brown *et al.*, 1998; Allen, 2000; Goodman *et al.*, 2007). These factors contribute to the balance between sediment supply and erosional process upon which saltmarsh stability depends (Harvey *et al.*, 2007).

The supply of sediment to coastal saltmarshes in northwest Europe is primarily allochthonous, with minor contributions from organic material; therefore the position of the marsh in the tidal frame and the hydroperiod are key determining factors in how much sediment is supplied to the surface (Marion *et al.*, 2009). The most important control on the hydrology of saltmarshes is the tidal regime. Tidal energy supplied to the saltmarsh influences a wide range of physiographic, chemical and biological processes, including sediment deposition and scouring, mineral and organic influx and efflux, flushing of toxins and the control of sediment redox potential (Mitsch and Gosselink, 1993). Above the neap high tide mark there is little energy to disturb the sediment and therefore the accumulating sediment tends to be fine grained and produces a relatively stable sediment surface (Davis and Fitzgerald, 2004). Consequently, initial marsh growth may be rapid once vegetation becomes established, but growth rates will decline rapidly

when the surface becomes constrained by the upper limit of the tidal frame (French, 2006; French *et al.,* 1995).

The tidal creek network, characteristic of saltmarshes, provides efficient sediment delivery to the marsh surface (Reed *et al.,* 1999). During tidal flood the creeks distribute tidal water and suspended sediment across the marsh surface. As the tide ebbs the surface is drained via the creeks and any un-deposited sediment returned to the sea (Allen, 2000). It has been shown by French *et al*. (1995) that proximity to major creeks is a main control on rates of sediment deposition.

Biological processes play an important role in stabilising sediment surfaces, promoting saltmarsh formation and in the processes of accretion and erosion (Brown *et al.,* 1998). Microflora, e.g. algae and diatoms, may precede pioneer saltmarsh plants binding fine intertidal mudflat sediments and promoting sediment accretion (Brown *et al.,* 1998). Once saltmarsh vegetation has become established the main method of sediment transportation on to the marsh is through sediment suspension (Davis and Fitzgerald, 2004). The vegetation surface has the effect of reducing flow across the saltmarsh therefore increasing sediment settling, dissipating wave energy and reducing erosion (Neumeier and Amos, 2006; Möller *et al*., 1999).

Storms are a major influencing factor increasing the sediment supply to the marsh surfaces and creating both temporal and spatial variations in the distribution of sediment supply over short time periods, i.e. less than 2 years (Marion *et al.,* 2009; Roman *et al.,* 1997; Stumpf, 1983). The tidal range is a significant factor on the effect of storm events as they will have a greater relative influence on micro-tidal systems than macro-tidal ones (French 2006). These storm events may be evident in the stratigraphical column by the presence of coarser grained particles and more massive sedimentary units. Storms may also be a potential cause of erosion of the saltmarsh and possible re-distribution of the sediment (Roman *et al.,* 1997). The potential for storm erosion and the severity of erosion is determined by the degree of exposure of the marsh.

Since coastal marshes are located within the transition zone between terrestrial and marine environments they are particularly susceptible to changes in the relative sea level (Arnaud-Fassetta *et al*., 2006). Several studies have examined the effect of predicted sea-level rise as a result of climate change on the evolution of coastal saltmarshes (e.g. Cahoon *et al*, 2000; Goodman *et al.,* 2007; Cundy and Croudace, 1996; Richards *et al.,* 2008; Chmura *et al.,* 2001; Reed, 2002). For coastal saltmarshes to survive any rise in relative sea level they require a vertical accretion rate equal to or greater than relative sea level rise (Goodman *et al.,* 2007). It is suggested by Roman *et al.* (1997) that episodic increases in sediment accumulation associated with storm events are an important mechanism enabling marshes to keep pace with sea level rise. Vertical growth will continue until the marsh surface is fully emergent; and ultimately they are limited by the tidal range (Harvey *et al.,* 2007), their ability to keep pace with rates of sea-

level rise (Cundy and Croudace, 1996) and accommodation space. There is greater risk of marsh loss if the relative sea-level rise is rapid as the marsh would not have time to recover from inundation (Kirwan and Temmerman, 2009).

Species assemblages and vegetation dynamics

Saltmarshes are among the most productive ecosystems of the world (Gallagher *et al*., 1996). They support high concentrations of photosynthetic organisms, the three major autotrophic units being marsh grasses, mud algae, and phytoplankton within tidal creeks (Mitsch and Gosselink, 1993). They also serve as a nursery ground for many organisms. In comparison to other wetland types they support a lower plant diversity as a result of the salinity (Keddy, 2000). However, the harsh saltmarsh conditions have resulted in the evolution of a community of plants specifically adapted to this environment, and there are around 40 species of higher plants that are found exclusively in saltmarshes (Boorman, 2003). Other species that occur in saltmarshes are often at the margins of their range of physio-chemical tolerances.

Often a clear zonation is present within saltmarsh vegetation communities (Table 1.2). This is a result of the physiochemical variations across the marsh driven by the tidal influenced hydrology. Species' ability to withstand environmental stress or to compete with other species is the cornerstone of saltmarsh vegetation zonation. In a study of the relative importance of physical factors and inter-species competition in saltmarsh vegetation zonation Pennings and Callaway (1992) found position in the marsh to be the major controlling factor determining whether environmental stress or competition was the dominant zonation determinant. In the lower marsh flooding frequency and soil water logging was the main species determinant whereas at higher marsh elevations inter-species competition was the main control on zonation. Emery *et al.* (2001) have shown that physically stressful areas of the marsh, i.e. high flooding frequencies and/or high salinities, provide refuges from competition for the less competitive stress tolerant species. However, they also show that when nutrient levels are high stress tolerators are also the dominant competitors, indicating the complex relationship between the physiochemical variation across the marsh and plant species dynamics.

Table 1.2 Typical plant species of European saltmarsh zones (after Boorman, 2003)

	Typical plant species
Pioneer	*Spartina* spp., *Salicornia* spp., *Aster tripolium*
Lower marsh	*Puccinellia maritima*, *Atriplex portulacoides*, *Spartina* spp., *Salicornia* spp., *Aster tripolium*
Middle marsh	*Limonium* spp. and/or *Plantago* spp, *Puccinellia maritima*, *Atriplex portulacoides*, *Spartina* spp., *Salicornia* spp., *Aster tripolium*
High marsh	*Festuca rubra*, *Armeria maritima*, *Elytrigia* spp., *Limonium* spp., *Plantago* spp, *Puccinellia maritima*, *Atriplex portulacoides*, *Spartina* spp., *Salicornia* spp., *Aster tripolium*
Transition zone	A combination of high marsh species and the surrounding non-halophytic species

Machair

The term "machair" has been applied to areas of coastal dune grassland, in particular in western Scotland, since 1926 (Angus, 2006). Gaynor (2006) describes machair as "a distinct geomorphological and ecological feature formed as a result of a unique combination of climatic, geographic, edaphic and anthropogenic factors"; as a result machair only covers about 30-40,000ha globally, all of which is found on the paraglacial Atlantic coasts of Britain and Ireland (Hansom and Angus, 2005).

Machair can be described as a gently sloping coastal dune-plain formed by wind-blown calcareous shell sand characterised by a lime rich surface which is subject to strong, moist, oceanic winds (Hansom and Angus, 2005), and typically lies behind dune ridges and forms on impermeable bedrock. The term "machair complex" is often used to refer to a whole system containing coastal dunes, fixed dune grassland, machair plain, wet slacks, marshland, etc (Owen *et al.*, 2004). The dramatic reduction in the presence of *Ammophila arenaria* is often used as a criterion for identifying the boundary between dune and machair grassland; inland, it is common for machair to grade into lake, heath or bog environments (Cooper *et al.*, 2005) (Figure 1.6). However, Gaynor (2006) describes a number of exceptions to this typical sequence; for example, flat machair may form over rock platforms adjacent to the sea, bypassing the dune building phase. A similar occurrence of machair formed on a planated bedrock surface is identified by Cooper *et al.* (2012) in the Outer Hebrides of Scotland. In these situations the morphology of the bedrock surface exerts a significant control on the topography of the machair. The fixed nature of the bedrock results in the absence of a mobile shore-face and therefore morphological adjustment to changing wave and tidal conditions is focused on the beach-face and dune or machair units behind. Tidal deposition of calcareous sediment may be promoted by gently sloping, submerged, sections of the bedrock surface. These Hebridean barrier islands are the only know example of barrier islands forming on and migrating over a

pre-Quaternary solid bedrock surface (Cooper *et al*, 2012). Another exception to the typical machair development sequence may occurs where wind speed is particularly high magnitude and of a suitable direction, resulting in large quantities of sand deposited on the seaward face of hills inland to form hilly machair. These variations in machair character highlight the importance of antecedent morphology on the form and evolution of the environment.

The majority of research on machair as a geomorphological feature and as an ecosystem has been based upon sites in Scotland (e.g. Ritchie, 1976; 1979; Gimingham, 1974; Angus, 1994; 2006; Mate, 1992). Very little research has been done on Irish machair sites and what research has been done focuses mainly on the vegetation.

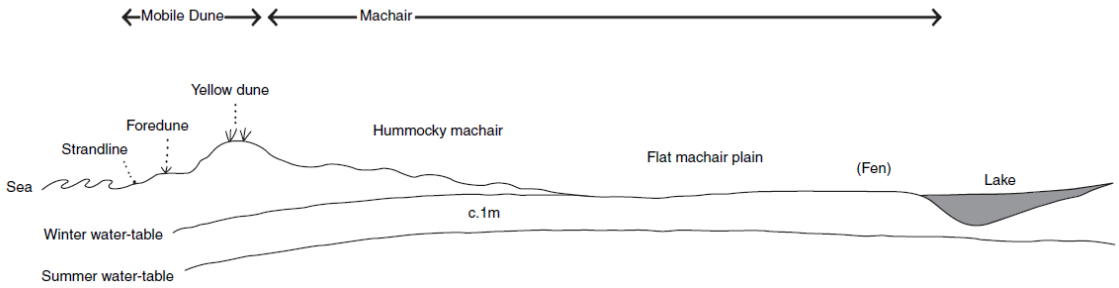

Figure 1.6 Diagrammatic representation of a "typical" machair profile (Gaynor, 2006).

Machair definition

Ritchie (1976) provides the only comprehensive attempt to define machair; he defined six main characteristics, based upon Scottish sites, that could be used to identify machair:

1. A base of wind-blown sand which has a significant percentage of shell-derived materials.
2. Lime rich soils with pH values normally greater than 7.0.
3. A level or low angle smooth surface at a mature stage of geomorphological evolution.
4. Sandy grassland type vegetation with long dune grasses and other key dune species having been eliminated. Core plants are *Festuca rubra, Lotus corniculatus, Trifolium repens, Achillia millefolium, Gallium verum, Plantago lanceolata, Euphrasia officinalis, Bellis perrenis* and *Rhytidiadelphus squarrosus* (Gimingham, 1974).
5. Biotic interference such as is caused by heavy grazing, sporadic cultivation, trampling and sometimes artificial drainage should be a detectable influence within the recent historical period.
6. An oceanic location with a moist, cool climatic regime.

Angus (2006) has subsequently added a seventh characteristic based on the work of Ritchie (1979):

7. Machair plains flood or are at least marshy in winter.

However, there still remains ambiguity in the definition of machair grassland as the distinction between machair grassland and other coastal grasslands has not been well defined. This is partly due to the derivation of the term machair from the Gaelic *mach* meaning "plain" or "field"; in northwest Scotland this is used to describe areas of level, stable, dune grassland over soils that are usually calcareous. Similarly in Irish, *machaire* means "plain", "stretch of level ground" or "links" and in Donegal (northwest Ireland) several place names of coastal areas contain the root word "maghera" (Bassett and Curtis, 1985). Also, machair is an extremely complex habitat and it can often be difficult if not impossible to distinguish dune grassland from machair, to the extent that Angus (2006) states that machair is "arguably no more than an extreme form of dune grassland on shell-rich sands". However, an ecological distinction has been made between the machair grassland or plain and the machair system as a whole (Angus, 1994) and it is the machair grassland which is listed under the EU habitats directive. Hansom and Angus (2005) believe that, although this distinction is useful in a landform context, it is important that a definition of machair should be based on both the geomorphology and vegetation.

Sediment supply and soil characteristics

The dominant source of sediment to machair systems is via the aeolian transportation of shelly marine sands onshore. A continuous supply of $CaCO_3$ is needed as rain will leach away any surficial shell debris after several decades. Therefore, the prevailing south-westerly winds of northwest Ireland and western Scotland provide ideal conditions for this to occur. The origin of the marine sand parent material is the glacial sands and marine shell skeletal remains transported landward during the Holocene marine transgression (Mate, 1992). Detrital carbonates from marine organisms, in particular shell fragments, make up much of the sediment of machair systems; as a result calcium carbonate content is typically in the region of 40-80% (Whittington and Edwards, 1997; Edwards *et al.*, 2005). Consequently the pH of machair soils is relatively high, between 6 and 8, although this may fall in older systems where leaching of $CaCO_3$ has occurred (Brayshay *et al*. 2000). Although high carbonate and shell fragment contents are characteristic of machair soils there are large variations both between and within systems. For example, Ritchie (1976) describes the carbonate content of the machair sites of the Outer Hebrides as ranging from less than 10% to over 80%. Machair soils contain low concentrations of nitrate, phosphate, potassium, copper and manganese; combined with summer water deficits, winter flooding and the calcareous nature of the sediment these result in low soil productivity (Cooper *et al.* 2005).

Within the Hebrides the volume of machair complex has been developing continually during the post-glacial period (Mate, 1992). Ritchie (1979) states that, as offshore sand banks are now rare, the only continuing supply of sand to machair systems is derived from organic sources and therefore shell sands would be present in higher proportions in younger sediments. However, sediment reworking will also provide a significant input into any more recent coastal sedimentary landforms. Mate (1992) suggests that during periods of dune growth, little sand is available for the formation of other units within the system. However, when maximum dune height is reached sediment will become available for the formation or growth of other units such as the machair grassland.

Morphology and geomorphological processes

Hansom and Angus (2005) describe machair grassland as "an extreme form of sand plain produced from the normal cycle of deposition and erosion of sand dunes". Machair surfaces are highly impacted by strong onshore winds creating deflation surfaces and once established the development of a machair surface is primarily erosion driven (Hansom and Angus, 2005). Machair is defined by Ritchie (1976) as tending to be flat or with a landward or seaward slope of less than 5 degrees. The machair plain is approximately parallel to the water table at a point where the moisture content of the sand prevents aeolian erosion of the plain (Gaynor, 2006). However, significant differences in morphology may occur depending on the underlying surface topography (de la Vega Leinert *et al*., 2000). Ritchie (1979) identifies 3 main groups of machair surfaces present in the Uists and adjacent islands, one group of hilly, hillocky hillside machair and two groups with plain surfaces; the explanation given for these differences is the subsurface control on morphology.

Ritchie (1976) states one of the defining characteristics of machair to be "an appearance of maturity in the machair plain landform". The age of the surface is probably in the order of centuries (Ritchie, 1976; Ritchie and Mather, 1974). The machair landforms described by Edwards *et al.* (2005) were found to have evolved at a slow and variable rate and the landforms displayed a long-term stability.

The main theory of the origin of the parent material of machair is proposed by Ritchie (1979) who states that the material is derived from glacial sands and marine shell and skeletal remains swept landward during the Holocene marine transgression, and that this volume of sand has since remained fairly constant within the beach/dune/machair system. A second theory, more specific to the exceptionally carbonate-rich machair of the Hebrides, is described by Mate (1992). He suggests that the machair complexes have been developing continually during the post-glacial period via the input of shell debris which has been continually forming offshore.

Ritchie's (1979) multi-stage model of the evolution of machair landforms is the dominant view of the longer scale geomorphological development of machair systems (Figure 1.7). As the large

dunes, produced as a result of the Holocene marine transgression, progressively blew out the subsequent re-working of the sand produced the present day "high machair" immediately inland of the shoreline and lower relief further inland that is common in the machair systems of the Outer Hebrides (Gilbertson *et al*., 1995). The high machair is thought to have eroded episodically and the sediment been re-worked and re-deposited further inland. Gilbertson *et al.* (1995) describe the two conditions under which this re-deposition is thought to occur. Firstly, "layer-cakes" made up of sheets of re-deposited sand accumulated further inland, with fossil soils marking periods of greater stability. Secondly the production of "low machair" through the in-filling of impounded lochs or marshy ground with sediment eroded from dunes and high machair on the seaward side. These areas of low machair are rendered almost completely resistant to further deflation by the presence of the winter water table above the surface (Gilbertson *et al*., 1995; Mate, 1992 and Ritchie, 2006). However, Gilbertson *et al.*, (1995) state that further geomorphological evaluation of these models would require a more detailed understanding of both the depositional environments and the chronology than is available at the present.

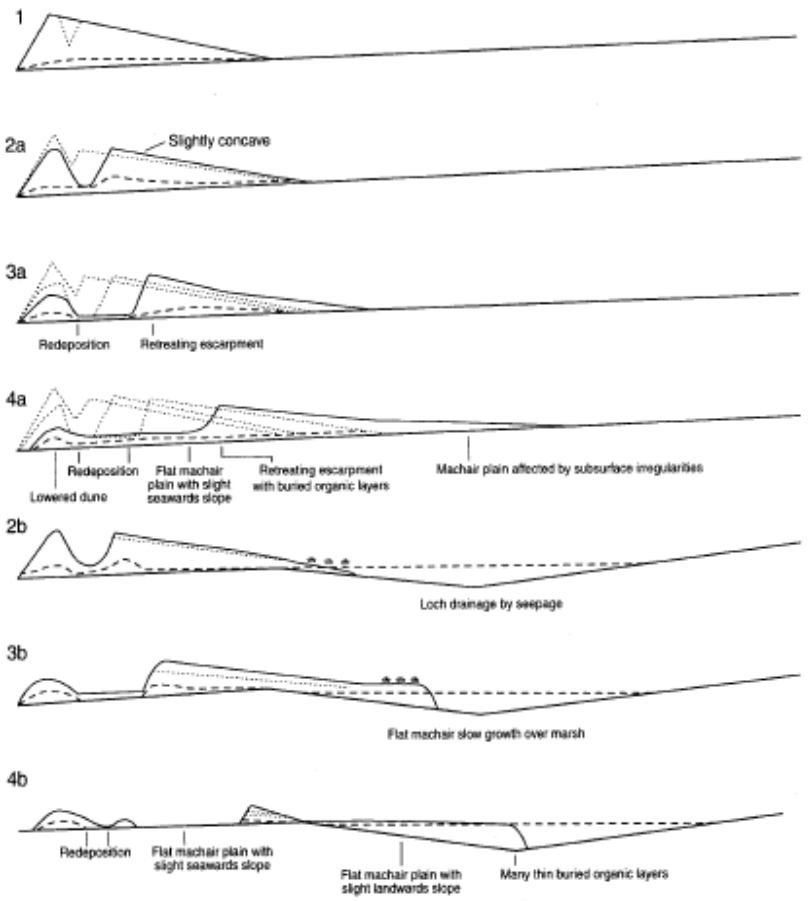

Figure 1.7 Ritchie's (1979) multi-stage model of machair development. Stage 1: initial build up of sand at the littoral. Stages 2a-4a: extension of the machair plain due to deflation and aeolian deposition. Stages 2b-4b: extension by sand encroachment into a pre-existing loch or mire (after Ritchie *et al*, 2001).

Species assemblages and vegetation dynamics

No assemblage of species is unique to machair; this is reflected in Gaynor's (2006) description of machair vegetation as "a mosaic of calcareous fixed dune, mesotrophic grassland, and dune slack communities". In their study of the machair vegetation of the Outer Hebrides Owen *et al.* (2001) identified 14 community types ranging from mobile dune to dune slack and swamp types. However, the main defining attribute of machair grassland vegetation is the absence of or significant reduction in the presence of the main dune building species, i.e. *Ammophila arenaria, Elytrigia farctus, Carex arenaria, Tortula ruraliformis*, etc (Gimingham, 1974). The species which occur most frequently are characteristic of calcareous grassland, i.e. *Festuca rubra, Trifolium repens, Lotus corniculatus, Achilliea millefolium, Galium verum, Plantago lanceolata, Euphrasia* spp., *Bellis perennis*, and *Rhytidiadelphus squarrosus* (Gimingham, 1974). As a result of the similarity of the most common species with those of other habitats Gimingham (1974) believes machair is better distinguished by the identification of the less common species groups; i.e. those associated with a high water table, orchids, annuals and species of open situations and a small number of arctic-alpines. Ritchie (1976) believes the botanical definition of machair can be expressed with reference to three main criteria:

1. A coastal location
2. The occurrence of lime rich soils
3. The elimination of long psammophilous grasses.

The composition of machair plant species communities varies according to soil calcium carbonate content, soil organic matter content, sand plain structure and the duration of winter flooding (Cooper *et al.*, 2005). A common characteristic of machair species is the ability to withstand a certain amount of sand burial. Owen *et al*. (2004) showed that machair communities are less able to withstand intermittent and repeated burial than a single burial event of greater magnitude. Where intermittent burial occurs or where burial is too deep the plants are unable to recover and a fossilised surface organic layer is produced; repeated occurrences of this process is termed "machair stratification" (Kent *et al*., 2005).

Role of humans

Human impact is a key factor influencing the formation and development of machair grassland (Owen *et al.*, 2001). A characteristic of machair surfaces is they show a detectable current or historic interference from grazing, cultivation, addition of fertiliser such as seaweed and sometimes artificial drainage (Hansom and Angus, 2005). There is a correlation in the occurrence of machair and the location of human settlements, with communities clustering at points along the coasts bordering the more fertile machair areas (Gaynor, 2006). Many machair grasslands have been managed by local communities for over 5000 thousand years (Edwards *et al.*, 2005, Ritchie *et al.*, 2001; Cooper *et al.*, 2005). In the more recent centuries, extensive cattle

and sheep grazing has been common with rotational cropping of potatoes, oats and rye at certain times of year (Gilbertson *et al.,* 1995; Knox, 1974). These human actions increase the sand erosion and deposition by destabilising the surface. Gilbertson *et al.* (1995) believe that these human actions, combined with natural climatological and oceanographic fluctuations, caused accelerated deflation, deposition and movement of machair sands between the 16th and 19th centuries. The machair had mostly stabilised by the end of the 19th century (Ritchie, 1979).

Sand dunes

Formation and dynamics

Coastal sand dunes show a great deal of variety in form; this is related to their sedimentation, climatic setting, both past and present, and ecological factors. The fundamental prerequisite for the formation of sand dunes is an abundant sediment supply and the wind to transport it (Łabuz, 2005). The sediment delivered to the back beach is composed predominately of fine to medium grained, well-sorted sand; this is due to the aerodynamics of grains of this particular size, i.e. entrainment of sand size grains requires a lower shear stress (Boggs, 1987). Shell fragments are often preferentially moved by wind, as they are less dense than the quartz sand grains. Where it is abundant this can lead to an accumulation of shell material.

Wind-blown beach sand can accumulate at various locations, ranging from the immediate backshore to back-barrier flats, to form embryo dunes. Sand accumulation may occur within and around discrete or relatively discrete clumps of vegetation, individual plants, driftwood, flotsam, etc (Hesp, 2002). Once the initiation of aeolian sediment accumulation begins it continues unless conditions change, such as loss of sediment supply, removal of the stabilising factor, or wave induced erosion. These small incipient dunes are typically 1 to 2 metres in diameter and between 0.5 and 1m in height (Davis and Fitzgerald, 2004). They are quite vulnerable and may be destroyed by moderate storm events; seasonal formation and destruction may also occur where they form around annual plants, invasion by perennial plants is required in order to attain more permanent survival. Morphological development of embryo dunes depends on wind velocity, rates of sand transport and plant density, distribution, height and cover. Tall, dense species such as *Ammophila arenaria* tend to produce higher hummocky dunes whereas lower, spreading plants such as *Spinifex* or *Ipomoea* tend to produce lower less hummocky dunes (Hesp, 2002).

Foredunes develop from embryo dunes and are commonly distinguished by the growth of intermediate, often woody plant species, and by their greater morphological complexity, height, width, age and geographical position. Typically they attain heights up to 5m (Waugh, 1995). Hesp (2002) lists the factors determining the morphological evolution of foredunes to include: sand supply; the degree of vegetation cover; plant species present, which is a function of climate

and biogeographical region; the rate of aeolian sand accretion and erosion; the frequency and magnitude of wave and wind forces; the occurrence and magnitude of storm erosion, dune scarping and overwash processes; the medium to long-term beach or barrier state i.e. stable, accreting or eroding; sea/lake/estuary water level; and extent of human impact.

Foredunes develop into fixed dunes as more dunes are created on the seaward side of the ridge and the dune becomes more sheltered. Wind velocities drop and therefore sand accretion stops and the dune ceases to grow. Organic matter deposited from the plants binds the soil particles, reduces sand movement and retains water and nutrient ions (King, 1989). Within the fixed dunes dune slacks may occur in interdune hollow where flooding occurs during the rainy season i.e. in winter and spring in Europe (Grootjans *et al,* 2004).

Attack by waves is a major factor in the de-stabilisation of vegetated dunes. Although dunes are out of the influence of regular waves, they are vulnerable to only modest storm surges. In these conditions embryo dunes can be destroyed and sand easily removed from the seaward edge of the main dune ridge. Dunes may also be eroded internally by the formation of blowouts. Blowouts are large depressions that develop as sand is eroded from the windward slope and crest of a coastal dune ridge and deposited as a depositional lobe on the leeward slope (Dech *et al*, 2005; Hesp 2002).

In the absence of vegetation, dune systems can exhibit significant mobility, where all or part of the dune can migrate (Short and Hesp 1982). The most common process for dune migration is blowover where onshore winds carry sand across the dune surface and down the lee slope by gravity, therefore facilitating a landward movement of the dune system (Davis and Fitzgerald, 2004).

The sediment budget of the littoral cell is a major controlling factor determining the presence of dunes and their morphology (Figure 1.8). Formation and progradation of coastal dunes will generally occur within systems with very positive sediment budgets (i.e. sediment input exceeds output). Where there is a change to a balanced sediment budget, i.e. sediment input equals sediment output, the sediment supply will be reduced; there may be areas of progradation and others of erosion, but there will be no change in the overall area of dune. Change to a negative budget will further reduce the amount of available sediment leading to a dissected dune system, characterised by erosional landforms e.g. blowouts, deflation hollows and plains, reactivation dunes and scarping (Carter, 1991).

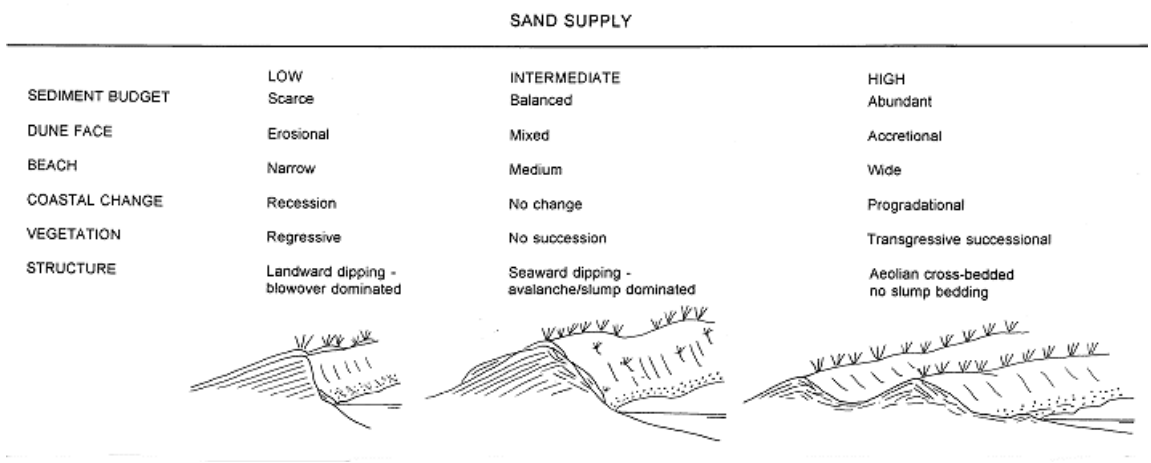

Figure 1.8 Irish dune morphology as a function of sediment supply (Carter, 1990)

Species assemblages and vegetation dynamics

The role of vegetation within coastal dune systems is important; the degree of vegetation stabilisation is a primary factor in determining the mobility of the system. Coastal dune vegetation falls into two broad categories sand fixing (e.g. *Atriplex* spp.) and sand building (e.g. *Ammophila arenaria* and *Leymus arenarius*) (Carter, 1991). Ecological succession is said to take place when the vegetation in a particular place changes with time and one unstable community progressively gives way to another until a stable climax community becomes established (Slingsby and Cook, 1986).

Initially, interspecies competition is not dominant on many dunes, but salt spray, mechanical stress (from moving sand), nutrient availability and water supply are key factors determining the species present and species diversity (Grunewald and Schubert, 2007; Greaver and Sternberg, 2006; Moreno-Casasola, 1986; Wilson and Sykes, 1999). Salt spray and a high permeability are major factors affecting the strandline and embryo dunes, and so colonising plants species need to have xerophytic and halophytic characteristics (Dowdeswell, 1984). The rough surface created by the plants decreases the wind speed causing mobilized sand to settle and build up embryo dunes and start primary succession (Grunewald and Schubert, 2007). As sand accumulates, the embryo dunes are colonised by various species of grass, e.g. *A. arenaria*, *Carex arenaria* and *Elytrigia juncea* in Europe; globally these species may vary, for example *Desmoschoenus spiralis* is the native colonising grass in New Zealand (Sykes and Bastow, 1991). The roots and rhizomes of these grasses have a stabilising effect on the sand (King, 1989). The grasses present in this area of the dune possess numerous adaptations to withstand burial. Maun (1998) states that growth of these plant species is stimulated by, improved soil resources, increase in soil volume, reactive plant growth, and enhanced mycorrhizal activity. As more sand is trapped the dunes grow and join to form foredunes.

Decaying organic matter from the colonising species initiates soil succession as humus starts to accumulate. The stabilising of foredunes is associated with the arrival of mosses and a wide range of perennial and annual plant species; *A. arenaria* becomes progressively less successful as succession proceeds and competition becomes more intense (Dowdeswell, 1984). As sand accumulation stops and fixed dunes become established, shell material is no longer delivered to the dune and $CaCO_3$ begins to leach out, and therefore pH decreases (Grunewald and Schubert, 2007). Nitrogen mineralisation increases as more soil organic matter collects (Berendse *et al*, 1998); soil moisture also increases. The change in the physiochemical conditions produces an environment favourable to more plant species and therefore more species can become established. Typical species of the fixed dunes include grasses such as *Festuca rubra*, *Festuca ovina* and herbs such as *Galium verum*, *Rhinanthus minor*, *Galium saxatile.* As species numbers increase inter-species competition becomes the dominant factor controlling species presence or absence (Grunewald and Schubert, 2007). Dune slacks and blowouts are exceptions to this successional trend.

1.4. Aims and objectives

This work focuses on the hitherto largely unstudied paraglacial marginal coastal environments of the barrier systems of northwest Ireland. The primary aim is to use records of environmental change to establish the main internal system controls (e.g. sediment supply, local physical context) and external driving factors (e.g. regional storminess, tidal regime, sea-level change) influencing the formation and morphological evolution of low-lying marginal coastal/estuarine habitats in this region. This region is of key importance. The northeast Atlantic margin is considered to be sensitive to climate (e.g. changes in storminess) and sea-level forcing (Devoy et al., 1996). The low-drift, sediment-rich coastline of west Donegal provides discrete morphosedimentary systems where the morphodynamic response to climate and sea-level forcing would be recorded within the accretional history of the inter- and supratidal sedimentary environments. Furthermore, there is a relative paucity of human impacts on the coastal zone here, which removes the added complications of morphological response to anthropogenic actions.

This study seeks to address to a certain extent the current paucity of information on the development, morphological evolution and distinguishing characteristics of the low-lying marginal environments (including machair) of northwest Ireland. Also a greater understanding of the functioning of these environments will be required in future studies to further the currently limited understanding of relative sea level change in this region. The primary aim of this study is achieved through a number of specific objectives:

- To establish the present day physical and ecological factors controlling and influencing the formation, presence and distribution of coastal/estuarine habitats of the study area.
- To establish the historical extent and morphological changes to the study area.
- To identify stratigraphic changes and compare historical sediment characteristics to present day sediment characteristics of varying local environments in order to determine the morphological and ecological development of the study site.
- To link historical changes to possible external driving factors.

The work also contains a significant methodological component. Various methods are assessed and their potential in multi-proxy analysis of marginal intertidal sediments evaluated.

The following chapter describes in more detail the physical characteristics of the paraglacial coastline of northwest Ireland and in particular County Donegal. The environmental history of the region and the occurrence and nature of the coastal environments are described and relevant previous studies and records assessed.

2. Physical Setting: Northwest Ireland and County Donegal

County Donegal is situated in the far northwest of Ireland (Figure 2.1). From Malin Head in the north to Donegal Bay in the south (Figure 2.1), the highly indented Donegal coastline is comparable to most of the Irish west coast and comprises a wide variation in the coastal environments represented. The presence of sediment-filled estuaries, of which there are 25 in Donegal, and bays separated by bedrock promontories and peninsulas ensures a high diversity of coastal habitat. Coastal physiography is strongly influenced by the regional geology and glacial history, which retains a strong structural and long-term imprint on the coastal framework. Coastal sedimentary environments such as sand flats, marshes and dunes occupying most of the coastal valleys are sensitive to changes in sea-level and wind and wave climates; as such, these systems are more dynamic and responsive over shorter time-scales (Duffy and Devoy, 1999).

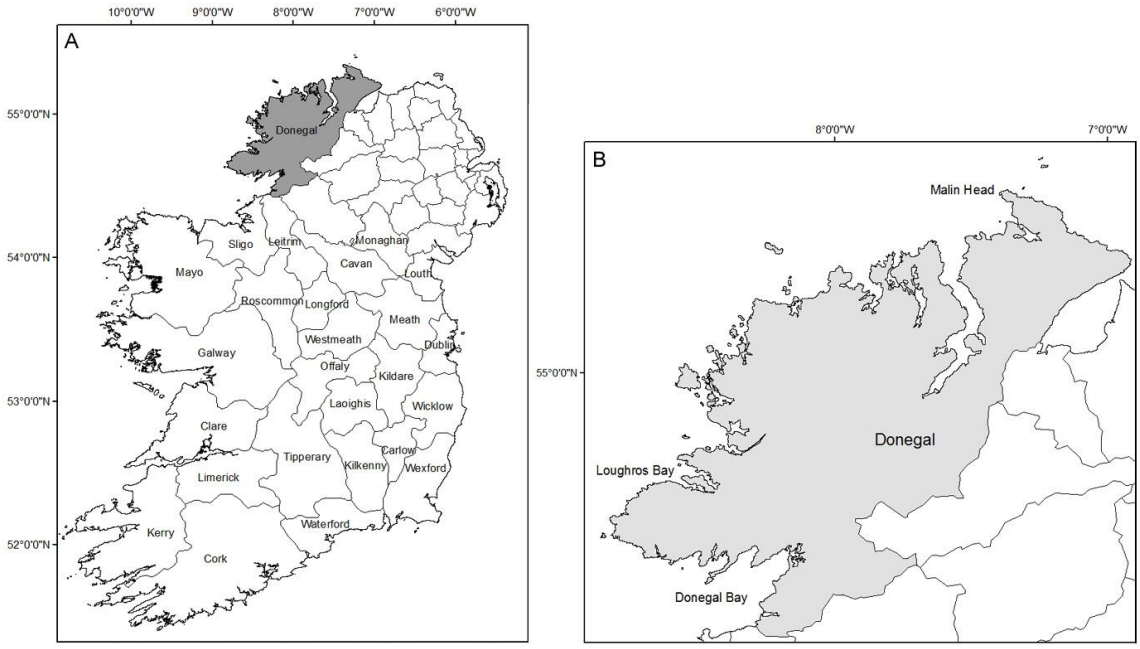

Figure 2.1 A: County Donegal; B: Donegal coastline and locations referred to.

2.1. Geology

The structural geology of Donegal is part of the NE-SW trending Caledonian fold belt of Lower Palaeozoic age, consequently many of the major rock groups and structures can be correlated with those found in the Scottish highlands (Pitcher and Berger, 1972). The basement rocks of Donegal are part of the Dalradian Supergroup deposited during the Early Ordovician (Woodcock and Strachan, 2002; Pitcher and Berger, 1972) and are primarily metamorphic in type. These basement rocks were deformed during a series of tectonic and metamorphic events

associated with the Grampian and Caledonian orogenic events (Woodcock and Strachan, 2002). Folding mainly followed the Caledonian NE-SW axis. In western Donegal, however, the structural trend changes to E-W. Subsequent to this period of structural and metamorphic change there was a major episode of granite emplacement associated with the Donegal Batholith; 8 different granite units have been identified (Pitcher and Berger, 1972). The contact metamorphism associated with each of these granite units resulted in a complete re-crystallisation of the surrounding rocks; for example the aureole rocks of the Ardara pluton were altered to contact-schists (Pitcher and Berger, 1972). This complex geological history has resulted in a great variety and contrast in the rock types present in the area including Carboniferous limestones; pelites, schists and quartzites of the Dalradian; and the Donegal Batholith granite complex. The present day coastal configuration is strongly influenced by the position and orientation of fault lines, with the majority of bays forming along the east-west trending faults in the south of the County and northeast-southwest trending faults in the north (Figure 2.2).

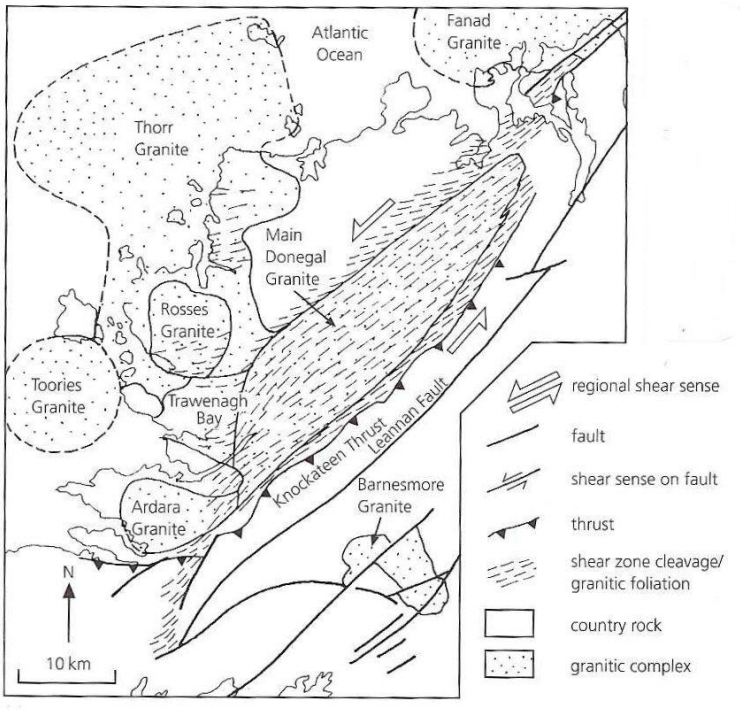

Figure 2.2 Relationships of the granites of the Donegal Batholith to Caledonian strike-slip faults or shear zones (adapted from Woodcock and Strachan, 2002).

2.2. Glaciology

2.2.1. Glacial history

Although the structural geology of the area provides an inherent control on the orientation and nature of the headland-bay configuration of the western coast of Donegal, the sea loughs and estuaries owe their presence to the erosional and depositional processes of the Quaternary glaciations.

Due to a lack of evidence, the number and extent of ice sheets that covered Ireland and extended onto the Atlantic continental margin to the west and south is unclear (Sejrup *et al.,* 2005). The Last Glacial Maximum (LGM) is thought to have occurred approximately 19-23ka, however extensive ice cover was present in Ireland 20ka prior to this period (McCabe *et al.,* 2007; Bowen *et al.,* 2002). During the LGM, rapid expansion of the Britain and Ireland ice sheets occurred. The west Donegal coastline was in close proximity to the limits of an extensive and thick (600-700m) ice sheet (Brooks *et al*., 2008) which covered much of north and central Ireland (Shaw and Carter, 1994; Lambeck, 1996). This Irish ice sheet is thought to have fluctuated during this period with at least three advances into the Irish Sea Basin identified. However, the western margin of the ice sheet remains poorly defined (McCabe *et al.,* 2007). Deglaciation is thought to have begun around 21ka with the retreat of ice from both Britain and Ireland almost complete by 15ka. Subsequently the Younger Dryas period (ca. 10-11ka) is marked throughout northwest Europe by a distinct change to periglacial environments and by the formation of features resulting from severe periglacial processes (Walker *et al.,* 1994). Such features are abundant on Muckish Mountain in the north of Donegal and are described by Wilson and Sellier (1995) to include blockfields and patterned ground on the plateau, and boulder lobes, talus and a relict lobate rock glacier on the surrounding slopes.

2.3. Sea-level change

Several studies have examined the changes in late- and post-glacial relative sea level on the coast of Ireland (e.g. Carter *et al*., 1989; Shaw and Carter, 1994; Lambeck, 1996; Brooks *et al.,* 2008). However, the history of relative sea level for the Holocene has never been fully established due to the lack of quantitative information available (Brooks *et al*., 2008).

During the early periods of deglaciation relative sea level was high due to isostatic depression; evidence the west coast of the Irish Sea indicates a sea level of +30m OD between 21 and 19ka (Clark *et al.,* 2004). From field evidence, Stephens and Synge (1965) describe a late-glacial (17-20ka) sea level in north Donegal of +22m compared to the present day; this decreases westward so that to the west and south of Bloody Foreland no late-glacial structures indicating a relative sea level higher than that of the present day have been identified. From this high stand sea level

fell during a period of isostatic recovery to a point where by 11.5-12ka the shoreline was some distance seaward of the present coast (Shaw and Carter, 1994). There are varying depths given for this Early Holocene low stand, ranging from -30m to -15m (Shaw and Carter, 1994; Schettler *et al.,* 2006). This fall in relative sea level corresponds to a similar fall to a Holocene minimum described in northwest Scotland for the period between 12 and 10ka (Shennan *et al.,* 1999; Shennan *et al.,* 1995) and highlights the regional effects of isostatic recovery in the area. Variation in the late Quaternary ice loading of Ireland led to a north - south gradient in isostatic recovery; as a result the relative sea level lowering in northwest Ireland never reach the same extent in southwest Ireland where glacial rebound was only slight (Devoy, 2008; Schettler *et al.,* 2006).

Shaw and Carter (1994) describe a rapid rise in sea level in northwest Ireland between 9000 and 7500 years BP which flooded coastal valleys and is thought to have reached present-day sea level ca. 6000 years BP in Donegal (Lambeck, 1996). This observational evidence has been used to validate Brooks (2008) model of sea level rise in this region (Figure 2.3). This early Holocene sea level rise is also evident in the northwest of Scotland where sea level is thought to have risen rapidly during the early Holocene, culminating in a mean sea level high stand of 1.5-5.1m OD at around 6000 years BP before a gradual fall to the present level (Wilson, 2002).

During the Holocene marine transgression the offshore glacial and periglacial sediments were remobilised and transported onshore (Burningham and Cooper, 2004). During this time, and under the influence of high energy waves, the northwest coast of Ireland segmented into a series of rock-bound embayments, within which the finite volume of sediment was, and continues to be, recycled under the control of wave and tidal energy (Carter *et al.,* 1989; Delaney and Devoy, 1995).

Due to the lack of observational evidence, both spatially and temporally, the relative sea-level record around Ireland is incomplete (Brooks *et al*., 2008) and much of the sea level change recognised is based on qualitative regional patterns. Therefore several attempts have been made to model the post-glacial sea level changes. The reconstruction described by Brooks *et al.* (2008) uses isostatic rebound modelling to predict the sea-level change at different points around the Irish coast. However, the model reports values on the Holocene high stand for west Donegal and north Wales that are contradictory to the available field evidence. The model proposed by Lambeck (1996) also has problems in predicting the pattern of sea level change along the west Donegal coastline due to the deeply penetrating coastal valleys, the close proximity to the ice sheet edge and the uncertainty over the data available for the Donegal area. The principal result from Lambeck's (1996) model for the Donegal area is that the present level was first reached around 6000 years BP, and was followed by a short-duration high stand; after about 4000 years BP sea level may have dropped below its current level.

Relative sea level along the Donegal west coast has fallen during the late Holocene and little or no mean sea level rise is thought to have occurred over the last 2000 years (Delaney and Devoy, 1995; Wheeler *et al.*, 1999; Brooks *et al*., 2008) (Figure 2.3). An associated influence on sediment recycling is therefore considered minimal. It is more likely that sediment recycling is forced by changes in coastal storminess and occurrence of high energy wind and wave conditions (Delaney and Devoy, 1995). As a result of the relatively stable recent sea level the supply of offshore sediment to the coast is low; and due to extensive reworking of the shelf during the mid-Holocence, most shelf-derived deposits are now contained within coastal compartments (Wheeler *et al.*, 1999). Evidence of 20th century sea level change points to a continuation of the late-Holocene trend. Analysis of tide gauge data from Malin Head (north Donegal, Figure 2.1) shows a linear rate in relative sea level changes of -0.16mm a^{-1} (±0.17mm a^{-1}) between 1958 and 1998 (Orford *et al*., 2006). The trend is not statistically significant, but despite this there is a general consensus that sea level in the north of Ireland is continuing to fall from the mid-Holocene highstand (Orford *et al*., 2006). However, the picture for west Donegal is less clear (Brooks *et al*., 2008).

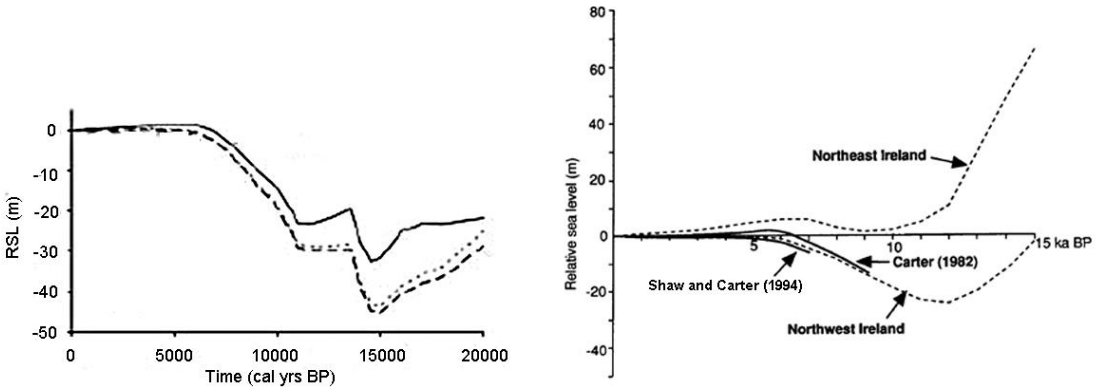

Figure 2.3 Left - Brooks (2008) models of relative sea level for West Donegal. Right - Shaw and Carter (1994) relative sea level from observational evidence (solid line) and predicted sea level (dashed line)

2.4. Wind, wave and tidal climate

2.4.1. Wind

Donegal has a West Maritime climate with mild, damp winters and cool, cloudy summers (Fossitt, 1994). The coastal region of northwest Ireland experiences a high energy wind climate dominated by south-westerlies (199.3 degrees) with an annual average hourly speed of 7.4ms^{-1} (14.3 knots) (Malin Head, north Donegal, and Belmullet, north west County Mayo, 1956–2009). This increases the further north on the coast with average wind hourly speed for Malin Head (1956-2009) alone being 8 ms^{-1} (15.6 knots) (Figure 2.4). There are on average 214 hourly occurrences of gale force winds, i.e. 17.5ms^{-1} (34 knots) or greater, per year; the majority of

which come from a westerly direction as well as those of greatest wind speed. The majority of storms affecting the west coast of Ireland are extratropical in type. These last a long time in the offshore fetch area allowing large waves to build up (MacClenahan *et al.*, 2001). This also creates the possibility of storm-generated surges affecting the coastal region (Wheeler *et al.*, 1999).

2.4.2. Tidal regime and wave patterns

The west Donegal coast is characterised by a semi-diurnal meso-tidal regime, with a mean tidal range of 3.5m at springs and 1.6m at neaps (Burningham, 2008; 2002).

The west Donegal coastline lies within the mixed wave-tide dominated part of the coastal energy spectrum. Wave data recorded offshore indicate an average wave height of 3.2m with 25% of waves exceeding 4m (Burningham, 2008). Mean wave height in the North Atlantic is thought to have risen since around 1950 by approximately 2% per year (Bacon and Carter, 1991).

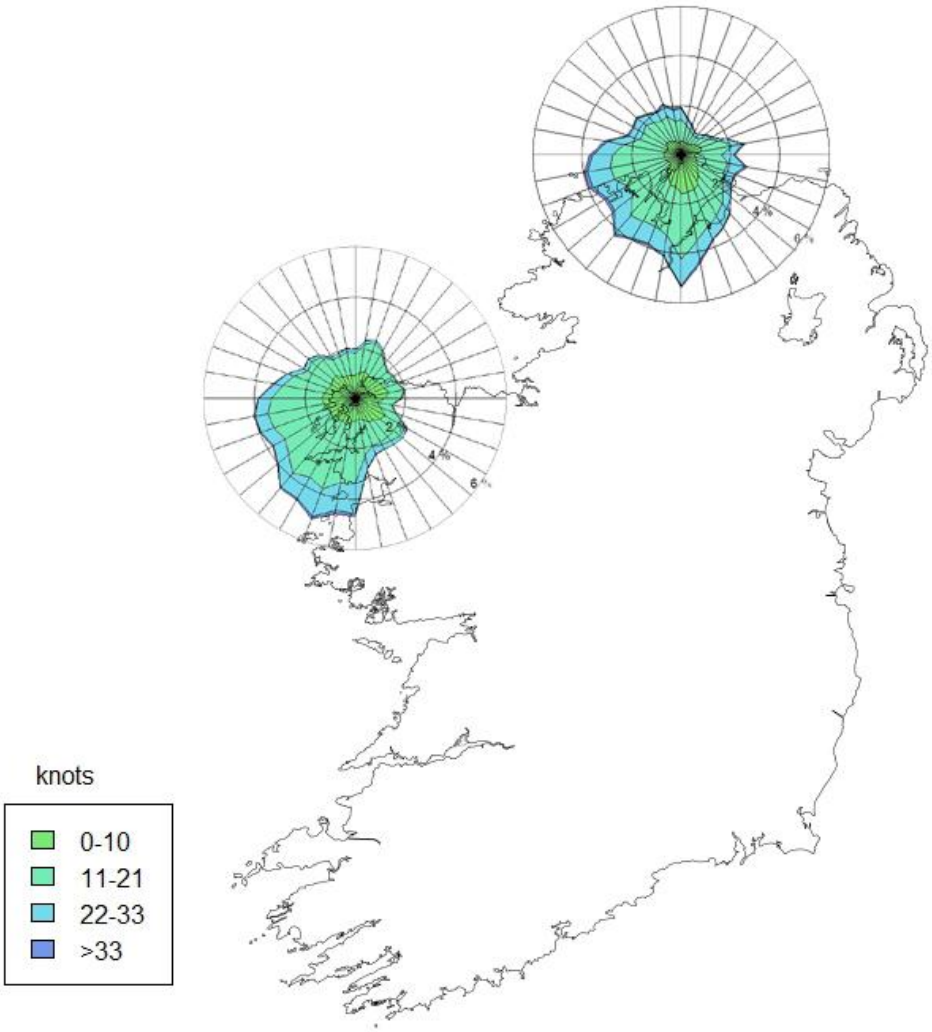

Figure 2.4 Wind frequencies recorded at Malin Head, north Donegal, and Belmullet, north west Mayo, for the period 1956 – 2009 (Source: see Appendix 1).

2.5. Coastal Environments

The coastal environments along the west coast of Ireland, in particular from County Galway to County Donegal, are dominated low lying marginal sedimentary systems separated by rocky headlands. These environments display some features that are distinct from similar environments elsewhere in Europe. For example, the dune-machair systems often show an increase in shell carbonate content from south to north due to the changing availability of marine shell material associated with the North Atlantic Drift. They generally lack any organic horizons or palaeosols, again distinguishing them from similar environments elsewhere in Europe (Duffy and Devoy, 1999).

2.5.1. Irish saltmarshes

Large areas of saltmarsh, commonly estuarine- or loch head-type, are found around the Irish coast (Boorman, 2003). Irish saltmarshes typically show some distinction from similar environments in the rest of Europe. For example, the saltmarshes along the western coast often lack a clear halophytic zonation; this may be due to the high annual rainfall in the region increasing the productivity and competitiveness of the euryhaline species (Duffy and Devoy, 1999). Also, Allen (2000) states that generally Irish marshes tend to be more organic rich due to restrictions in mineral sediment supply. There are also differences in the vegetation of Irish saltmarshes for example *Limonium vulgare* is replaced by *L. humile* and *Attriplex portulacoides* does not occur on the northern coasts between County Mayo and County Antrim (Boorman, 2003).

Curtis and Sheehy Sheffington (1998) produced an inventory and classification based on the morphology and nature of the substrate of Irish saltmarshes. 238 saltmarshes were identified in the Republic of Ireland and 12 in Northern Ireland. They defined 5 types of saltmarsh which were used in their classification (Table 2.1). Although the typical substrate is used in the definition they point out that this may vary depending on the local physical conditions, for example fringe salt marsh soils may contain portions of sandy and mud sediment if other types of coastal formations, such as dunes, occur nearby. Estuary types were found to occur in large estuaries such as those in Limerick, Dublin and Cork as well as in smaller estuaries in Donegal for example. Bay types were primarily found on the west coast in sheltered conditions around Donegal, Clew Bay and Galway Bay. The lagoon type is very rare in Ireland and Curtis and Sheehy Sheffington (1998) speculate that this may be due to the high rainfall promoting brackish vegetation rather than saltmarsh. The fringe type was found to be wide spread on the west coast of Ireland where it may be extensive if the tidal prism is sufficient. Mud was found to be the predominate substrate in the majority of marshes across Ireland with the exception of those marshes in the northwest and west, in counties Donegal and Mayo Sand was the most common substrate, and in west Galway peat was the dominate substrate.

Table 2.1 Definition of saltmarsh types used by Curtis and Sheehy Skeffington (1998) in the classification of Irish saltmarshes.

Saltmarsh type	Substrate	Saltmarsh characteristics
Estuary	Silts and clays	Occurs at the mouth on medium to large rivers. *Spartina* grasses present.
Bay	Silts and clays (not necessarily marine)	Occurs in very sheltered bays, direct river or stream input is minimal. *Spartina* grasses usually absent.
Sand flats	Sandy	Alongside dune systems in a sheltered corner or as extensive seaward extensions of machair plains.
Lagoon	Muds/sand/gravel	Along the edge of lagoons formed behind sand or shingle bars. Rare in Ireland
Fringe	Muds/ peat	Overlying reedswamp and/or *Sphagnum* peats. Only in western Ireland.

In their study of two "estuary" type saltmarshes in County Donegal and County Sligo, Wheeler *et al.* (1999) identified distinct, alternating, clay and silt lamination sequences within the saltmarsh stratigraphy. At the Donegal site, at the head of the Loughros Beg estuary, these laminations can be clearly identified along a 70cm cliffed margin of the saltmarsh. They interpreted the alternation between these sediment facies to be indicative of the occurrence of storm-surge events. Periodicities were noted within these sequences and are seen to represent changes in the storminess of the north-east Atlantic over the period of deposition (i.e. approximately the last 150years). Wheeler *et al.* (1999) estimate the average annual deposition rate at the County Donegal saltmarsh to be 5mm/yr however this deposition rate was seen to not be constant throughout the sequence; they were not able to determine a deposition rate for the County Sligo marsh.

2.5.2. Irish machair

As described previously machair is a highly specialised calcareous dune grassland habitat which, in Ireland, is confined to areas of the northwest, from the Aran Islands, Co. Galway, to Malin Head, Co. Donegal (Ryle *et al*. 2009) (Figure 2.5). It is estimated that the total area of machair within Ireland is approximately 2750ha. However, a large proportion of this is deemed to be of unfavourable-inadequate or unfavourable-bad status due to agricultural and recreation pressures (Arroyo and Bolger, 2010). Machair is one of the rarest habitats in Europe occurring only in northwest Scotland and Ireland. It is designated as a priority habitat under the European Habitats Directive (European Commission, 1992) and as such is offered a high level of protection in Ireland. Despite this recognition of its rarity and importance there have only been a few studies on the machair of Ireland (Gaynor, 2006; Cooper *et al*., 2005; Bassett and Curtis, 1985). Due to its low lying morphology and high winter water levels machair is particularly vulnerable to sea level rise and increased storminess (Angus and Hansom, 2006).

Bassett and Curtis (1985) produced the first comprehensive description of the occurrence of machair in Ireland, up until this point the term machair had only been applied to the extensively described landforms in west and northwest Scotland. In their paper, Bassett and Curtis (1985) assess the characteristics of Irish dune grassland sites in order to ascertain if there is any

similarity with Scottish machair. Twenty six Irish machair sites were identified; these closely resembled the machair of the Scottish Western Isles. However, some differences between the Irish and Scottish systems were apparent: the organic content soils of Irish machair was not seen to increase landward as is observed in Scottish systems; and differences in the presence or absence of some core plant species were also noted. Bassett and Curtis (1985) consider the core species of Irish machair to be *Festuca rubra, Plantago lanceolata, Bellis perennis, Lotus corniculatus, Galium verum, Trifolium repens, Carex arenaria, Poa subcaerulea* and *Brachythecium ablicans*, they also found the common occurrence of *Luzula campestris* to be of note. However, they considered the main difference between the Scottish and Irish machair sites to be the human use; in Ireland it is universally grazed and used for amenity purposes.

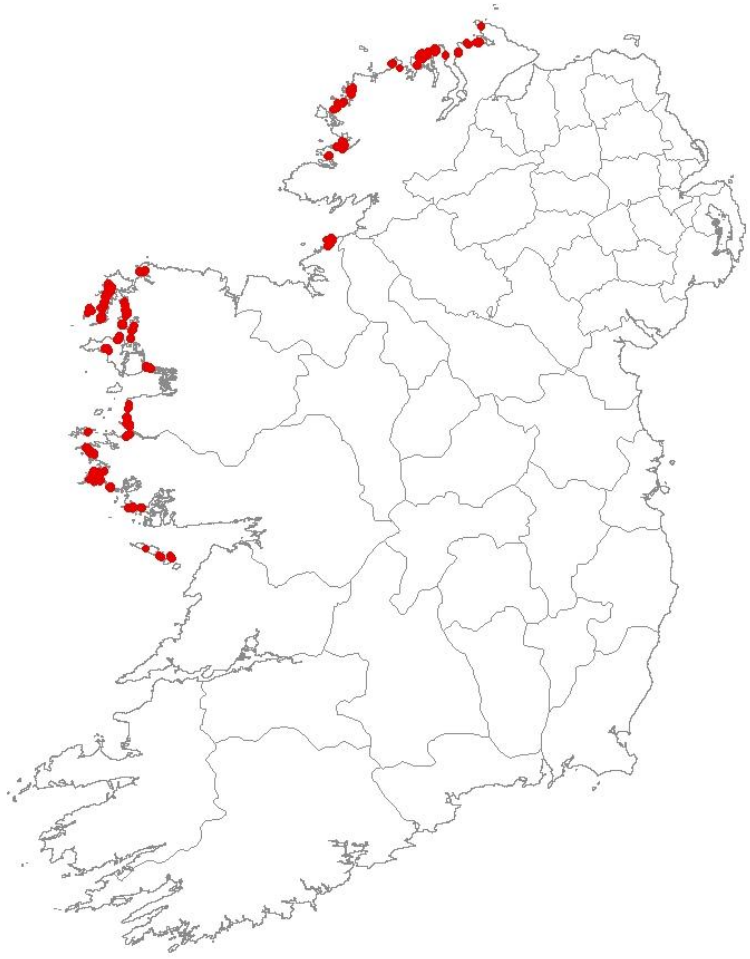

Figure 2.5 Distribution of machair in Ireland (Ryle *et al.* 2009)

Cooper *et al.* (2005) assessed the effect of livestock grazing and recreation the vegetation of 22 machair sites from Malin Head to Galway Bay. They showed that grazing intensity and recreation use had a much greater impact on the species and amount of bare ground present than the key soil variables.

Gaynor (2006) described the vegetation of Irish machair in order to examine how climatic, edaphic, geographic and anthropogenic factors influence the distribution and formation of

machair and the plant communities present. She concluded that the highly dynamic nature of machair makes it difficult to classify the vegetation. However, she did identify distinct wet and dry communities. Also, she found the vegetation of Irish machair to be comparable to that of Scottish machair but with some differences and found that, with the exception of *Poa subcaerulea* and *Brachythecium ablicans*, the core species described by Bassett and Curtis (1985) dominated this survey.

The research into Irish machair to date has been focused on identifying machair sites and on the vegetation. In contrast, little attention has been paid to the geomorphology or sedimentary systems and processes associated with the formation, development and occurrence of Irish machair.

2.6. Study area

2.6.1. Geomorphology

The west facing Loughros More estuary (Figure 2.6) is one of 25 Donegal estuaries. It is typical of west Donegal coastal systems, which are inherently dynamic, often comprising large dune environments along one or both inlet margins. In these systems bedrock and structural features of the valley often impose strong controls on estuarine morphodynamics (Burningham 2002). Metamorphic rocks underlie most of the seaward parts of Loughros More, in particular Loughros Group and Upper Falcarragh Pelites, and Falcarragh limestone. These are overlain by extensive aeolian sand deposits across the northern margin of the estuary. The majority of the inner reaches of the estuary are underlain by intrusive igneous granodiorites (National Parks and Wildlife Service, 2005).

The Magheramore dune system covers the northern edge of the estuary mouth and covers 280ha (Figure 2.6). The majority of this system comprises fixed dunes that stretch for approximately 600m eastward and inland from the west-facing, open-coast Tramore beach and 400m northward / northeastward and inland from the intertidal zone along the northern margin of the estuary inlet. The system is bound to the southwest by a pelite bedrock headland (Figure 2.6). Tramore beach bounds the system to the west; here, mobile foredunes and embryo dunes extend approximately 100m seaward of an area of dune slack/wetland. This dune slack/wetland is fed by springs at the base of the fixed dunes. Immediately behind this is a 1 to 5m steep erosional dune escarpment. This escarpment formed during a period of erosion and dune front retreat between the mid-twentieth century and the 1970s. The embryo and foredunes are evidence of a period of rapid progradation (approximately 200m) since the 1970s (Barrett-Mold and Burningham, 2010). A second area of progradation is present at the southeastern margin of the Magheramore system (northwest of Sandfield). Here, approximately 350m of dune progradation, dominated by recurve growth of foredune ridges and inter-ridge lows, has occurred since the 1950s (Barrett-Mold and Burningham, 2010). Associated with the period of

erosion and dune front retreat in the mid-twentieth century was wide spread dune surface destabilisation. Numerous blowouts were present across the fixed dunes during the early 1950s, predominantly aligned with the prevailing wind direction (SW-NE). By the 1970s the dune surface showed signs of recovery and stabilisation and vegetation had re-colonised many of the blowouts. Presently, many of these blowouts are only present as relict topographic features on the fixed dune surface; a few are partially active, i.e. areas of bare mobile sand on the steep sides, but with vegetation and/or dune slack in the base of the depression.

Since the early 1900s, the estuary ebb tidal channel has shifted northwards to its current position adjacent to the Magheramore dunes. This equates to a northward shift of 650m, resulting in 500m of erosion into the dunes (reducing the breadth of the dunes to half its 1835 extent) (Burningham, 2002) (Figure 2.7). The progradation seen at Tramore and northwest of Sandfield is thought to be a direct result of this northward channel migration and dune erosion. This caused significant release of dune sand which was subsequently available for transport and deposition elsewhere in the system (Burningham, 2008). The northward shift in channel position has also facilitated the formation of foredunes and a supratidal sediment point bar on the southern margin of the inlet.

Behind the dunes to the northeast is Sheskinmore Lough. This is a shallow lake fed by the Duvoge and Abberachrin rivers from the northeast and east respectively, and is fringed by areas of fen and wet grassland (Figure 2.6). The Magheramore dunes are instrumental to the existence of Sheskinmore Lough, having dammed a tributary to Loughros More approximately 1000 years ago during extensive dune destabilisation and sediment reworking (Shaw & Carter, 1994). The lake drains southeast through the dunes before entering the estuary where it runs along the intertidal margin at Sandfield. A sluice at the dune/sandflat margin is used to regulate the discharge from the outflow to control the water level in the lake.

At Sandfield and Derryness are areas of low lying grassland surface (Figure 2.6). These have a distinct and unusual morphology comprising large and relatively flat surfaces, with few other morphological features. They occupy a narrow elevation zone at or around high intertidal / low supratidal. There are conflicting views on the definition of these areas with some authors defining the area at Sandfield as machair or partially machair and Derryness as saltmarsh (e.g. Gaynor, 2006) and others defining both areas as saltmarsh (e.g. Curtis and Sheehy Skeffington, 1998; McCorry and Ryle, 2009). Additionally, the area between Sheskinmore Lough and the fixed dunes displays many of the typical machair characteristics as described by Ritchie (1976). For example, it has a low angle surface morphology at a mature stage of geomorphological evolution, distinct calcareous grassland vegetation and sandy substrate with a high proportion of shell derived material. However, unlike the areas at Sandfield and Derryness, this area does not comprise an abrupt morphological boundary, but rather it grades into the fixed dunes to the southwest and the wetland surrounding the Lough to the northeast.

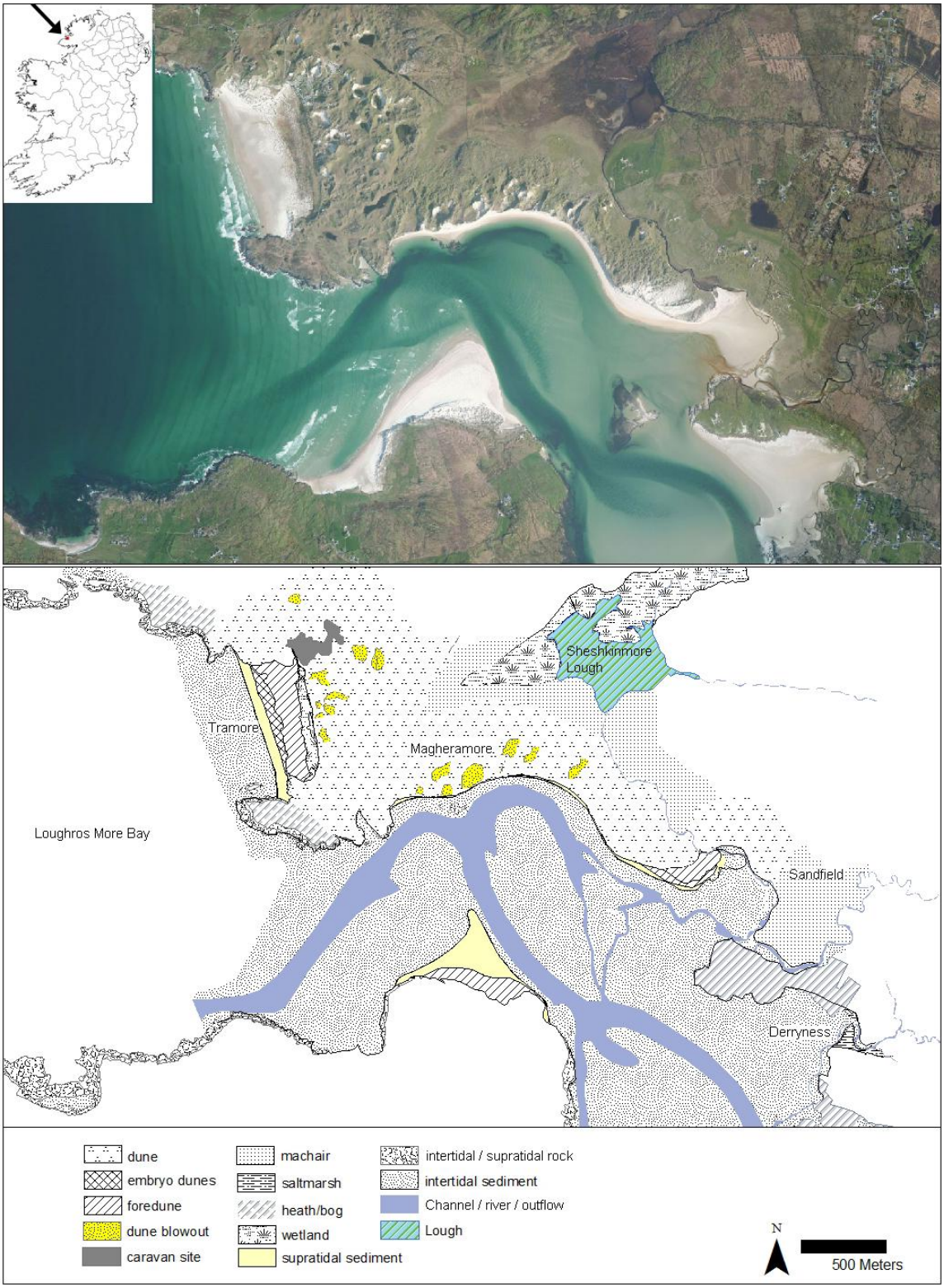

Figure 2.6 Aerial image of Loughros More estuary (2010) (above); Indicative map of marginal environments of the Loughros More estuary (below) (after Burningham, 2002) (Image source: see Appendix 1)

Figure 2.7 Relative change in position of low tide channel and dune margin between 1907 and 2010. (Image source: see Appendix 1)

The low lying grassy surfaces of Sandfield and Derryness are, in part, framed by the course of small rivers and drainage channels. At Sandfield the Sheskinmore Lough outflow forms the west boundary of the vegetated site, and the Bellanagoal runs along the southern boundary. Derryness straddles and unnamed river draining from marsh and land to the east. These outflows and rivers are tidal within the vicinity of Sandfield and Derryness. Both rivers have a natural, sinuous and meandering morphology and there is no evidence of present or historic modifications. The channels range from 1-5m in width and bank heights are generally 0.5 to 1m. There are no obvious signs of levee development, aggradation or incision. The bed material of reaches within the study site is dominated by sand size material.

These two areas of shoreline-margin, exposed vegetated sandflat / machair / saltmarsh at Sandfield and Derryness are the focus of this study (Figure 2.8). These sites were chosen because of their distinct morphology and the uncertainty over their definition and process of formation. The Sandfield vegetated platform covers a single site 13.6ha in area. At Derryness tow marginal grassy sandy platforms lie to the north (2.5ha) and south (0.9ha) of an unnamed river (Figure 2.8). Both areas occupy the high-intertidal – low-supratidal zone from mean high water to beyond the level of highest astronomical tides.

2.6.2. Species and habitat designation

The seaward portion of the Loughros More estuary is protected under the European Commission Birds Directive 79/409/EEC and Habitats Directive 92/43/EEC (European Commission 1979 and 1992) by both a Special Protection Area (SPA) and a Special Area of Conservation (SAC) (Figure 2.8). The Sheskinmore Lough SPA covers the Loughros More estuary inlet, Tramore strand, Magheramore dunes, Sheskinmore Lough and Sandfield vegetated area. The SPA designation lists 944ha of intertidal flats, sand dunes, machair, salt and freshwater marshes and partially sand filled lough (BirdLife International, 2007). The SPA was designated for the internationally important wintering populations of Greenland White-fronted Goose and Barnacle Goose. However, since the 1980s the populations of these species have declined. In the present day wintering populations of Greenland White-fronted Goose seldom reach 50 individuals in this area. This decline is attributed to a general trend to improved grassland (National Parks and Wildlife Service, 2005).

The 'West of Ardara/Maas Road' SAC is designated for 23 habitats listed under Annex 1 of the habitats directive, six of which have priority status, and the presence of several rare species listed under Annex II of the Habitats Directive including slender naiad, freshwater pearl mussel, marsh fritillary, petalwort, Atlantic salmon, common seal, whorl snail and otter (National Parks and Wildlife Service, 2005). This SAC covers the areas of both Sandfield and Derryness.

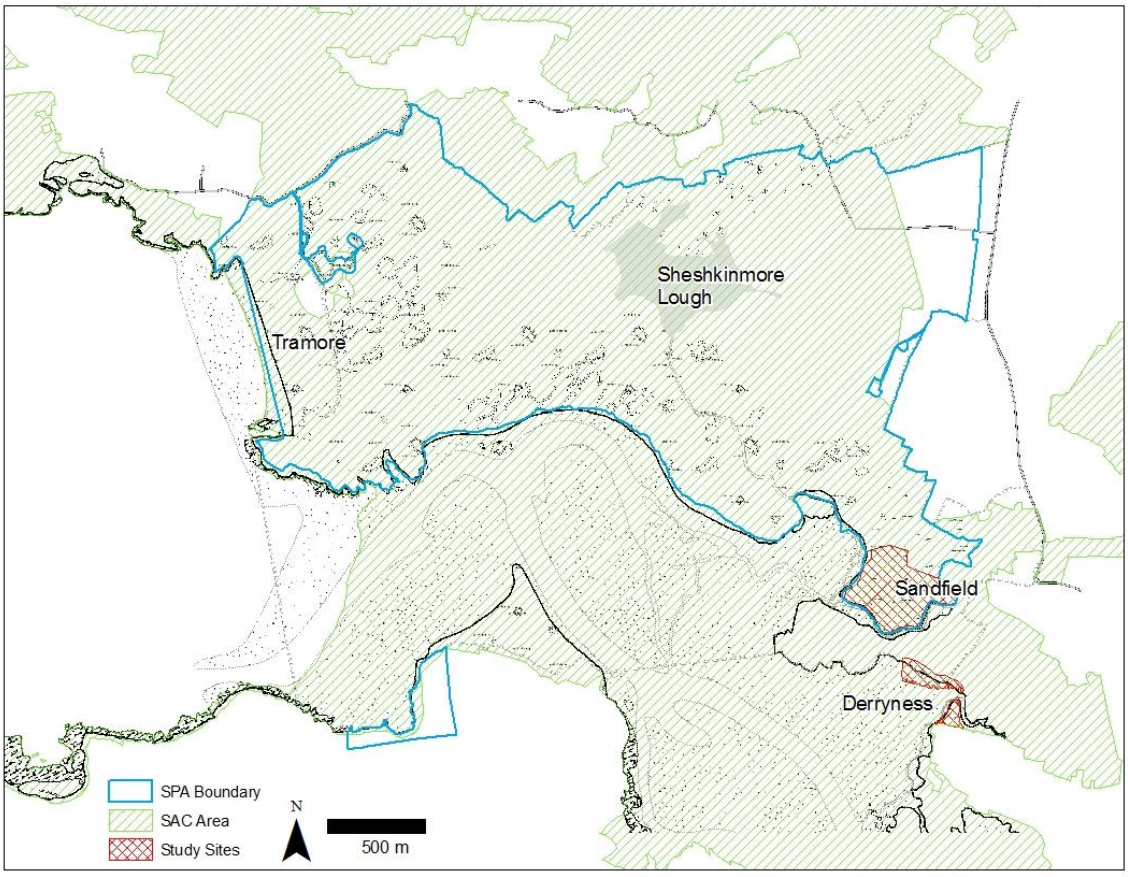

Figure 2.8 Loughros More estuary with study sites, SPA and SAC designation boundaries shown.

2.7. Summary of the physical setting

Along the Donegal coastline, in northwest Ireland, sediment-filled estuaries, separated by bedrock promontories or peninsulas, are common and coastal habitat diversity is high. Much of this sediment is of glaciogenic origin and was bought onshore during the late Holocene marine transgression and is now contained within these coastal embayments with little or no connectivity between estuaries. Recent sea level change over the last 2000 years is relatively uncertain and is complicated by the complex relationships between eustatic sea level rise and isostatic land adjustments.

This study focuses on the west facing Loughros More estuary. Here, there is evidence of significant morphological change over the last 200-300 years. Perhaps most significantly the shift of the main tidal channel from the southern margin of the estuary to the north and the consequent 500m erosion of the Magheramore dune system. This has remobilised a large amount of sediment within estuary and resulted in the formation on new depositional features. The estuary contains a high diversity of coastal sedimentary environments including, fixed and mobile dunes, saltmarsh, tidal flat and machair. Much of these environments are recognised and protected under the European habitat and birds directives. Of particular interest are the low lying grassland surfaces at Sandfield and Derryness. These areas occupy the high intertidal / low surpratidal zone and are unique within this estuary due to their distinct morphology of large, relatively flat surfaces. There are contradictions in the definition of these habitats with some authors describing both areas as machair and others describing a mixture of machair and saltmarsh.

3. Research design and techniques

This chapter describes the research design developed to address the aims and objectives of the research. And secondly, presents the methodologies of the techniques used to achieve these objectives.

3.1. Research design

In order to evaluate present day characteristics, influencing forcing factors, historic changes within the site and the possible mechanisms of change, the research is split into three distinct areas of study: spatial environment, stratigraphic characteristics and coastal forcing.

3.1.1. Spatial environment

Within this area of the study present day environmental conditions and historical morphological change are assessed. Spatial analysis methods are used to characterise the surface environment and identify changes across and between the sites.

The analyses focus on the areas of Sandfield and Derryness which were identified as unique within Loughros More estuary due to their distinct, low lying and flat morphology (Figure 2.6). These areas were examined within a GIS (ESRI ArcGIS 9.3) and discrete sample points identified across the vegetated surfaces and adjacent tidal sandflat using a stratified random sampling approach: 31 vegetated surface points and 53 sandflat points at Sandfield and 13 vegetated surface points and 20 sandflat points at Derryness (Figure 3.1) (see Appendix 2 for grid references).

3.1.2. Stratigraphic characteristics

This area of research analyses stratigraphic variations down-section at each of the study sites. Both stratigraphic and time-series methods are used to identify and characterise historical change.

Sediment cores were taken from each of the sites (Figure 3.1), 3 at Sandfield and 2 at Derryness (see Appendix 2 for grid references). Core sample sites were chosen to provide a representative sample of different periods of landform development as identified in the analysis of site environmental history (see chp 4.2). From the retrieved records SFD3 represents an area that has been continually vegetated since at least 1850, SFD2 has been vegetated since at least 1951 and SFD1 since at least 1907. At Derryness, both DYN1 and DYN2 have been vegetated since at least 1850. To enable examination of the core structure and sub-sampling the cores were split in half lengthways. Where non-destructive, scanning, methods were used the cores were sampled at a 1mm resolution, for all other destructive methods the core sediment was extracted into samples at a 1cm resolution. Before any analysis was undertaken on the downcore data the effects of compression of the sequence during core collection was taken into account. The

amount of compression, i.e. the distance between the top of the core tube and the sediment, was divided by the compressed length of the core and the result added cumulatively to each 1mm sample point. Although compression is unlikely to have been uniform throughout the core this was seen as the most effective way of "uncompressing" the core.

Due to time and resource limitations it was not possible to apply all analyses to all cores therefore cores SFD3 and DYN1 were selected for further analyses. Based upon GIS analysis of the environmental history of the sites (see chp 4.2) cores SFD3 and DYN1 represent the longest periods of vegetation cover at each site and therefore are likely to contain the longest, most complete record of sedimentation.

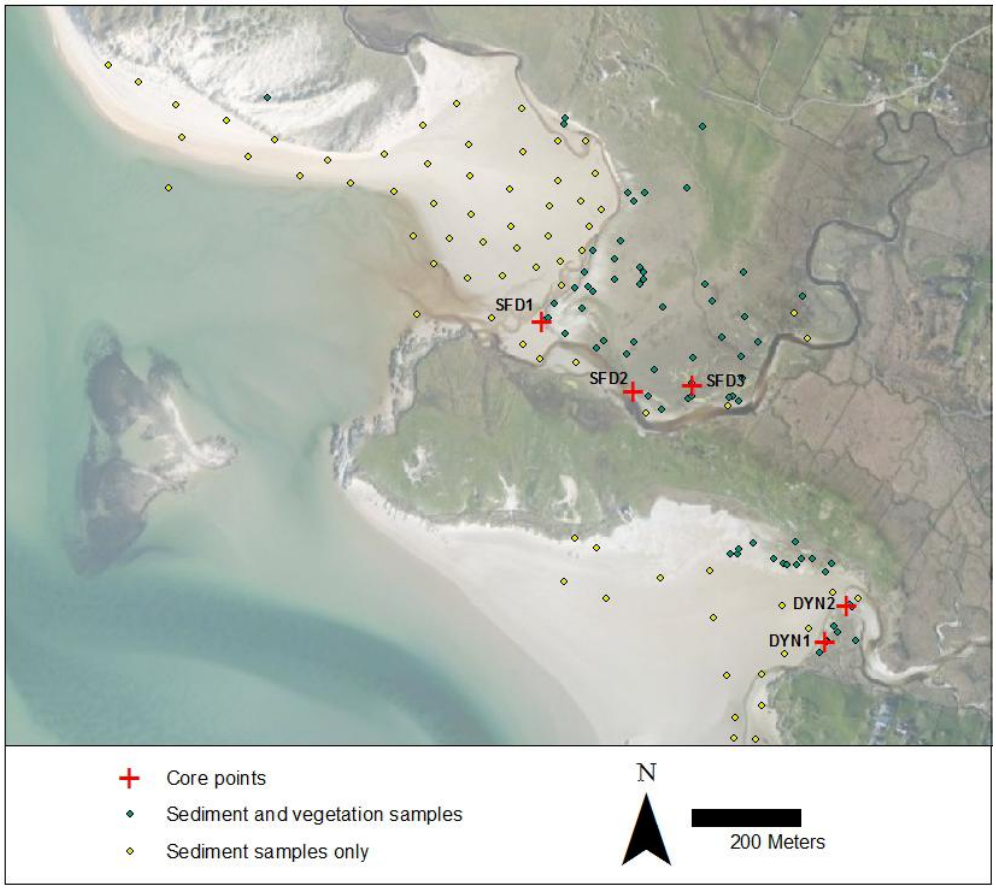

Figure 3.1 Location of core and sampling points (see Appendix 2 for grid references)

3.2. Multiproxy studies

Multiproxy studies are frequently used in the study of sea-level and coastal evolution. The use of a number of different but complimentary techniques enables a more secure reconstruction of coastal evolution (Freund *et al.*, 2004) and characterisation of processes and driving factors affecting the system. Therefore a multiproxy approach was applied to this research in order to address the multiple forcing factors influencing these types of system and also to more fully

evaluate changes occurring both spatially and historically. To an extent the nature of the sediment determines the most effective techniques; therefore, the methods used were chosen based upon their suitability to this intertidal, sand dominated environment. However, some of the methods used do have significant constraints in this type of environment. Diatoms are often poorly preserved very sandy units, however, other palaeoecological records (e.g. macrophytes and pollen) are equally poorly represented. The potential for the examination of foraminifera was considered however previous analysis of this revealed very low species diversity and therefore it was not considered suitable as an indicator of environmental change. It was therefore considered that although diatom sampling may not produce a complete record it could provide valuable insights when combined with other methods. ^{210}Pb and ^{137}Cs are also often problematic in very sandy environments therefore OSL dating was also used to provide additional chronological information. Table 3.1 summarises and evaluates the techniques used in this study.

3.3. Research techniques

3.3.1. Fieldwork

Fieldwork was mainly conducted in April 2008 although subsequent visits were made to check for any change and to collect additional samples for dating analysis; in May 2010 a confirmation of the plant species previously identified was made when the plants were in flower. Photographs were taken on all visits to provide a visual record of change; where possible permanent reference points were included in these photos to aid assessment of change.

Sample positions were numbered to ensure cross-correlation with the field data. A handheld GPS (Garmin eTrex) was used in the field to locate the sample points and to delineate landform boundaries.

Vegetation sampling was made at each of the vegetated surface points. As the vegetation is predominately of grassland community a 1m x 1m quadrat was used; this also allows direct comparison with other works on similar habitats, for example the National Vegetation Classification (Rodwell, 2000). The species present were recorded and their percentage cover estimated. Identification and nomenclature of vascular plants followed Rose (1981), Blamely *et al*. (2003), Fitter *et al*. (1984); those that could not be identified in the field were sampled and identified later; mosses and lichens were recorded, but not identified to species level.

At each of the vegetated surface and sandflat sample points sediment samples were collected to 5cm depth. Samples were placed in sealed plastic bags and were kept refrigerated until analysis to prevent decay.

Table 3.1 Summary of techniques used in this study

Technique	Purpose	Sampling	Output	Benefits	Constraints
Sediment peels	Aids stratigraphical correlation	Whole sample site sections	Detailed stratigraphic logs	Enables detailed logging; provides a record of sections	Some very fine sediments may not adhere
Geochemistry	Aids stratigraphical correlation	XRF – whole core scanning Organic & $CaCO_3$ content – every 1cm of core and all surface samples	Multi-element analysis	Allows correlation and comparison with other geochemical data sets	Problems relating elemental analyses to sediment compounds
Diatoms	Reconstruction of palaeo-environment	Representative samples of main sedimentary units	Diatom plots of counts of identified species	Indicator of palaeo-salinity, morphodynamics and environmental changes	Poor preservation in very sandy units
Grain size analysis	To aid stratigraphical correlation	Every 1cm of core and all surface samples	Grain size distributions	Enables correlation of samples based on physical characteristics	Difficulties in comparing with other datasets due to differing methods used
SEM	Reconstruction of palaeo-environment / modes of deposition	Representative samples of main sedimentary units	Descriptive analysis of surface microtextures	Provides a method of determining between aeolian and tidal deposits	Semi-qualitative, difficulties in identifying structures
^{210}Pb and ^{137}Cs Dating	Independent chronology	Subsamples from cores	Age determination and rates of sediment deposition	Provides an independent chronology and allows correlation between cores	Lack of datable material in very sandy deposits
OSL dating	Independent chronology	Subsamples from cores	Age determination	Provides an accurate age for a specific point downcore	Problems if quartz grains have been partially bleached or remobilised

Elevation data for each of the sites was collected using a Leica 500/1200 differential GPS (dGPS). The dGPS equipment was mounted to a backpack and multiple transects walked across the vegetated surfaces and down onto the sandflat immediately adjacent in order to establish the elevation change at this boundary. Positions and elevations are accurate to 1cm and were referenced initially to WGS (World Geodetic System) 1984 coordinate system, and then transformed to Irish Grid (TM (Transverse Mercator) 1965 geodetic datum, Malin Head OD (Ordnance Datum) vertical datum) using the GridInQuest software (version 6.6). Malin Head OD is equivalent to mean sea level in Ireland, and was assigned the national vertical datum in 1970: elevations (and OD) on the earlier OS (Ordnance Survey) maps refer to Poolbeg Lighthouse, Dublin which is approximately 2.7m below Malin Head OD (OSi, 2013).

Core samples were collected at each of the core sample locations in 0.5m to 1m length plastic tubes; these were hammered into the ground and removed by digging them out from the escarped edge. The amount of compaction in each core was recorded, i.e. the distance from the top of the core tube to the core sample when the top of the tube was flush with the surface.

In order to assess the local tidal regime a tide gauge was placed at the estuary mouth at Rossbeg for the period 4th – 13th April 2008 with measurements being recorded at 5 minute intervals.

A weather station was set up on the dune ridge of the Sandfield dune system to the north west of the site. Local temperature, humidity, wind speed and direction and atmospheric pressure information was recorded at 10 minute intervals for the period 4th – 13th April 2008.

A wave buoy was also placed in the main channel of the estuary for the period 4th – 13th April 2008; however, this piece of equipment did not work and therefore no results were obtained.

3.3.2. Stratigraphic peels and sediment logs

Sediment peels are not widely used in the study of coastal and estuarine environments. The methods traditionally used to record details of exposed sediment sequences and sections, i.e. field notes, sketches, logs and photographs, are often unsuccessful because they may fail to reveal subtle changes in colour, texture, sedimentary structures and sedimentology, and the often-complex relationship between beds and units (Goldberg, 1974). However peels are an effective way of capturing sedimentary sequences and the approach provides a permanent record that can be later used for laboratory study of mineralogy, grain size distributions and geometric relationships of layers (Yasso and Hartman, 1972).

There are a number of different materials and methods that can be used for the production of sediment peels and these have been described by various authors (e.g. Kidwell *et al.*, 1985; Yasso and Hartman, 1972, Goldberg, 1974; Burger *et al.*, 1969; Skipper *et al.* 1998). Skipper *et al.* (1998) summarised a number of methods and materials that can be used to produce peels of loosely consolidated and unconsolidated sediments, these include: PVA glue, Latex, epoxy

resin, polyester resin, acrylic resin and Portland cement. However, many of these methods are unsuitable for use in littoral and intertidal environments due to the time needed for the adhesive to set sufficiently for the peel to be removed, which can range from 3 to 72 hours.

Skipper *et al.* (1998) advocate the use of polyurethane foam as a simple, rapid and inexpensive technique for producing sediment peels. This method produces a ridged and lightweight peel within 30 minutes of application, ideal for intertidal environments and enabling several peels to be collected in a day. It was therefore decided that this would be an effective method of obtaining a record of the sections exposed at the cliffed margins of the Sandfield and Derryness sites.

In this study, peels were collected from 5 sample sites immediately adjacent to the positions where the cores were taken (Figure 3.1), exploiting existing exposures within the saltmarsh. The sections were exposed down to the level of the surrounding tidal flat, and cleaned using a hand trowel to render the face approximately flat. The polyurethane foam method outlined by Skipper *et al*. (1998) was followed with slight modifications. A wooden board or plank was prepared by covering with cling film to create a non-stick surface onto which the polyurethane foam was sprayed. This was then pressed up against the section and held in place for approximately 5 minutes in order to allow the foam to begin to expand and to adhere to the surface. The board was then left in place for approximately 30 minutes until the foam had fully expanded and set. The peels were then pulled away from the surface and stored for transport back to the lab. Each peel took approximately 45 minutes to acquire. This method is also described in Barrett-Mold *et al*. (2009).

Peels obtained were then transported back to the lab where they were analysed stratigraphically. From the degree of detail retained on the peels it was possible to identify discrete stratigraphic units and draw schematic logs of the sections to a 2mm resolution. The units identified were recorded using a modified Troels-Smith scheme as described by Long *et al.* (1999). This involved four stages:

1. visually identifying discrete stratigraphic units and marking them with a pin;
2. recording the depth from the top of the section of the upper and lower boundaries of the unit;
3. an examination of the physical components of the unit, i.e. sedimentology and organic content;
4. an examination of the physical properties of the unit, i.e. degree of darkness and stratification.

Long *et al*. (1999) also record the degree of elasticity and dryness of the unit however this was not possible using the peel method due to the small amount of sediment collected.

3.3.3. Geochemistry

Organic content

The organic content of the sediment was determined via the loss on ignition method. The SFD3 and DYN1 cores were sampled at 1cm intervals, and 1g from each subsample was placed in a crucible and left to dry in a furnace set to 105°C overnight and the dried sediment weight recorded. The dried sediment samples were placed back in the furnace set to 550°C and kept at this temperature for 2 hours. The samples were removed and reweighed and the percentage of the dry weight lost on ignition (organic content) calculated.

$CaCO_3$ content

The remaining ash sample from the LOI was placed back in the furnace set to 925°C for 4 hours. The amount of carbon dioxide lost in this process, as carbonates are converted to oxides, is used to determine the original carbonate content. The difference between the ash weight and the weight lost at 925°C was multiplied by 1.36 (the difference between the molecular weights of CO_2 and CO_3) to calculate the carbonate content.

XRF

An understanding of the total concentrations of rock-forming elements within sediment can provide valuable information about the evolution of a system (Boyle, 2000). High resolution data are particularly useful when looking at century and decadal scale cyclic events and small scale structures within the sediment (Jansen *et al*., 1998).

X-ray fluorescence (XRF) is an elemental and chemical analysis method used in a variety of fields, e.g. metallurgy, ceramics, forensic science, archaeology and geochemistry. Within geochemistry, scanning XRF is a commonly used, non-destructive, method of logging the major element concentrations of split sediment cores. Jansen *et al.* (1998) believe the four main advantages of using scanning XRF analysis to be the very high resolution at which cores can be sampled, i.e. 1mm, enabling production of near continuous records; the quickness at which XRF measurements can be carried out; the method is non-destructive; and it provides data about the actual composition of the sediment.

The XRF method works by bombarding the sample with high energy X-rays causing the emission of fluorescent X-rays which are characteristic of the element they have been emitted from. The emitted fluorescent X-rays are counted to determine the various proportions of the different elements within the sample. In part, the response of the elements exposed to the X-rays depends on the different physical and chemical properties at the split core surface, such as density, surface roughness, matrix effects (absorption and enhancement), sediment composition, grain size and water content (Spofforth *et al*., 2008). As such the core surface is not ideal for

producing highly accurate XRF readings, however, Jansen *et al.* (1998) believe that the advantages of the method, as stated previously, merit its use in many situations.

The geochemical use of the scanning XRF method has primarily and traditionally been in the analysis of marine sediment cores (e.g. Jansen *et al*., 1998; Rothwell *et al*., 2006; Palike *et al*., 2001; Spofforth *et al*., 2008). Application of the scanning XRF method to coastal intertidal sediment cores is less common. Where the method is used it is often for the detection of heavy mineral contamination (e.g. Pirrie *et al*., 1997) or for looking at specific elements and their profile and behaviour throughout the sediment core (e.g. Rae, 1989)

Cores were split in half lengthways and were placed in an Avaatech XRF scanner. Readings were taken every 1mm with a count time of 45 seconds per sample point. Multiple runs were done at 30kV and 10kV in order to analyse a greater proportion of elements. Initial exploration of the XRF results revealed a number of sample points in which a the element counts were lower than elsewhere in the core, these are likely to be false results due to the scanner foot not making proper contact with the sediment surface due to surface roughness.

Discrete subsamples were also run through a non-scanning XRF in order to provide quantitative values to the compositional data and also as a control on the scanning XRF data. Subsamples from SFD 1, 2 and 3 and DYN1 and 2 were identified based upon the scanning XRF analysis. Subsamples were chosen where there were distinct peaks or troughs in the scanning XRF data and to provide a representative sample of the whole core. Subsamples were taken from the core on a 1cm scale due difficulties and inaccuracies associated with removing smaller samples and the need to obtain a sample greater than 2 grams for reliable analysis. The subsamples were freeze dried to remove moisture and then ground to a homogeneous powder in an agate pestle and mortar. Between 2 and 4 grams of each sample was then placed into an XRF pellet and the exact weight of the sample recorded ready for analysis.

Samples were analysed on a Spectro x-lab 2000 energy dispersive XRF spectrometer and sample percentages or proportions were measured for a total of 49 elements. 2 standards were run with each batch of samples to ensure consistency and accuracy; these consisted of a sediment sample of known composition.

3.3.4. Sedimentology

Particle size distributions

Laser diffraction is a commonly used method of obtaining particle size distributions. The method measures the refractive indices of light scattered by a sample in order to calculate the size of particle. Results are dependent on the refractive indices of the material and medium into which it is suspended; therefore the particle size distribution obtained depends critically upon assumptions made about the optical properties of the study materials (Wedd, 2003). The

conversion from the light scattering data to particle size distributions uses Mie theory which assumes all the particles are spherical (Campbell, 2003).

In this study, measurements were carried out using a Malvern MS2000 Laser Sizer with a Hyrdo2000 MU pump and cell; this enabled a size range of 0.02 to 2000μm to be measured. A standard operating procedure (SOP) was set up and used for all samples so the conditions of each measurement would be the same. A standard (24/013W) of known grain size composition was measured to ensure accuracy; there was found to be no significant difference between the known and measured values (p-value = 0.007). Initial examination of the sedimentology of the samples showed the majority of grains to be quartz sand grains, therefore within the SOP the particle refractive index of and particle absorption index for silica, 1.544 and 0.01 respectively, were entered for the conversion to grain size data calculations. The dispersant used was tap water and therefore a dispersant refractive index of 1.33 was entered into the SOP. An appropriate amount of sample was placed into 500ml of tap water until a suitable laser obscuration was reached (i.e. between 10% and 20%); this amount varied depending on the sample but was approximately 2g. The pump speed was set to 2000rpm and the ultrasonic stirrer used for 10 seconds to disaggregate the sample before measurements were taken. Three measurements of a count time of 30 seconds per sample were made with a 10 second gap between measurements. The output data is in the form of volume of sample between size classes.

The particle grain size fractions of the samples were analysed using GRADISTAT (Blott & Pye, 2001) to examine the grain size distributions, statistics and textural descriptions. The working unit for sediment size analysis in this study is phi (ϕ) as converting the geometric size scale to a arithmetic size scale via log transformation aids the statistical analysis of the sediment size distribution data (Hobson, 1979).

Grain size trend analysis

There have been numerous different methods applied to sediment data in order to characterise grain size distributions and attribute distribution mechanisms and potential sediment sources (e.g. Folk and Ward, 1957; Buller and McManus, 1972; Bui *et al*, 1990).

McLaren (1981) and McLaren and Bowles (1985) showed that the trend of sediment grain size properties as they progressively move further downstream from the sediment source must follow one of two cases:

1. Sediments at a downdrift site are better sorted, finer and more negatively skewed than at an updrift site.
2. Sediments at a downdrift site are better sorted, coarser ad more positively skewed than at an updrift site.

These two cases relate to transport directions for fining and coarsening sediments respectively. From this they developed a grain size trend analysis model that identifies the linear sediment transport direction and strength at individual sample sites based upon the relationships between mean grain size, sorting and skewness between sediment samples. This model was developed further by Gao and Collins (1992) to enable grain size trend analysis across a 2D surface, with particular thought to applying the model to coastal environments, such as tidal flats. The output of this model is a transport vector of particular strength for each sample point included in the analysis.

Particle size distribution modelling

Traditional descriptive grain size statistics of observed grain size, whilst effective in exploratory analyses, often fail to model the size distribution well enough to permit discrimination between sedimentary environments and sub-environments (Sutherland and Lee, 1994). The log-hyperbolic distribution has been shown to be a more suitable model of particle size distribution (Barndorff-Nielsen, 1977; Fieller *et al*, 1992). One of the benefits of applying this model is that the skewness (χ) and kurtosis (ξ) of the log-hyperbolic distribution can be calculated and plotted within the hyperbolic shape triangle (Figure 3.2). This allows the shape of a distribution to be visualised and individual samples and sample groups compared (Hartmann and Christiansen, 1992). However Hartmann and Christiansen (1992) suggest that the tilt parameter ($\rho = \chi/\xi$) is the best parameter to express the shape difference between samples. Barndorff-Nielsen and Christiansen (1988) defined an erosion-deposition model in which it is envisaged that erosion will move the χ,ξ position to the right hand side of the shape triangle and deposition will move the position to the left hand side.

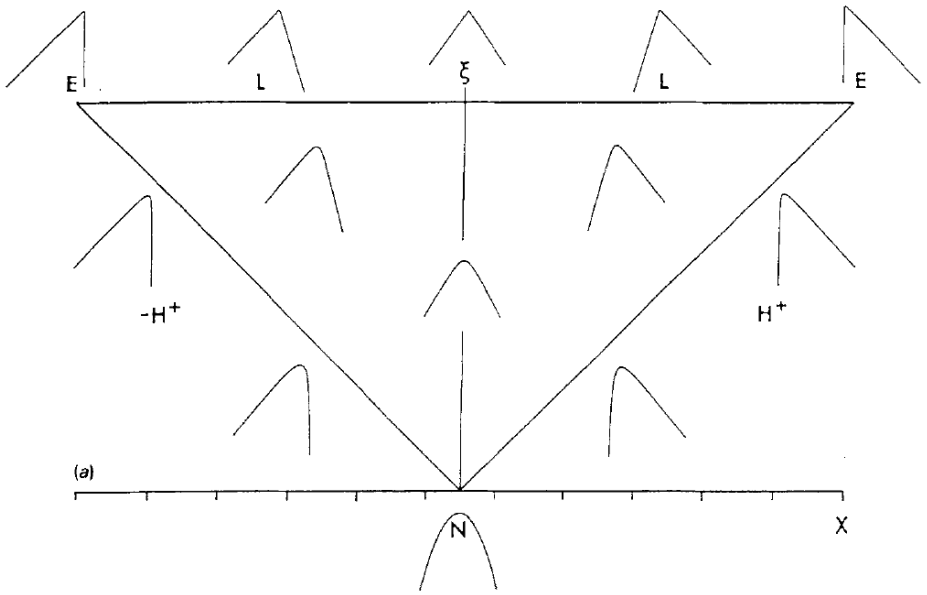

Figure 3.2 The hyperbolic shape triangle. Limit distributions indicated: N, Normal; L, Laplace; E, Exponential; H+ and H-, positive and negative Hyperbolic (interpreted as erosional and depositional sediment distributions, respectively) (Hartmann and Christiansen, 1992).

Fitting a four-parameter log-hyperbolic model involves significant additional computational effort (Julia and Vives-Rego, 2008). Consequently, Fieller *et al* (1992) presented the log-skew-Laplace distribution model as a simple but effective alternative. This model is more straight forward to compute yet has the flexibility to handle more complex problems. When fitted to dune and beach sediment samples from the Hebrides, Fieller *et al* (1992) found this model to be more effective at modelling their distribution than the log-hyperbolic model.

In this study, the *Shefsize* statistical program (Robson *et al*. 1997) was used to fit the log-hyperbolic, log-skew-Laplace and log-normal distributions to each downcore sample. The goodness of fit of each model was assessed using the modified chi-squared statistic *Ncrit* (Fieller *et al*, 1992).

Quartz grain microtextures

Work on the examination of quartz grain surfaces via scanning electron microscopy (SEM) by Krinsley and Takahashi (1962a; 1962b; 1964), Krinsley *et al.* (1964) and Krinsley and Funnell (1965) established the possibility of distinguishing between littoral (beach), aeolian (dune) and glacial environments on the basis of the surface textures generated on the grains. Subsequent works have proven it to be a valid method of determining the mode of transport and environment of deposition of sand grains (e.g. Madhavaraju *et al.*, 2009; Krinsley and Donahue, 1968; Coch and Krinsley, 1971). During the sedimentary history of a sand quartz grain a number of different mechanical and chemical processes will act upon the surface of the grain creating a variety of textures depending on the environment. Different impact features and

abrasion marks form on the quartz grains during transportation in different dynamic environments and features of chemical origin consist of various types of etching and overgrowth (Madhavaraju *et al.,* 2009). However, many textural patterns cannot be related to specific mechanical or chemical events. The features described in Table 3.2 are widespread and consistently present in specific coastal environments and considered to be reliable qualitative environmental indicators (Krinsley and Donahue, 1968).

Table 3.2 Summary of coastal quartz grain surface textures and their environmental interpretation (after Krinsley and Donahue, 1968; Krinsley and Funnell, 1965; Margolis and Krinsley, 1971)

Depositional environment	**Characteristic surface textures**
Littoral – high energy	V-shaped patterns, irregular orientation. Straight or slightly curved grooves. Blocky conchoidal breakage patterns. Chatter marks, a series of sub-parallel indentations (rare)
Littoral – Medium and low energy	En echelon V-shaped indentations (as energy level increases orientation becomes more random)
Aeolian	Meandering ridges. Graded arcs. Upturned cleavage plates.

Core subsamples were taken from depth locations identified via analysis of XRF profiles. A stratified random subset of surface sediment samples was taken to include sandflat and quadrat samples from Sandfield and Derryness and aeolian deposits on the sandflat at the base on the dunes adjacent to the Sandfield site. Approximately 0.5g of sediment was placed in a 63µm sieve and washed with distilled water in order to remove any silt or clay particles adhering to the sand grain surfaces and within the sample generally. The washed sample was left to dry. A suitable number of grains, i.e. so all exposed sides of the grain could be seen clearly, were then stuck onto an SEM stub using double-sided tape. The surface of the stub was gold plated prior to SEM analysis. 10 grains per sample were analysed and their surface textures documented and photographed.

3.3.5. Geochronology

Application of ^{210}Pb dating

Since its development in the 1960s, ^{210}Pb dating has primarily been used in establishing the chronology and accumulation rates of lake sediments within the time range of 1-150 years (Walker, 2005). The method has also been successfully applied to coastal environments with sedimentation rates ranging from millimetres to centimetres per year (e.g. Chanton *et al.,* 1983; French *et al.,* 1994; Cundy and Croudace, 1996). The method is based on the escape of radon

gas from the earth to the atmosphere; through the ^{238}U decay series this results in the production of the unstable isotope ^{210}Pb, with a half life of 22.6±0.22 years (Walker, 2005). This is removed from the atmosphere via precipitation, and in coastal marine waters it readily adsorbs to suspended particles which may be incorporated in the sediments (Kirchner and Ehlers, 1998) and subsequently decay to the stable form of lead, ^{206}Pb. The measurement of excess ^{210}Pb activity that is incorporated in to the sediment allows the calculation of accumulation rates (Cundy and Croudace, 1996). However all sediments contain varying amounts of supported ^{210}Pb as a result of the decay of ^{238}U series radionuclides in the sediment itself and therefore this has to be accounted for in the analysis of excess ^{210}Pb.

There are two models used for ^{210}Pb dating age calculations. The first assumes a constant initial concentration (CIC) of excess (unsupported) ^{210}Pb at each depth in the profile, irrespective of variations in sediment accumulation rates. The second assumes a constant rate of supply (CRS) of unsupported ^{210}Pb over approximately the last 150 years (Walker, 2005). The problem with the CIC method is variations in accumulation rate will influence the excess ^{210}Pb concentration and therefore lead to under or over-estimates of age; consequently the most applications use the CRS model (Walker, 2005). Sedimentation rates are therefore most commonly determined using the "simple" model (Robbins, 1978) described by Cundy and Croudace (1996) as "where the rate is given by the slope of the least squares fit for the natural log of the $^{210}Pb_{excess}$ activity plotted against depth."

Application of ^{137}Cs dating

^{137}Cs is an artificial radioisotope found in sediments as a result of atmospheric nuclear testing and discharge. Detectable concentrations can be found from 1954 onwards with a peak at 1963 and locally within northwest Europe in 1986 as a result of the Chernobyl accident (Walker, 2005). These peaks, identifiable in sediments, are often used to calculate sediment accumulation rates over the last few decades (Milan *et al.*, 1995), although the small amounts from 1954 may now no longer be detectable (Kirchner and Ehlers, 1998). Evidence of the fallout of ^{137}Cs from the 1986 Chernobyl accident can be found in sediment records across northern much of Europe and produce a peak much sharper than that of 1963 (Callaway *et al.*, 1996). Callaway *et al.* (1996) measured high ^{137}Cs activities associated with the 1986 peak in the sediment of a number of northern European saltmarshes and therefore conclude that given the half-life (30.0 years) this will serve as a valuable sediment marker for at least 50-60 years. They also believe it will be particularly useful for short-term sedimentation studies and comparisons of sediment process over different time scales. However, Kirchner and Ehlers (1998) believe the main shortcoming of basing a sediment chronology on a few point markers is that is makes little use of the information within the ^{137}Cs distribution, in particular changes in sedimentation rates. However these problems are overcome when using ^{137}Cs geochronology in combination with other

methods such as ^{210}Pb, as the ^{137}Cs peak dates can then be used as time markers on which to place the accumulation rate data from the ^{210}Pb analysis.

There are problems with ^{137}Cs dating associated with the mobility of the isotope which is much greater than that of lead (Foster *et al.,* 2006). This mobility can result in a "tail" of activity which extends to some depth below that of the 1954 first occurrence, although in many cases the 1963 peak tends to remain reasonably well fixed (Foster *et al.,* 2006). Bioturbation of sediment by root growth or invertebrate feeding may cause vertical movement of the isotope and as a result decrease the accuracy of data collected (Milan *et al.,* 1995). ^{137}Cs is absorbed more strongly by smaller particles, particularly clays; therefore it is not possible to obtain a geochronology based on ^{137}Cs unless a suitable proportion on the sample is within the clay fraction.

Method for ^{210}Pb and ^{137}Cs analysis

Core sub-samples from SFD3 and DYN1 were sent to the laboratories of the University of Brighton, School of Environment and Technology for standard ^{210}Pb and ^{137}Cs analysis.

Core sub-samples were counted on a Canberra well-type ultra-low background HPGe gamma ray spectrometer to determine the activities of ^{210}Pb, ^{137}Cs and other gamma emitters. Spectra were accumulated using a 16K channel integrated multichannel analyzer and analysed using the Genie 2000 system. Energy and efficiency calibrations were carried out using bentonite clay spiked with a mixed gamma-emitting radionuclide standard, QCYK8163, and checked against an IAEA marine sediment certified reference material (IAEA 135). Detection limits depend on radionuclide gamma energy, count time and sample mass, but were typically *ca.* 15 Bq/kg for ^{210}Pb, and 5 Bq/kg for ^{137}Cs, for a 150,000 second count time. Core samples with very low activities received extended count times of up to 350,000 seconds.

The $^{210}Pb_{excess}$ activity in core SFD3 was estimated by subtraction of the ^{210}Pb activity in deeper core sections (6 Bq/kg) (e.g. Cundy and Croudace 1996). Sediment accretion rates were determined using the "simple model" of ^{210}Pb dating (e.g. Robbins 1978), where the sedimentation rate is given by the slope of the least squares fit for the natural log of the $^{210}Pb_{excess}$ activity versus depth. Data for the naturally-produced radionuclide ^{214}Pb were also included. ^{214}Pb can be used as an approximate indicator of the supported ^{210}Pb activity, and large-scale variations in its activity-depth distribution may indicate significant changes in sediment composition with depth.

Optically stimulated luminescence

The optically stimulated luminescence (OSL) method is often used to determine when quartz rich sediments were last exposed to daylight. It can therefore be an effective method for determining burial/deposition age (Murray and Olley, 2002). Ionisation of quartz and feldspar

minerals is induced when they are exposed to radiation from surrounding naturally occur radionuclides within the sediment matrix, and from cosmic rays. This charge is released by heating (thermoluminesense) or by exposure to light (OSL) (Madsen *et al*, 2005). OSL effectively empties the sediment of charge during transportation; this is termed resetting, zeroing or beaching (Madsen *et al*, 2005). The time period since the sediment was deposited can be calculated by determining the amount of charge which has built up in the sediment since burial (Rhodes, 2011). It is therefore important that grains are fully bleached for an accurate age to be determined. Quartz is the most commonly used mineral in OSL dating due to the faster bleaching time than that of feldspar (Madsen *et al*, 2005).

OSL dating has several advantages over ^{210}Pb and ^{137}Cs dating as these methods are restricted to sediments younger than 120 and 50 years respectively and generally to fine grained muddy sediments. However, within the intertidal environment incomplete bleaching can be a problem for determining an OSL date. Water and higher levels of turbidity attenuate the UV end of the spectrum therefore reducing bleaching rates; this can result in overestimating the burial age (Rhodes, 2011; Madsen *et al*, 2005).

The most common measurement procedure used to determine burial age is the single aliquot regenerative-dose (SAR) protocol (Rhodes, 2011) due to its accuracy and reliability (Murray and Olley, 2002). Using SAR, OSL dates may be obtained for single quartz grains and problems with incomplete bleaching recognised (Rhodes, 2011).

Method of OSL analysis

Two samples were collected in opaque sample tubes from known depths immediately beside the DYN1 and SFD3 sample points. Precautions were taken not to expose the sample to any light source both during collection and transportation. The samples were sent to the Sheffield Centre for International Drylands Research (SCIDR) luminescence laboratory where all luminescence work was carried out.

The samples were prepared under subdued red lighting following the procedure to extract and clean quartz outlined in Bateman and Catt (1996). Prepared aliquots of the samples were taken from a size range between 90-250 μm with the exact size range utilised varying according to the abundance of quartz and the dominate grain size. All prepared quartz was mounted as 9.6 mm diameter aliquots onto 9.6 mm diameter disks for measurement. The purity of the quartz extract was checked using infrared stimulated luminescence and no feldspar contamination was seen. All OSL measurements were carried out using an upgraded DA-15 Risø luminescence reader fitted with blue LEDs for stimulation. OSL was measured through a Hoya-340 filter in placed in front of the photomultiplier tube. Samples were dosed using a calibrated ^{90}strontium beta source. All samples were analysed using the single aliquot regenerative (SAR) approach (Murray and Wintle 2000, 2003), in which an interpolative growth curve is constructed using data derived

from repeated measurements of a single aliquot which has been given various laboratory irradiations. The last irradiation dose replicated the first to check if sensitivity changes cause by repeated measurement of the same aliquot had been correctly monitored and corrected for by the SAR protocol. All aliquots where the ratio of first and last dose point exceeded ±10% of unity were excluded from further analysis. The most appropriate preheat temperature for each sample was selected using a dose recovery preheat plateau test. Results of this test were scattered with no systematic trend of palaeodose with preheat temperature. This resulted in selection of preheat temperatures of 160 °C for 10 seconds, which were applied to each sample prior to OSL measurement to remove unstable signal generated by laboratory irradiation. Given the weak OSL signal of the samples, poor recycling and a tendency to over-estimate palaeodose, a hot bleach (OSL for 80s at 260°C) was introduced into the SAR protocol to mitigate this.

Radiocarbon dating was not considered appropriate for these core samples due to the very low organic contents throughout the cores.

3.3.6. Diatoms

The presence and diversity of diatom species in coastal and freshwater wetland environments makes them a valuable indicator of past and present environments and conditions. Consequently, diatom analysis is a well established palaeoecological method used in resolving the sedimentary conditions of marine, coastal and freshwater deposits (Denys, 1994). Diatom analysis is frequently used either on its own or in combination with other environmental proxies in the determination of Holocene sea level changes and coastal morphological and sedimentological evolution (e.g. Vos and de Wolf, 1994; Shennan *et al.,* 1995; Plater and Shennan, 1992; Hemphill-Haley, 1995).

Diatoms are found wherever there is moisture and sufficient light for photosynthesis; however, habitats vary significantly depending on the chemical and physical properties of the environment. As a result each habitat supports a specific and characteristic flora which once defined can be used to identify that habitat (Hendey, 1964).

In the littoral zone the diatom flora is to a large extent determined by the properties of the substratum, e.g. rocky platforms are only able to support those species which can physically attach to the surface whereas sand and mud flats can also support species which lie as a film across the surface (Hendey, 1964). The other factors influencing the distribution of intertidal diatom species include the strength of wave action, nutrient supply, temperature, pH, salinity, vegetation, exposure to sunlight and competition with other organisms (Battarbee *et al.*, 2001; Roe *et al.,* 2009). Diatoms are regarded as very sensitive indicators of salinity (Freund *et al.,* 2004) and are often used to record palaeoenvironmental changes in salinity and tidal exposure

(Vos and de Wolf, 1993a). A number of studies have looked at the effect of altitude within the tidal frame on the distribution of diatom species, with the view of enabling reconstruction of tidal levels through the zonation of characteristic species (e.g. Nelson and Kashima, 1993; Hemphill-Haley, 1995; Shennan *et al.*, 1995; 1996; Zong and Horton 1999). Zong (1997) identified four diatom groups related to altitude within the tidal frame (Table 3.3).

Table 3.3 Description of diatom groups identified by Zong (1997) (Zong, 1998).

Diatom Group	Position within the tidal frame	Species types	Life form	Typical species
Sand-mudflat	Between the local MHWST and MHWNT or lower	Diverse marine and brackish	Epipelic and episammic, often with high numbers of marine planktonic	*Delphineis surirella, Diploneis smithii, Navicula flanatica, Nitzschia navicularis, N. sigma Actinoptychus senarius, Cyclotella striata, Odontella rhumbus, Paralia sulcata,*
MHWST	Low marsh around the local MHWST level	Brackish and salt-tolerant freshwater	Epipelic, episammic and epiphytic, low number of marine planktonic	*Diploneis interrupta, Navicula peregrina, N. cryptocephala*
Midmarsh	Transition between high and low marshes	Salt-tolerant freshwater with some brackish and aerophilous	Epipelic, episammic and epiphytic	*Navicula halophila, N. pusilla*
HAT	Top end of the tidal frame, high marsh occasionally flooded by abnormal tides	Mainly freshwater, including some salt-hating and aerophilous	Epipelic, episammic and epiphytic	*Navicula mutica and Cymbella spp., Eunotia spp., Pinnularia spp., Tabellaria spp*

Vos and de Wolf (1993a) proposed a method for diatom analysis in which each diatom species encountered is given an ecological code determined from seven key factors and their subcategories:

1. Life form

   Plankton, tychoplankton, epiphytes, benthos epipelon, benthos episammon or benthos aerophilous

2. Salinity

   Polyhalobous, mesohalobous, oligohalobous halophilous, oligohalobous indifferent or halophobous

3. pH spectrum

   Alkalibiotic, alkaliphilous, indifferent, acidophilous or acidobiotic

4. Nutrient content spectrum

   Eutrophic, meso-eutrophic, mesotrophic, meso-oligotrophic or oligotrophic

5. Temperature

   Warm, temperate or cold

6. Tides

   Pseudo-ampotiphilous, tide-indifferent or ampotixen

7. Current

   Rheophilous, indifferent or limnophilous

Vos and de Wolf (1993a) were able to place the classified diatoms into ecological groups for palaeogeographical reconstructions. Vos and de Wolf (1993b) related these groups to different near-shore palaeo-sedimentary environments in order to describe palaeo-salinity and palaeo-tidal changes and reconstruct sedimentary environments. Zonation of littoral diatoms can therefore provide important information relative sea level and environment and mode of deposition of the sediment.

An advantage of using intertidal diatoms as a proxy for environmental and sea-level conditions, and in particular those inhabiting mud flat surfaces is that they tend to be present throughout the year (Hendey, 1964). This increases their usefulness as an environmental proxy as it negates the problems associated with species migration as seen in other indicator species such as foraminifera (Roe *et al.,* 2009). The siliceous cell walls of diatoms generally fossilize well (Vos and de Wolf, 1993a) and as a result are a valuable palaeo-environment indicator. However, the issue of the accuracy with which diatom assemblages in sediments represent the composition of the source communities from which they were derived is raised by Battarbee *et al.* (2001); they state that in some extreme cases some diatom species are completely absent from the sediment record due to dissolution problems. Although this research is based upon lake diatoms, where preservation is largely determined by the pH of the lake, dissolution may also occur in marine sediments. In the coastal environment one of the main problems is distinguishing between autochthonous and transported, allochthonous species (Freund *et al.,* 2004). This is particularly important in the estuarine and tidal environments were zonation based upon this distinction is of major importance. Freund *et al.* (2004) have used the percentage of broken diatom frustles as an indication of the amount of transportation they have been subjected to and also the energy level of the environment. They also state that the presence of fragile species indicates they have lived at the place of deposition, and therefore, are a better indicator of palaeoenvironment than the more heavily silicified species.

In this study 5mls of 30% H_2O_2 was added to a test tube containing approximately 0.1g of wet sediment. This was placed in a water bath at room temperature if the sediment did not react violently the temperature was increased to 80°C and left for 2-4 hours until all organic material had been removed. The tubes were then removed from the bath and 1-2 drops of 50% HCL

added to eliminate any remaining H_2O_2 and any carbonates. The tubes were centrifuged at 1200rpm for 4 minutes and the supernatant decanted off, they were then topped up with distilled water and the washing process repeated at least 3 times.

The cleaned diatom suspension was diluted to a suitable concentration before being pipette onto a cover slip and left to dry. 1 drop of Naphrax was placed onto a glass slide and the cover slip inverted and placed onto the drop. The slide was then heated on a hotplate at 130°C for 15 minutes then allowed to cool.

Diatoms were identified according to Hendey (1964) and Krammer and Lange-Bertalot (1986, 1988, 1991a, 1991b). The valves were counted under phase contrast illumination at x1000 magnification. To obtain data on the relative abundance diatom frequencies are expressed as percentages of total diatom valves counted (TDV). A minimum of 200 valves were counted per sample.

3.3.7. Regional climate

Tidal

Information on the regional tidal regime was obtained from the Marine Institute's tide gauge network. 6 minutely water level observation data was retrieved for the Killybegs and Malin Head tide gauges from 1st Jan 2009 to 10th June 2011.

Wave

Information on the regional wave patterns was obtained from the Marine Institute's Databuoy (M4) off the northwest coast of Ireland. Hourly data on wave height and wave period was retrieved.

Wind

Information on the regional wind patterns was obtained from the Irish Metrological Office. Hourly wind direction and magnitude data was retrieved for the Belmullet and Malin Head stations from 16th October 1956 to 31st December 2009.

3.3.8. Maps and aerial images

Historical maps from 1850 and 1907, aerial photographs from 1951 and 1977 and satellite images from 1995, 2000, 2005 and 2009 were obtained for the area containing the Sandfield and Derryness sites (see Appendix 1 for sources). These images were digitised using ArcGIS 9.3 to allow analysis within the GIS.

The errors associated with GIS analysis are a combination of inaccuracies resulting from the georeferencing of maps and aerial photos which in this environment is more difficult due to the lack of permanent static landmarks to reference to. The root mean squared error (RMSE) was at

maximum 5m for all the maps and aerial photos georeferenced in this study. The error associated with the hand held GPS was approximately 5m whereas for the differential GPS it was approximately 15cm. There are also inaccuracies to take into account when comparing the historical map data with aerial photos and present day measurements as the map data will be simplified to some extent and boundaries recorded on the map are more likely represent landform feature edges rather than vegetation edges. Therefore in all subsequent analyses of boundary change an error of ± 20m has been used where definitive vegetation boundaries cannot be identified and of ± 10m where vegetation limits can be delimited.

3.4. Datasets

Table 3.4 summarises the datasets collected as a result of the methods used in this study and described above. The following analyses use these data to describe and interpret both the present day environmental characteristics and also the stratigraphic record of the Sandfield and Derryness sites.

Table 3.4 Summary of data sets collected

Data set	Location	Sampling method	Variable measured	Data type
Scanning XRF	All cores	Scanning XRF every 1mm down-core	Al, Si, P, S, K, Ca, Ti, V, Cr, Mn, Fe, Zn, Br, Sr, Zr, Mo, Pb, B.	Counts per area per element.
Sample pellet XRF	All cores	1cm subsamples of cores	49 elements	Element percentage of proportion of sample composition
Organic and carbonate contents	Sandfield and Derryness sandflats and vegetated surfaces. Cores SFD3 and DYN1	Sand flat and vegetated surface sample points, 1cm subsamples of cores	Sample weight loss on ignition and at 950°C	Percentage organic and carbonate content
Grain size distributions	Sandfield and Derryness sandflats and vegetated surfaces. Cores SFD3 and DYN1	Sand flat and vegetated surface sample points, 1cm subsamples of cores	Grain size	Percentage frequency distributions
SEM	Surface samples, cores SFD3 and DYN1	Selected surface and core sub samples	Quartz grain surface microstructures	Presence/absence of different structures.
Vegetation	Sandfield and Derryness vegetated surface	1x1m quadrat at vegetated surface sample points	Plant species	Percentage cover
Palaeoecology	Vegetated surface samples, cores SFD3 and DYN1	All surface sample points, selected core sub samples	Diatoms	Species counts per sample
Tidal	Rosbeg	Ceradiver tide gauge, recording every 5mins	Pressure	Pressure variations
Wind	Magheramore Dunes	Davis weather station, recording every hour	Wind speed and direction	Wind speed and direction variations

4. Contemporary geomorphology, sedimentology and ecology

This chapter assesses the present day physical and environmental factors influencing the Sandfield and Derryness study sites. The aim is to provide a detailed classification of the sites based upon their geomorphological, sedimentary and ecological features and provide a detailed assessment of the present day environment that can be used as a benchmark against which to compare this study's subsequent stratigraphic analyses.

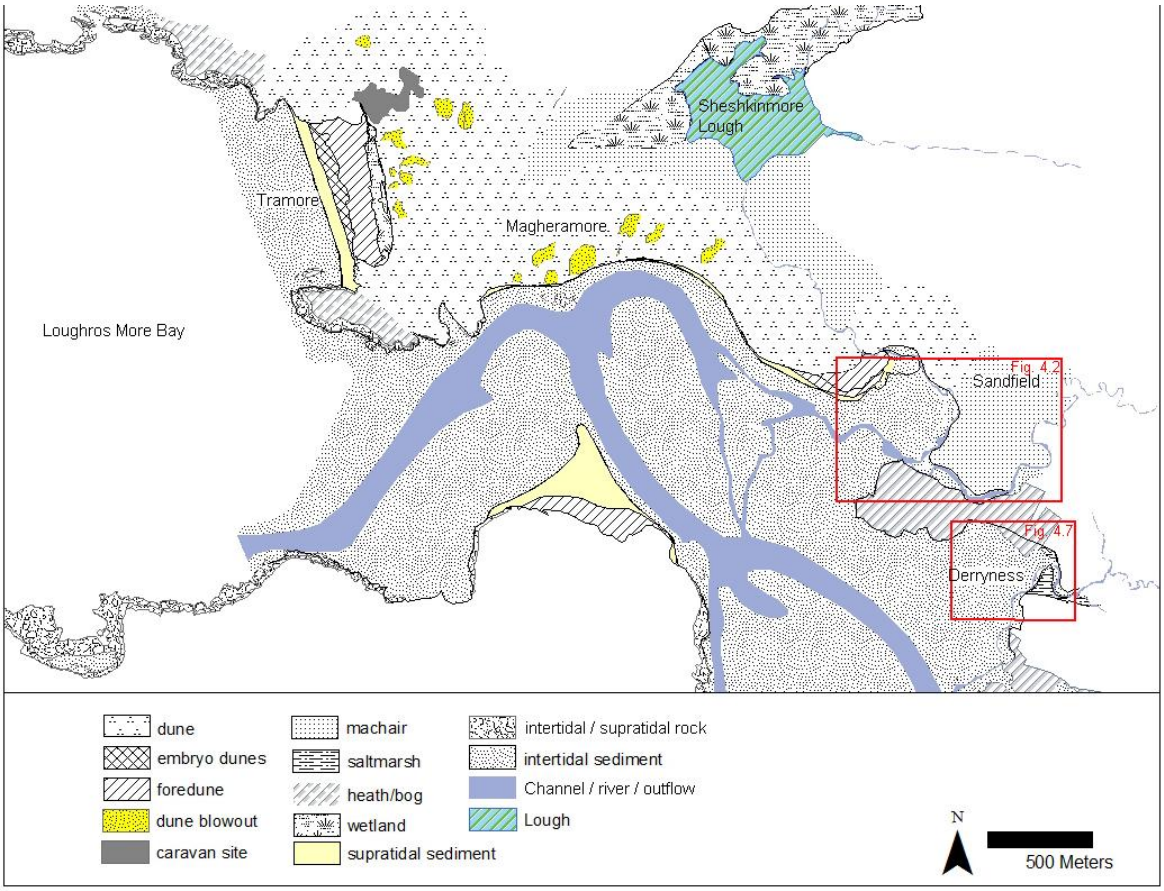

Figure 4.1 Overview map of sites and place names referred to in this chapter.

4.1. Physical features

4.1.1. Sandfield

The Sandfield site is comprised of an 18.4ha vegetated surface with an elevation about 1 – 1.5m above the adjacent tidal flat (Figure 4.1). It is bounded to the north by low dunes which form the easterly extent of the Magheramore – Tramore dune system. To the east and south the vegetated surface is bounded by the Bellanagoal River (Figure 4.2). To the west is a very shallow low tide channel that drains from Sheskinmore Lough to the north, through dunes. This channel joins the Bellanagoal outflow to the south west of the site. Whilst the majority of the raised surface is vegetated, there are some unvegetated patches, notably in the south west of the site where

disturbance (possibly turf cutting, recreation and grazing) has degraded the surface integrity (Figure 4.2).

The drainage network across the vegetated surface is poorly developed. There is one main channel from the centre of the site to the southeast margin where it joins the river channel (Figure 4.2). This main channel is predominately straight (i.e. no meanders) and has no tributaries or offshoots. The channel is 0.5m – 0.8m in depth and between 0.5m and 1m wide for the majority of its length, increasing to 2m wide at the mouth. There is a second, smaller channel, to the south of the site. This is much more convoluted than the main channel and is approximately 0.5m in depth and width. In addition to the drainage channel there are also a number of depressions across the surface ranging in depth from a few cm to 30cm; these are vegetated and flooded (standing water) to varying degrees. The major surface depressions are shown in Figure 4.2. However, there are many smaller depressions which occur over the majority of the eastern half of the site.

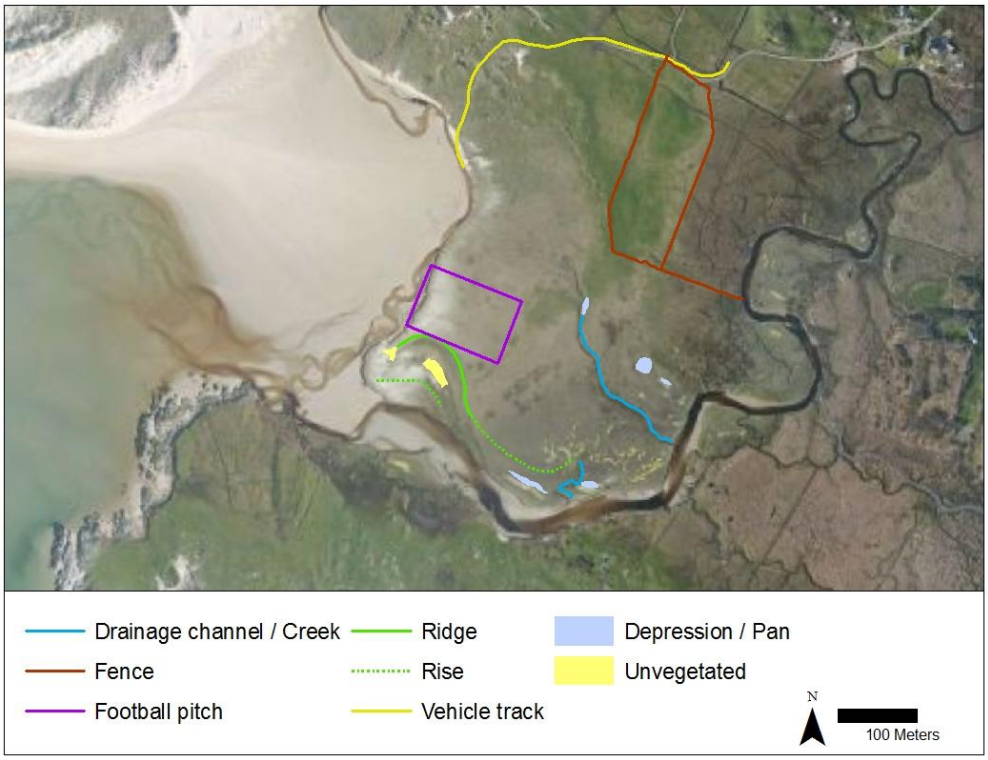

Figure 4.2 Physical features of the Sandfield environment

Over the majority of the vegetated surface variations in elevation are small and gradual (Figure 4.3). There is an overall gradual rise of approximately 70cm to the north where it grades into dunes (Figure 4.4). There is also a slight rise of about 50cm from east to west across the site; topography is more variable across this southern part of the vegetated area (Figure 4.4). A noticeable acute ridge is present in the southwest of the site leading into a 10cm stepped rise that runs round to the south of the site (Figure 4.2, Figure 4.6). This ridge may be related to a previous meander of the river running along the southern margin.

Using the DEM and local tide data the hydroperiod of the vegetated zones was calculated and is represented here as a proportion of time (i.e. number of days of flooding per 365 days). In the context of the tidal frame the elevation of vegetated surface at Sandfield means that the majority of the surface is tidally flooded for 5 days or less per year (Figure 4.5). Only the lower lying areas along the southern margin of the site are flooded more frequently than this, with the areas containing the majority of the surface depressions likely to flood between 15 and 20 days per year.

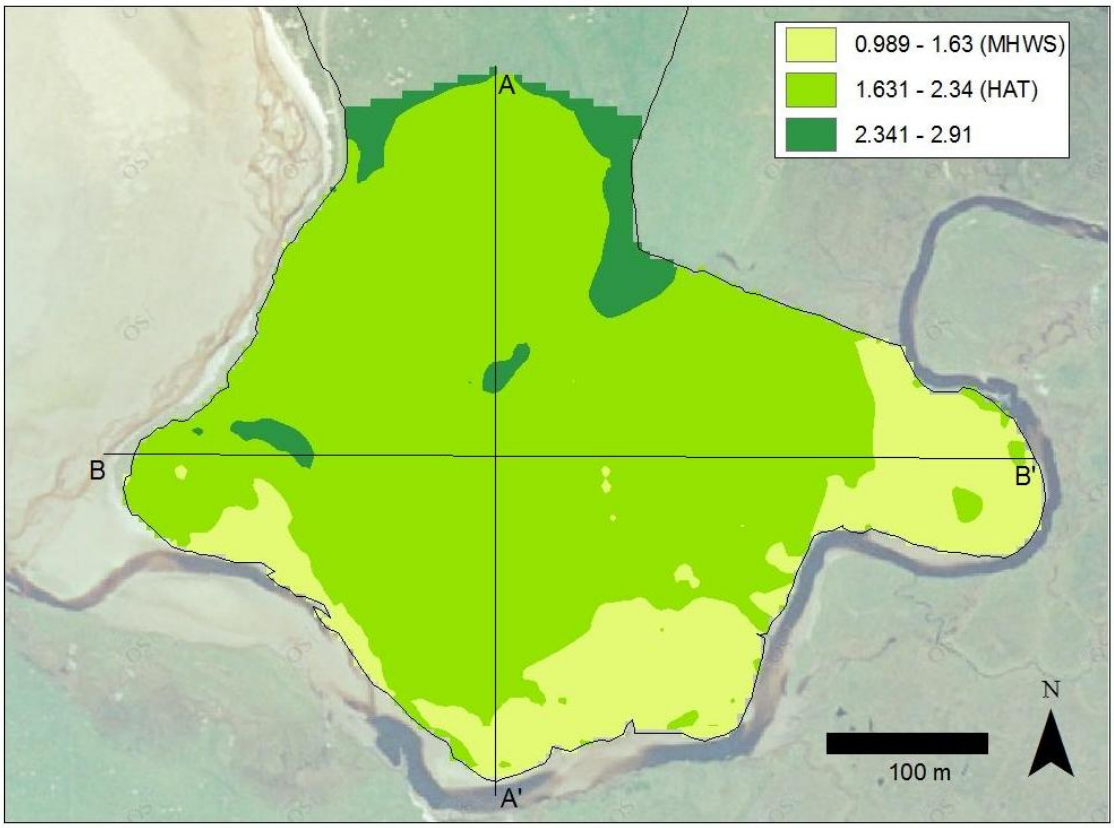

Figure 4.3 Digital elevation model (DEM) of Sandfield (elevations shown in mOD).

The edge of the vegetated surface is characterised by a steep, cliffed rise from tidal flat / low tide channel to vegetated platform. On these margins vegetated blocks of the collapsed surface form a ramp up against the present day intact surface as the substrate below has been undermined (Figure 4.6). Eroded blocks dominate the west boundary between tidal flat and vegetated platform, but reduce in number and extent to the north, and disappear entirely to the south (Figure 4.6). Allen (1989) describes a similar occurrence of cliffed margins and eroded blocks in the sandy salt marshes of the Solway Firth and Morecambe Bay estuaries. In these instances Allen (1989) determined that the sandy nature of the sediment is the main control on the mechanism of cliff failure. The relatively non-cohesive sands below the root-strengthened vegetation mat are susceptible to wave erosion at high tide. This undercutting eventually leads to cantilever and beam type failure and collapses along subvertical shears and the creation of cobble to boulder sized eroded blocks and the base of the cliff.

At Sandfield the fallen vegetated blocks are dynamic over seasons and years. Between April 2008 and July 2010 many of the blocks in front of the western margin were removed, causing further recession of the microcliff and a steeper cliffed edge. This was also associated with the introduction of greater amounts of wind blown sand both onto the sand flat adjacent to the vegetation and on the surface along the western margin of the site (Figure 4.6).

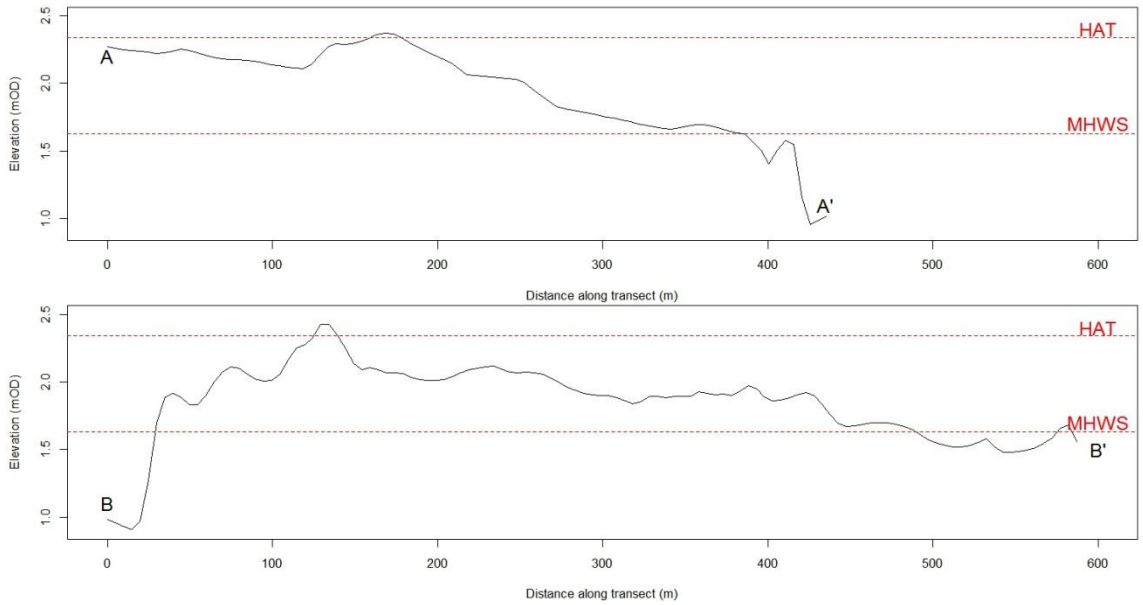

Figure 4.4 Sandfield elevation profiles (see Figure 4.3 for transect locations).

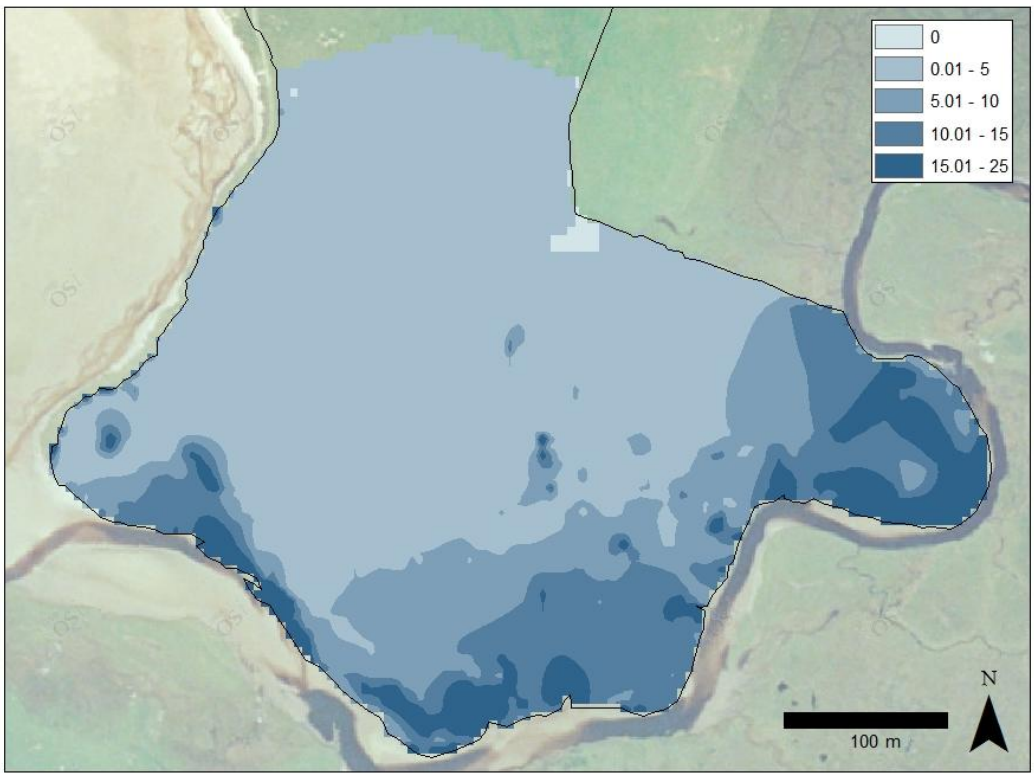

Figure 4.5 Sandfield hydroperiod map (values indicate number of days per year the area is tidally flooded).

Figure 4.6 A) View northwest across Sandfield along the southern margin with Bellanagoal River. The small surface depression shown is approximately 1m across. The ~10cm stepped rise can also be been (Apr 2008). B) View south at Sandfield along the western margin with the Sheskinmore Lough outflow. The ramping effect of the eroded vegetated blocks can be seen: vegetated blocks here are approximately 50cm x 80cm and some may be over 1m in length (Apr 2008). C) View south at the western margin of Sandfield showing the removal of many of the eroded vegetated blocks and the deposition of wind blown sand along the margin (May 2010).

4.1.2. Derryness

Derryness is located just to the south of Sandfield (Figure 4.1). Here, two vegetated systems occupy the high intertidal zone either side of a small river input to the estuary (Figure 4.1). To the south of the small river is a 1.4ha vegetated surface, with a similar appearance to Sandfield, which lies 1 – 1.5m above the tidal flat. This area is bounded to the east, north and west by a small river / low tide channel (Figure 4.7); to the south a rise in elevation and a fallen stone wall forms the boundary with agricultural grazing land. North of the small river the tidal flat rises gradually to a 3ha area of vegetated sand flat formed along the southern edge of Derryness Point. This bedrock, sand covered promontory, separates Derryness from Sandfield to the north. This area is bounded to the north by a fence separating it from higher elevation agricultural grazing land on the promontory (Figure 4.7). Vegetation cover is more continuous over the elevated surface than the vegetated flat which appears to be in the initial stages of colonisation.

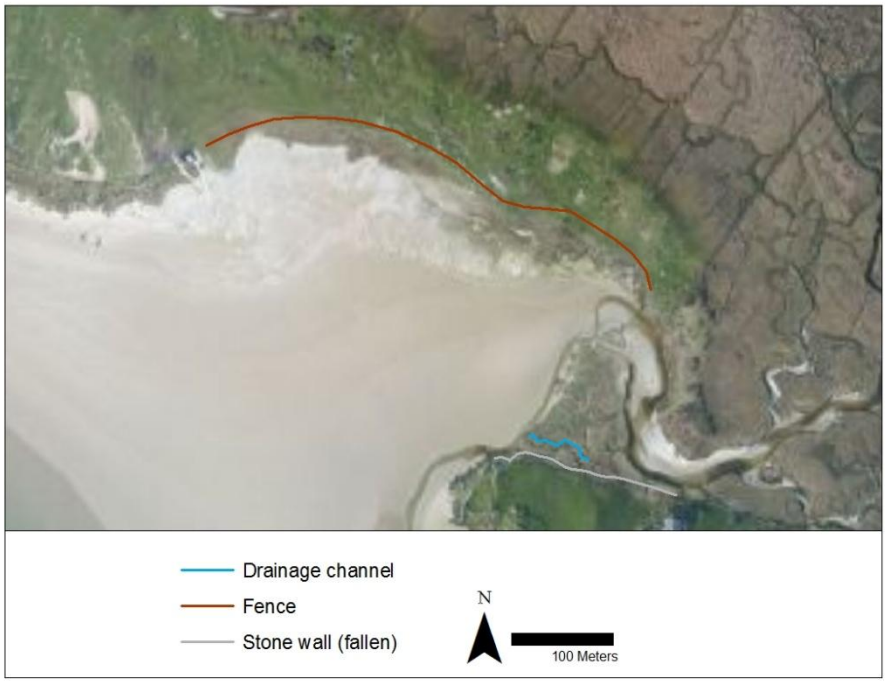

Figure 4.7 Physical features of the Derryness environment

As at Sandfield the drainage network is poorly developed across the vegetated systems. Within raised vegetated surfaces there is a channel at the southern end adjacent to the stone wall running from the middle of the site to the western edge. This channel is approximately 1m deep and wide. There is also a channel running across the northern tip of the elevated section effectively creating an island at the northern point of the site, although this channel has little effect on the drainage of the site (Figure 4.7, Figure 4.11).

Across the southern vegetated area there is little variation in the elevation and no surface depressions or ridges such as those seen at Sandfield (Figure 4.8, Figure 4.9). However, as at

Sandfield, there is a ~1m cliffed step between the intertidal flat and the vegetated zone. Along the western margin eroded vegetated blocks are ramped up along the edge of the site (Figure 4.11). To the north the vegetated sandflat rises from approximately 1.3mOD to 2.6 – 3mOD where it joins agricultural land (Figure 4.8, Figure 4.11); the steepness of this slope increases significantly toward the back of this area (Figure 4.9).

The raised surface at Derryness lies lower in the tidal frame compared to that at Sandfield, the majority of this site flooding between 5 and 10 days per year (Figure 4.10) with slightly less frequent flooding in the south eastern corner (0 to 5 days per year). The island on the northern tip of this area floods more frequently, the majority flooding between 40 and 80 days per year. The majority of the vegetated sand flat in the north of the site is comprised of an area of steeper slope towards the back of the vegetated area and this only floods 0 to 5 days per year. More frequent flooding occurs on the flatter section and the front and eastern margin of the area flood regularly (between 40 and 80 days per year; Figure 4.10).

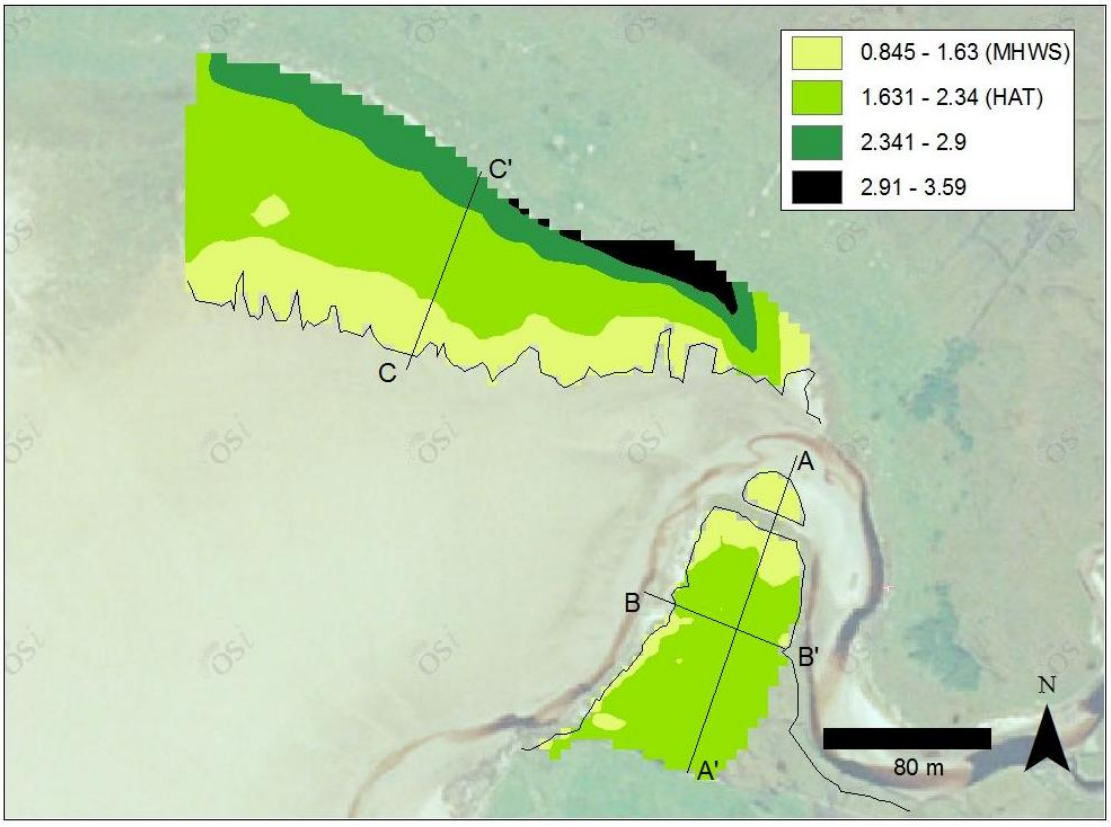

Figure 4.8 Digital elevation model (DEM) of Derryness (elevations shown in mOD).

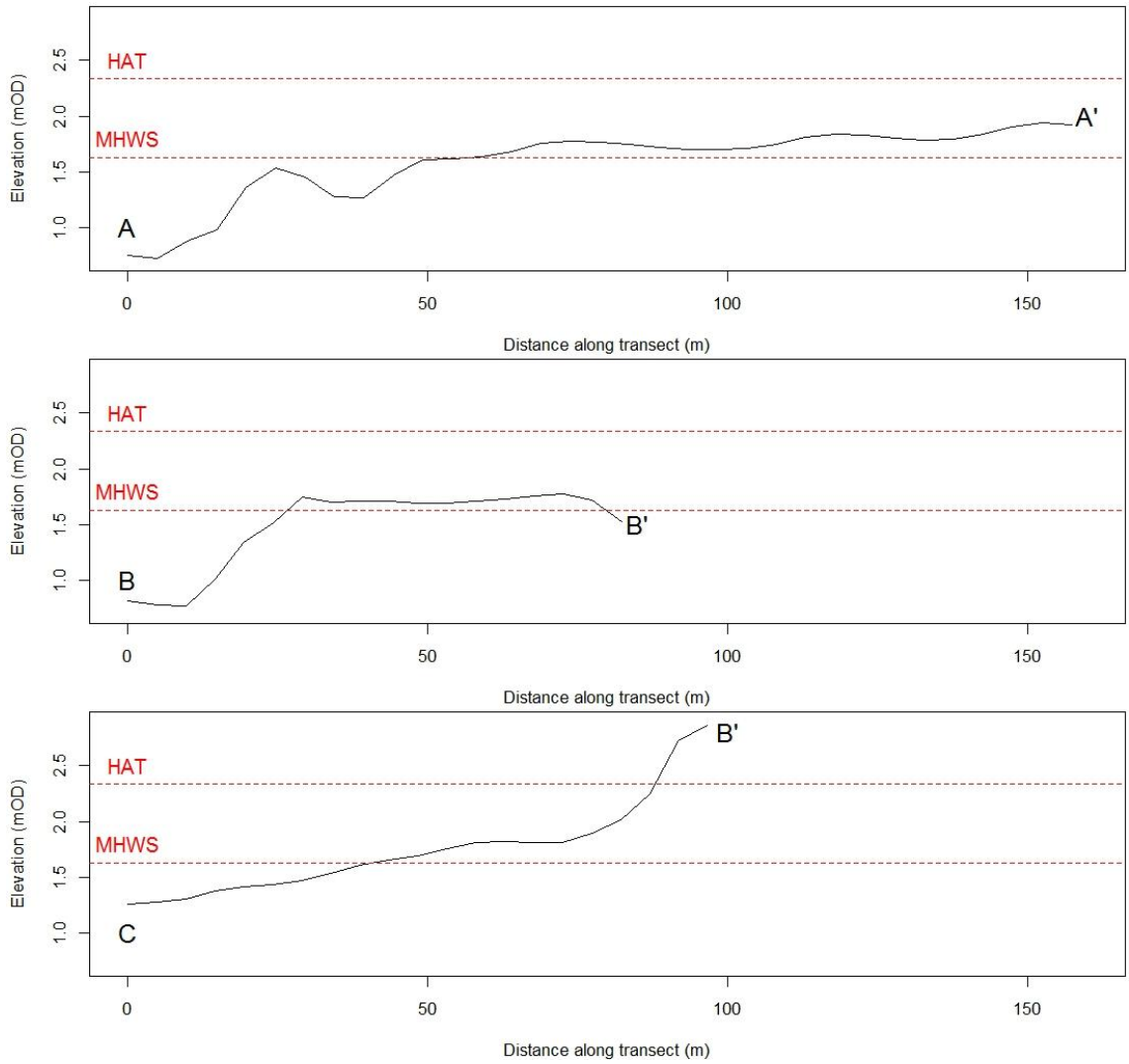

Figure 4.9 Derryness elevation profiles (see Figure 4.8 for transect locations).

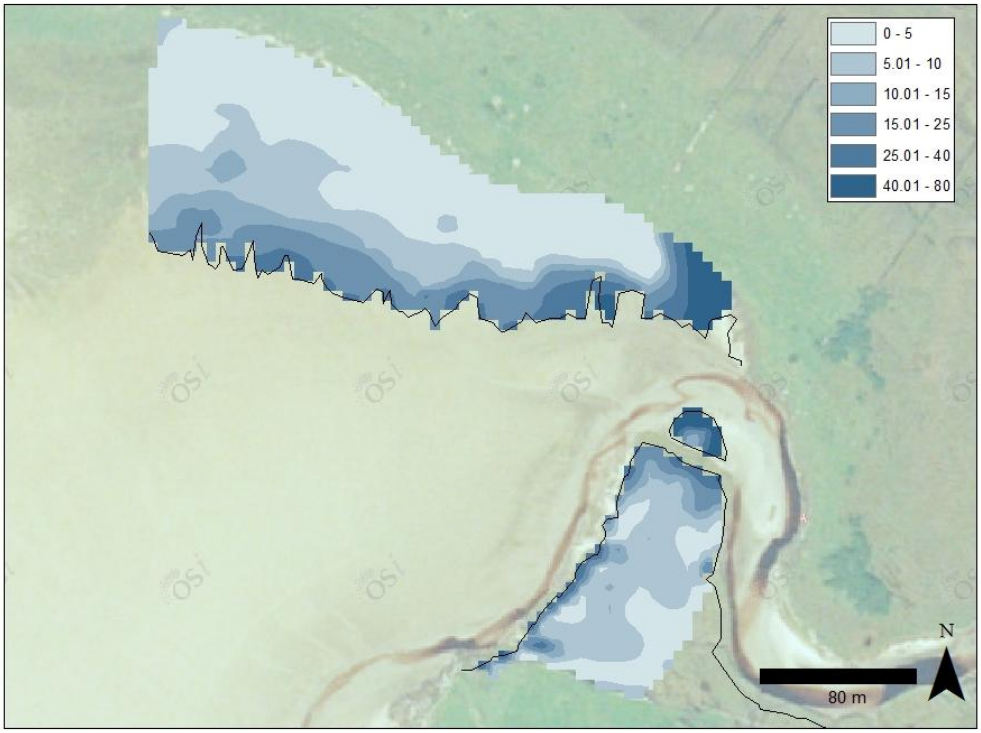

Figure 4.10 Derryness hydroperiod map (values indicate number of days per year the area is tidally flooded).

Figure 4.11 A) View south along Derryness raised surface western margin showing eroded vegetated blocks forming a ramp along the margin, blocks are approximately 50cm in width and up to 2m in length (Apr 2008). B) View north at Derryness showing island at northern tip of the raised surface and vegetated sand flat behind (May 2010).

4.2. Historical geomorphology

The geomorphological history of the study sites was ascertained from a GIS analysis of historical maps and aerial photographs, covering the mid-1800s to present. Historical vegetation limits were delineated, surface features identified and morphological change determined. Wherever possible vegetation limits have been used to define site edges and boundaries.

4.2.1. Sandfield

There has been a large amount of localised morphological change at Sandfield (Figure 4.12) the majority of which has taken place along the western boundary between vegetated surface and tidal flat. There have been two phases of change between 1850 and the present day; firstly a period of progradation between 1850 and 1977 and secondly a period of retreat between 1977 and the present day.

Site boundaries defined from the maps and aerial photos between 1850 and 1977 indicate the maximum growth on the western edge being 200m ±20m (Figure 4.12). The 1850 map indicates that at this time the westerly edge of the site was fronted by sand dunes extending down from the main Magheramore dune system to the north of the site (Figure 4.12). Mobile foredunes would provide a sediment supply to enable the rapid expansion seen in this portion of the site. These dunes are not drawn on the 1907 map but the latter does indicate that the western half of the site is sandier than the eastern half. The 1951 aerial photo shows no distinct dune forms on the western edge. However, there is a large area of exposed sand extending 90m further west from the edge of the vegetated surface raised above the level of the sand flat which appears to be a deflated feature. It is therefore possible that the Sandfield site extended a further ~90m west from the 1951 vegetation boundary equating to a progradation of approximately 300m ±20m from 1850. The Sheshkinmore Lough outflow is not drawn on the 1850 map; this maybe due to insignificant low flow at the time the map was drawn or the river may have had a different course through the dunes to the north west of the site. The Sheshkinmore Lough outflow channel is, however, present on the 1907 map. At this time the outflow runs approximately 300m west of the vegetated area margin. By 1951, both the westward progradation of the vegetated area and an eastward migration of the channel resulted in the channel running alongside the western margin of the site. Between 1951 and 1977 there is little change in the extent of the vegetated area and the Sheskinmore Lough outflow continues to run alongside the western margin.

Between 1977 and 1995 there was a retreat of the western edge of the site ranging from 60m ±10m on the northern section edge to 30m ±10m at the southern end. This retreat of the western edge has continued steadily from 1995 to the present day (Figure 4.13). The Sheskinmore Lough outflow has retained its position alongside the western margin of the site gradually moving eastwards with the retreat of this area. The Sheskinmore Lough Management plan states

the Lough has been subjected to a number of drainage schemes and in 1981 the present day outlet channel was excavated. Between 1982 and 2004 several ineffective attempts at controlling the outflow from the lough were made via a sluice and other softer options. In 2004 reconstruction of a previous sluice structure was made which has been effective in controlling the outflow from the Lough (National Parks and Wildlife Service, 2011).

The ridge feature that is found in the south west corner of the vegetated surface (Figure 4.2) appears to be the result of a northward extension of the Bellanagoal River meander running along the south western margin. There is no evidence from the historical maps or aerial photographs of the Bellanangoal River having been this far north between 1850 and the present day. However, the 1907 south western margin profile does run further north than at any other period and aligns well with the smaller arched rise seen to the southwest of the ridge. It is therefore likely that the river occupied a meander within this part of the site at some point between 1850 and 1907, and the northern bank of this ran along the line of the ridge.

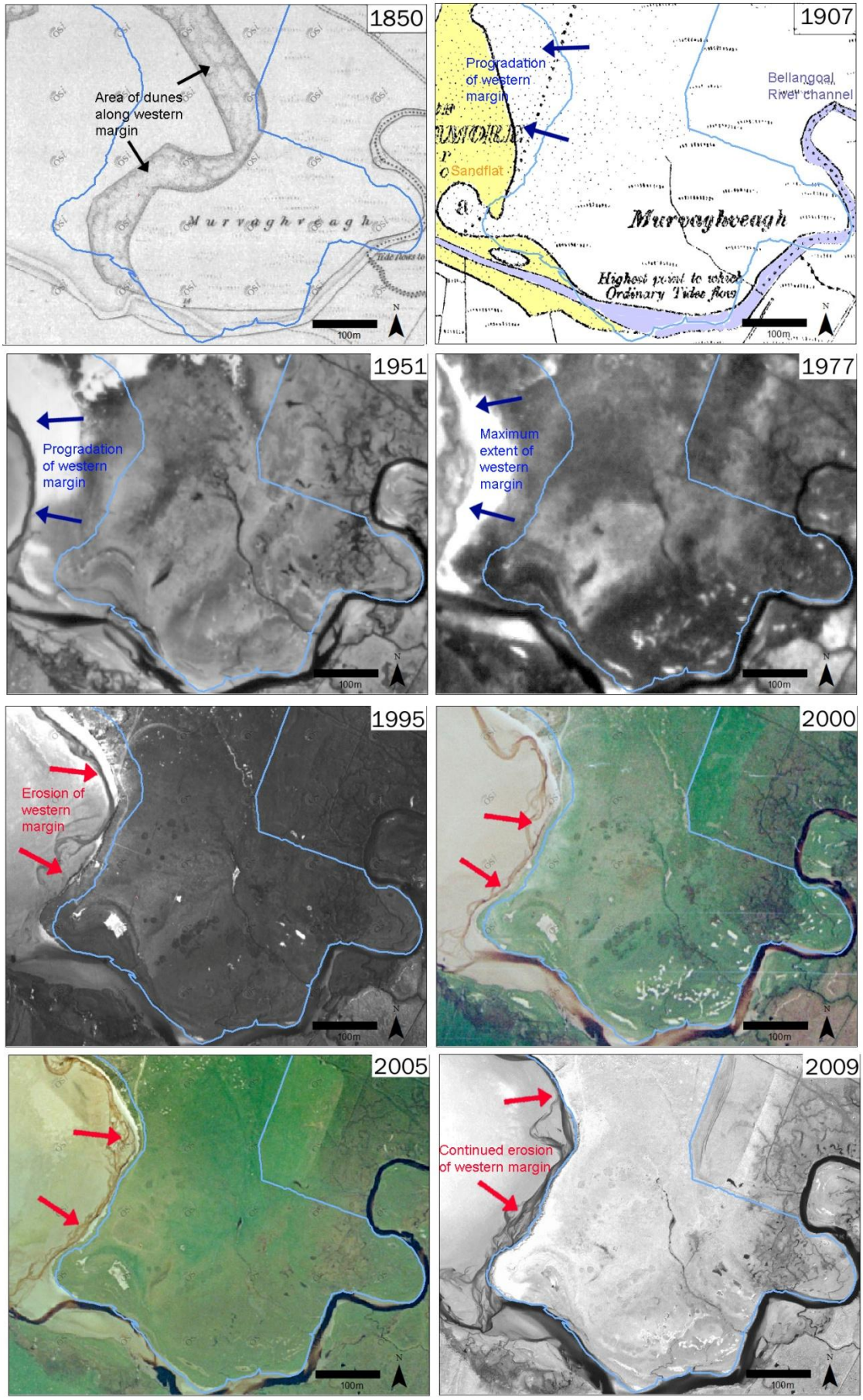

Figure 4.12 Historical maps, aerial photographs and satellite images of Sandfield. The April 2008 surveyed vegetation edge is also shown in each image as a reference (blue line).

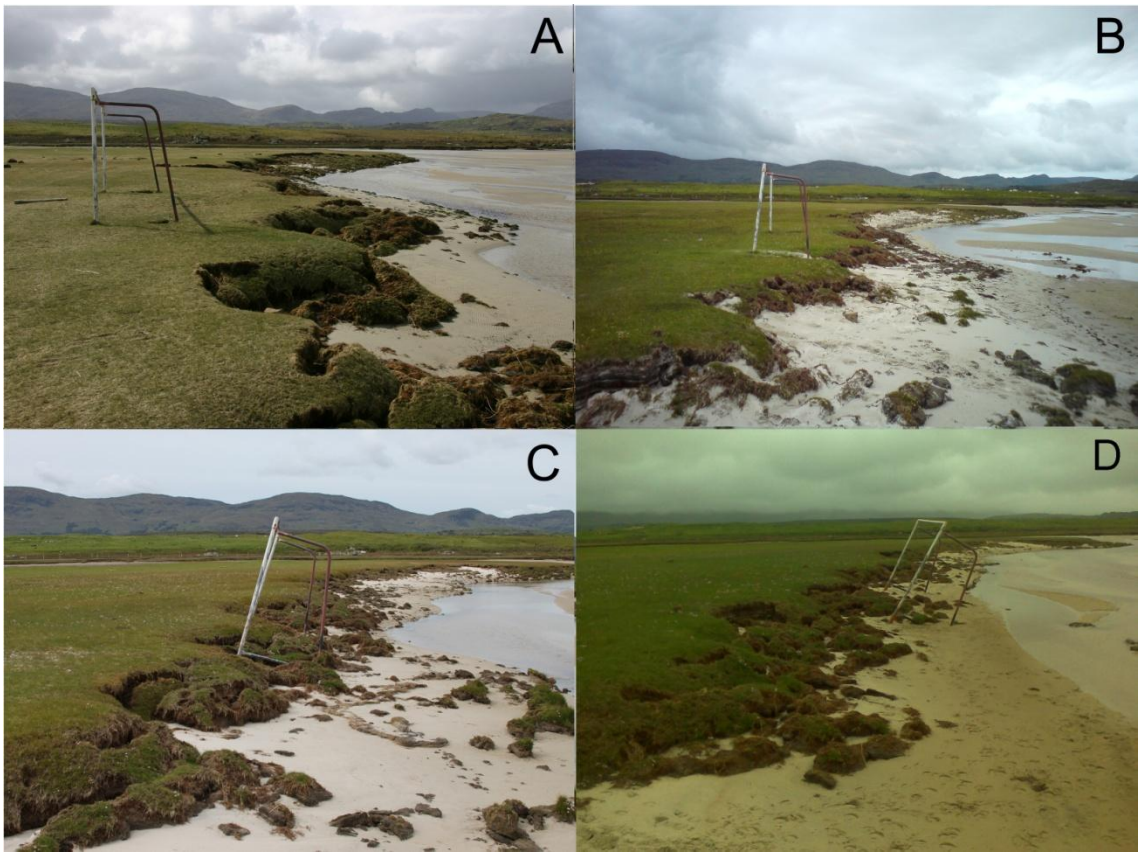

Figure 4.13 Photographs (looking south) showing retreat of the western margin at Sandfield between April 2008 (A), May 2010 (B), June 2011 (C) and June 2012 (D).

4.2.2. Derryness

Historical morphological change at Derryness has been less substantial than at Sandfield particularly at the raised vegetated surface in the southern section of the site; however, these changes are still significant (Figure 4.15). The two phases of change seen at Sandfield are not repeated at Derryness. Here both the southern elevated area and northern area of vegetated sand flat experienced a period of retreat between 1850 and 1951. From 1951 to the present day the elevated area experiences little morphological change whereas the vegetated sand flat shows a period of progradation through to the present day when it reaches its greatest extent.

The 1850 map indicates that the northern part of the raised area extended a further 30m ±20m westward of its present day position. The boundary of the vegetated flat was 100m ±20m further north at the western end of the area however there is little change with the present day position at the eastern end as here extension of the site is limited by the presence of the river channel. There is little change in extent of both areas between 1850 and 1907. However, the 1907 map does show a channel running south west to north east across the tip of the elevated section creating an island; this is the first indication of the presence of this channel.

As at Sandfield, the 1951 vegetation boundaries indicate a major period of erosion shortly before these aerial photographs were taken. The northerly portion of the elevated area had retreated to approximately its present day position and the island at the tip is not visible in the aerial photograph; it is unclear whether the landform has been completely eroded or whether it has significantly reduced in size, i.e. receded on the seaward side, and the remaining portion covered in fresh wind blown sand. As the island is present in later aerial photos through to the present day the latter is more likely. By 1951 the vegetation boundary of the sand flat area had retreated 90m ± 20m northwards from is 1907 position. This is approximately 35m further inland than the position of the present day fence which effectively marks the boundary between the high intertidal zone and the natural rise in the bedrock promontory. Again, it is likely that a large amount of fresh wind blown sand has been deposited inland as a result of erosion within the intertidal area.

The 1977 aerial photo shows the limits of the southern elevated area to have retreated by approximately 5m, i.e. within the margin of error; however, the island on the northern tip is present. To the north the vegetated sandflat had prograded from its 1951 minimum to approximately the 1850/1907 limit with a slightly greater extension to the western end.

From 1977 to the present day there is little morphological change to the raised area (Figure 4.15); however new vegetation growth was noted between site visits in April 2008 and May 2010 particularly around the channel area separating the island at the northern tip (Figure 4.14). Where the vegetation had established the channel was narrowed and the surface elevated by 10-20cm due to the presence of the vegetation and also additional sediment build up associated with the vegetation. It is possible this channel periodically opens and closes depending on the position of the river outflow around the northern tip of the site; it is also likely to change seasonally due to changes in storminess and vegetation growth. The vegetated sand flat continues to prograde southwards to its present day position.

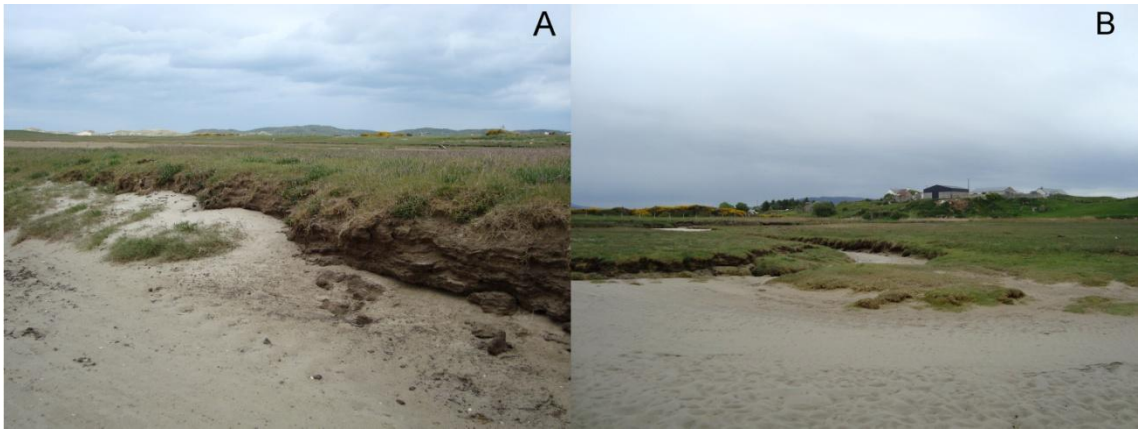

Figure 4.14 Areas of new vegetation growth around the island channel area at Derryness. A - looking north west, B - looking east.

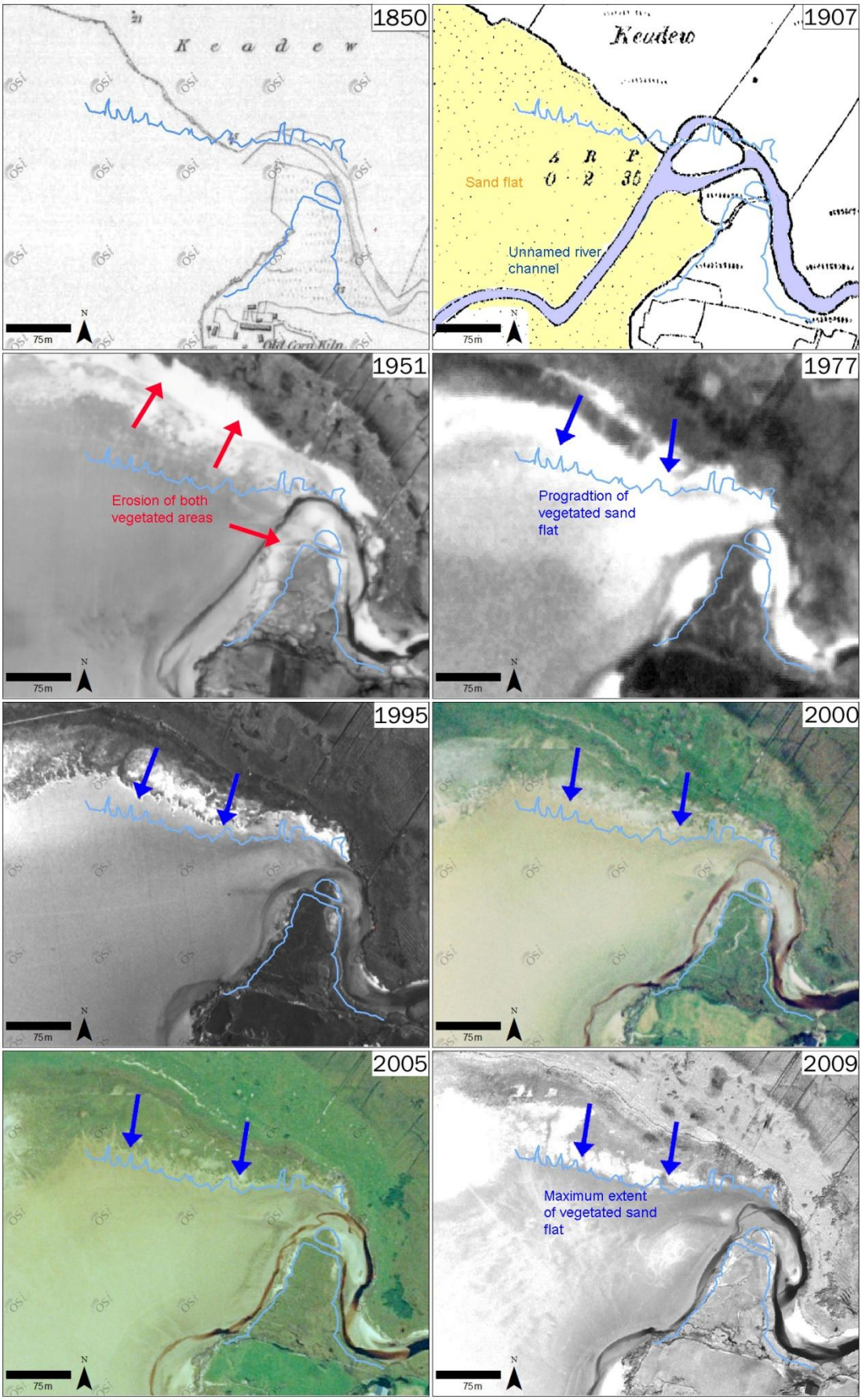

Figure 4.15 Historical maps, aerial photographs and satellite images of Derryness. The April 2008 surveyed vegetation edge is also shown in each image as a reference (blue line).

4.3. Sedimentology

Surface sediment samples were taken from across the sand flat and vegetated areas at both Sandfield and Derryness. The sediment budget within the Loughros More estuary is dominated by sand and this is reflected in the grain size distributions of the samples collected. The majority of this sediment is minerogenic although shell material and organic matter does contribute a varying proportion.

4.3.1. Grain size distributions

At Sandfield sediment samples were taken from 53 locations across the sand flat to the west of the vegetated site and 31 locations within the vegetated area (Figure 3.1). Across both the sand flat and vegetated area the samples are dominated by sand (Figure 4.16).

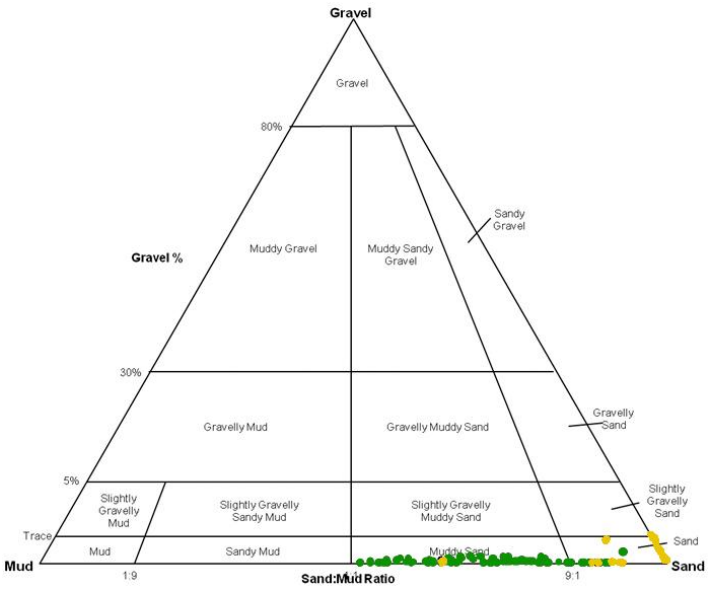

Figure 4.16 Sandfield sediment grain size diagrams for the sand flat samples (yellow) and vegetated area samples (green).

The sand flat samples are well sorted and are dominated by medium and fine sand with an average mean grain size of 2.04ϕ (standard deviation = 0.25ϕ). There is some variation across the flat where patches contain a higher proportion of very coarse and coarse sand (Figure 4.17); where this is the case it is usually due to the presence of shell fragments.

The vegetated area samples are dominated by the sand fraction and have an average mean grain size of 2.92ϕ (standard deviation = 0.48ϕ). However a large proportion of these samples contain a significant percentage within the silt fraction; this percentage increases to the east and south corresponding to areas of lower elevation. However, the samples within this area also have a higher percentage of coarse sand than the samples in the west of the vegetated area. This variation is reflected in the sorting across the site: samples in the east and south are predominately very poorly sorted (3.5ϕ to 5ϕ) and samples in the west being poorly sorted (1.7ϕ to 3ϕ) (Figure 4.17).

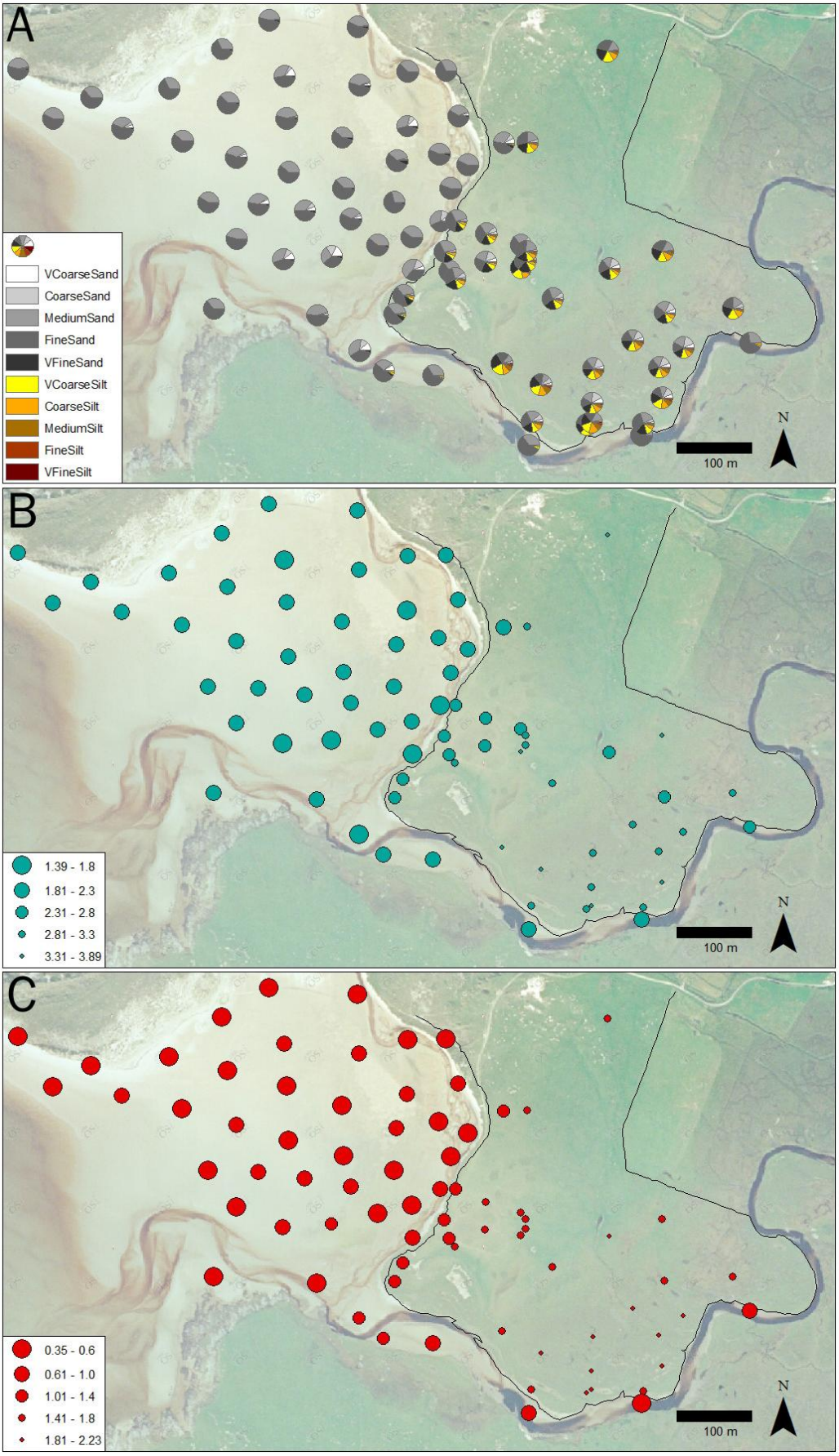

Figure 4.17 Sandfield sediment characteristics. A) Grain size distributions; B) mean grain size (values in ϕ units); C) sorting (values in ϕ units).

At Derryness sediment samples were taken from 20 locations across the sand flat to the west of the vegetated areas and 13 locations within the vegetated areas, 4 on the raised marsh and 9 on the vegetated sand flat. As at Sandfield both the sand flat and vegetated area samples are dominated by sand (Figure 4.18).

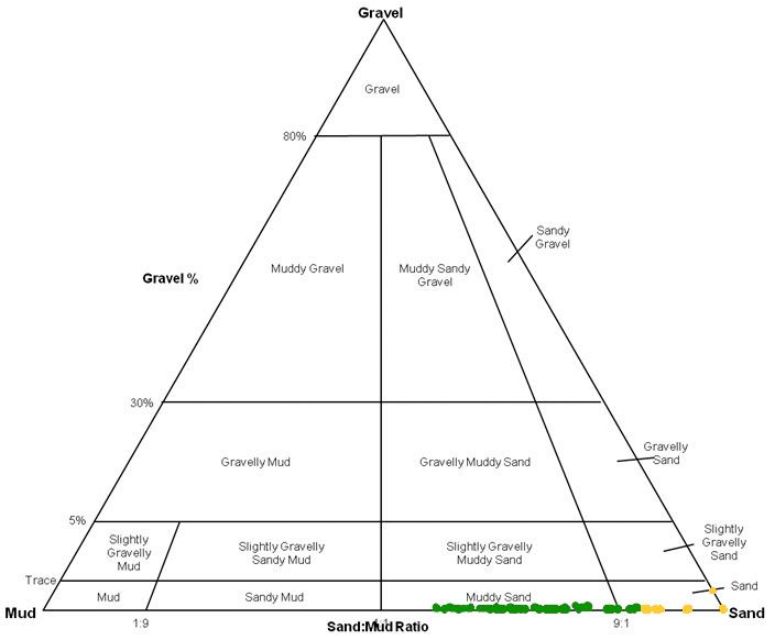

Figure 4.18 Derryness sediment grain size diagrams for the sand flat samples (yellow) and vegetated area samples (green).

Sediment across the Derryness sand flat is well sorted and dominated by medium and fine sand (Figure 4.19) with an average mean grain size of 2.22ϕ (standard deviation = 0.10ϕ). However unlike at Sandfield only one of these samples contains sediment coarser than medium sand; this may indicate a lack of shell debris in this part of the estuary sand flat.

The vegetated areas are dominated by the sand fraction although also contain a significant proportion from the silt fraction. The samples from the raised surface have an average mean grain size of 3.2ϕ (standard deviation = 0.22ϕ) and there is little variation in the grain size distributions across the area (Figure 4.19). The majority of the samples from the vegetated sand flat contain a higher percentage of medium and fine sand than the samples from the raised surface; this is reflected in the mean grain size value, 2.75ϕ (standard deviation = 0.33ϕ). There is some variation in grain size distribution across the vegetated sand flat area with the samples along the front margin of the area containing less fine (sub-sand) sediment; more northerly samples in this area contain a higher proportion of silt fraction sediment. This variation is reflected in the decrease in sorting from the front margin (1.9ϕ – 2.0ϕ) to further back (2.7ϕ and 3.0ϕ) (Figure 4.19).

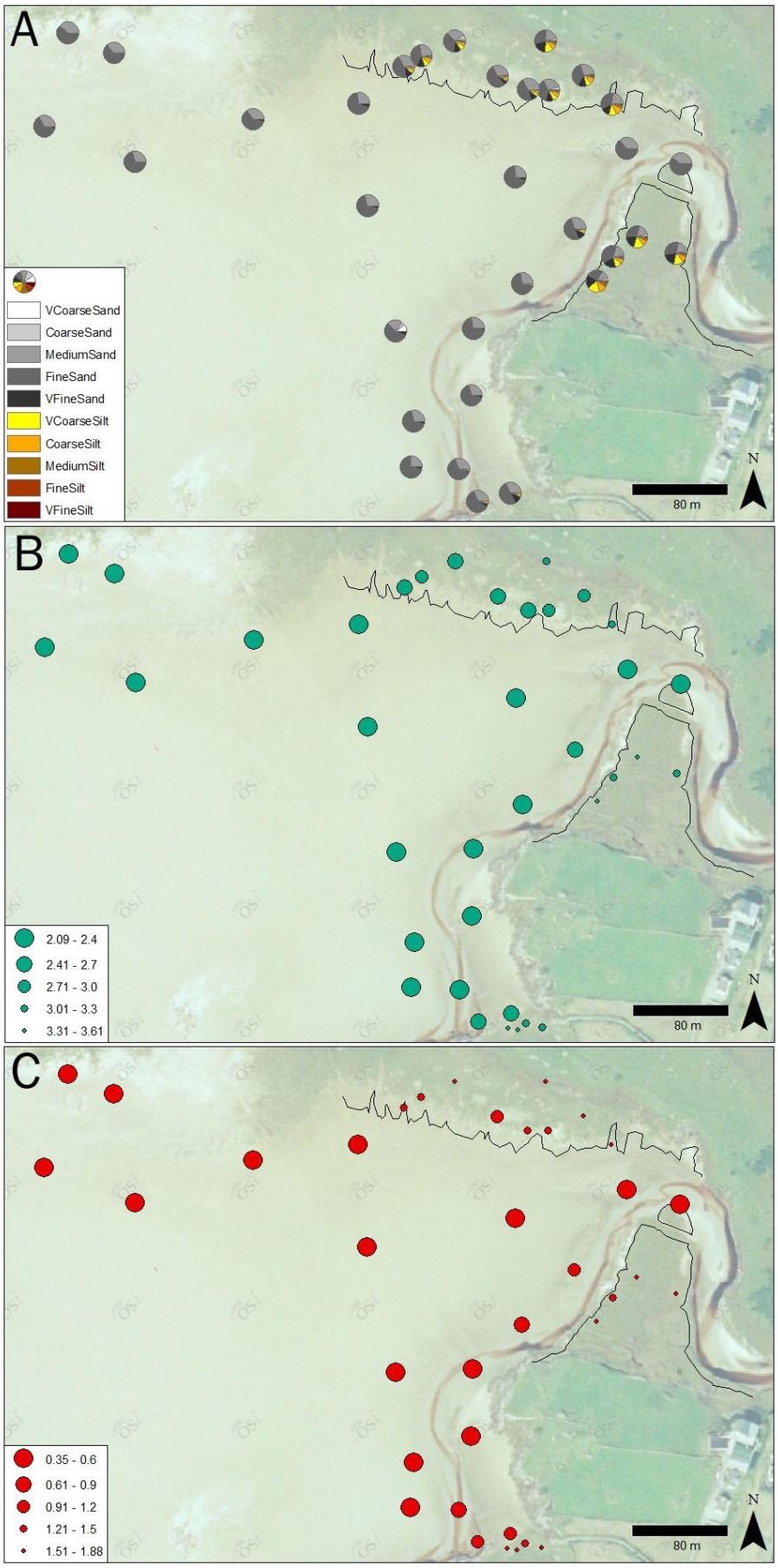

Figure 4.19 Derryness sediment characteristics. A) Grain size distributions; B) mean grain size (values in ϕ units); C) sorting (values in ϕ units).

4.3.2. Grain size trend analysis

The Gao and Collins (1992) grain size trend analysis model was applied to the Sandfield and Derryness sediment samples. The model was run on the sand flat and vegetated area samples separately as it is likely that the processes acting on these areas are significantly different. A characteristic distance of 123m and 150m for sand flat samples and 100m and 50m for vegetated area samples was used for Sandfield and Derryness respectively; this reflects the different sample intervals between environments and sites. The results of this analysis are shown in Figure 4.20.

For the Sandfield sand flat there appear to be two main directions of sediment transport: north east towards the dunes and south east towards the vegetated portion of the Sandfield site (Figure 4.20). Using this method it is not possible to distinguish between aeolian and aqueous transport and therefore results indicate an overall transport direction. On the vegetated portion of the Sandfield site the model predominately indicates transport away from the centre of the site. However, these results are likely to be influenced by the addition of fine grained organic material to the sediment. Given the observed aeolian deposition onto the western margin of the site where westerly transport direction is indicated towards this area this is likely a result of wind blown sand being deposited and creating a sorting gradient, i.e. becoming more well sorted, from the centre to the edge.

For the Derryness sand flat there are also two main transport directions with sediment to the south moving northwards and sediment in the north moving south although less significantly than the northerly transport (Figure 4.20). Again within the vegetated areas the sediment transport direction indicated by the model are likely to be confused by the addition of fine grained organic material to the sediment. This is particularly the case for the vegetated sand flat where there is an increase in organic material from the front to the back of the site (south to north) and therefore a decrease in the sorting.

Sediment traps were used to try and validate these modelled results and to attempt to determine the relative importance of water transport. However these were not successful as although they were effective at trapping any tidally deposited sediment they were also covered by wind blown sand and therefore quantifying the different transport methods was not possible. In future research sediment sampling during a storm event or on the retreat of the tide may be more effective.

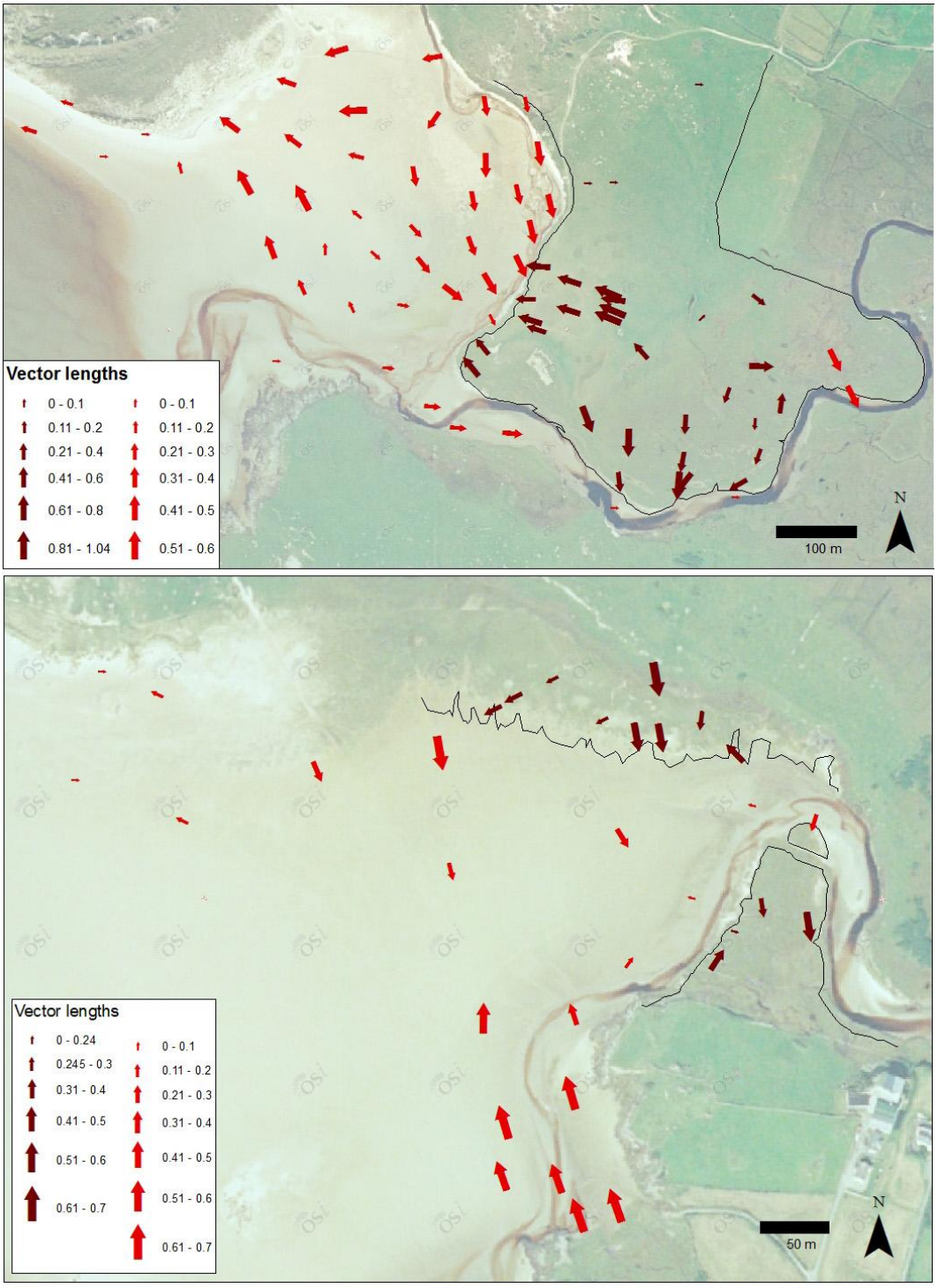

Figure 4.20 Grain size trend analysis for Sandfield (above) and Derryness (below).

4.3.3. Quartz grain microtextures

A stratified random subsample of the surface sediment samples was selected for quartz grain microtexture analysis under scanning electron microscopy (SEM). This method can enable the determination of transport mode and environment of deposition of the sand grains (e.g.

Madhavaraju *et al.* 2009 and Krinsley and Donahue, 1968). This environmental interpretation is based upon the presence of characteristic surface textures (Table 4.1).

Table 4.1 Summary of coastal quartz grain surface microtextures and their environmental interpretation (after Krinsley and Donahue,1968; Krinsley and Funnell, 1965; Margolis and Krinsley, 1971)

Depositional environment	Charateristic surface textures
Littoral – high energy	V-shaped patterns, irregular orientation, Straight or slightly curved grooves, Blocky conchoidial breakage patterns Chatter marks, a series of sub-parallel indentations (rare)
Littoral – medium energy	En-echelon V-shaped indentations (as energy increases orientation becomes more random)
Aeolian	Meandering ridges Graded arcs Upturned cleavage plates.

The presence of V-shaped indentations, conchcoidial breakage and upturned cleavage plates was recorded for each sample. The analysis focuses on these three textures as they can be considered indicative of the high energy littoral, medium and low energy littoral and aeolian depositional sub-environments encountered within the study setting. Moreover they are readily identifiable in the samples. V-shaped indentations are formed as a result of grain to grain collision in moderate to high energy littoral sub-aqueous environments (Madhavaraju *et al*. 2009; Williams and Thomas, 1989) with their orientation becoming more irregular as the energy level increases (Margolis and Krinsley, 1971). Blocky conchoidal fractures form during periods of high energy transportation in the littoral surf zone (Udayaganesan *et al*. 2011). Upturned cleavage plates are the result of aeolian abrasion of the grains (Tomas, 1987; Krinsley and Donahue, 1968).

Three samples from the machair, two from the sand flat at Sandfield and 1 from each of the raised surface and the sand flat at Derryness were chosen and 10 grains from each sample analysed. The occurrences of the indicative quartz grain surface features are shown in Figure 4.21. Within Sandfield machair the main difference between the samples is the lack of conchoidal breakage in the surface ridge sediment. This suggests this sediment has been subjected to a lower energy littoral environment than the other sediment samples from this area. The surface ridge sediment also has a higher occurrence of upturned cleavage plates suggesting this sediment has been subjected to a higher proportion of aeolian transport. Within the Sandfield sand flat samples the reason for the lack of v-shaped indentations in the dune edge sediment is unclear as the presence of conchoidal breakage patterns still suggests a high energy subaqueous environment. The appearance of the east sand flat sediment is similar to that of the machair sediment from the western margin and east of the area.

The Derryness sediment from both the saltmarsh and the sand flat differs from the Sandfield sediment in that it has fewer occurrences of upturned cleavage plates. This suggests that sediment from the Derryness area is subjected to less aeolian transportation. The sediment from vegetated area contains a greater occurrence of conchoidal breakage than the Derryness sand flat sediment; it is therefore likely that the zone B sediment has been transported in a higher energy subaqueous environment.

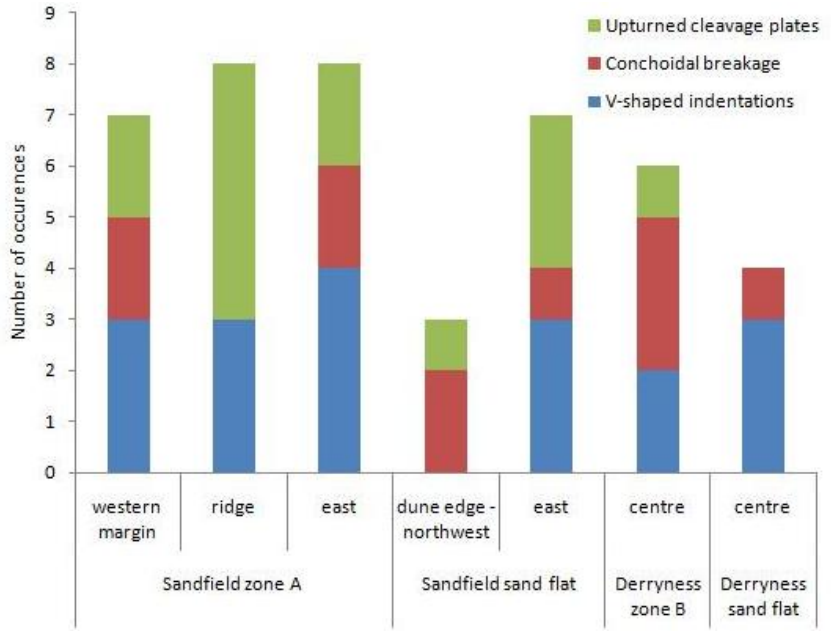

Figure 4.21 Number of occurrences per sample of indicative quartz grain surface microtextures.

4.4. Geochemistry: carbonates and organics

The grain size characteristics attributable to the presence of shell material in the sediment are confirmed by the spatial pattern in calcium carbonate ($CaCO_3$) content. Samples of the Sandfield sand flat / vegetation / river margin contain the highest $CaCO_3$ content (9 - 15%) (Figure 4.22). Across the seaward portion of the Sandfield sand flat $CaCO_3$ percentages are lower, i.e. 6 - 9%. The $CaCO_3$ percentages within the vegetated area are relatively low compared to those of the sand flat. However, there is some variation. The samples along the western margin of the machair contain levels akin to the sand flat, i.e. 3 - 9%; this could be attributed to the deposition of wind blown sand from the sand flat. There is also a slight peak in $CaCO_3$ to the east of the vegetated area (3 - 6%); it is possible this is due to the tidal deposition of shell material onto this lower elevation portion of the site although it could also be due to the presence of terrestrial mollusc species in this area.

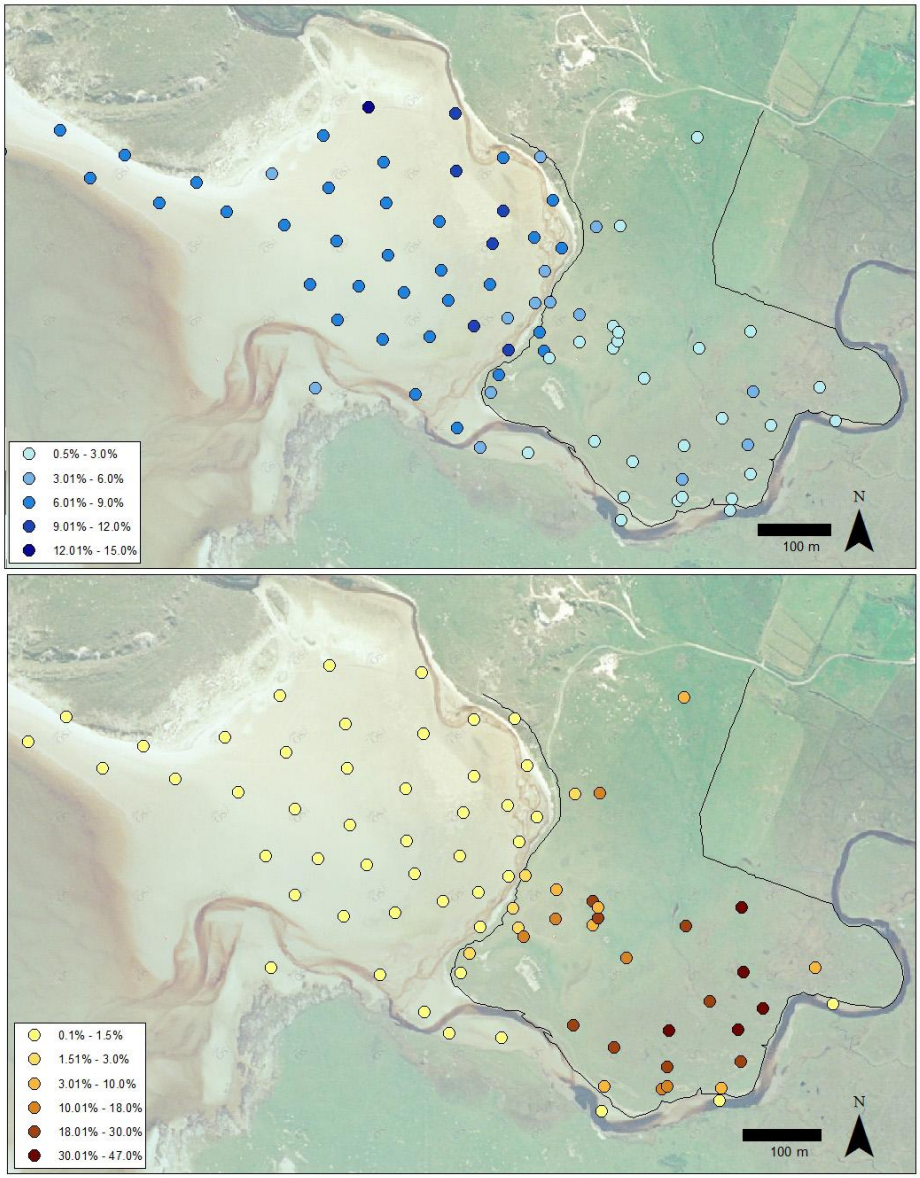

Figure 4.22 Sandfield carbonate contents ($CaCO_3$) (above) and organic contents (below)

Organic content within all the sand flat and near-river samples is minimal with little or no significant variation (Figure 4.22). Across the vegetated area the samples in the east tend to have the highest organic contents while those in the centre and along the western and southern margins have lower organic contents (Figure 4.22). This variation is likely due to greater allochthonous minerogenic input to the sediment along the margins of the vegetated area due to aeolian and tidal transportation of sediment from the tidal sand flat combined with a lack of deposition of allochthonous organics and reduced autochthonous organic build up (i.e. less productive in terms of vegetation). This would suggest that there is little minerogenic input to the sediment in the lower elevation east of the area and therefore that a greater proportion of the sediment in this area is derived from organic productivity.

Derryness tidal flat sediments contain less shell material than the Sandfield tidal flat: 3 – 6% compared to 6 – 9% (Figure 4.23). There is some variation across the sand flat with the central area having a higher $CaCO_3$ percentage (6 - 9%) and sites adjacent to the river channel north of zone B and along the rocky outcrop in the south of the site having lower percentage content (0.5 - 3%). $CaCO_3$ percentages of elevated area in the south of the site are low (0.5 - 3%) and do not vary across the area. The $CaCO_3$ percentages of the vegetated sand flat in the north of the site increase towards the south and west this is likely due to the influence of the tidal sand flat processes becoming more dominant at the sand flat / vegetation margin.

There is minimal organic content within the Derryness sand flat and near-river samples (Figure 4.23). In comparison to Sandfield the organic content of the vegetated areas are significantly lower (Figure 4.23). The organic content of the raised saltmarsh surface range from 3 - 10% (Figure 4.23) this is similar to the values seen for Sandfield along the western and southern margins. It is likely that due to the small size and flatness of this area the effect of minerogenic input from tidal and aeolian transportation of sand flat sediment and deposition onto the vegetated area is more-or-less equal across this elevated section. The organic content of the samples from vegetated sand flat are on the whole lower than those of raised vegetated surface (Figure 4.23). Within the vegetated sand flat area there is variation in the distribution of organic content with, in general, values decreasing from north east to south west. This corresponds to the amount of vegetation and the length of time the area has been vegetated, i.e. the areas that are more densely vegetated and have been vegetated for longer have a greater organic content. There a couple of samples that seem to be exceptions to this pattern. This is likely due to the patchy nature of plant colonisation and the high sensitivity of this type of environment.

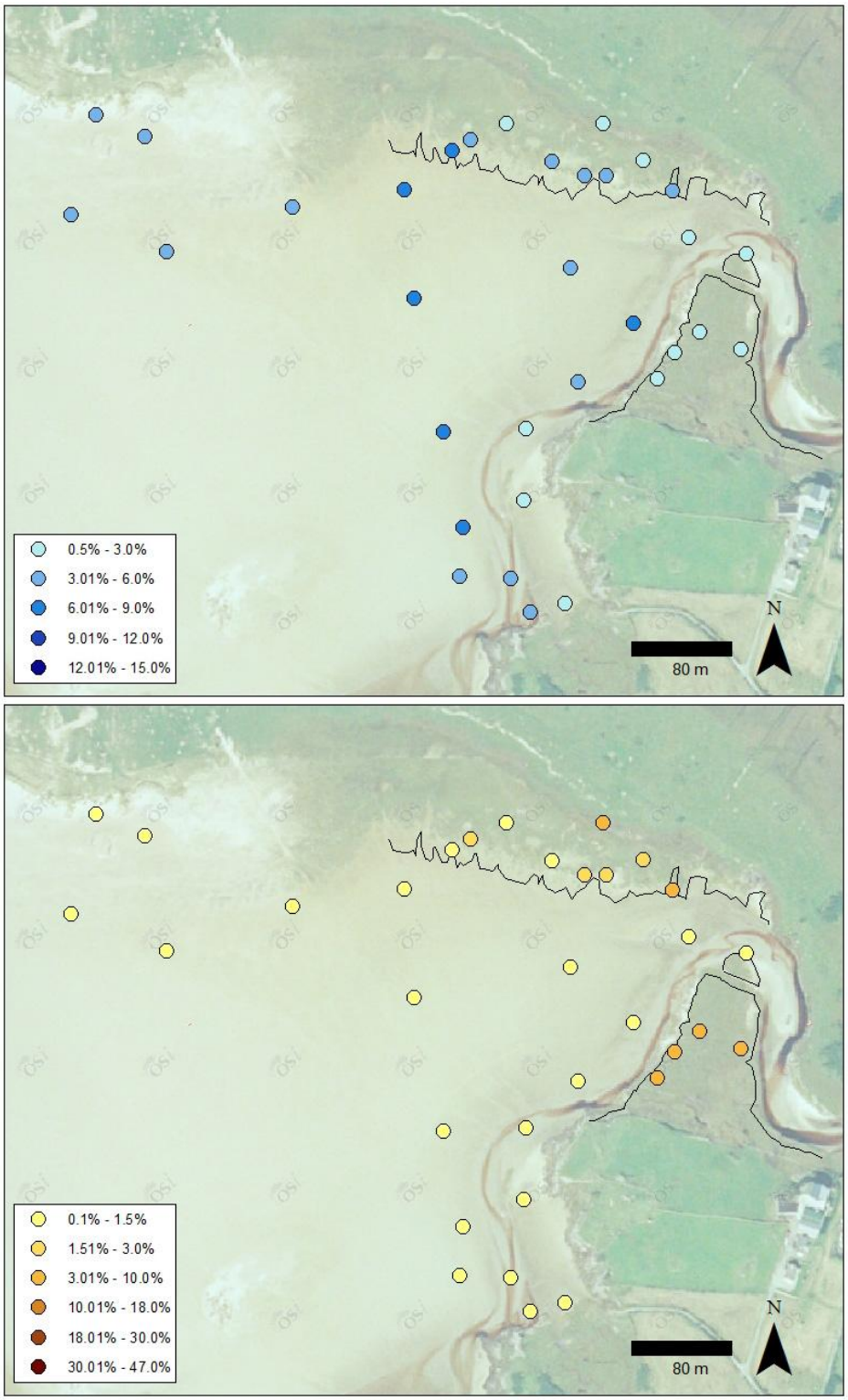

Figure 4.23 Derryness carbonate contents ($CaCO_3$) (above) and organic contents (below)

4.5. Ecology

4.5.1. Vegetation communities

Plant species across the vegetated areas at Sandfield and Derryness were surveyed in terms of their percentage cover within a 1m x 1m quadrat. In total 20 species of vascular plants were identified. Of these species 6 were only seen at Sandfield and 5 only seen at Derryness leaving 9 common to both sites (Table 4.2). The species unique in this study to Sandfield are predominantly more terrestrial grassland type species (e.g. *Bellis perenis, Taraxicum officinalis* and *Lotus corniculatus*). Whereas the species unique in this study to Derryness are predominantly high intertidal species (e.g. *Elytrigia juncea, Glaux maritima* and *Puccinella maritima*); these are generally found in the vegetated sand flat.

Table 4.2 Plant species identified in the vegetation survey and their locations.

Sandfield only	Both sites	Derryness only
Bellis perenis	*Ameria maritima*	*Elytrigia juncea*
Juncus gerardii	*Aster tripolium*	*Glaux maritima*
Lotus corniculatus	*Carex flacca*	*Poa trivialis*
Plantago media	*Cochlearia officinalis*	*Puccinellia maritima*
Schoenus nigricans	*Festuca rubra*	*Triglochin maritima*
Taraxicum officinalis	*Plantago coronopus*	
	Plantago maritima	
	Poa pratensis	
	Trifolium repens	

Principal Component Analysis (PCA) of the vegetation data shows distinct clustering related to the sample site location (Figure 4.24). The Derryness vegetated sand flat samples form a distinct group and are significantly different from the samples from the elevated areas at both Derryness and Sandfield; these are associated with *Glaux maritima* and *Puccinellia maritima.* Three of the four Derryness elevated area samples also form a group separate from both the other Derryness samples and the Sandfield samples. Their position on the ordination plot suggests they have greater similarity to the Sandfield samples although they are still significantly different. The majority of the Sandfield samples cluster together in the centre of the plot and are associated with the high intertidal and grassland type species. One Sandfield sample is separate from the main cluster in the bottom right of the ordination plot; this sample is from the north of the eastern half of the Sandfield site and is partially covered by one of the surface depressions described earlier. As a result the vegetation is split between that of the depression, e.g. *Juncus gerardii*, and of the surrounding area, e.g. *Festuca rubra* and *Poa pratensis*.

When the vegetation data are considered in combination with the environmental data collected for each of the sample sites within a constrained correspondence analysis (CCA) the three

sample groups can again be seen (Figure 4.25). Elevation exerts a strong control on the plant species composition of the Derryness vegetated sand flat samples as would be expected with such a relatively large change in elevation and consequent flooding periods. The more dominant controls on the Sandfield samples appear to be the moisture and organic contents of the soil.

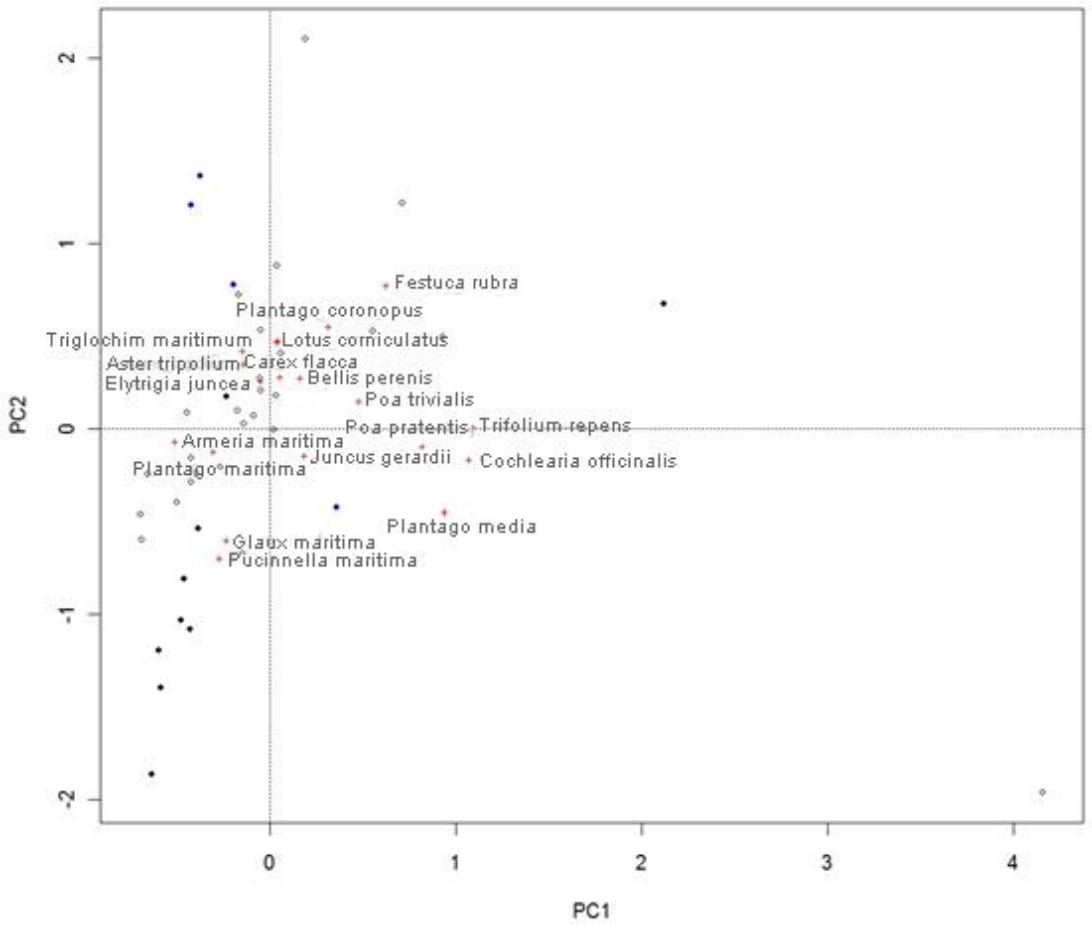

Figure 4.24 Ordination plot of principal components analysis (PCA) of vegetation data. Sandfield samples shown as white circles, Derryness vegetated sand flat shown as black circles and Derryness elevated vegetated area shown as blue circles. Plant species recorded are shown as red crosses and labelled. Eigenvalues: PC1 = 21.04%, PC2 = 11.13%.

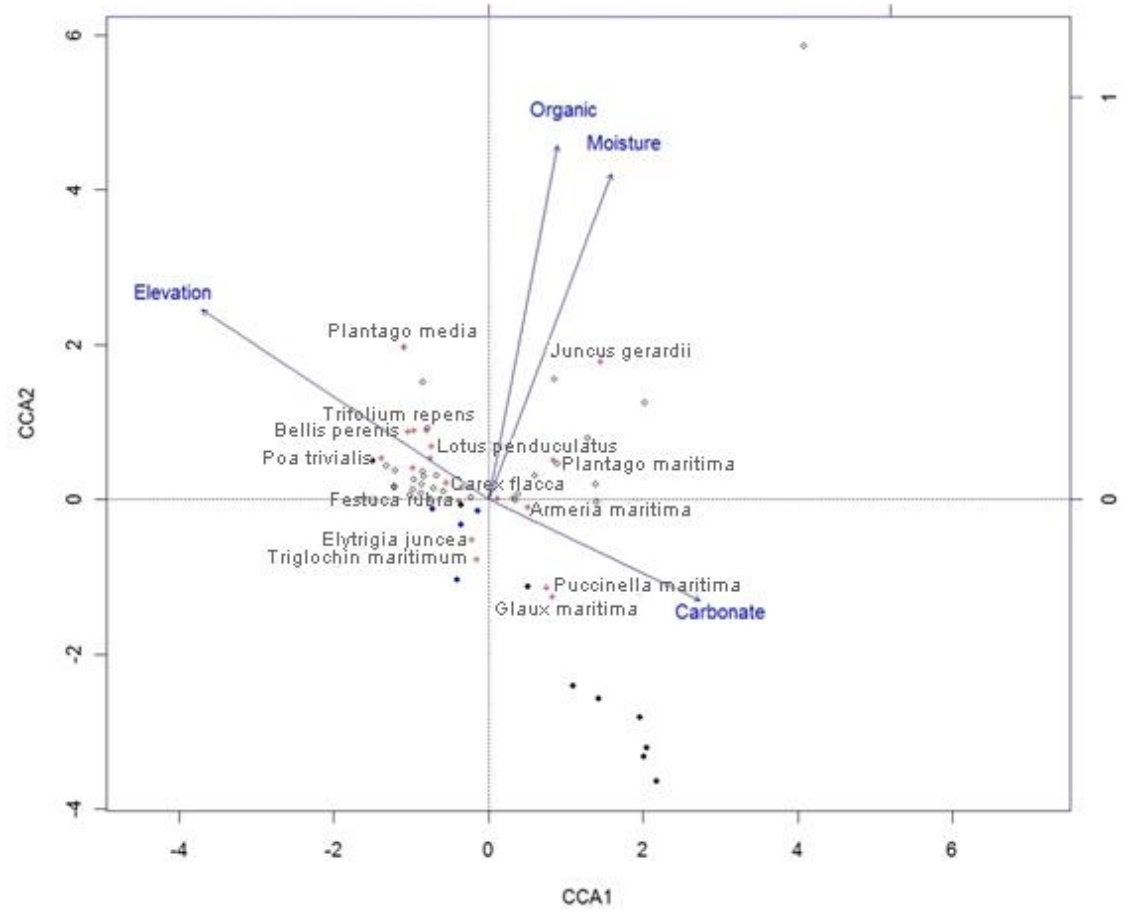

Figure 4.25 Ordination plot of Constrained correspondence analysis (CCA) of vegetation and environmental data. Sandfield samples shown as white circles, Derryness vegetated sand flat shown as black circles and Derryness elevated vegetated area shown as blue circles. Plant species recorded are shown as red crosses and labelled. Eigenvalues: unconstrained axes CA1 = 25.27%, CA2 = 20.81%; constrained axes CCA1 = 46.53%, CCA2 = 39.82%.

The vegetation data were analysed using TABLEFIT (Hill, 1996) in order to assign vegetation types to the quadrat samples in terms of both their NVC community type (UK based classification) and their CORINE biotype (European based classification). This analysis was based upon both species composition and species dominance; where the overall goodness of fit value was less than 50, i.e. very poor, the samples were removed from the analysis. The analysis indicates that the majority of the Sandfield samples are of the NVC MC8 type, i.e. *Festuca rubra – Armeria maritima* maritime grassland (Figure 4.26). Four samples in the south east of the site are classified as *Festuca rubra* saltmarsh (SM16) or *Puccinellia* saltmarsh (SM13). These samples are located in the lower elevation portion of the vegetated site associated with surface depressions. Although there are other areas indicated as maritime grassland at lower elevations which are more frequently flooded the surface depressions in this area retain the tidal water consequently increasing the flooding period and salinity in these areas; this will affect the vegetation species composition and is most likely the reason for saltmarsh communities in this area. There is also one sample indicated as saltmarsh community in the north west of the site,

this is an outlier due to the input of wind blown sand reducing the vegetation percentage cover and also the number of species present. Consequently the goodness of fit for the species composition component of the analysis is very poor.

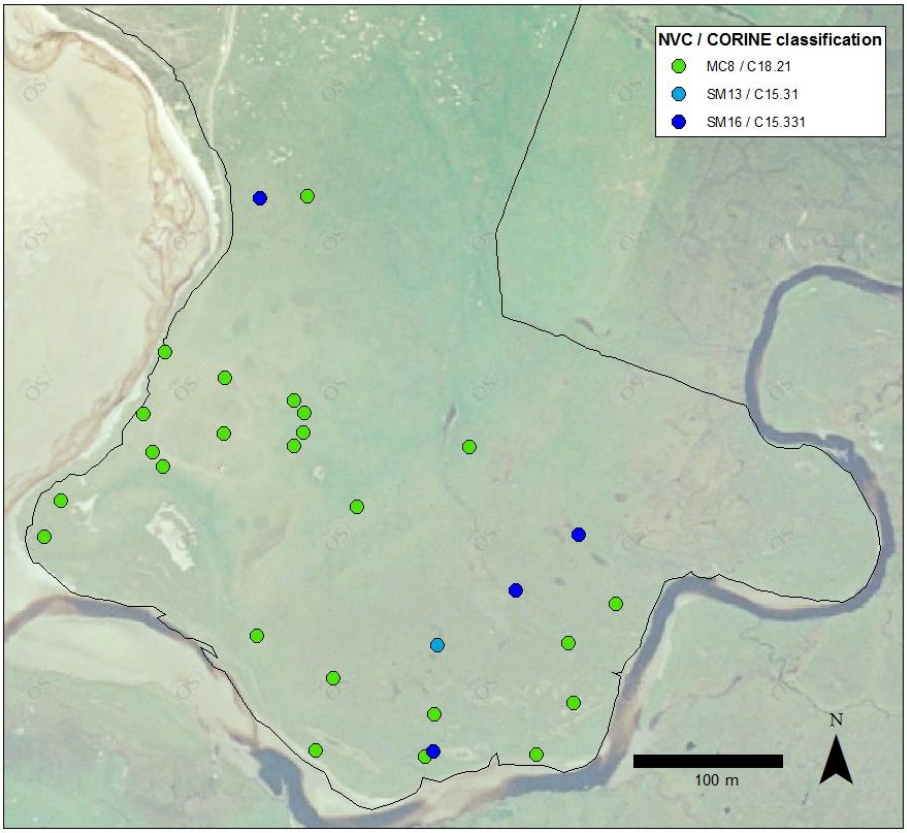

Figure 4.26 Sandfield vegetation types from TABLEFIT analysis.

The samples in elevated area at Derryness are a mix of maritime grassland (MC8) / maritime cliff (MC1) and saltmarsh communities (SM13 and 16) (Figure 4.27). This difference from the Sandfield elevated area reflects the lower elevation and more frequent flooding at Derryness. The vegetated sandflat is dominated by saltmarsh communities (Figure 4.27) as would be expected in this area, which is more frequently flooded than the rest of the vegetated areas within the site. However, one sample is indicated as maritime grassland towards the rear of the site; this suggests that if this area continues to develop and be raised above the tidal flat the vegetation is likely to change to a maritime grassland type composition.

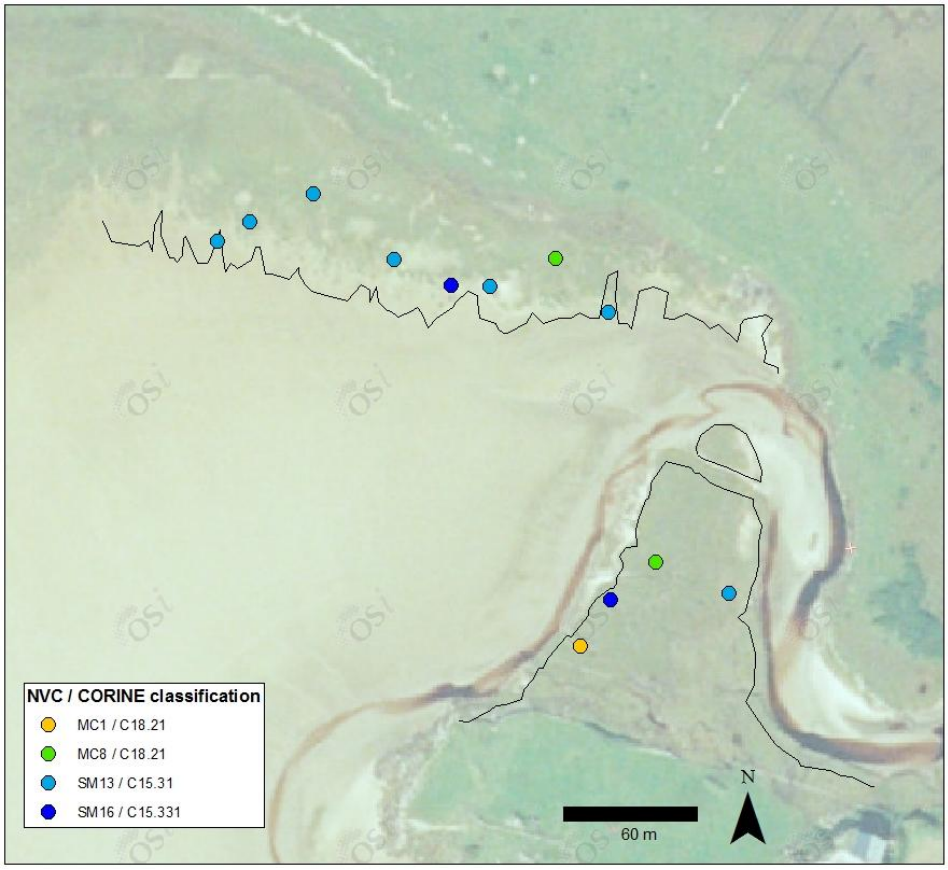

Figure 4.27 Derryness vegetation types from TABLEFIT analysis.

4.5.2. Diatom communities

Diatom analysis was carried out on a randomly selected subsample of the vegetated area and tidal sand flat sediment sample points at both Sandfield and Derryness. Diatoms were sampled from sediment samples to a 0.5cm depth. These samples included any living diatoms from the surface and recently deposited dead diatoms. This method was preferred over sampling of only living species as it enabled assessment of allochthonous deposition and therefore allows direct comparison with downcore samples. However, many of the sand flat samples contained very few or no diatoms as did some of the more sandy vegetated area sediment samples; therefore this analysis is based upon 6 vegetated area, 1 sand flat and 1 drainage channel samples from Sandfield and 4 vegetated area and 1 sand flat samples from Derryness (Figure 4.28). Due to this small sample size analysis based upon differences between vegetated zones and sand flat areas is not possible; therefore, analysis is based upon variations between vegetated area and sand flat communities. In total 33 diatom species were identified. Of these 5 species were only found in the sand flat samples, 8 only in the vegetated areas leaving 20 common to both sand flat and vegetated areas (Table 4.3). The majority of these species are common along the western British coast (Hendy, 1964) and therefore are likely to be typical of northwest Ireland communities.

PCA analysis of the diatom data shows a clear grouping of the vegetated area samples separate from the sand flat samples (Figure 4.29). This analysis also reveals one sample which lies outside of the main vegetated area sample group; this sample was taken from the vegetated sand flat at Derryness. This would suggest that the diatom assemblages here have more in common with those of the sand flat than that of the Derryness and Sandfield elevated vegetated areas.

Figure 4.28 Location of diatom surface sample points where diatoms were present.

Table 4.3 Diatom species identified and their locations

Vegetated areas only	Both areas	Sand flat only
Caloneis branderii	*Actinocyclus normanii*	*Fragilaria construens*
Cocconeis sublittoralis	*Actinoptycus senarius*	*Navicula arvenis*
Diploneis lineata	*Caloneis westii*	*Navicula cryptolyra*
Hantzschia virgata	*Cocconeis placentula*	*Navicula halophiloides*
Navicula abrupta	*Cosinodiscus radiatus*	*Surirella ovata*
Navicula forcipata	*Diploneis didyma*	
Navicula maculosa	*Diploneis interrupta*	
Navicula pennata	*Diploneis notablis*	
	Eunotia intermedia	
	Fragilaria exigna	
	Fragilaria pinnata	
	Hantzschia marina	
	Navicula arenaria	
	Navicula cincta	
	Navicula halophila	
	Navicula humerosa	
	Paralia sulcata	
	Pinnularia cruciformis	
	Pleurosigma strigosum	
	Rhaphoneis suriella	

Diploneis interrupta is the most dominant species in the quadrat samples with an average 45% of total diatom valves (TDV); within the sand flat samples this value drops to 1.5% TDV. The *Diploneis* genus is considered to be mainly littoral and the *D. interrupta* species in particular is described as common on the sandy beaches of north east Atlantic coastlines (Hendy, 1964) and therefore by implication western Ireland. The presence of species such as *Paralia sulcata* and *Actinoptychus senarius* in many of the vegetated area samples indicates tidal transport onto the vegetated surface as these are planktonic species.

Due to the relatively few samples with diatoms present it is not possible to infer or establish changes in species composition with, for example, change in elevation or hydroperiod on the vegetated areas.

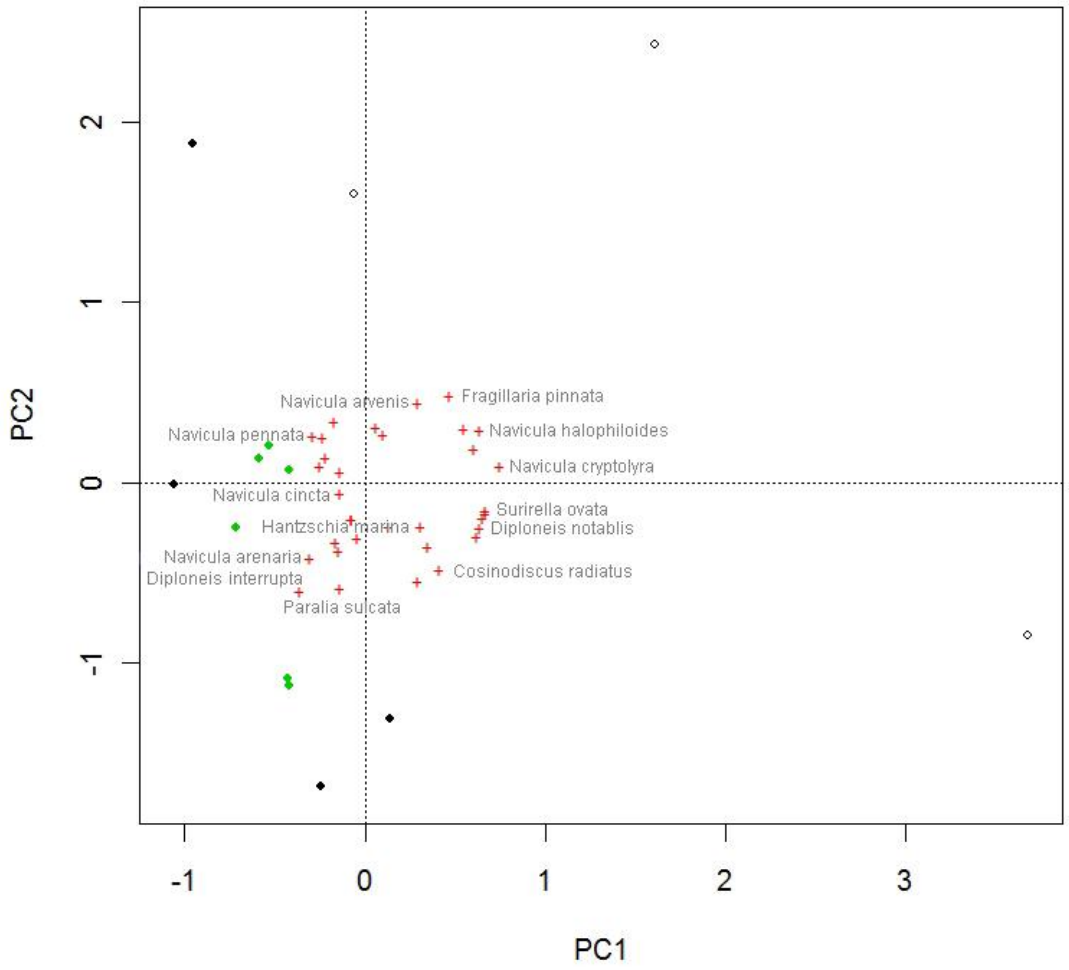

Figure 4.29 Ordination plot of principal components analysis (PCA) of total diatoms. Sand flat samples shown as white circles, Derryness vegetated area samples shown as black circles and Sandfield vegetated area samples shown as green circles. Diatom species identified are shown as red crosses and a selection labelled. Eigenvalues: PC1 = 26.43%, PC2 = 17.12%.

4.6. Human impacts

At Sandfield in particular there is evidence of disturbance of recreational vehicle driving across the site leaving areas of cut up vegetation and exposed soil. There are also football goals on the site. Although they are apparently rarely used (one of them is eroding with the microcliff at the seaward margin), they are clearly associated with areas of erosion around the goal mouths. In the south west corner of the site there is an area of exposed soil, approximately 5m x 3m, where it appears the turf has been cut and removed. It is also common for people to practice golf on the site and often divots associated with this can be found. Although is less disturbance at Derryness, vehicles are often driven onto the sand flat in front of the site.

The Sandfield site is grazed by cattle and there are obvious signs of nutrient enrichment from the manure in the vegetation on the site. The sward height here in April 2008 (i.e. 10-15mm) was lower than at Derryness (15-20mm) where there is no agricultural grazing although there is evidence of some grazing by rabbits. In the spring/summer of 2011 the cattle were removed from Sandfield this resulted in a noticeable change in the sward height, i.e. an increase to 15-20mm, and in June 2011 a notable increase in the number of *Armeria maritima* flowers.

4.7. Site classification

The habitat inventory of the Sheskinmore SPA states that a significant proportion of the designated area is a machair complex (European Environment Agency, 2010) and it is the opinion of Gaynor (2006 and pers comm. 2008) that the vegetated area at Sandfield is machair. However, McCorry and Ryle (2009) describe the majority of the vegetated areas at both Sandfield and Derryness as Atlantic salt meadows, i.e. CORINE C15.31 / NVC SM13.

The seven main characteristics of machair as defined by Ritchie (1976) and Angus (2006) are:

1. A base of wind-blown sand that has a significant percentage of shell-derived materials.
2. Lime rich soils with pH values normally greater than 7.0.
3. A level or low angle smooth surface at a mature stage of geomorphological evolution.
4. Sandy grassland type vegetation with long dune grasses and other key dune species having been eliminated. Core plants are *Festuca rubra, Lotus corniculatus, Trifolium repens, Achillia millefolium, Gallium verum, Plantago lanceolata, Euphrasia officinalis, Bellis perrenis* and *Rhytidiadelphus squarrosus* (Gimingham, 1974).
5. Biotic interference such as is caused by heavy grazing, sporadic cultivation, trampling and sometimes artificial drainage should be a detectable influence within the recent historical period.
6. An oceanic location with a moist, cool climatic regime.
7. Machair plains flood or are at least marshy in winter.

The Sandfield vegetated site displays all of these characteristics with the exception of the variety of core plant species. However, these core plant species are based solely upon the study of Scottish machair and whilst there is likely to be little difference between the species composition of Irish and Scottish machair greater research needs to be done to establish this. It is also unclear whether the recent heavy grazing on the Sandfield site has depleted the species richness. Now summer grazing has been reduced there may be an introduction or reintroduction of species to the site. As the distinction between machair grassland and other maritime grasslands has not been well defined (Bassett and Curtis, 1985), the NVC classification places the Sandfield site as maritime grassland and the presence of key machair characteristics it is reasonable to classify the Sandfield site as machair. The method of formation of this machair will be examined further in the subsequent chapters however; initial examination of the historical records has identified a dune barrier along the western margin of the site in 1850. By 1907 this barrier is no longer present although the vegetated surface remains in a somewhat modified morphological state. The formation of machair in the Western Isles of Scotland has frequently been attributed to the deflation of dune barriers to create the flat machair surface (e.g. Ritchie, 1979). It is therefore possible that deflation of the 1850 Sandfield dune barrier between 1850 and 1907 initiated the formation of the present day machair seen here.

The elevated area at Derryness displays many similar characteristics to that of Sandfield; however it does lack some of the key characteristics of machair (i.e. the evidence of historical biotic interference and also the shell content in this area is lower). The slightly lower position of this area within the tidal frame results in a greater proportion of saltmarsh type species; this is reflected in the NVC classifications for the sample sites in this area. This area can therefore be described as transitional between saltmarsh and maritime grassland/machair. The vegetated sand flat at Derryness is low enough in the tidal frame to be dominated by saltmarsh species. It is an area that is still forming as is evidenced by the angle of slope of the surface and is highly susceptible to tidal surge and storm events. This area can be classified as saltmarsh. If it continues to develop and become raised above the tidal flat it is likely to transition into maritime grassland/machair.

4.8. Summary of the contemporary environments

The two raised vegetated areas at Sandfield and Derryness, although initially similar in their appearances, display distinct differences in their sedimentology and ecology. It has been seen that the area at Sandfield contains all the typical attributes of machair with the exception of some of the core plant species; however, this may be due to differences between the Scottish and Irish typologies and/or the current grazing regime on the site. The lower position of the Derryness site within the tidal frame has determined a plant species composition with attributes

of both saltmarsh and maritime grassland. The lower $CaCO_3$ content of the sediment here also distinguishes it from the Sandfield site. The vegetated sandflat area at Derryness is subject to more regular tidal inundation, particularly at the seaward edge, than either of the raised surfaces at Sandfield and Derryness; this area is more akin to saltmarsh.

The variation in $CaCO_3$ (attributed to shell content) is the only distinction between the sedimentology of the Sandfield and Derryness sites. The differences in sediment transportation, suggested by the quartz grain surface textures, may explain the lower shell content seen in the Derryness sediment. The grain size trend analysis is unable to confirm this suggestion due to the inability to distinguish between aqueous and aeolian transportation using this method. Also the method is not appropriate for use on the vegetated surface samples due to the additional input of autochthonous organic sediment.

The history of the evolution of the sites, determined from the historical records obtained (maps and aerial photos), suggest significant differences in the timings of morphological change at the two sites. At Sandfield two periods of morphological change have been identified; firstly, a period of progradation between 1850 and 1977. Notably, on the 1850 map a dune barrier is indicated along the western margin of the site, this is no longer present by 1907. The margin of the machair reaches it most westerly extent by 1977. The second period of morphological change, between 1977 and the present day, is marked by erosion and retreat of the western margin. The change to an erosional environment is approximately coincident with the excavation of the Sheskinmore Lough outflow channel which flows along this western margin. Conversely, at Derryness, a period of erosion is identified between 1850 and 1951 at both the raised maritime grassland area and saltmarsh area in the north of the site. Subsequently the saltmarsh undergoes a period of progradation to the present day whereas there is little change in the lateral extent of the raised maritime grassland. There appear to be no correlations between the significant periods of morphological change seen at the Sandfield and Derryness sites.

The following chapter explores the evolution of the two sites in more detail via examination of the stratigraphy of the sediment columns.

5. Stratigraphic interpretations

This chapter describes and attempts to explain temporal (down core) and spatial (intra-/inter-site) variations and trends in the estuary margin sedimentary sequences of the of the study area. Stratigraphies are presented for the five cores obtained from Sandfield (n=3) and Derryness (n=2) machair/maritime-grassland sites. This is followed by more intensive, sample-based, analysis of one core from each site. Chronological information contained within the two latter cores is also evaluated.

5.1. Core site environmental history

Based upon the environmental history of the sites presented in the previous chapter (chapter 4.2) the spatial context of the core sites, in terms of their historical evolution, can be defined based upon their relative positions (Table 5.1). It can be seen that within the Sandfield site SFD3 has been stable in terms of vegetation for the longest period. SFD1 represents a transition from tidal flat to dune/machair up to 5m from the seaward edge to its 2009 position on the edge of the platform. Much of SFD2 represents channel deposits from the Bellanagoal River followed by a transition to machair up to 5m from the river channel edge to its 2009 position on the river edge.

Table 5.1 Position of core sites relative to site evolutionary stage.

	SFD1	SFD2	SFD3	DYN1	DYN2
2009	Edge	Edge	Machair (~40m from Bellanagoal)	Edge	Edge
2008	Edge	Edge	Machair (~40m from Bellanagoal)	Edge	Edge
2005	<5m from seaward edge	Edge	Machair (~40m from Bellanagoal)	Marsh (<5m from seaward edge)	Edge
2000	Machair	Machair (<5m from Bellanagoal)	Machair (~40m from Bellanagoal)	Marsh (<5m from seaward edge)	Edge
1995	Machair	Machair (<5m from Bellanagoal)	Machair (~40m from Bellanagoal)	Marsh (~10m from seaward edge)	Edge
1977	Machair	Channel edge	Machair (~40m from Bellanagoal)	Marsh (~10m from seaward edge)	Marsh
1951	Machair/dune	Channel edge	Machair (~50m from Bellanagoal)	Marsh (~20m from seaward edge)	Fragmented marsh
1907	Machair/dune	Mid-channel	Machair (<20m from Bellanagoal)	Marsh (<5m from seaward edge)	Marsh (~20m to channel to E; ~50 to seaward edge)
1850	Tidal flat	Mid-channel	Machair (<20m from Bellanagoal)	Marsh (<5m from seaward edge)	Marsh (~20m to channel to E; ~50 to seaward edge)

Within the Derryness site both DYN1 and DYN2 represent periods of maritime grassland/marsh for the majority of their historical evolution. Their positions relative to the seaward edge of the environment has changed between 1850 and the 2009 with a retreat of the seaward margin.

All five cores are also likely to represent periods of sediment deposition prior to the historical evidence obtained.

5.2. Core stratigraphy

Stratigraphic logs were produced from the sediment peels collected from exposed sediment sequences immediately adjacent to the core sample locations (Figure 3.1) (Figure 5.1 and Figure 5.2). These enabled the identification of the main stratigraphic characteristics by examination of down-section variation in sediment texture and composition. Sedimentological descriptions of the units identified were based upon a modified Troels-Smith scheme described by Long *et al.* (1999). Using this method focused the detailed examination of the sequences. The light and dark layering is clearly visible in the field sections (Figure 7.4) however due to the effects of drying out the contrast between the layers, although visible on closer inspection, is less clear in the peels and core surfaces. Therefore, the sediment logs provide a record of downcore changes not always immediately visible in the core or peel photographs.

SFD1 is the most seaward of the three Sandfield cores and is located on the westward margin of the Sandfield machair area. The surface elevation of the top of this core is 1.972mOD, i.e. 0.34m above MHWS (Figure 5.1). The surface sediment here is dominated by wind-blown sand deposited onto the machair surface and there are several patches of bare sand where the vegetation has become buried. SFD2 is located on the southern margin of the area of machair on the edge of the Bellanagoal river channel. The elevation of the top of the core is 1.774mOD, i.e. 0.14m above MHWS (Figure 5.1). Here, the surface sediment is again dominated by sand, although there is less evidence of recent aeolian deposition. However, whilst vegetation cover is more continuous than at SFD1 bare patches still occur. SFD3 is the most landward of the Sandfield cores. It is located approximately 30m inland from the margin with the Bellanagoal River on the edge of a small creek running from the centre of the vegetated area to the river. The surface elevation at the top of the core is 1.728mOD, i.e. 0.10m above MHWS (Figure 5.1). The surface sediment is again predominantly sandy. However, compared to SFD1 and 2, a larger silt and clay fraction is present. Vegetation cover is complete across the surface.

DYN1 is located on the seaward/western margin of the elevated area of maritime-grassland adjacent to the river outflow at the Derryness site. The elevation at the top of the core is 1.946mOD, i.e. 0.32m above MHWS (Figure 5.1). The surface sediment is dominated by sand and vegetation cover is complete. DYN2 is located on the northern tip of the area of elevated maritime-grassland where the river channel turns south and flows out onto the tidal flat. The

elevation of the top of this core is 1.434mOD, i.e. 0.20m below MHWS (Figure 5.1). Here vegetation cover is not continuous with occasional patches of bare sediment occurring.

There is a clear down-section shift in sedimentary character within all sections from an organic-silica mix to silica-dominated. The depth of this transition varies between samples and sites; in SFD1 it is at 30cm (1.67 mOD), SFD2 22cm (1.55 mOD), SFD3 26cm (1.47 mOD), DYN1 42cm (1.53 mOD) and DYN2 22cm (1.21 mOD). This zone is interpreted as a transition from a predominantly clastic tidal flat to more organic-rich vegetated marsh/machair. This interpretation is corroborated by the presence of ripple structures and other non-planar laminations in the lower parts of the sections from SFD2 and SFD3 and DYN1. The ripple structures are approximately 1cm in height and occur frequently within silica-dominated units. They are probably indicative of wave-generated ripples formed on the tidal flat.

Small-scale bedding (<2cm) in the form of alternating light (silica-rich) and dark (silt and/or clay increase) layers is evident throughout the sequences. Within the lower, tidal flat, units these are often non-planar and intermittent, forming ripple structures as previously described or larger lenses of finer grained material within a sand dominated unit; within the Sandfield sections, discontinuous layers or lenses dominated by comminuted shell fragments are also found. Within the lower tidal flat units there is often little change in sedimentology between the light and dark layers. It is therefore likely that this colour change is due to the characteristic darkening of sediments in the 'sulphide system', i.e. anaerobic conditions in sub-surface sediments resulting in anaerobic decay and the production of sulphides (Libes, 2009). Therefore the alternation of numerous light and dark layers is likely to represent repeated episodes of surface burial.

Within the upper units of the sections the alternating light and dark layers can be attributed to a change in sedimentology, i.e. light silica-rich layers and dark silt and/or clay rich layers. Bedding is generally planar with a greater portion of the finer particle fraction consisting of organic deposits. Fining upwards sequences, often in repeating groups, are present in all the samples but are more common at Sandfield. Within many of these fining sequences, the sand at the base of the unit forms a discontinuous contact with the unit below. The form and structure of these beds imply repeating periods of enhanced sediment supply followed by vegetation growth and the development of organic horizons. At Sandfield there is a wedge shaped finer organic rich unit increasing in thickness from west to east, i.e. SFD1 to SFD3 (Figure 5.1); this organic upper unit is not present in the Derryness sections.

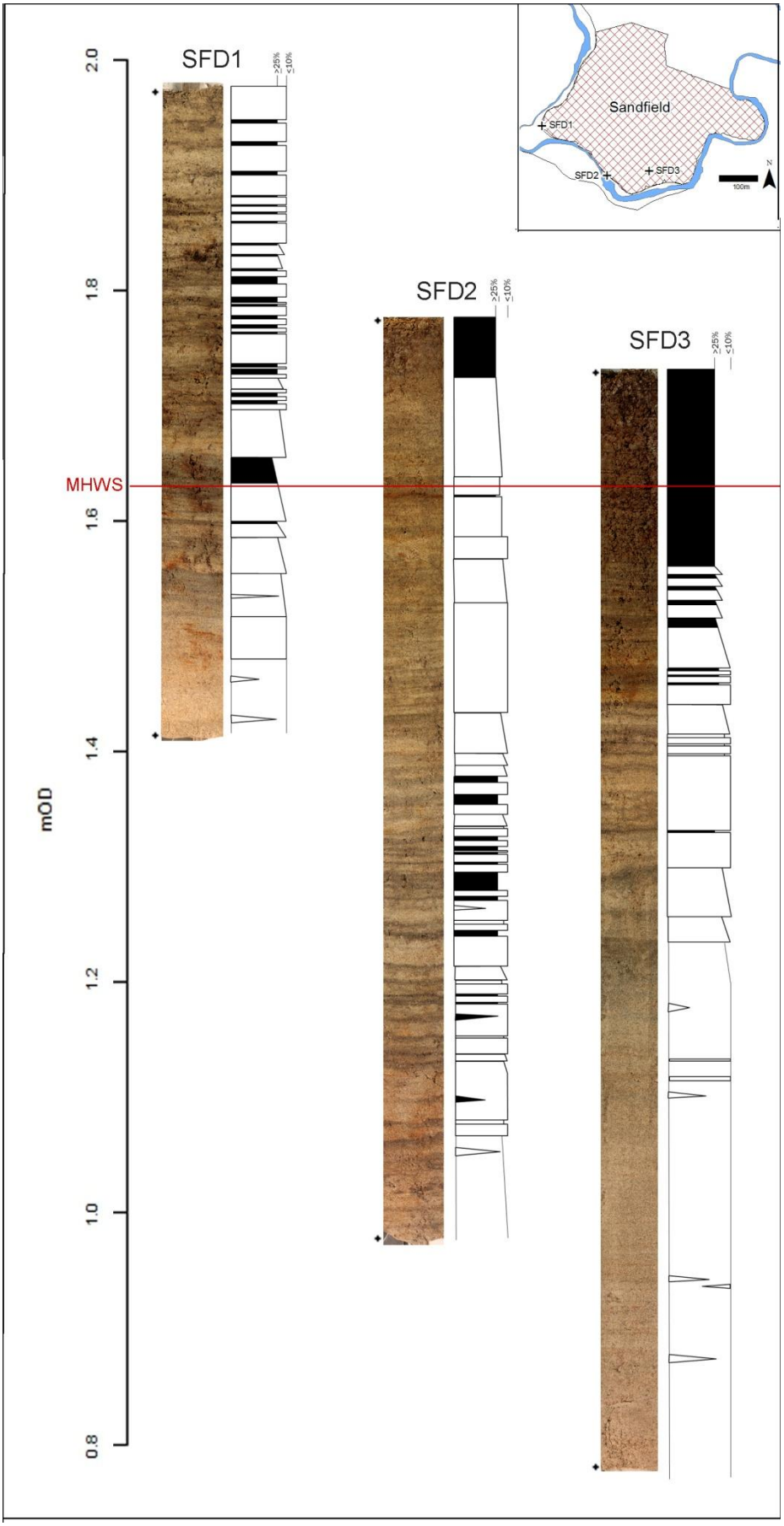

Figure 5.1 Sandfield stratigraphic logs. Black units = ≥25% silt or clay, white units = <25% silt or clay. Images on the left of the logs show the split core surface. Core locations indicated.

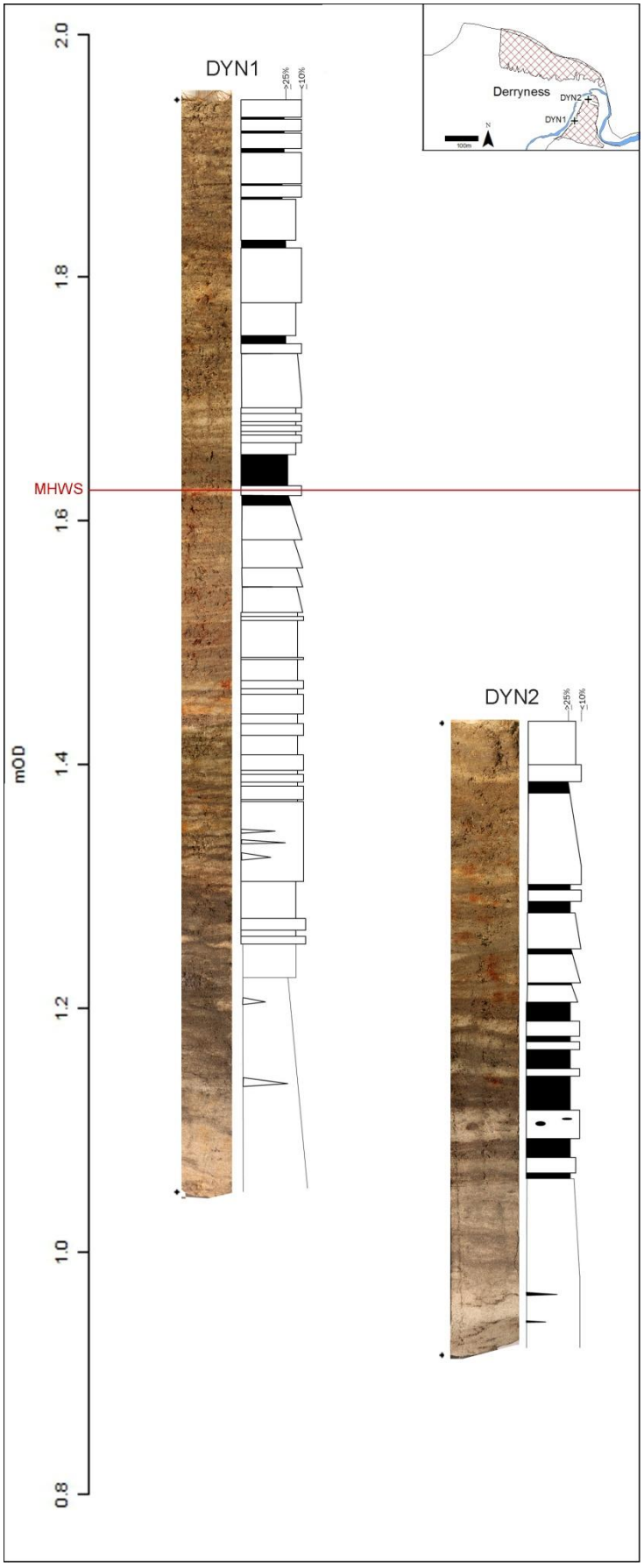

Figure 5.2 Derryness stratigraphic logs. Black units = ≥25% silt or clay, white units = <25% silt or clay. Images on the left of the logs show the split core surface. Core locations indicated.

Sediment texture varies between Sandfield and Derryness, notably in terms of sand content. The Sandfield sections have a significantly higher number of units classified as ≤10% silt or clay; whereas at Derryness the sandier units often have a silt/clay fraction between 10 and 25%. It is common at Sandfield, particularly at sites 2 and 3, for the finer units (≥25% silt or clay) to occur as thin bands, between 2mm and 5mm in thickness, within the more sandy units throughout the section. In contrast, the finer units at Derryness are of greater thickness particularly in DYN2 (Figure 5.1 and Figure 5.2).

There are some similarities between cores at the two sites. The identification of the shift from silica to organic-dominated sediments, inferring the change from tidal flat to vegetated surface, allows a single point of correlation between all the sequences. However further correlation of other beds can only be tentative at best as there are no unique distinguishing features identified from this descriptive analysis. At both SFD1 and DYN1 a fine unit occurs between ~1.62 and 1.65mOD. In both cores this unit is significantly thicker than other finer units within the individual core. In both cores below this unit the sediment is coarser with the units becoming more massive towards the base of the core. Above this unit both cores exhibit an alternation between light coloured, coarser, more clastic units and narrower, darker, finer, more organic layers. These finer layers are more prevalent in SFD1.

In previous analysis of these samples (Barrett-Mold *et al.*, 2009) it was determined that the relative sandiness of the tops of DYN1 and SFD1 was due to their positions within the machair or maritime grassland (i.e. along the western margin) and therefore they receive more wind-blown sand. It was also considered that the alternating light silica-rich and dark organic mud-rich bedding above the tidal flat – marsh transition infers significant periodicity and continuity in sediment supply and saltmarsh accretion. Within the lower (tidal flat) units light sandy sediments dominate and where finer sediments do occur it is in discontinuous, non-planar beds or in lenses. This is thought to indicate that the conditions required for deposition of these sediments was not common, only occurring episodically and in discrete, localised pockets. Within the upper marsh / maritime grassland / machair units, the alternating bands are more regular and often associated with a fining upwards sequence. These sequences are consider to infer an input of sand associated with a higher energy event, creating an erosional contact with the unit below, grading up to finer sediments, increasingly organic in character with the renewed biogenic contribution associated with vegetation growth.

The inter-site similarities between Sandfield and Derryness are significant as they indicate that, in addition to local core or site specific factors influencing sediment stratigraphy there are also processes active on a larger estuary-wide scale.

5.3. Sedimentology

Selected cores, SFD3 and DYN1, were sub-sampled at 1cm resolution to permit further sedimentological analyses for sediment texture and composition. The effects of core compression were also taken into account. At Sandfield, core SFD3 underwent 8cm of compression; its uncompressed length is 0.95m, extending from a surface elevation of 1.73mOD down to 0.78mOD. At Derryness DYN1 underwent 2cm of compression; its uncompressed length is 0.89m, extending from a surface elevation of 1.94mOD down to 1.05mOD.

A 1cm sampling resolution was used primarily due to the amount of sediment required for the analyses but also due to the practicalities and accuracy limits in extracting the samples from the core. To ensure repeatability of the results, in addition to the accuracy of the equipment being tested with a known standard (see Chp 3.3.4), three repeats were run within each sample: all p-values = $< 2.2e^{-16}$; R^2 values ranged between 0.9186 and 0.9999.

5.3.1. Grain size distributions

Sediment obtained from cores at both Sandfield and Derryness is dominated by sand-sized material (Figure 5.3, Figure 5.4).

Within the bottom 15cm of the SFD3 core there are several occurrences of coarse sand to very fine gravel size sediment this can be attributed to the presence of the shell material identified in the sediment logs. Between 0.95mOD and 1.2mOD mean grain size remains consistent at around 2.25ϕ (0.21mm). This material is dominated by fine and medium sand with very few occurrences of very fine or coarse material. The sorting within this unit is also at its maximum for the core (Figure 5.3). The top of this unit, i.e. 1.2mOD, coincides with the start of the fining upwards sequences identified in the sediment logs. Between 1.2mOD and 1.54mOD there is an increase in finer material, i.e. very fine sand to clay. However, between 1.2mOD and 1.4mOD there is also an increase in coarser material, which is again attributed to a greater content of shell material. Between 1.54mOD and the top of the core mean grain size decreases further with an associated increase in coarse silt to clay sized material. This is reflected in a decrease in mean and sorting values (Figure 5.5). This increase in finer material can be attributed to the more organic rich sediment within this upper unit (Figure 5.1, Figure 5.3). Mean grain size in the SFD3 core ranges from very fine (3.55ϕ; 0.085mm) to medium (1.24ϕ; 0.42mm) sand and sorting values from 1.65ϕ to 0.36ϕ (Figure 5.3, Figure 5.5). The relationship between the mean grain size and the sorting and skewness values, shown in Figure 5.5, reflects the presence of finer material at the top of the core with increasing mean grain size downcore corresponding to increasing sorting and skewness. The highest kurtosis values are found in the samples from the top and bottom of the core (Figure 5.5). Within the biplots of grain size statistics for the SFD3

core (Figure 5.5) the bottom and top core samples form clusters distinct from each other, the samples in between being transistionary between the two clusters.

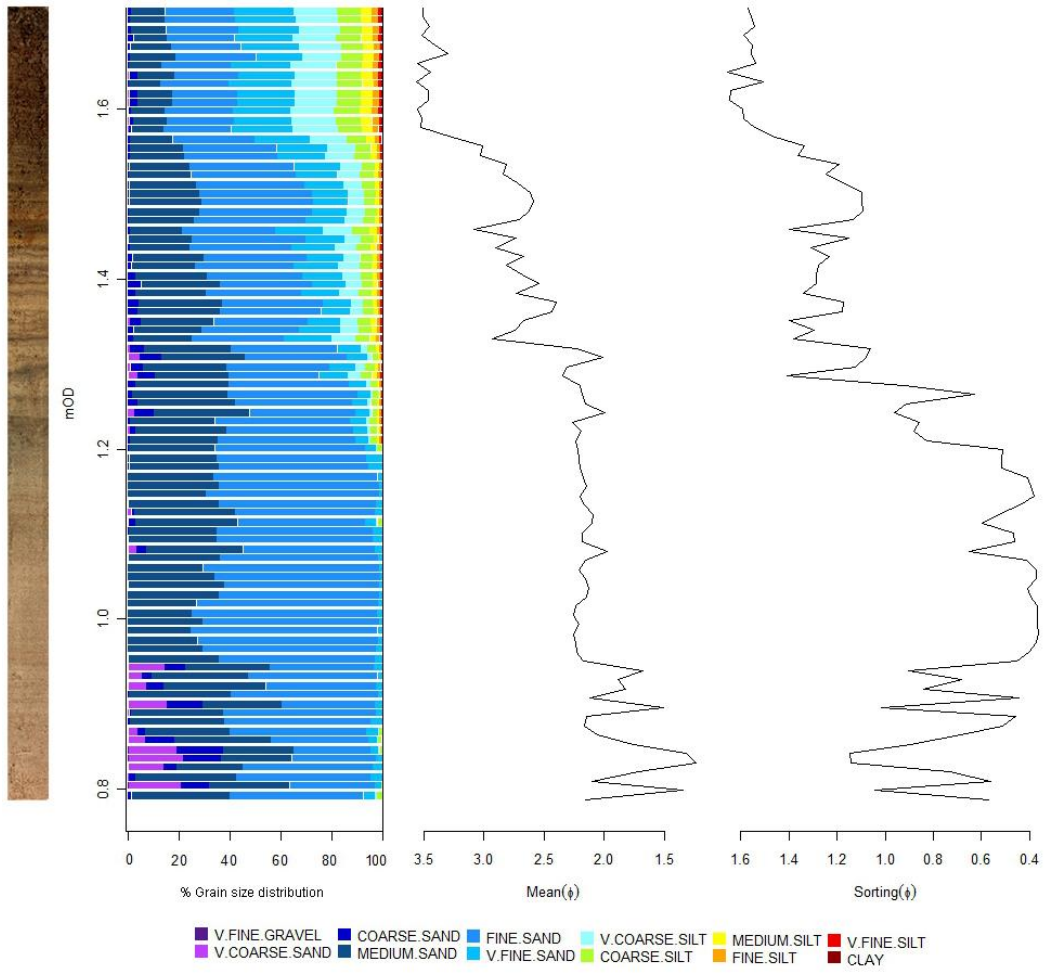

Figure 5.3 SFD3 downcore grain size distributions and mean and sorting values.

The bottom 10cm of the DYN1 core is dominated by fine sand with small percentages of very fine and medium sand. Above 1.15mOD the mean grain size decreases with an introduction of silt-sized material. Between 1.15mOD and 1.48mOD there is no overall increase or decrease in mean grain size. However, there is some variation, with several peaks and troughs in both mean grain size and sorting; this correlates with several alternating light (coarser) and dark (finer) layers in the stratigraphic log of this unit (Figure 5.2). Between 1.48mOD and 1.62mOD there is a decrease in mean grain size with an increase in percentage content of silt and clay sized material. Within this unit both mean grain size and sorting reach their minimum values within the core (Figure 5.4). Above 1.62mOD the mean grain size increases due to the slight decrease in the percentage content of silt and clay size material and the presence of coarse and very coarse sand. This coarse sand portion remains present to the top of the core.

Although similar to SFD3 in that it is dominated by sand sized material the range of mean and sorting values of DYN1 is less, i.e. 3.23 - 2.24ϕ (0.11-0.21mm) and 1.39 - 0.40ϕ respectively. The biplots of the grain size statistics are also noticeably different. Within the DYN1 core the

top and bottom samples are similar to each other predominately plotting in the same area on the biplots (Figure 5.5). The mid-core samples are distinct reflecting the decrease in grain size in the 1.48-1.62mOD unit. Similar to SFD3 an increase in mean grain size corresponds to an increase in both sorting and skewness values. The kurtosis values are highest in the mid-core samples. Comparison between the SFD3 and DYN1 biplots would suggest that the DYN1 mid-core samples are most similar in terms of their grain size characteristics to the top of core samples from SFD3. The bottom core samples are better sorted in SFD3 and more positively skewed.

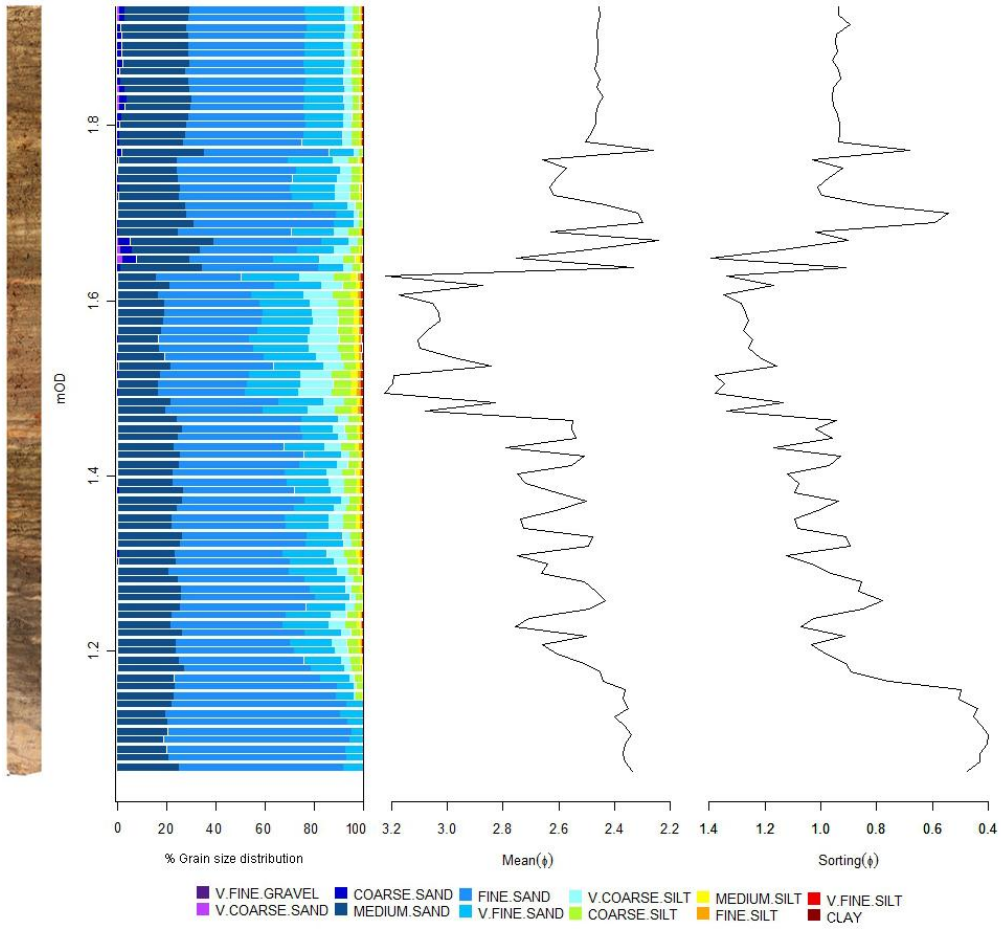

Figure 5.4 DYN1 downcore grain size distributions and mean and sorting values.

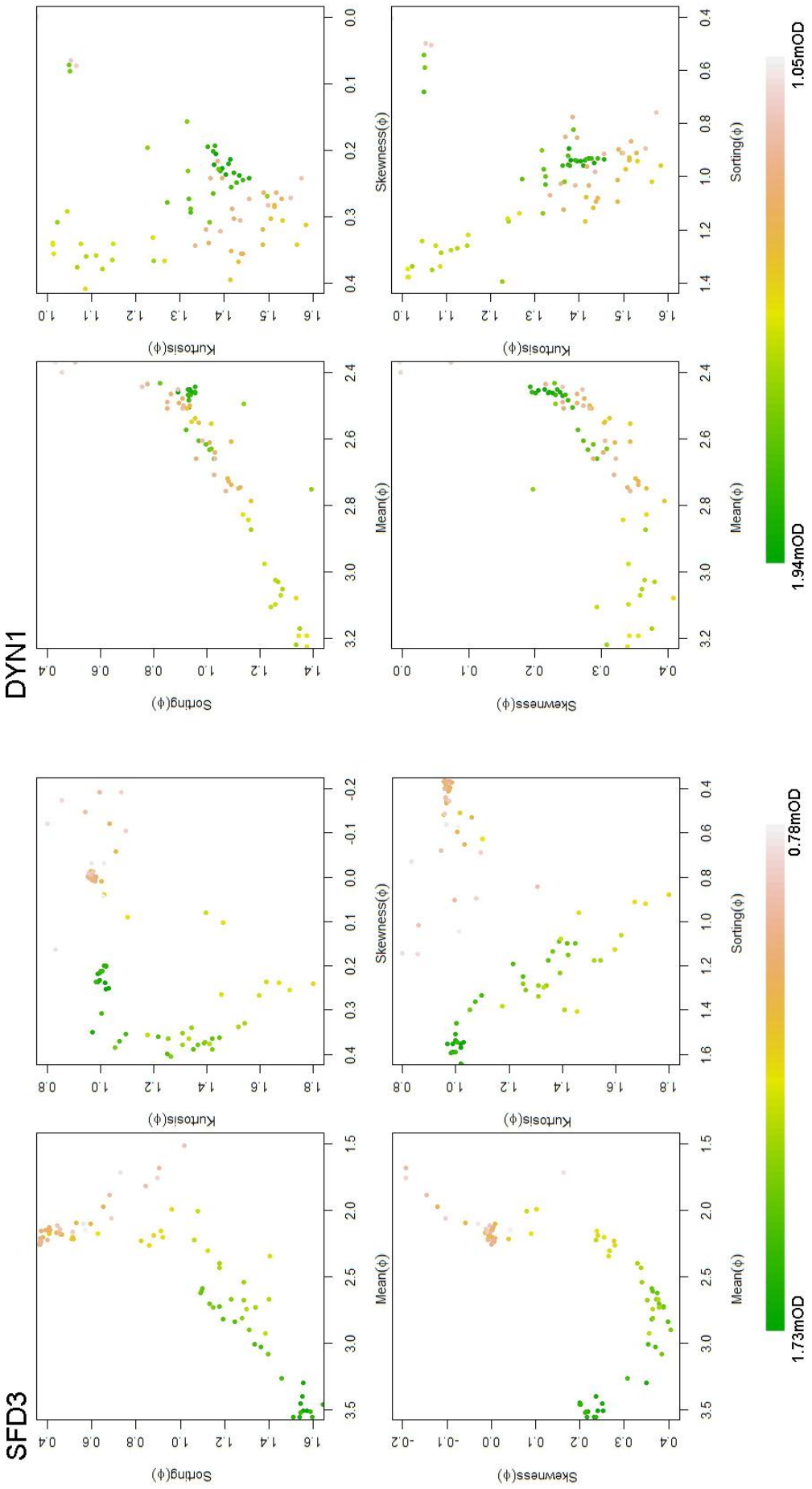

Figure 5.5 Biplots of grain size statistics for SFD3 and DYN1, position in core indicated by colour gradient.

Particle size distribution modelling

The *Shefsize* statistical programme (Robson *et al.* 1997) was used to fit the log-hyperbolic, log-skew-Laplace and log-normal distributions to each downcore sample. However, computational problems were encountered in fitting the log-hyperbolic model to some of the samples and therefore for these samples only log-skew-Laplace and log-normal statistics are available.

Problems fitting the log-hyperbolic model were encountered mostly in the SFD3 core where, for 22 out of 87 samples, log-hyperbolic statistics were not calculated. These are all in the bottom half of the core and often arise due to the coarser shell material fraction creating a distinct bimodal distribution. Of the 65 samples where all three models were fitted the log-hyperbolic had the highest *Ncrit* value (best fit) in 42 samples and the log-skew-Laplace in 23 samples. Of the 22 where log-hyperbolic was not fitted log-skew-Laplace was the best fit. Interestingly, the log-normal model was not a good fit for any of the distributions.

Figure 5.6 shows the log-hyperbolic shape triangle plot for the 65 SFD3 samples where all models were fitted. The log-hyperbolic values for the samples where the log-skew-Laplace was the best fit are also included to enable a more complete comparison of core samples. There is a clear clustering of samples based on their relative core depth: samples from the base of the core plot to the right and samples from the middle and top plot to the left. Within the middle and top samples there is also a clear distinction between the samples of the top ~20cm and the rest. This plotting path of samples from the left of the shape triangle to the right is indicative of an up-core transition from an erosional sedimentary environment in the bottom 10cm of the core to a depositional sedimentary environment above.

Due to the incomplete log-hyperbolic downcore record the similarity to the log-skew-Laplace values was assessed to establish its usefulness in providing information on the characteristics of the distribution. There is a good correlation between the tilt values for the log-hyperbolic and log-skew-Laplace values ($p = <2.2e\text{-}16$, $R^2 = 0.919$) it can therefore be assumed that the log-skew-Laplace tilt value profile provides an accurate representation of the downcore tilt values. Downcore variation in the log-skew-Laplace tilt factor for SFD3 (Figure 5.7) indicates a change in sediment characteristic at approximately 1.32mOD this corresponds approximately to the beginning of the right to left transition on the hyperbolic shape triangle. Between 1.32 and 1.58mOD the tilt factor is low and with little variation; above 1.58mOD the log-hyperbolic tilt factor becomes more variable and there is a slight increase in the variability of the log-skew-Laplace tilt factor (Figure 5.7). The log-skew-Laplace tilt factor plot suggests that the missing log-hyperbolic values would be more similar to the base of the core than those above 1.32mOD.

For the 86 DYN1 core samples the log-hyperbolic model could not be fitted to the bottom 8 samples. For the 78 samples where all models were fitted the log-hyperbolic model was the best

fit in 73 and the log-skew-Laplace in 5. These 5 are distributed throughout the core. Where the log-hyperbolic wasn't fitted the log-skew-Laplace was best fit in 3 and log-normal in 5.

Figure 5.6 shows the log-hyperbolic shape triangle plot for the 78 samples where all models were fitted. All samples plot on the left side of the triangle and although there is some clustering evident, i.e. samples from similar depths within the core plot closer together, the amount of downcore variation between sample groups seen in SFD3 is not present. This plotting pattern suggests a depositional sedimentary environment with little change throughout the core.

Again due to the incomplete log-hyperbolic downcore record the similarity to the log-skew-Laplace values was assessed to establish its usefulness in providing information on the characteristics of the distribution. There is a good correlation between the tilt values for the log-hyperbolic and log-skew-Laplace values ($p = <2.2e\text{-}16$, $R^2 = 0.832$) the log-skew-Laplace tilt value profile, therefore, provides an accurate representation of the downcore tilt values. Compared to SFD3 the variation in tilt factor throughout the DYN1 core is much less (Figure 5.7). The log-skew-Laplace tilt factor indicates a significant change between the sediments at the base of the core and those above 1.15mOD. This change is not seen on the hyperbolic shape triangle as log-hyperbolic values were not able to be calculated for samples below 1.15mOD. The tilt factor is low and consistent to 1.63mOD above which it is more variable.

When comparing the tilt factors between SFD3 and DYN1 there appear to be very few similarities between the two profiles. There is a coincident section of low and consistent values seen in both cores between 1.32 and 1.62mOD. This may be indicative of similar processes influencing sediment deposition at each of the core sites during this period assuming deposits at a similar elevation within the core were deposited at the same time. However the differences between the two cores are potentially more significant as they highlights that environments that may initially appear visually similar are affected by different sediment depositional processes. The location of the sites within the estuary is likely to have a significant effect on the sediment depositional characteristics. The suggestion of a more erosional environment in the base of SFD3 (tidal flat section) is likely to be a result of its greater exposure to the prevailing winds and therefore greater aeolian action over the then tidal flat surface. Conversely, Derryness's position further within the estuary and to the south of the rocky promontory of Derryness Point affords it some protection from these prevailing winds.

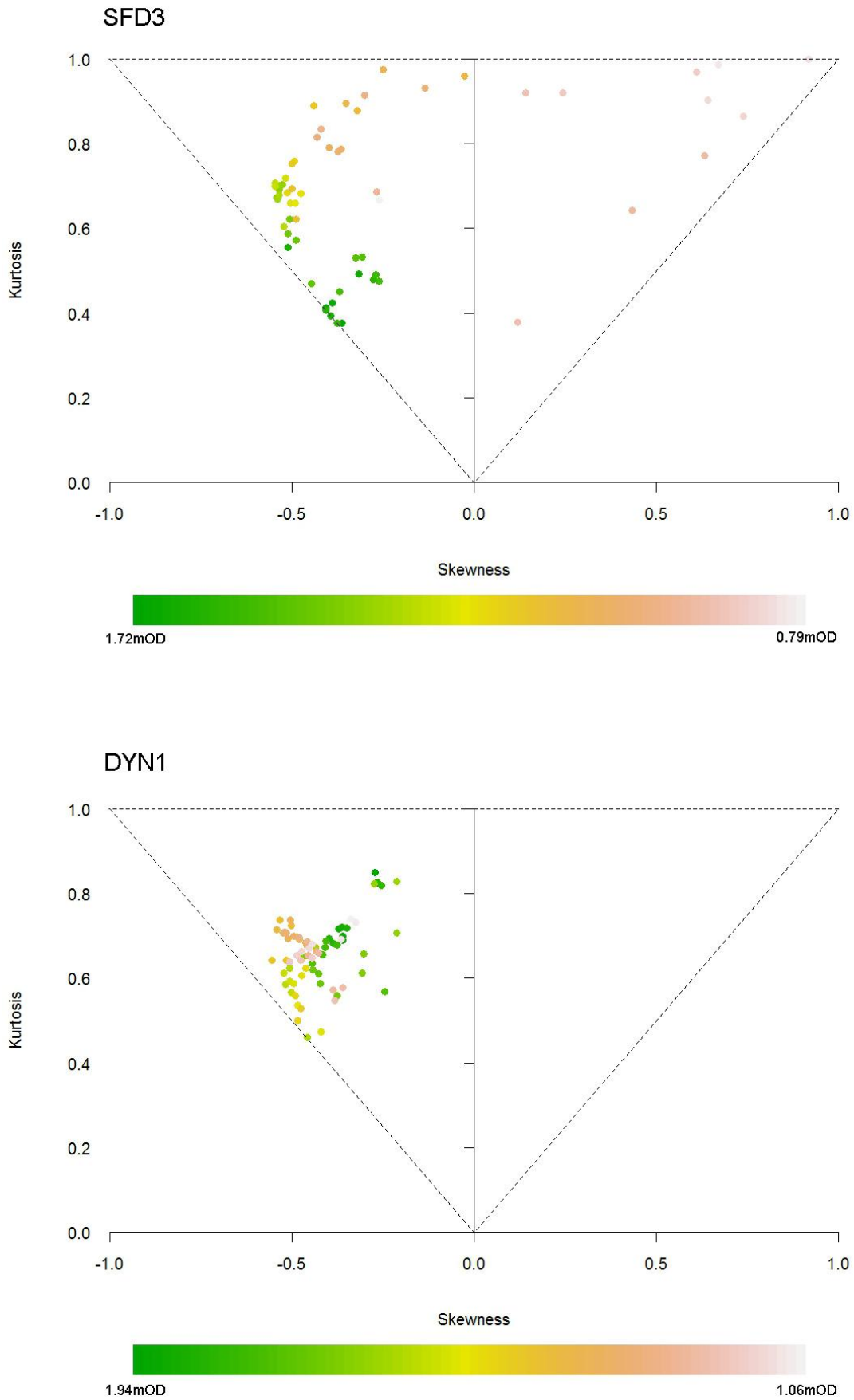

Figure 5.6 Log-hyperbolic shape triangle plot of SFD3 and DYN1 core samples (interpreted as depositional on the left of the diagram and erosional on the right). Position in core indicated by colour gradient.

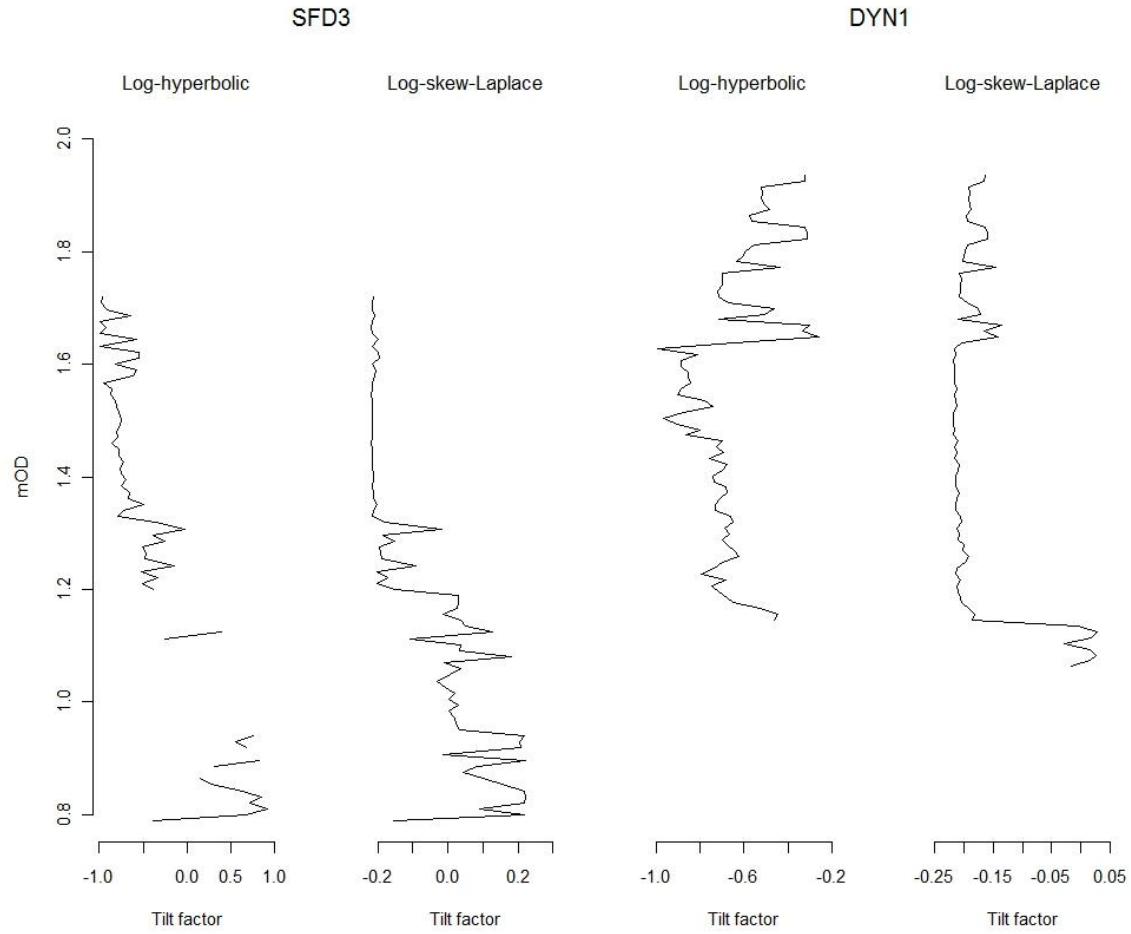

Figure 5.7 Downcore variations in log-hyperbolic and log-skew-Laplace tilt factors (Skewness/Kurtosis) for SFD3 and DYN1.

5.3.2. Quartz grain microtextures

Examination of quartz grain surface textures via SEM can enable the determination of transport mode and environment of deposition of the sand grains (e.g. Madhavaraju et al., 2009 and Krinsley and Donahue, 1968). Accordingly, selected subsamples of the SFD3 and DYN1 cores were analysed in this way. This environmental interpretation is based upon the presence of characteristic surface textures (Table 4.1) The presence of V-shaped indentations, conchoidal breakage and upturned cleavage plates was recorded for each of the SFD3 and DYN1 subsamples (see section 3.3.4). The identification of these features was based upon examples described by Krinsley and Funnel (1965) and Krinsley and Donahue (1968) from various coastal environments and laboratory produced samples. Downcore variation in the occurrence of the quartz grain surface textures is summarised in Figure 5.9. Quartz grain roundness was also recorded.

Within SFD3, the presence of upturned cleavage plates (Figure 5.8) is more common below 1.2mOD, possibly indicating greater influence of aeolian actions on these sediments. The two samples between 1.2mOD and 1.4mOD are dominated by conchoidal breakage features.

However, the number of occurrences of conchoidal breakage feature in these samples is similar to throughout the rest of the core, therefore, likely indicates, a reduction in the actions producing V-shaped indentations and upturned cleavage plates. V-shaped indentations are present both below 1.2mOD and between 1.4mOD and the top of the core. There is little variation in the number of occurrences of this feature, which may indicate that the subaqueous collision is fairly constant throughout the deposition period. The quartz grain roundness is predominately sub-angular and also exhibits little variation between samples and no apparent increasing or decreasing trends.

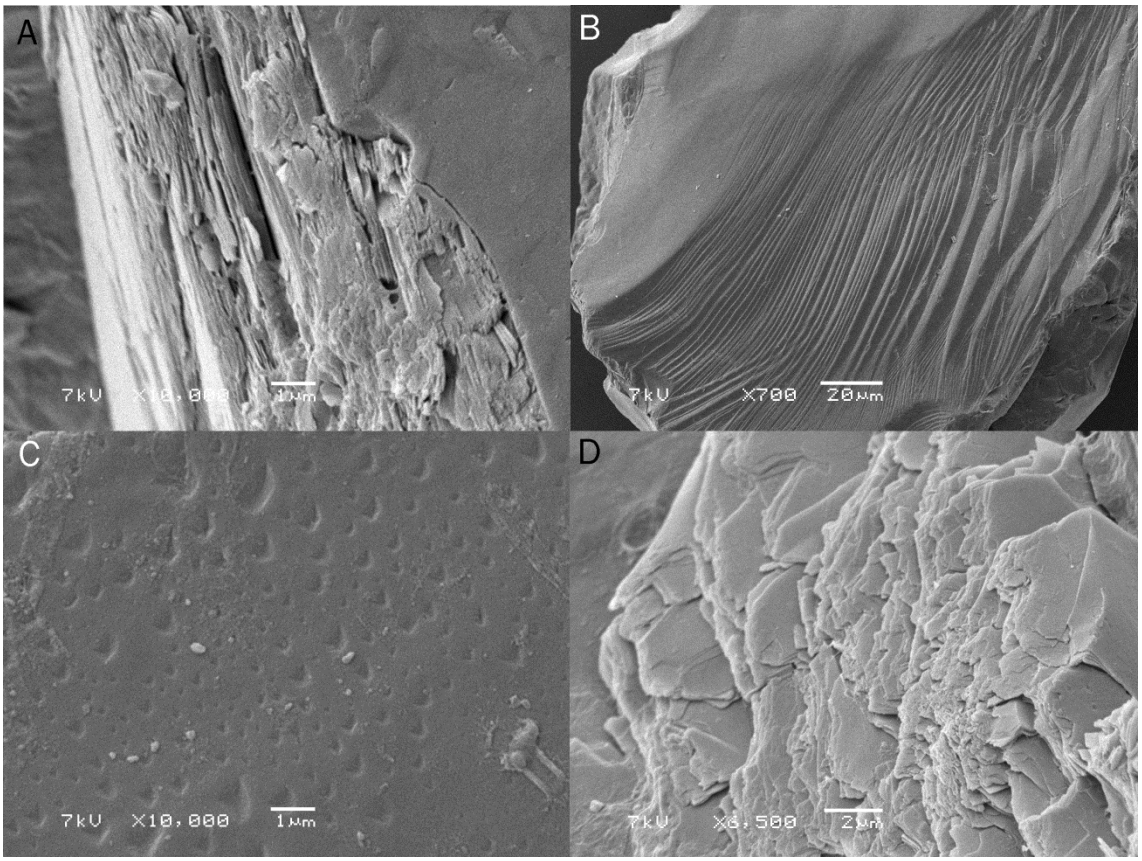

Figure 5.8 Examples of surface textures identified in the sediment core samples: A) upturned cleavage plates SFD3 1.7mOD; B) Conchoidial breakage SFD3 1.53mOD; C) V-shaped indentations DYN1 1.75mOD; D) upterned cleavage plates DYN1 1.42mOD.

Within the DYN1 core, there are no occurrences of upturned cleavage plates (Figure 5.8) below 1.4mOD, which implies a predominately subaqueous depositional environment. Within the three samples below 1.4mOD there is an increase in the presence of conchoidal breakage and decrease in V-shaped indentations (Figure 5.8) upcore possibly indicative of an increase in the energy of the depositional environment. Between 1.4mOD and 1.8mOD upturned cleavage plates are present in all samples indicating the influence of aeolian actions on the sediment. However, V-shaped indentations and conchoidal breakage patterns are also present within these samples. The two samples immediately above 1.8mOD only display conchoidal breakage surface features; this may indicate a higher energy depositional environment in the

corresponding time interval. As in the SFD3 core, the majority of grains are sub-rounded with little variation throughout the core.

The majority of the samples analysed contained two or more types of microtexture on one grain surface. This may suggest a mixed depositional environment or grains having gone through several periods of transportation and retaining the surface textures imposed by previous phases. This is significant as it highlights the importance of reworking of sediment within the sediment supply limited estuary in the creation and evolution of new depositional features.

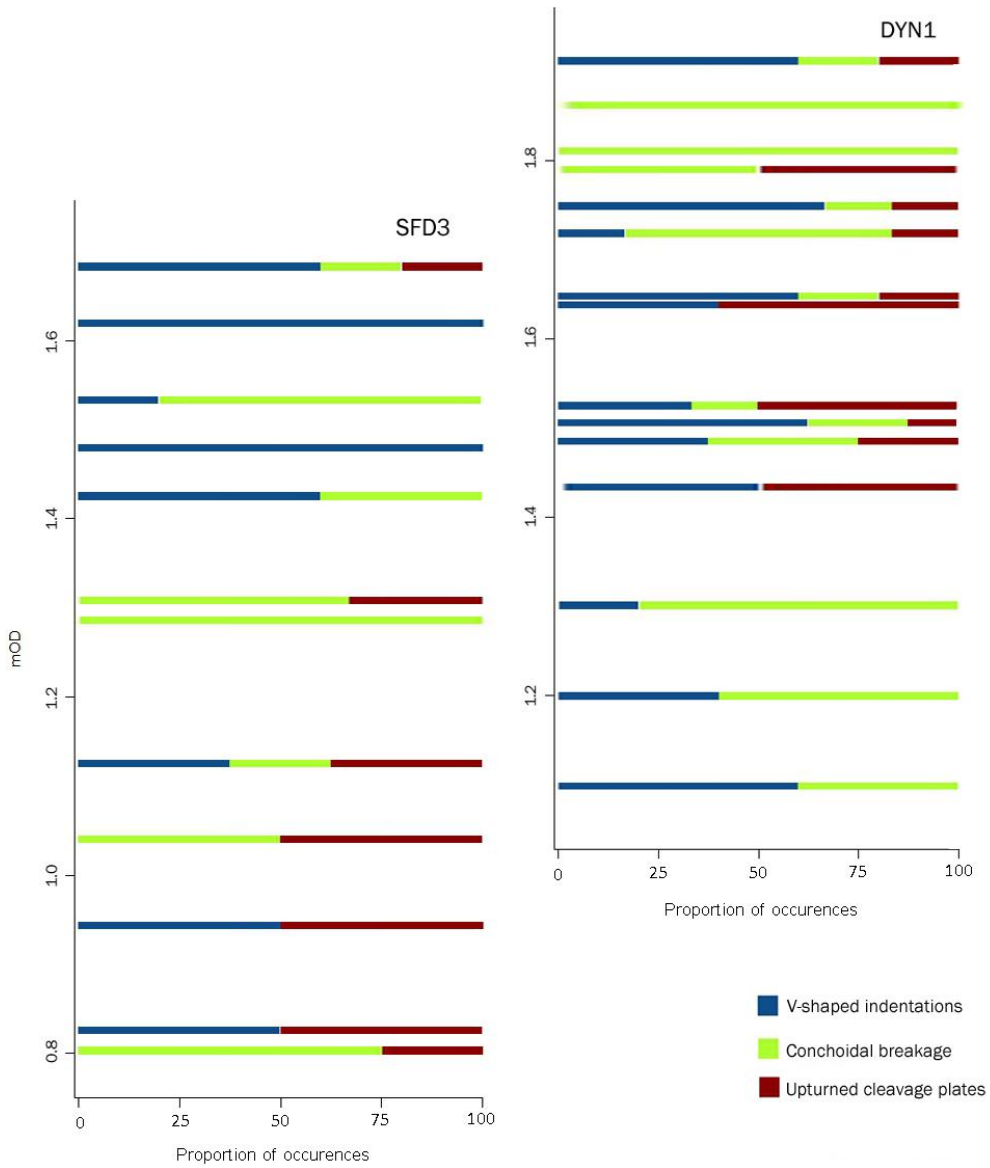

Figure 5.9 Proportion per sub-sample of quartz grain surface microtexture features for SFD3 and DYN1.

5.4. Geochemistry: organics and carbonates

Organic and carbonate contents were analysed for each 1cm subsample of the SFD3 and DYN1 cores.

Within the SFD3 core organic content is low (approx. 1%) from the base of the core to around 1.21mOD (Figure 5.10). From 1.21mOD to approximately 1.55mOD organic content rises gradually to ~4% with two peaks of 4% at 1.34mOD and 1.41mOD corresponding to darker layers within the unit (Figure 5.10). Above 1.55mOD to the top of the core the organic content rises significantly to a maximum of 14%. This increase corresponds to the transition to darker organic rich sediment at the top of the core.

Carbonate content within the SFD3 core decreases from 10% at the base to 4% at 1.17mOD. Within this unit there is some local variability and a dominant peak at 1.12mOD. Above 1.17mOD the carbonate content rises quickly to 18%. There are four peaks ranging from 17-20% between 1.17 and 1.42mOD. Throughout this lower half of the core local variability reflects the repeated occurrence of shell-rich layers (Figure 5.1, Figure 5.10). Above this there is a dramatic decrease in carbonate content with values dropping to ~0%, i.e. within measurable limits, at 1.45mOD (Figure 5.10). This sudden decrease in carbonate values correlates with the initiation of the rise in organic content toward the top of the core and the transition (interpreted from the stratigraphic log) from probable tidal flat to vegetated marsh/machair and related soil development.

The organic content at the base of the DYN1 core is approximately 0.5% increasing to 2% between 1.18mOD and 1.47mOD with three peaks reaching 3% (Figure 5.10). Immediately above this unit there is a sharp peak at 1.52mOD where organic content reaches its maximum within the core (6%). This appears to be associated with a slightly darker layer within the core and also with the possible tidal flat to marsh/machair transition previously identified. It is therefore probable that this increase in organic content is indicative of vegetation and soil development. Above this peak organic content gradually drops from ~4% to ~2% at the top of the core, although there is some variation. The organic content within this core is 1 to 2% higher than those seen within majority the SFD3 core with exception of the higher contents within the relatively organic rich top to the SFD3 core.

Carbonate content within the DYN1 core is low with values of around 0.5% for the majority of the section. There is a peak at 1.79mOD where values reach 3.5% and this is associated with a lighter, sandier layer within the section and also a trough in the organic content (Figure 5.10). With exception of the peak described, the carbonate content of the DYN1 core is similar to that of the low values seen at the top of the SFD3 core, i.e. background values.

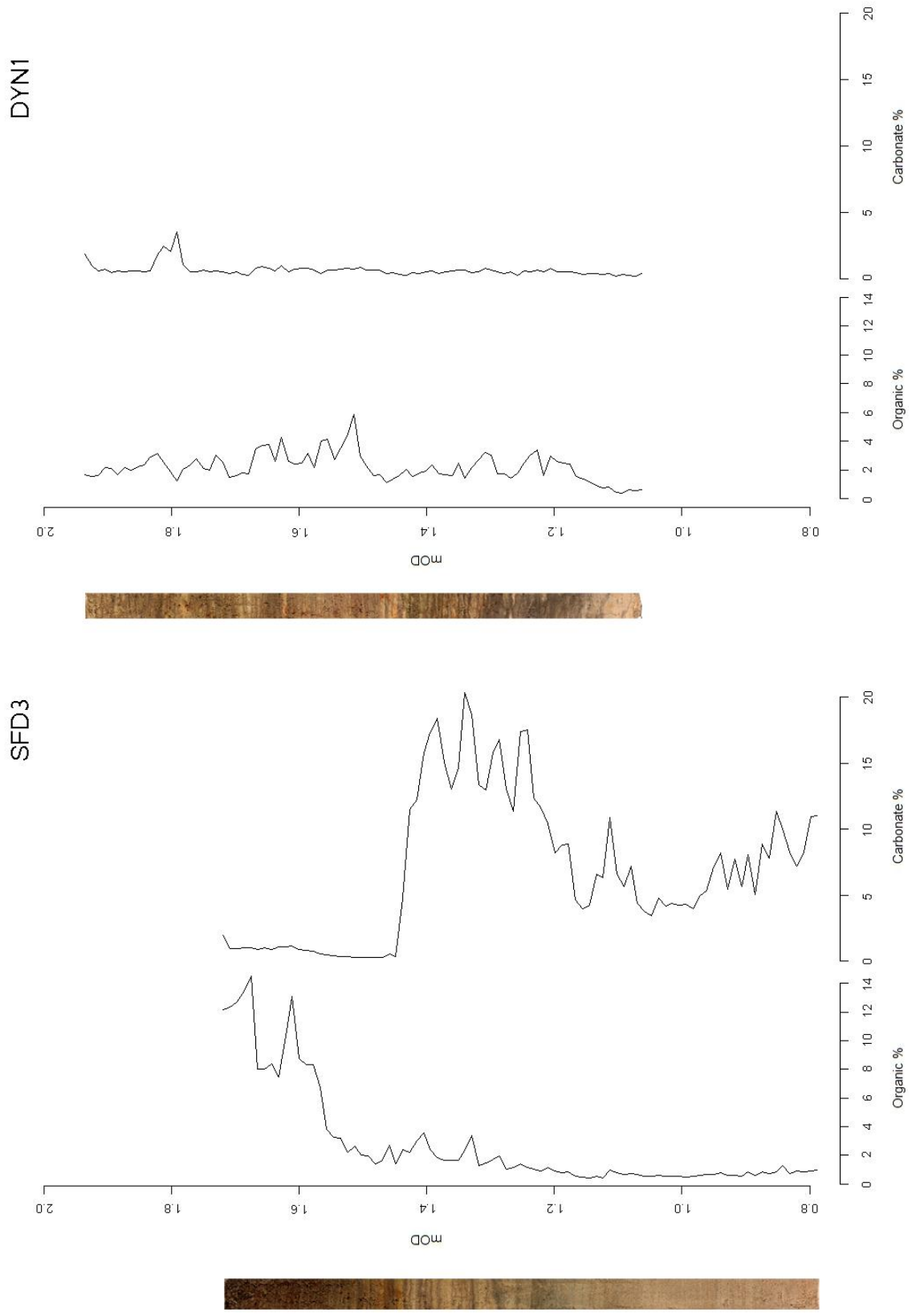

Figure 5.10 Organic and carbonate percentage content of SFD3 and DYN1.

5.5. Downcore diatom assemblages

Diatom counts were made on the selected subsamples of the SFD3 and DYN1 (see section 3.3.4). A total of 12 samples were taken from SFD3 and 15 from DYN1. However, of the samples taken, 14 from DYN1 and only 5 from SFD3 contained diatoms. A total of 38 species were identified within the core samples; 27 present in SFD3 with 2 of these only seen in this core and 36 present in DYN1 with 11 only seen in this core (Table 5.2).

The absence of any diatoms in many of the samples is potentially due to two reasons. Firstly, a lack of diatoms on the surface or within the sediment at the time of deposition. As has been seen in the analysis of the present day environment diatoms are mostly absent from the tidal flat area and present in varying abundances on the vegetated areas. It is therefore likely that in some of the more sandy layers within the core the lack of diatoms is due to their absence from the environment at the time of deposition. However, the second potential reason for their absence is dissolution of the values post-deposition. Therefore care has to be taken when drawing conclusions from these results. For example the general trend of increasing percentage of broken valves towards the top of the core may be a result of the lower valves dissolving.

Table 5.2 Diatoms species list for the Sandfield (SFD3) and Derryness (DYN1) cores.

Life form	SFD3	Both	DYN1
Planktonic		*Actinocyclus normanii* *Actinoptycus senarius* *Cosinodiscus radiatus* *Paralia sulcata*	
Benthic	*Navicula cryptolyra* *Navicula jaernefeltii*	*Caloneis westii* *Cocconeis placentula* *Cocconeis sublittoralis* *Diploneis didyma* *Diploneis interrupta* *Diploneis lineata* *Diploneis notablis* *Eunotia intermedia* *Fragilaria exigna* *Fragilaria pinnata* *Hantzschia marina* *Hantzschia virgata* *Navicula cincta* *Navicula forcipata* *Navicula halophila* *Navicula halophiloides* *Navicula humerosa* *Navicula pennata* *Navicula arenaria* *Pinnularia cruciformis* *Rhaphoneis suriella*	*Achnanthes longipes* *Amphora ostrearia* *Caloneis branderii* *Cosinodiscus maginatus* *Diploneis suborbicularis* *Navicula abrupta* *Navicula maculosa* *Navicula palpebralis* *Pinnularia rectangulata* *Pleurosigma strigosum* *Tabellaria flocculosa*

Paralia sulcata can be either a benthic or planktonic species (Witon etal, 2006). Here it is treated as a planktonic species as it is common in coastal plankton (Tomas, 1996) and its presence in the study environment is likely to be indicative of tidal deposition. In the majority of core samples *Diploneis interrupta* was the dominant species with *Navicula cincta,* and *Navicula arenaria* making up significant contributions (Figure 5.11). *Navicula halophila* is a significant contributor to the total diatom valves counted in the lower core samples of DYN1 (i.e. 1.3mOD and 1.2mODcm). Comparatively, the DYN1 samples contain a significantly higher proportion of *D. interrupta* than SFD3. Of the remaining dominant species the proportions are similar.

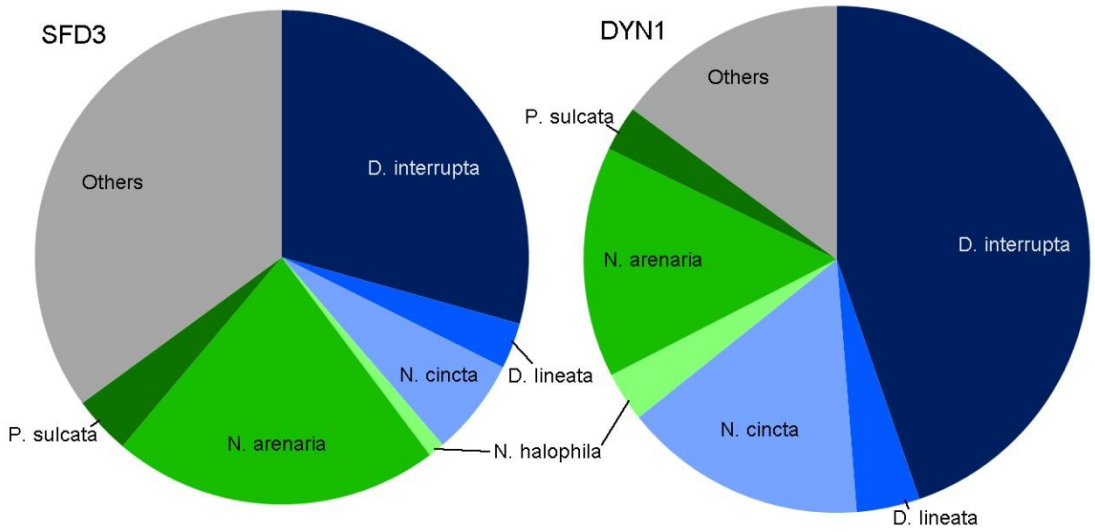

Figure 5.11 Comparison of proportions of most abundant diatoms species in SFD3 and DYN1

PCA analysis of the diatom core samples (Figure 5.12) shows the limited presence of diatoms in SFD3. It also highlights the importance of the four diatom species identified above together with *Fragularia pinnata* and *Navicula forcipata* in explaining the variation seen in the core samples. The main gradient in species data, i.e. PC1, is represented in the DYN1 samples. It is notable that variation between the SFD3 and DYN1 samples is less than within the DYN1 samples alone. This is likely in part due to the lack of samples containing diatoms from the SFD3 and therefore a reduced variety in the environments represented.

For interpretation and reconstruction of sedimentary environments Vos and De Wolf (1993a) advocate the classification of coastal diatoms by life form and salinity (Figure 5.13). Benthic/epiphytic diatoms species from all halobian groups and planktonic species from the marine and brackish groups were present in the cores. Figure 5.15 shows the results of this analysis for the DYN1 core together with the downcore variations in the relative abundance of the most important diatom species, i.e. those with a relative abundance >1%. Species with relative abundances <1% were not included to aid visualisation of the data. A cluster analysis was performed on the DYN1 diatom data to determine groupings of samples that could be used

to identify different units within the core (Figure 5.14). The cluster analysis was carried out using Ward's method which forms clusters by maximising the within group similarities (Primpas et al, 2008). This method is generally regarded as being very efficient and produces a well-proportioned hierarchical structure (Swan and Sandilands, 1995).

It was not possible to assess the downcore variation in any detail for the SFD3 core due to the lack of samples containing diatoms.

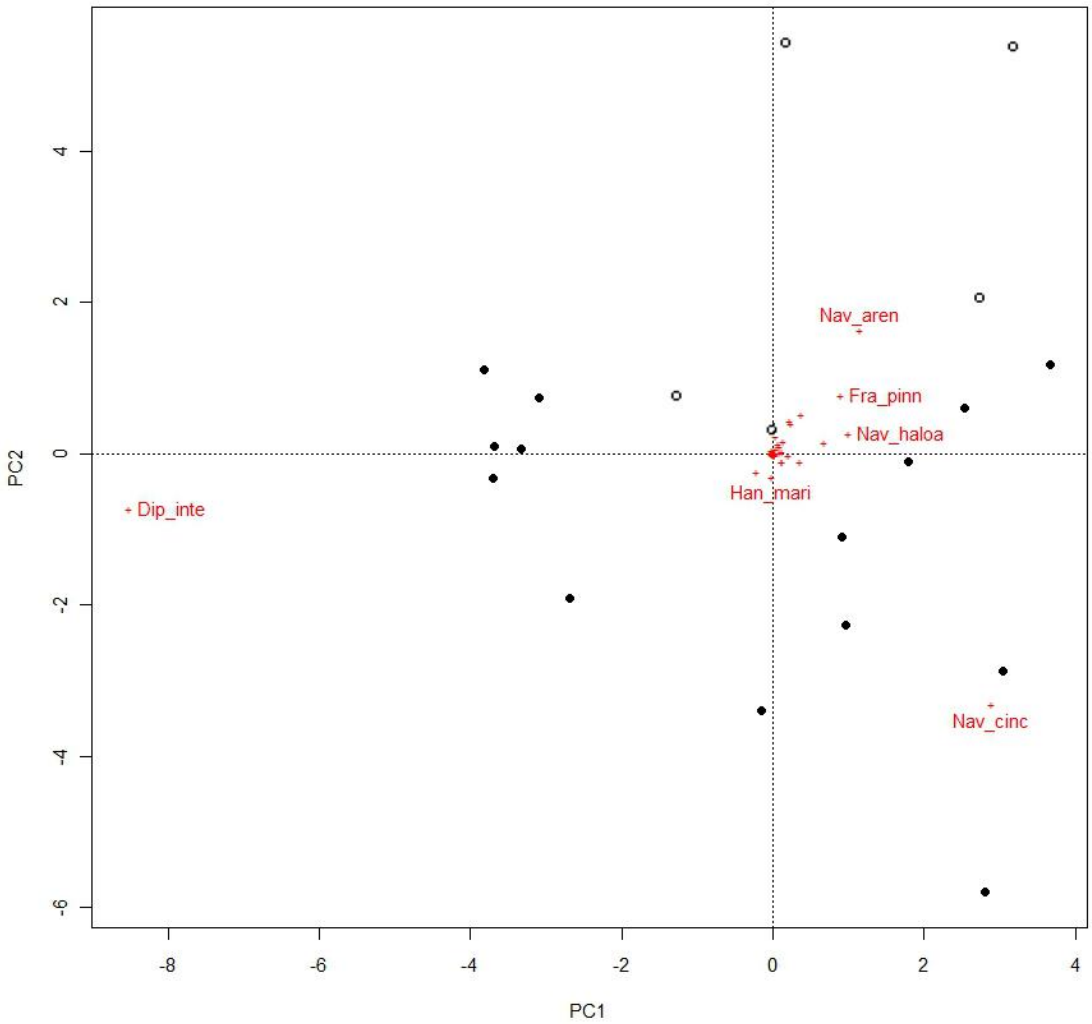

Figure 5.12 Ordination plot of PCA analysis of diatom data for SFD3 (white circles) and DYN1 (black circles). Diatom species shown as red crosses and a selection labelled. Eigenvalues: PC1 = 64.86%, PC2 = 12.08%

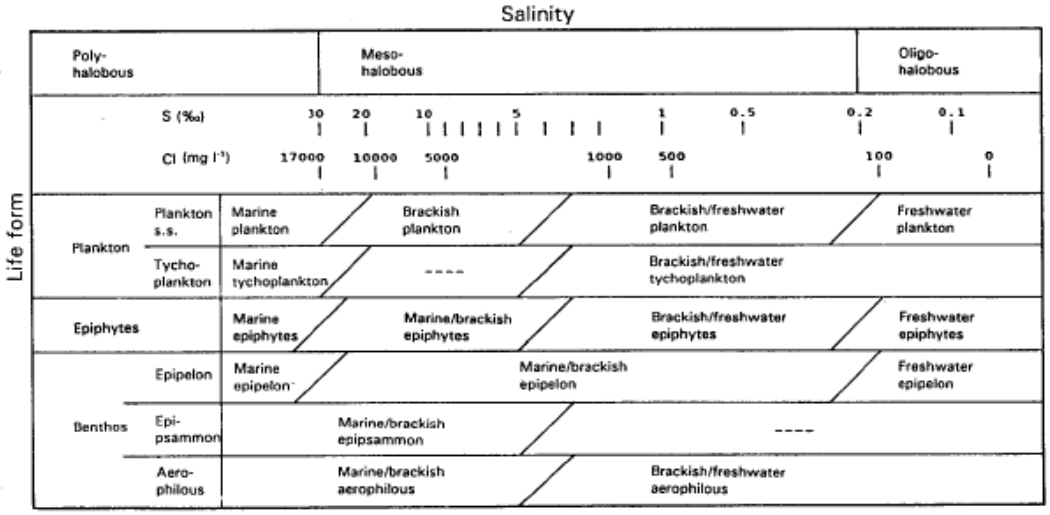

Figure 5.13 Classification of diatom ecological groups based on life form and salinity (Vos and De Wolf, 1993a).

The results of the cluster analysis suggest three distinct groups of samples within the DYN1 core at distance 60 (Figure 5.14). Of these, group 1 is the most distinct and contains all samples from 1.63 to 1.81mOD. Groups 2 and 3 are more similar with group 2 containing samples from above and below the group 1 samples. Group 3 contains the two lowest depth samples and also one sample from above the group 1 samples.

As a result of the cluster analysis and visual interpretation of the downcore variation the DYN1 core can be divided into three units based the diatom content: Unit A – 1.19 to 1.58mOD; Unit B – 1.58 to 1.84mOD and Unit C – 1.84 to 1.91mOD (Figure 5.15).

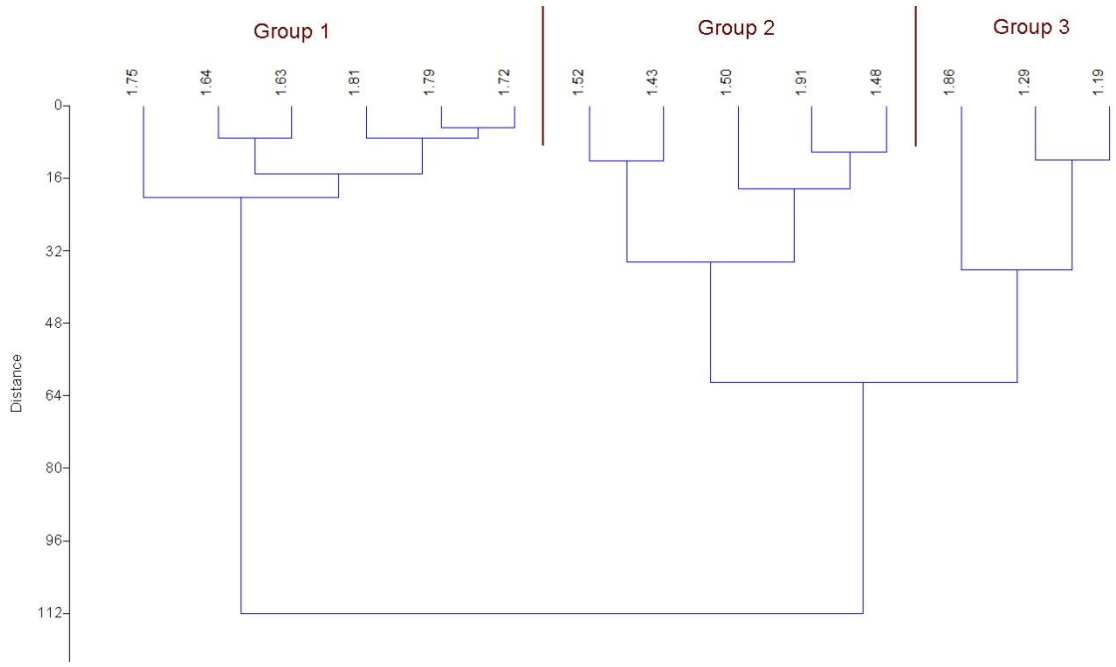

Figure 5.14 Cluster analysis of the DYN1 diatom data. Groupings of samples indicated at Distance of 60 (individual sample values represent mOD).

There is little downcore variation in the abundance of the majority of the pelagic species and no appreciable change between the three units. However, there is a slight increase in *Paralia sulcata* in the middle of the core between 1.48mOD and 1.64mOD. *P. sulcata* is the dominant pelagic species present. This is likely to be because it has a highly silicified frustule which withstands transport and dissolution well (Witon *et al*, 2006) thereby enhancing its preservation potential. The presence of these marine/estuarine pelagic species in relatively low abundances throughout the core could be due to regular tidal inundation and deposition or aeolian transport and deposition onto the sample site. With exception of some of the highly silicified *P. sulcata* valves the pelagic valves within the subsamples are all broken, again indicative of transport post-mortem and prior to deposition.

The most common benthic species are those that were identified as explaining the most variation in the PCA analysis (Figure 5.12), i.e. *Navicula arenaria, N. cincta* and *Diploneis interrupta*. These three species are present throughout the core but there is a clear transition in the diatom assemblage downcore. Within Unit A, *N. cincta* dominates and its relative abundance increases upward through this unit. *N. arenaria* and *D. interrupta* are also present in significant abundances in this part of the core. *D. interrupta* increases in abundance to the top of the unit whereas the abundance of *N. arenaria* decreases slightly. Due to the lack of diatoms in some samples the exact position and nature of the transition between Units A and B cannot be described. Within Unit B *D. interrupta* dominates with abundances of approximately 70%. Within this section the relative abundances of *N. cincta* drop considerably to approximately 3% in the majority of subsamples. The abundances of *N. arenaria* also drop slightly but are still present at 10-20%. *D. interrupta* is still the dominant species in Unit C. However its relative abundance drops to between 20-40%. The relative abundances of *N. arenaria* and *N. cincta* increase in this unit.

These changes are reflected in the plot of the salinity group changes throughout the core (Figure 5.15). The representation of the polyhalobous, mesohalobous, and oligohalobous – halophilous groups in approximately equal amounts and the presence of the oligohalobous – indifferent group in Unit A is possibly indicative of a mixing coastal environment where diatoms were being deposited, both autochthonously and allochthonously, from marine and brackish environments. There is an increase in the mesohalobous percentage within Unit B due to the increase in *D. interrupta*. Within this unit the oligohalobous – halophilous and indifferent percentages significantly decrease. *D. interrupta* is an aerophilous species present in supratidal environments (Vos and de Wolf, 1993b). It is therefore possible that the increase in *D. interrupta* is indicative of an environment emerging above MHWS. However, the continual presence of pelagic species suggests a continuing marine influence. Within Unit C the mesohalobous percentage decreases and oligohalobous – halophilous increases associated with the decrease in *D. interrupta* and increase in *N. cincta*. *N. cincta* is a brackish water epipelon

species common on salt marshes (Vos and de Wolf, 1993b; Witkowski, 1991). Its presence above and below the *D. interrupta* maximum of Unit B may be suggestive of a more vegetated marsh environment.

The percentage of broken valves ranges from 30 to 80%. The lowest percentage of broken valves is at the base of the core. This may be due to the preferential preservation of stronger frustules. The percentage broken increases up-core reaching a maximum at the top of Unit B; above this the percentage broken decreases. The increase in broken valves within this section suggests a more disturbed environment or greater transportation of diatoms onto the area of deposition during this period.

The downcore variations and cluster analysis suggest a significant change in the depositional environment of the core sediment from Unit A to B. Unit C is more similar to Unit A suggesting a change, approaching a return to the initial conditions, towards the top of the core.

Within the SFD3 core *D. interrupta*, *N. cincta* and *Fragilaria pinnata* are the most abundant diatom species; *P. sulcata* is also present in all 5 samples that contain diatoms. These four species represent the mesohalobous, oligohalobous – halophilous, oligohalobous – indifferent and polyhalobous salinity groups respectively, again indicative of a mixing coastal environment in which they were deposited.

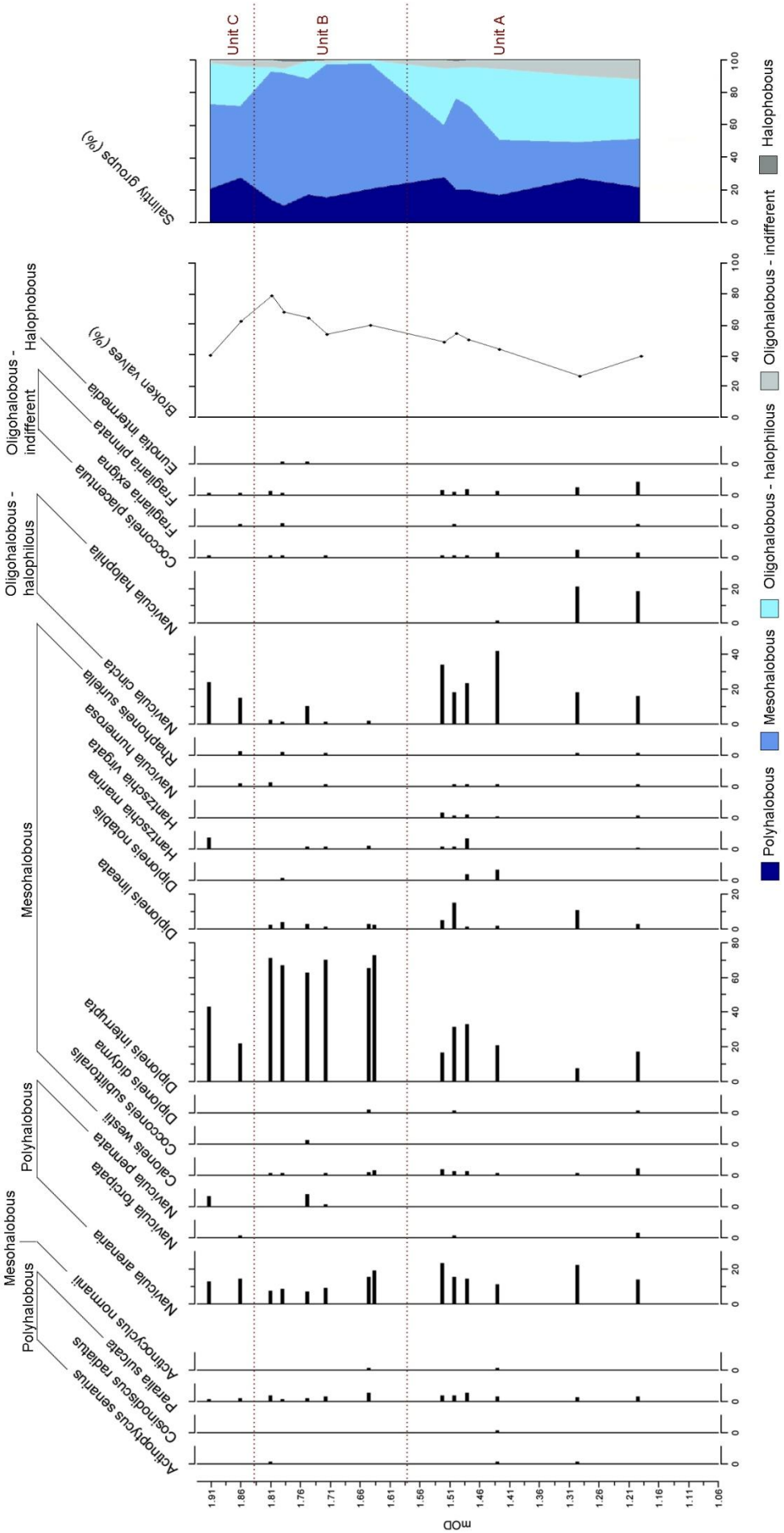

Figure 5.15 Downcore variations in relative abundance of individual diatom species and salinity groups for DYN1 (see pg 129 for further description of the downcore changes in salinity groups)..

5.6. Core dating results

5.6.1. ^{210}Pb and ^{137}Cs

^{210}Pb activities in SFD3 show a rapid decline with depth (Figure 5.16), from near-surface activities exceeding 100 Bq/kg, to 6 Bq/kg at 1.51mOD. The simple model of ^{210}Pb dating was applied and an accumulation rate of 1.2mm/yr calculated. ^{137}Cs shows two distinct subsurface activity peaks at 1.70mOD and 1.66mOD depth, with values rapidly decreasing to at or near detection limits (2 – 3 Bq/kg) below 1.60mOD. These peaks are likely to be discrete ^{137}Cs spikes as there is little evidence (based on the ^{214}Pb activity-depth profile) of significant variation in sediment composition over the 1.70mOD - 1.66mOD interval. The west coast of Ireland is unlikely to receive much Sellafield-derived ^{137}Cs but will have received appreciable Chernobyl fallout. The ^{137}Cs spikes, therefore, most likely correspond to 1986, Chernobyl fallout maximum, and 1963, the year of peak ^{137}Cs fallout from above-ground nuclear weapons testing. A similar distribution of ^{137}Cs was observed in saltmarsh cores from the Donegal/Sligo region by Wheeler *et al.* (1999b), who also attributed the observed subsurface activity maxima to ^{137}Cs input from Chernobyl and above ground nuclear weapons testing. Attributing the 1.70mOD spike to 1986 gives a sediment accumulation rate of 1.4mm/yr, while attributing the 1.66mOD spike to 1963 gives a sediment accumulation rate of 1.3mm/yr, in good agreement with the ^{210}Pb-derived rate.

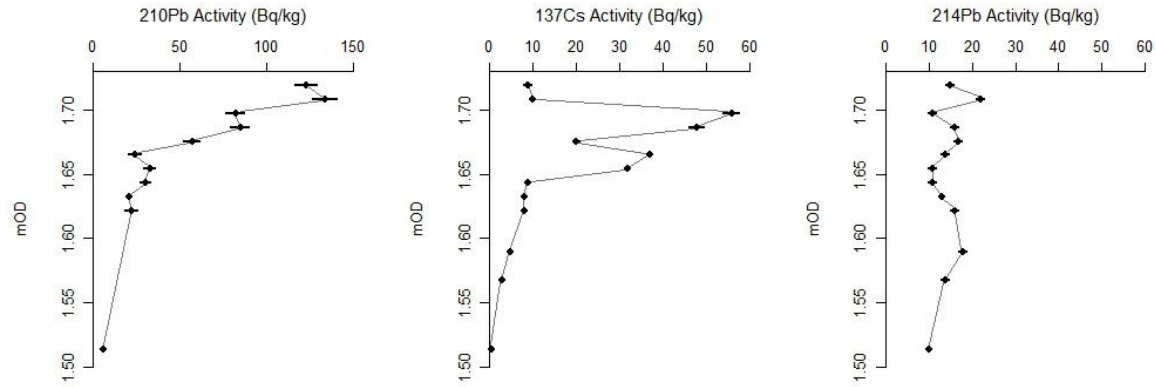

Figure 5.16 ^{210}Pb, ^{137}Cs and ^{214}Pb activity vs. depth for SFD3.

A sediment accumulation rate of 1.3 ± 0.1mm/yr would make the base of the SFD3 core between 676 and 789 years old in 2008, dating the base of the core to around 1220 to 1330 AD. However, due to the lack of datable sediment lower in the core, this calculated accumulation rate is based upon samples from the top 25cm of the core. As discussed previously the characteristics of the SFD3 core change significantly downcore, i.e. upper organic-rich units above the tidal flat/vegetated machair transition (1.47mOD) and minerogenic units below. This dating evidence, therefore, relates specifically to the upper units and accumulation rates may

change significantly within the sediments below 1.50mOD consequently there is a large amount of uncertainty in dating the base of the core. However dating of the tidal flat/vegetated machair transition can be more accurate. A sediment accumulation rate of 1.3 ± 0.1mm/yr would position this boundary to between 186 and 217 years old, dating it to approximately 1790 - 1820 AD.

^{210}Pb activities in core DYN1, while slightly exceeding those of ^{214}Pb, are significantly lower than those in the surficial layers of core SFD3, and show a relatively erratic profile with depth (Figure 5.17). The slight subsurface maximum in ^{210}Pb activity at 1.83 - 1.81mOD corresponds to a similar maximum in ^{137}Cs and ^{214}Pb activity, indicating that this activity maximum most likely reflects a change in sediment composition or supply, rather than variations in atmospheric fallout. ^{137}Cs is present throughout core depth at relatively low, but clearly detectable, activities, and shows no discrete activity maxima that can be definitively linked to atmospheric fallout events. The presence of ^{137}Cs throughout the core depth, the lack of clear decline of ^{210}Pb activity with depth, and the broad correlation between the activity-depth profiles of ^{137}Cs, ^{210}Pb and ^{214}Pb are all consistent with the "linear" or "erratic" profile type described by Cundy *et al.* (2003). Large-scale variations in sediment composition and/or rapid sediment accumulation rates mean that the vertical distribution of ^{137}Cs and ^{210}Pb is controlled by input on reworked sediment particles and by variations in sediment composition, rather than by atmospheric fallout. As such, it is not possible to accurately ascribe a sediment accumulation rate to this sequence.

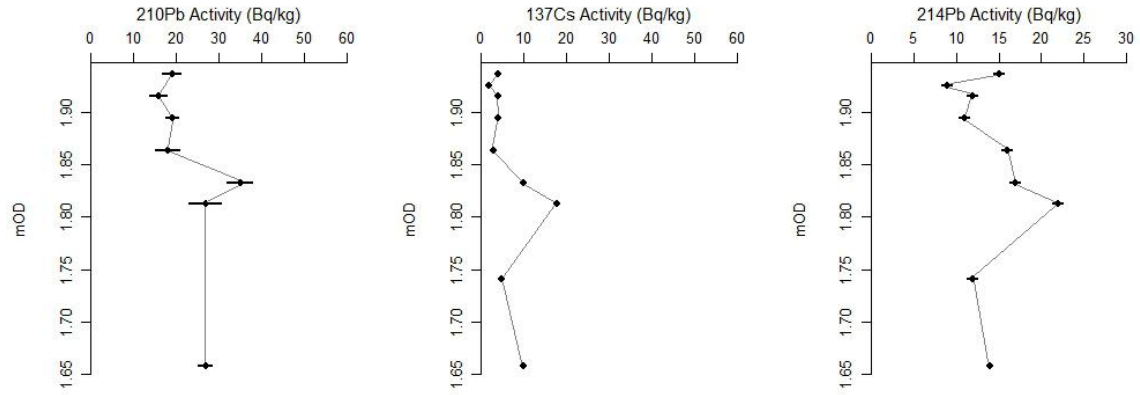

Figure 5.17 ^{210}Pb, ^{137}Cs and ^{214}Pb activity vs. depth for DYN1

5.6.2. Optically stimulated luminescence

Samples from the base of the SFD3 (at 1.33m OD) and DYN1 (at 1.44m OD) cores, well within sand-rich, organic-poor units, were submitted for optically stimulated luminescence (OSL) dating. Both samples showed a weak naturally acquired OSL signal which grew relatively slowly with artificial radiation dose. Consequently although 31 replicate measurements were

made per sample a number of these had to be disregarded as their recycling ratios were not within 10% of unity and/or the single aliquot regenerative (SAR) growth curve was not well constrained by the SAR regeneration points. Ultimately, 5 from SFD3 and 9 from DYN1 were unusable.

The effects of incomplete bleaching of the sediment during the last period of transport or exposure *in situ* can be profound. Typically, poorly bleached sediments retain a significant level of residual signal from previous phases of sedimentary cycling, leading to inherent inaccuracies in the calculation of a palaeodose value. This is difficult to establish with any certainty from OSL data and should be taken in consideration with the site stratigraphy. In principle, a well-bleached undisturbed (post-deposition) sample should have replicate palaeodose (De) data that are normally distributed (Bateman *et al.* 2003).

The reproducibility of the OSL data shows that both the SFD3 and DYN1 samples have a high amount of replicate scatter reflected in overdispersion (OD) values >20%. The De distribution of both samples is skewed. Whilst some of the distribution shape may reflect the limited population size of replicates, it also may reflect incomplete bleaching and/or post- depositional disturbance of samples. If it is assumed that the aliquots that give the lowest De values have the most fully bleached grains on them and are least post-depositionally disturbed then an age based on these will be closest to the true burial age. Accordingly, the final De value used to calculate ages was derived by analysing the De replicate data using the Minimum Age Model (Galbraith and Green, 1990). This attempts to statistically extract the youngest (and presumed to be best bleached and therefore closest to burial age) De replicates. However as single aliquot measurements are an average of OSL signal palaeodose over-estimation of burial age is still possible. Table 5.3 summarises the results of the OSL dating analysis.

Table 5.3 Summary of OSL dating results for SFD3 and DYN1

Sample	Depth	Total number of aliquots measured	Usable aliquots	De (Gy)	Dose rate ($\mu Gy/a^{-1}$)	Age (ka)
SFD3	1.33mOD	31	26	1.16±0.16	943±47	1.23±0.18
DYN1	1.44mOD	31	22	2.35±0.13	1229±64	1.91±0.14

5.6.3. Core dating interpretation

The estimated OSL burial ages calculated for SFD3 and DYN1 are 1.23±0.18ka and 1.91±0.14ka respectively. These dates are significantly different to those suggested by the accumulation rates from simple linear extrapolation of the ^{210}Pb and ^{137}Cs dating. For the SFD3 core where the ^{210}Pb and ^{137}Cs accumulation rates are better defined the predicted time of

deposition for the depth of 1.33mOD is 307.9±23.7 years ago, a difference of approximately 920 years with the OSL date.

There are several possible reasons for the discrepancies between the dating analyses. Over-estimation of burial age in the OSL analysis is a more likely occurrence in intertidal environments where subaqueous transport of the sediment could result in incomplete bleaching of grains. The disturbance history of the sediment sequence is also unknown and therefore not able to be taken into account in the dating process. The characteristically high sand content and lack of a finer fraction in the sediment in this environment also hinders ^{210}Pb and ^{137}Cs dating, this is particularly apparent in DYN1.

However, as already noted, the ^{210}Pb and ^{137}Cs dating refers specifically to the upper more organic rich units and therefore the derived accumulation rate cannot be realistically extrapolated to the lower units. It is therefore possible that the OSL date for the lower units is representative of the age of sediment deposition. This would imply two broad periods of sediment movement and accumulation, firstly between 1ka and 2ka when the lower minerogenic units were deposited and secondly between 200yrs ago and the present day when the upper organic units are deposited. This scenario fits with current understanding of the evolution of the Loughros More estuary, i.e. instability and large-scale movement of the Magheramore dune system around 1000 years ago which cut off the Sheskinmore Lough to the north of the Sandfield site (Figure 2.4) (Shaw and Carter, 1994). A significant increase in North Atlantic storminess is recognised between 1400-1420AD and the present day by Meeker and Mayewski (2002). Therefore although the large scale movement of the dune system approximately 1000 years ago may have triggered the formation of the environments at Sandfield and Derryness this period of increased storminess is likely to have been key in their evolution. More recently, the historical maps indicate the development of vegetated land surfaces by 1850 (Figure 4.12).

From a comparison of layer frequency with the dating controls for SFD3 it can be seen that for the 13cm immediately above 1.47mOD (i.e. transition to vegetated environment) 32 layers are identifiable (Figure 5.18). Based upon a deposition rate of 1.3mm/year for this section of the core this would suggest layer alternation occurs on average once every 3 years. However, as can be seen in Figure 5.18 this alternation is not regular rather the timing of change from sandy to more organic is episodic. This evidence therefore excludes the possibility of annual rhyhmicity causing the alternation of light (sandy) and dark (organic) layers. Identification of individual layers in the SFD3 core above 1.6mOD is not possible as the organic content increases and bioturbation has caused disturbance of the stratification.

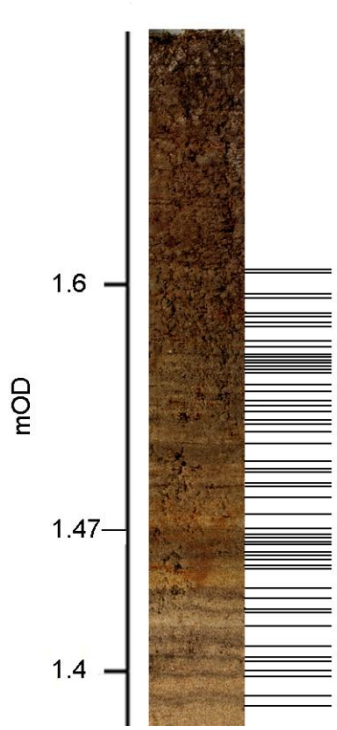

Figure 5.18 Identification of individual layers within SFD3 above the tidal flat / vegetated area transistion at 1.47mOD (bars on right hand side mark boundaries between layers).

5.7. Downcore summaries and environmental interpretation

The most striking visual feature of the sediment sequences is the 1-5mm light and dark layering present in all 5 cores. This is caused by the alternation of light coloured, minerogenic sand layers and darker more organic rich layers. Also clearly identifiable within all the cores is a transition from deposition on a tidal flat to sediments deposited in an environment separated from the influence of tidal processes. There is a maximum variation of 20cm in the elevation of this transition between the Sandfield cores and of 33cm between the Derryness cores.

The further stratigraphic analyses carried out on the SFD3 and DYN1 cores reveal significant downcore variations in the sedimentology, geochemistry and palaeoecology and distinct differences between the cores.

5.7.1. SFD3

Within the SFD3 core three distinct features occur. Firstly, the change in sediment characteristics at 1.32mOD indicated by a marked decrease in the mean grain size and sorting values decrease and tilt factors (Figure 5.19). This is associated with the introduction of finer organic material into the sequence as evidenced by the increase in organic percentage from this point. This change is also reflected in the quartz grain surface textures where below 1.32mOD there is a greater occurrence of upturned cleavage plates which are almost completely absent above this boundary. The second distinct feature is the abrupt decrease in percentage carbonate

content at 1.45mOD (Figure 5.19). This dramatic reduction in carbonate content does not correspond with any other significant changes in the other variables. This change could either relate to change in sediment supply to a source with little or no shell derived material or a major reduction in the post mortem deposition of mollusc species in the source area. The third feature is the increase in organic content between 1.55mOD to the top of the core (Figure 5.19); this is also reflected in the lower mean grain size and sorting values due to the input of finer organic material.

These three features can also be interpreted as representing significant changes in the evolution of the site. The increase in organic content and associated changes in sedimentology seen above 1.32mOD is likely to represent the initiation of plant colonisation of the tidal flat. Tidal processes were still prevalent in this area during this time as evidenced by the position of the boundary from tidal flat to vegetated marsh (i.e. at a higher elevation (1.47mOD)). It is likely that the conditions during this early colonisation are analogous to the present day conditions of the saltmarsh area in the north of the Derryness site as attested to by the similar sedimentology (i.e. mean grain size and sorting values). The timing of this initial plant colonisation at SFD3 cannot be determined with any certainty, due to the paucity of datable material; however it is likely to have been pre 1800.

The abrupt drop-off in $CaCO_3$ content is also significant. This can be interpreted as a sudden cut-off in the supply of shell material to the east of the Sandfield site. The sudden nature of the cut-off suggests a short-lived event rather than a gradual process change. It is possible that this change in shell material supply is linked to the presence of a dune barrier along the western margin of the Sandfield site identified in the 1850 map of the area. It is not known when this dune barrier formed, however, if this $CaCO_3$ cut-off is taken to be indicative of its formation, the limited dating information suggests a timing between approximately 1800 and 1850.

The increase in organic content toward the top of the core highlights the more recent organic productivity of this area and the more sheltered nature of the site possibly as a result of its increasing distance from the western margin as this prograded between 1850 and 1977. The more sheltered nature of the site is also suggested by the decreasing influence of aeolian sediment deposition as indicated by the reduction in occurrence of upturned cleavage plates on the quartz grain surfaces in this upper section of the core.

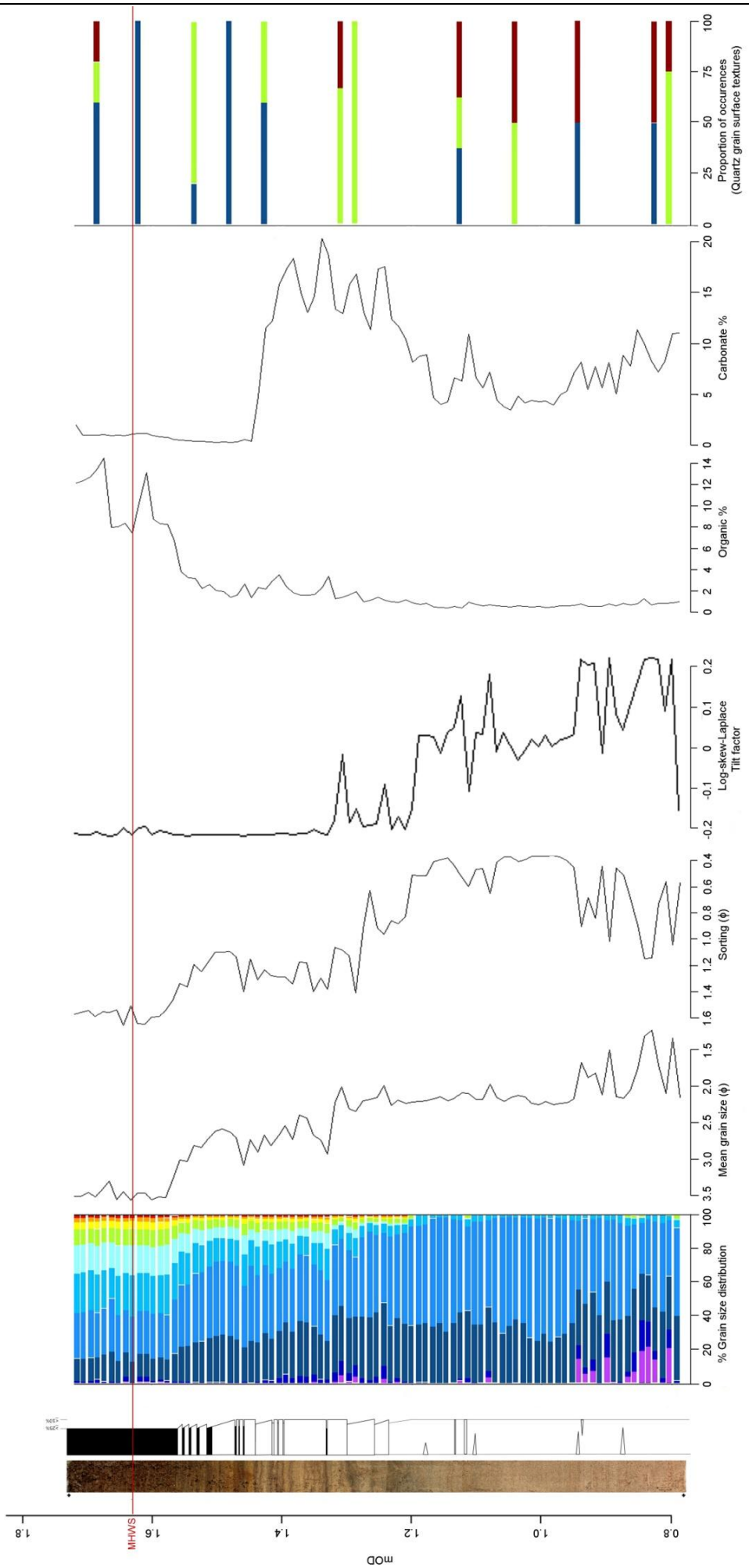

Figure 5.19 SFD3: Summary of downcore profiles.

5.7.2. DYN1

The main features of the DYN1 core are the unit between 1.48 and 1.62mOD where mean grain size decreases significantly this is associated with a slight rise in organic content (Figure 5.20). The top of this unit occurs at approximately the same level as mean high water springs (MHWS), i.e. 1.63mOD. Above this level is another distinctive unit identified by diatom analysis; between 1.63 and 1.86mOD there is a shift from a mix of *Navicula arenaria*, *N. cintca* and *Diploneis interrupta* to a dominance of *D. interrupta* (Figure 5.20). This unit is not as apparent in the other downcore variables. Between 1.86mOD and the top of the core again there is no significant change in the profiles other than the diatoms where species proportions return to similar to that below the previous unit.

Linking any of the changes seen within the DYN1 core periods in the sites evolution as identified in the previous chapter (4.2.2) is difficult due to the problems encountered in trying to determine the chronology of this core. The slight rise in organic content and the associated changes in sedimentology between the base of the core and 1.62mOD are likely due to initial plant colonisation of a tidal flat area, similar to the transition seen at Sandfield. The log-hyperbolic analyses suggest this area has been depositional for the whole of the period represented by the core. Continued deposition after the initiation of plant colonisation raised the vegetated surface above the influence of tidal flat processes, represented by the boundary between tidal flat and vegetated area identified at 1.53mOD in the sediment logs. As a result of this increasing elevation the surface emerges above the MHWS level and the ecology of the area changes accordingly with a greater occurrence of mesohalobous diatom species. The change in the diatom communities in the top 6cm of the core (i.e. above 1.86mOD), although not appearing significantly different in the majority of the variables examined, may be indicative of a change in the vegetation structure to greater marsh coverage. It is therefore possible that the present day Derryness raised maritime grassland surface is similar to that of Sandfield prior to the increased rate of organic content increase towards the top of the core. Therefore this suggests that if deposition continues on the Derryness site and organic content increases as it is shown to have done at Sandfield the maritime grassland may evolve into an environment more characteristic of machair.

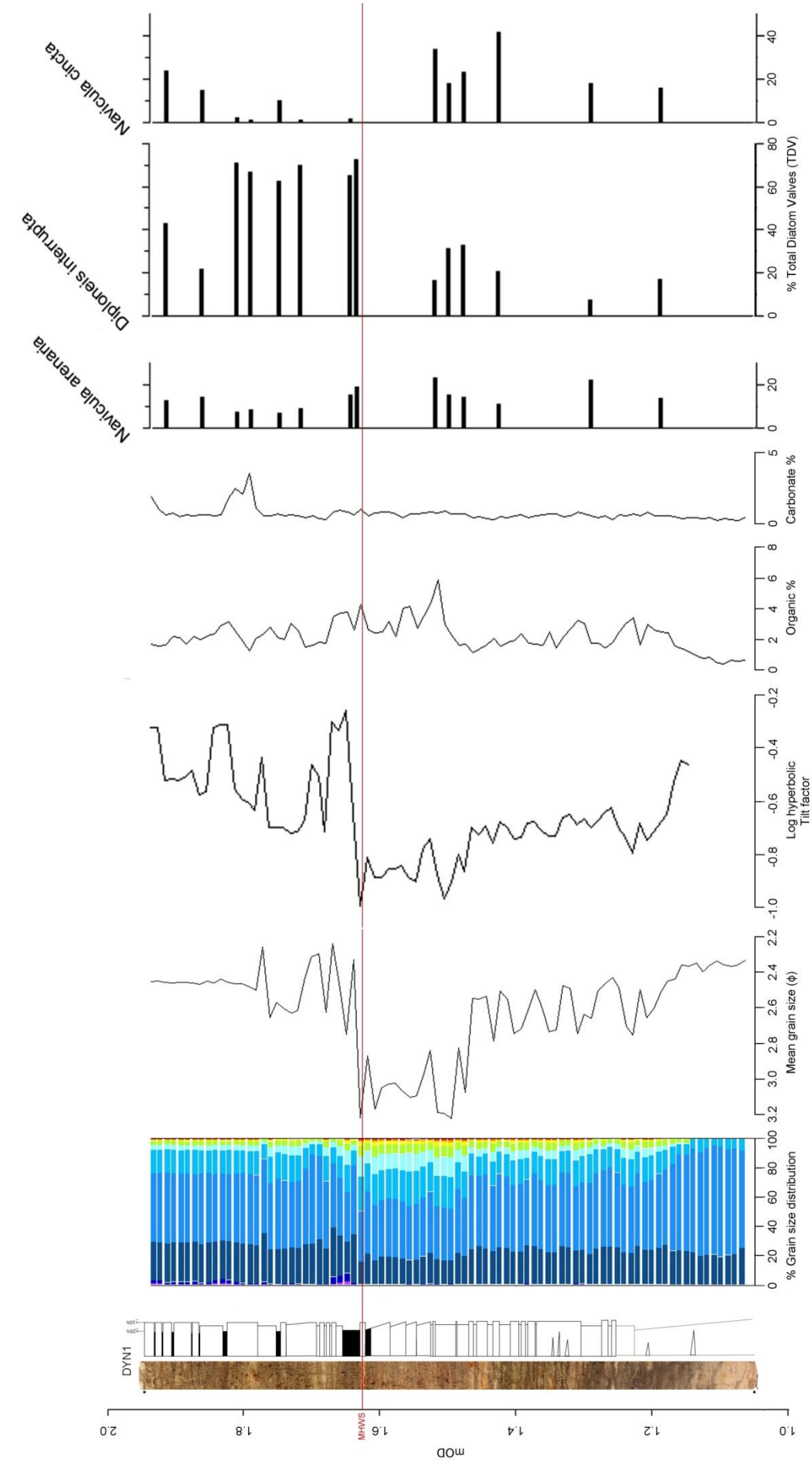

Figure 5.20 DYN1: Summary of downcore profiles

The stratigraphic analyses of SFD3 and DYN1 were carried out on 1cm sub-samples due to the requirement for a sufficient volume of sediment to be available for the various methods. As a result of this sub-sampling resolution the finer detail of the 1-5mm layers will be lost. The following chapter describes the application of scanning XRF to examine the downcore stratigraphy at a higher resolution.

6. Application of high resolution scanning XRF

This chapter describes the use of scanning X-ray florescence (XRF) in the high resolution examination of the core stratigraphy. Additionally, the suitability and effectiveness of using scanning XRF as both a method of indentifying geochemical downcore variations and as a proxy for environmental change on sediment sequences from intertidal marginal coastal environments is assessed. Previously scanning XRF has been predominately used in the marine environment and also, less frequently, in lacustrine environments; there are, however, very few examples of its use in coastal environments.

The analyses carried out in the previous chapter have identified significant downcore stratigraphical variations indicative of environmental change. The majority of these analyses have been carried out at a 1cm resolution to allow for sufficient volume of sediment to be analysed. However, the most apparent visual feature of the sediment sequences in both the field sections and split cores is the banding of light and dark layers of between 1 and 5mm thickness. In the eroded edges of the raised areas at Sandfield and Derryness these are particularly apparent, as there is greater erosion of the lighter, sandier layers leaving the darker finer layers protruding. These layers are very clear in the photographic images of the cores and the more sandy layers are easily picked out using an analysis of the image intensity (variation in lightness/darkness) (Figure 6.1). The ability of scanning XRF to analyse the downcore geochemical variations at a high resolution (1mm) enables these layers to be examined in much greater detail.

An Avaatech XRF core scanner was used to measure elemental composition of all five cores retrieved from Loughros More. Measurements were undertaken at 1mm intervals downcore (the maximum resolution achievable) and count per area data retrieved for 18 elements (Al, Si, S, K, Ca, Ti, V, Cr, Mn, Fe, Zn, Br, Rb, Sr, Zr, Mo, Pb and Bi) (see chp 3.3.3 for method).

6.1. Data preparation and validation

6.1.1. Acuracy and precision

To test repeatability of results, reruns were made on sections of selected cores. The results of this showed mixed agreement, ostensibly dependent on magnitude of signal. A good correlation (R^2 values ranging from 0.796 – 0.979) was achieved when values exceeded 600 counts per area (cpa). Sample measurements below 600 cpa showed more variation between sample repeats with R^2 values ranging between 0.254 – 0.756. Therefore, it is likely that values below 600cpa are dominated by background noise rather than significant signals, and 600cpa represents the threshold of repeatability.

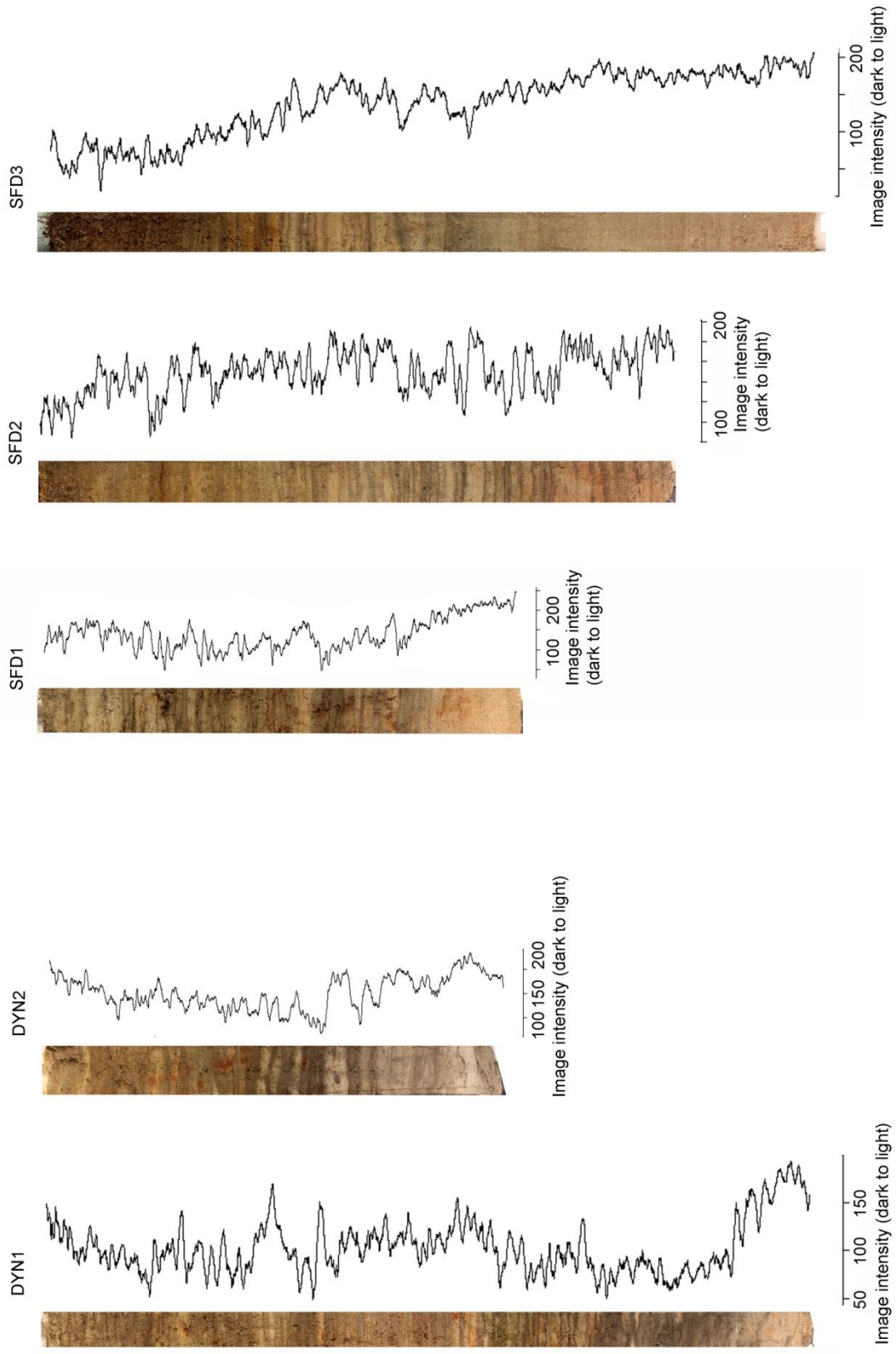

Figure 6.1 Analysis of image intensity to highlight light and dark layers within cores

As a method of validation, non-scanning, bulk sample XRF (using a Spectro XLAB 2000 spectrometer) was run on discrete subsamples of the cores and compared to the scanning XRF data. The non-scanning XRF provides quantitative information on the percentages of each element present throughout the core. Larger sediment samples (1cm units used here) are required for this instrument, so for comparison, the 1mm scanning analysis data was averaged over the 1cm sample section associated with the subsamples. Linear regression was used to compare individual element results from the two methods and identify significant similarities; the results of this validation process are shown in Table 6.1.

Throughout the five cores, some specific elements exhibit significantly different results between the scanning and non-scanning XRF methods: these are predominately those with low count per area values (i.e. below 600). As mentioned previously, measurements below this level are likely to be dominated by background noise and this could explain the differences between the results. The exception to this is Si which has high count per area values. However the results for this element do not show a significant similarity between methods for the Sandfield cores. This is possibly due to the relatively large variations in count per area values which change dramatically over short distances down-core and the effects of averaging these over the 1cm subsample section to allow comparison.

6.1.2. Noise reduction

In order to reduce noise in the scanning XRF datasets and to aid visual interpretation, several smoothing or re-sampling strategies were applied to the data and assessed to determine the most appropriate. The smoothing and re-sampling approaches were applied at a scale of 3-5mm as this corresponds to the thickness of the thinner bands within the sections. Three filters were tested on the data, a 3-point moving average, a 5-point moving average and a 5-term quadratic polynomial (Figure 6.2). Of these 3 filters the 5-term quadratic polynomial filter was most effective at removing noise from the dataset whilst still retaining the finer detail of sharp peaks and troughs. When comparing the residuals of each method the 5-term quadratic filter is again the most effective (R^2=0.98). Therefore the 5-term quadratic filter was used to process all element profiles prior to subsequent analyses.

Table 6.1 Comparison between scanning and non-scanning XRF results. Statically significant similar results highlighted in yellow.

	Al	Si	S	K	Ca	Ti	V	Cr	Mn	Fe	Zn	Br	Rb	Sr	Zr	Mo	Pb	Bi
SFD1																		
Count range	275 - 500	4000 - 12000	530 - 730	1500 - 4000	5000 - 32000	300 - 1000	20 - 120	220 - 400	300 - 700	2000 - 12000	04-Sep	0 - 260	40 - 120	190 - 640	140 - 260	105 - 150	03-Oct	3.5 - 4.8
% range	1 - 4	19 - 24	0 - 0.08	0.6 - 1.8	3 - 13	0.05 - 0.26	0 - 0.007	0 - 0.0045	0 - 0.035	0.5 - 3.25	5 - 45µg/g	0 - 290µg/g	25 - 85µg/g	100 - 425µg/g	30 - 100µg/g	2 - 3.5µg/g	4 - 16µg/g	0.4 - 0.9µg/g
P value	0.2531	0.8996	0.1244	0.02017	0.2227	1.19E-03	0.475	0.1754	0.62	9.96E-04	0.00469	1.05E-05	1.29E-04	0.1645	7.73E-03	0.3339	2.92E-03	0.6748
R^2 value	0.2103	0.00288	0.347	0.6211	0.2357	0.8472	0.0882	0.2823	0.04353	0.8556	0.7614	0.9679	0.9263	0.2949	0.72	0.1554	0.7953	0.03136
SFD2																		
Count range	275 - 370	5000 - 11000	480 - 600	1400 - 2600	0 - 32500	300 - 800	60 - 115	150 - 400	250 - 450	2000 - 11000	3.5 - 7	10 - 240	20 - 90	100 - 700	170 - 265	115 - 150	5 - 13	3.5 - 5.2
% range	0.5 - 2.5	20 - 33	0	0.6 - 1.4	0 - 10	0.05 - 0.18	0 - 0.0035	0 - 0.0035	0.005 - 0.025	0.4 - 1.8	4 - 29µg/g	10 - 270µg/g	22 - 49µg/g	40 - 350µg/g	30 - 90µg/g	1.5 - 4.0µg/g	5 - 14µg/g	0.4 - 0.8µg/g
P value	0.3783	0.07268	NA	7.09E-03	1.56E-04	0.1093	0.4702	6.78E-03	0.8532	0.02979	0.04919	9.07E-06	8.84E-04	1.90E-04	0.08568	0.5492	0.5519	0.4619
R^2 value	0.1122	0.389	NA	0.6686	0.8852	0.3246	0.07683	0.6726	0.005236	0.5137	0.4464	0.9487	0.8134	0.8788	0.3635	0.05352	0.05283	0.07963
SFD3																		
Count range	200 - 370	3000 - 14000	300 - 1400	1100 - 2900	0 - 65000	300 - 800	40 - 120	150 - 470	200 - 650	2000 - 17000	3 - 11	0 - 600	30 - 110	100 - 1300	140 - 270	100 - 180	2 - 14	3.5 - 7
% range	0 - 3.5	14 - 40	0 - 0.7	0.55 - 1.65	0 - 21	0.05 - 0.2	0 - 0.005	0 - 0.02	0 - 0.04	0.4 - 2.5	0 - 35µg/g	0 - 700µg/g	10 - 60µg/g	100 - 900µg/g	50 - 110µg/g	2.5 - 4.0µg/g	2 - 12µg/g	1 - 13µg/g
P value	0.4975	0.01211	1.96E-04	0.02198	8.30E-16	0.02295	0.5037	0.6494	0.01939	4.33E-05	1.78E-05	1.07E-07	5.35E-05	8.55E-09	0.5702	9.58E-03	6.99E-05	0.8754
R^2 value	0.04721	0.483	0.7652	0.4232	0.8739	0.4187	0.0459	0.02149	0.4363	0.8253	0.8534	0.9468	0.8179	0.9679	0.03331	0.505	0.8081	0.00258
DYN1																		
Count range	250 - 400	6000 - 14000	500 - 2400	1700 - 3500	1000 - 12000	400 - 110	60 - 160	200 - 425	300 - 650	3800 - 12000	4.5 - 9.5	10 - 200	50 - 105	90 - 350	160 - 280	115 - 155	5 - 10	2 - 5
% range	1.0-3.5	23-34	0 - 3	1.0 -1.7	0-7	0.05-0.25	0-0.007	0-0.0045	0.005-0.020	0.5-2.8	8-42µg/g	10-250µg/g	30-67µg/g	40-180µg/g	35-120µg/g	2-5µg/g	4-19µg/g	0.3-0.9µg/g
P value	0.1615	7.99E-04	5.10E-09	1.76E-03	4.51E-07	5.95E-04	0.8428	0.5845	0.3793	2.76E-05	1.43E-03	1.54E-08	1.76E-05	1.18E-10	9.84E-05	0.3634	1.97E-03	0.8784
R^2 value	0.186	0.6915	0.971	0.6409	0.9292	0.7086	0.004124	0.03094	0.07801	0.8401	0.6551	0.9638	0.8538	0.9863	0.7948	0.08313	0.633	0.002456
DYN2																		
Count range	280 - 360	6000 - 14000	600 - 1600	1600 - 2500	3500 - 13000	400 - 800	40 - 130	150 - 400	270 - 520	3000 - 11000	4 - 10	0 - 180	54 - 84	110 - 340	160 - 220	110 - 160	5 - 10.5	3.6 - 5.0
% range	0.4 - 3.1	21 - 32	0.1 - 0.85	0.75 - 1.6	1 - 6	0.05 - 0.225	0 - 0.006	0 - 0.004	0 - 0.05	0.4 - 2.2	6 - 50µg/g	0 - 200µg/g	25 - 50µg/g	50 - 230µg/g	40 - 80µg/g	2 - 7µg/g	4 -19µg/g	0.3 - 0.8µg/g
P value	0.08831	1.72E-03	7.97E-06	0.7423	1.25E-04	0.1806	0.03436	2.96E-04	0.2573	4.33E-03	0.03704	2.98E-03	3.46E-03	7.20E-05	0.2998	3.18E-03	0.4215	0.7505
R^2 value	0.2887	0.6827	0.9015	0.01261	0.8199	0.1897	0.4081	0.7829	0.1398	0.614	0.3992	0.6433	0.6318	0.8404	0.1186	0.6383	0.07305	0.0118

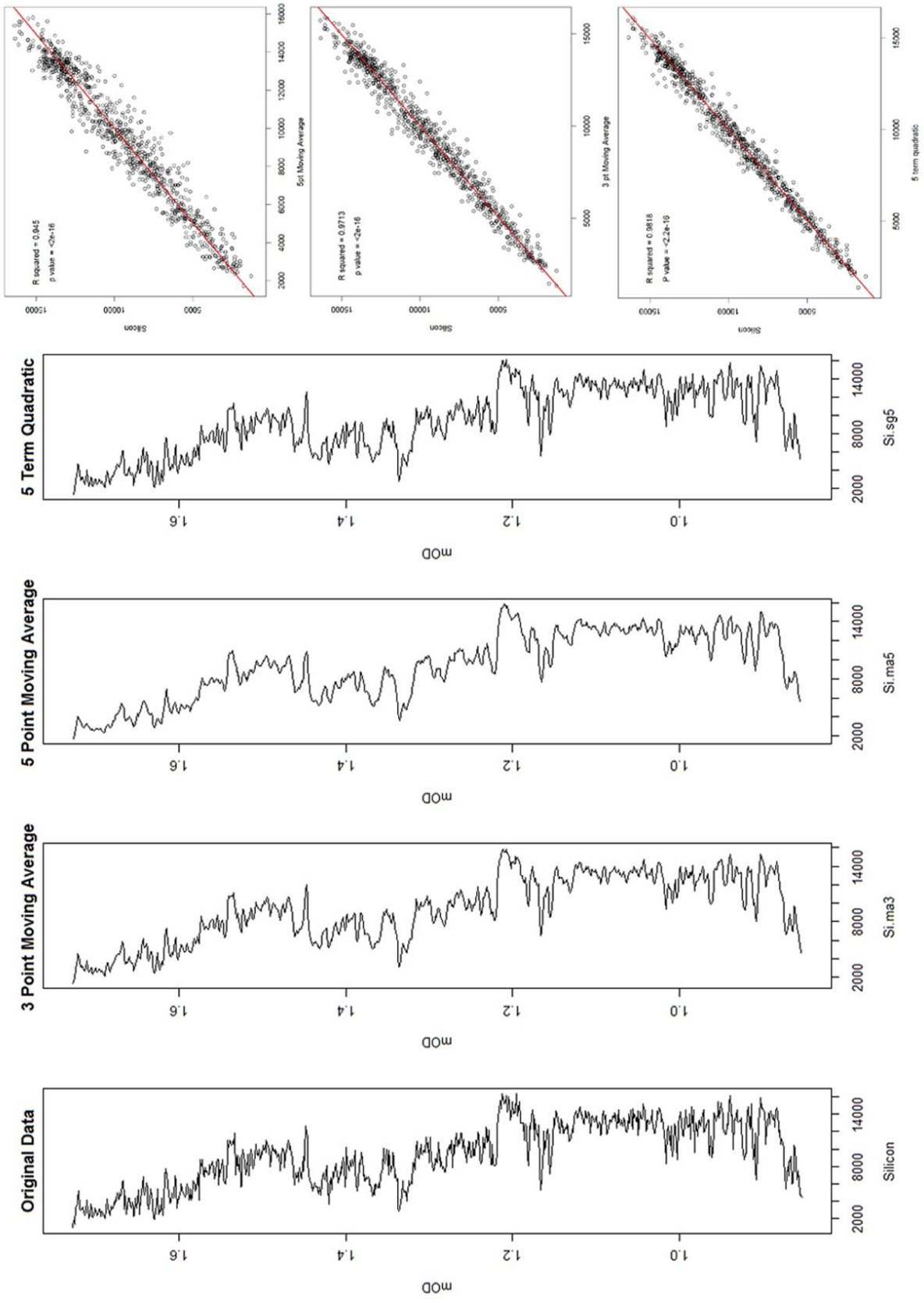

Figure 6.2 Comparison of smoothing strategies applied to Si data from the SFD3 core showing the visual effects of the filter and also the correlations between the original and filtered data and the associated residuals.

6.2. Individual element profiles

Within this section the individual element profiles of each core are described in detail. For ease of comparison, elements that exhibit similar profiles are considered together. Where the count per area values of an element profile are low, i.e. below 600, and the profile shows no overall trend or similarity with other elements this element has been omitted from the descriptions.

6.2.1. SFD1

Al, K, Ti, Fe, Zn, Br, Rb and Zr comprise core profiles that are characterised by an increasing trend from the base to a peak at 1.54mOD, on the upper side of which, is a sharp drop to a flat bottomed trough between 1.55 and 1.56mOD (Figure 6.3). The increasing trend continues to a broad or double peak at 1.63-1.65mOD followed by a sharp trough above. At 1.67mOD values return to mid-range and gradually decrease to the top of the core. K and Fe are the dominant elements in this group. Al, Zn, Br, Rb and Zr values are all below 600cpa and Ti partially below (i.e. ranges 200-1200cpa).

Maximum Si values are at the base of the core. There is an overall decreasing trend to a broad trough at 1.62-1.65mOD (Figure 6.3). Values return to mid-range on the upper side of this trough and the envelope of variability remains wide, but constant to the top of the core. There is, however, a narrow, deep, broad, trough at 1.83mOD where values drop to just above 0.

The S values are low ranging between 400 and 800cpa. The S profile is the opposite of the Si profile, i.e. minimum at the base of the core increasing to a broad peak at 1.62-1.65mOD (similar to that seen in Al, K, Ti, etc) (Figure 6.3). Above the peak values remain constant to the top of the core. However, the deep, broad, trough seen in the Si profile is not represented in the S profile.

Ca and Sr profiles are very similar (Figure 6.3) although the Sr values are significantly lower (200-1000cpa). Values are highest at the base of the core with sharp peaks at 1.45mOD and 1.54mOD, the latter corresponding with peaks present in the Al, K, Ti, etc profiles. There is a decreasing trend between 1.54mOD and 1.64mOD where values reach background noise levels. There is then a rapid increase to 1.66mOD from which high frequency fluctuations dominate through to the top of the core, with broad minima at 1.75mOD and 1.83mOD and maxima at 1.81mOD and 1.95mOD.

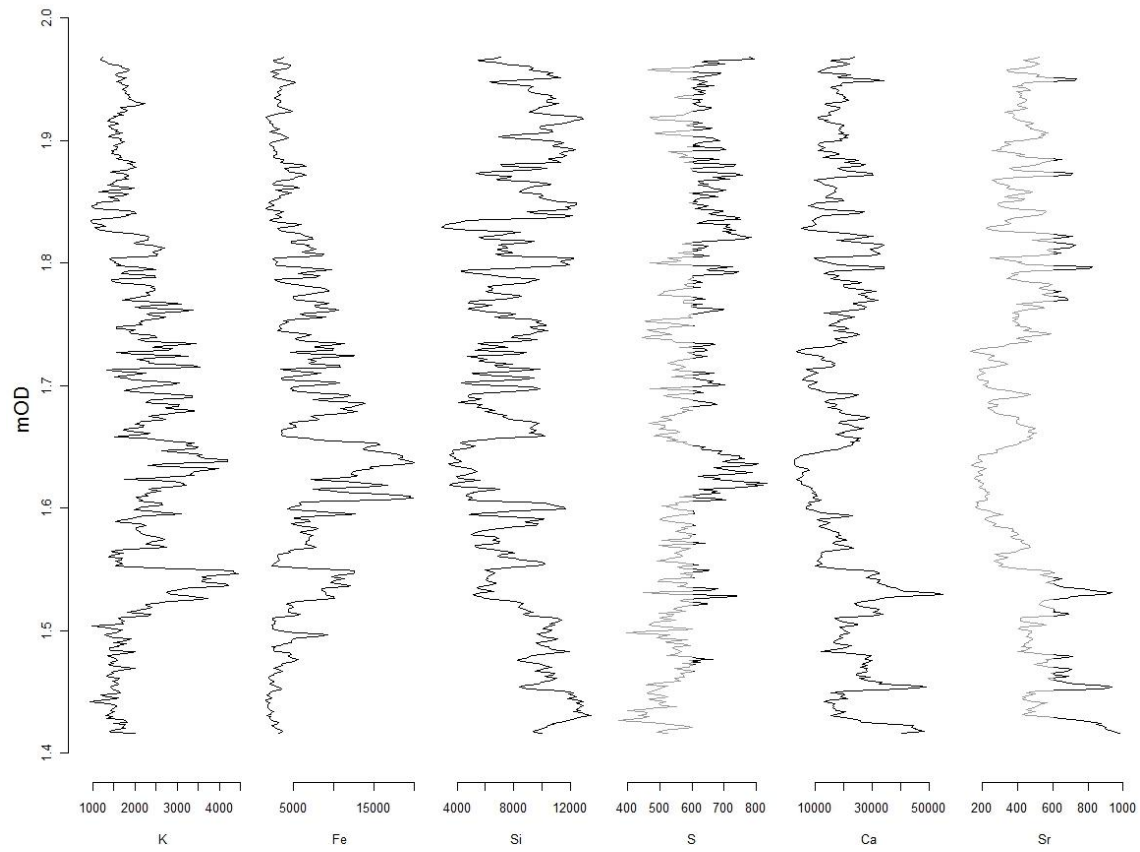

Figure 6.3 Examples from each of the downcore profile groups identified for SFD1. Values below 600cpa (corresponding to the threshold at which signal can be separated from noise) are plotted in grey.

6.2.2. SFD2

Al, K and Ti values are broadly low at the base of the core and increase to a section of higher values with high variability between 1.22mOD and 1.4mOD (Figure 6.4). Values remain relatively high above 1.4mOD increasing gradually to their highest at 1.51mOD then sharply decrease to the top of the core. Only K values are above 600cpa throughout the core.

There is no clear increasing or decreasing trend in Si throughout the majority of the core, there is, however, greater variability between the base and 1.41mOD where there are numerous peaks and troughs (Figure 6.4). From 1.7mOD to the top of the core there is a rapid decrease in values.

The S profile again appears to be negatively correlated with that of Si with no overall increasing or decreasing trend but with numerous peaks and troughs and an increase from 1.7mOD to the top of the core (Figure 6.4). The values range from 400-800cpa.

The Ca and Sr profiles are very closely correlated with relatively high values at the base of the core that remain constant to 1.42mOD at which point values sharply drop to approximately 0 (Figure 6.4). This effectively splits the profile into 2 sections. Within the lower section, where there is no overall trend, there are 2 sharp peaks at 1.06mOD and 1.33mOD.

The Fe and Br profiles display relatively low values for the majority of the core with a sharp increase from 1.7mOD to the top of the core. The Br values range between 20-400cpa and only in the top 10cm of the core do they rise above ~50cpa. Additionally Fe has a sharp narrow peak at 1.62mOD (Figure 6.4).

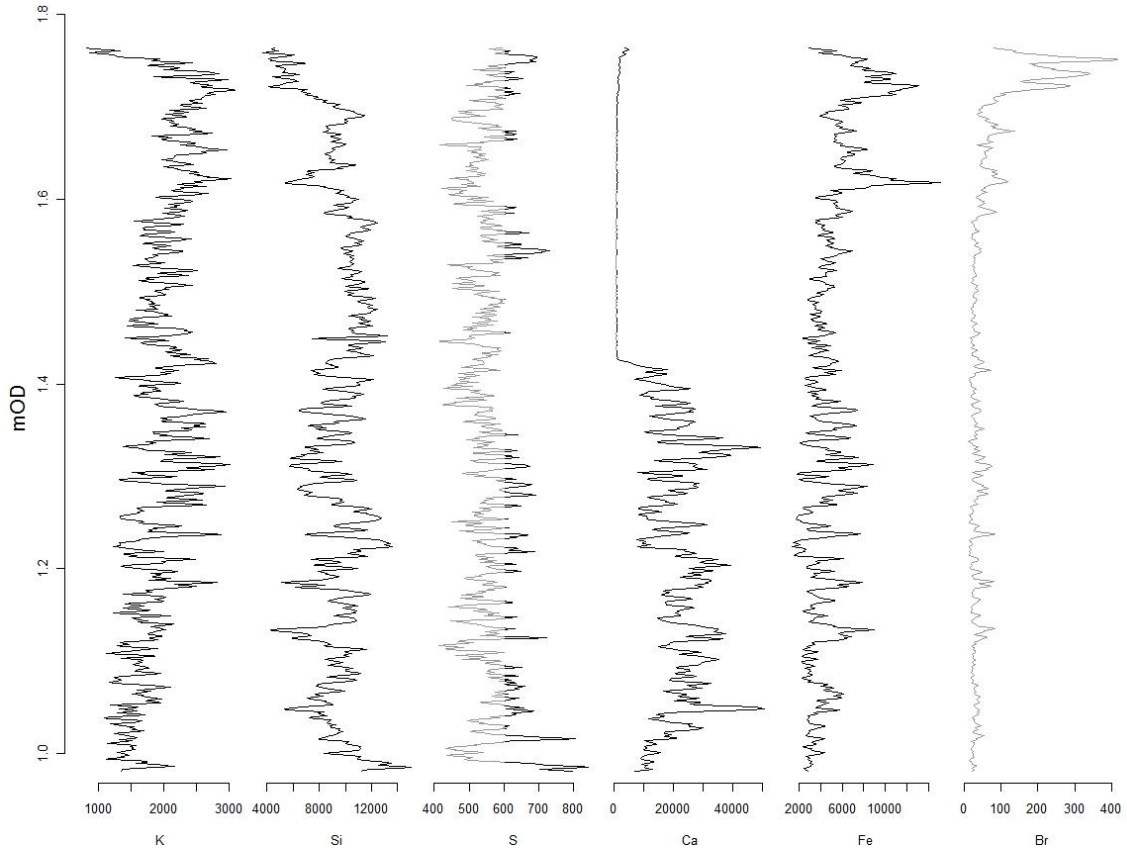

Figure 6.4 Examples from each of the downcore profile groups identified for SFD2. Values below 600cpa (corresponding to the threshold at which signal can be separated from noise) are plotted in grey.

6.2.3. SFD3

Values for Al, K, Ti and Zr are lowest and remain relatively constant from the base to 1.3mOD at which point there is a sharp trough present in the Al, K and Ti profiles (Figure 6.5). Above 1.3mOD values increase to a maxima at 1.6mOD. A peak at 1.46mOD in the Al, K and Ti profiles correlates with peaks seen in the Fe, Br and Rb profiles. From 1.6mOD values decrease to the top of the core. K is the only profile with values consistently above 600cpa

Element count values for the Si profile are highest at the base of the core and remain consistently high until approximately 1.18mOD; however there is quite high variability (Figure 6.5). From 1.18mOD to the top of the core there is a gradual overall decreasing trend. There are several small peaks within this section of gradual decline notably at 1.31mOD and 1.43mOD.

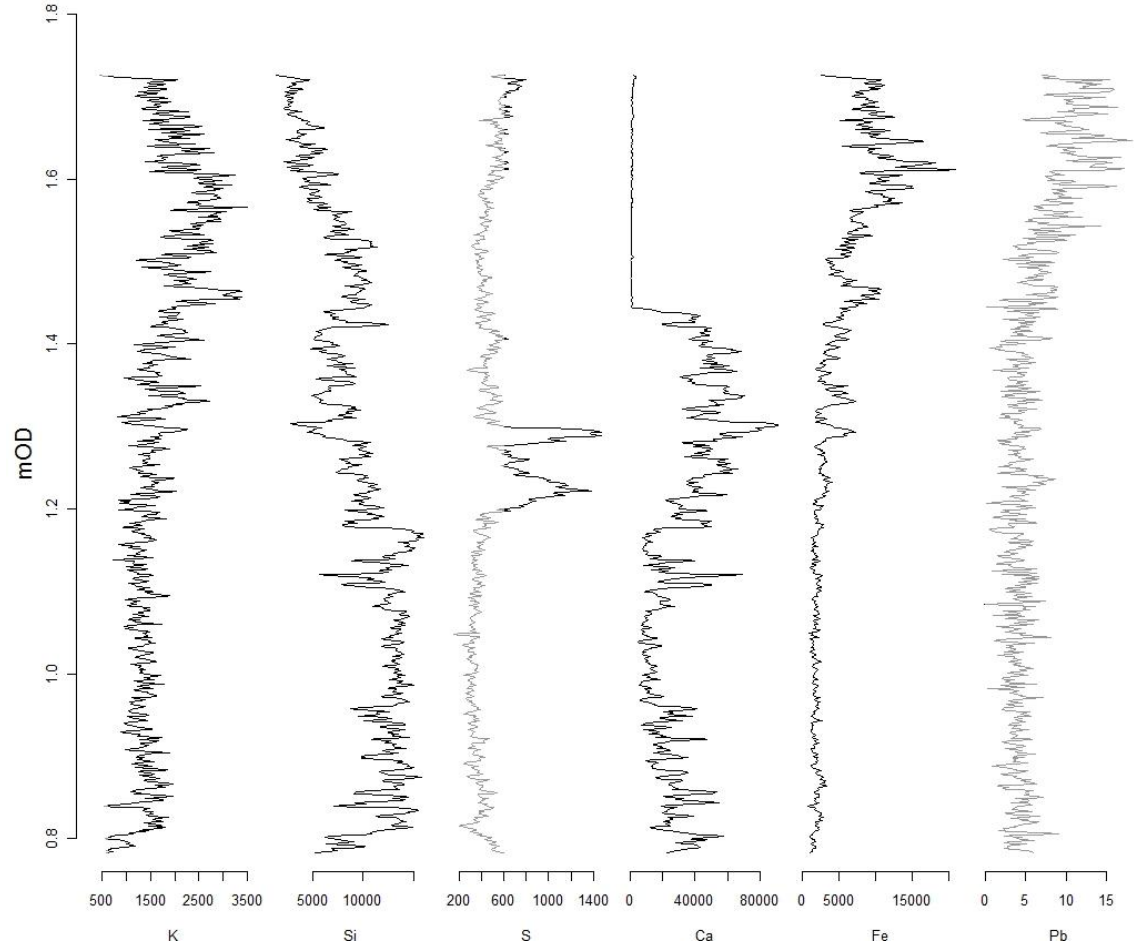

Figure 6.5 Examples from each of the downcore profile groups identified for SFD3. Values below 600cpa (corresponding to the threshold at which signal can be separated from noise) are plotted in grey.

The S downcore profile is distinct from those of the other elements in this core (Figure 6.5). Generally, values are low throughout the core, less than 600cpa, indicating this is probably just noise. Values rise slightly between 1.6mOD and the top although still within noise levels. However there are two broad peaks between 1.2mOD and 1.3mOD where values rise to their highest within this profile with a steep short trough between the two peaks.

The Ca and Sr profiles are closely correlated. Count values are highest at the base of the core to 0.81mOD where there is a sharp drop. Values remain constant between 0.81mOD and 0.96mOD although with relatively high variability (Figure 6.5). The variability is less between 0.96mOD and 1.08mOD where the count values are also slightly lower. From 1.08mOD to 1.44mOD count values and variability increases with several peaks present, the most notable at 1.3mOD where Ca values reach a maximum for this core. At 1.43mOD values drop sharply to approximately 0 and remain constant to the top of the core. This profile is almost identical to that of Ca and Sr in SFD2 with the sharp drop in count values occurring at a similar elevation.

Fe, Br, Rb and Pb profiles are all below the noise-signal threshold throughout the majority of the core with no overall increasing or decreasing trend and with some variability (Figure 6.5). Values and variability increase between 1.3mOD and 1.62mOD with significant peaks at 1.46mOD and 1.62mOD present in the Fe, Br and Rb profiles. Between 1.62mOD and the top of the core values decrease slightly, except in the Br profile where values continue to increase to the top of the core. Fe and Br are the only elements whose values rise above 600cpa towards the top of the core.

6.2.4. DYN1

Al and Si have similar downcore profiles although the Al values are low throughout the core (100-500cpa) (Figure 6.6). Maximum values occur at the base of the core, decreasing to mid-range at 1.21mOD. Values remain within a constant envelope of variability to approximately 1.48mOD where they drop again to the minima of the profile. They remain at this level to 1.62mOD. At approximately 1.63mOD there is a sharp peak in the Si profile whereas in the Al profile there is a trough; this is the only point within this core where these two elements are negatively correlated. Above this point this is an increase from the lowest values to mid range values between 1.64mOD to 1.69mOD; they then remain constant at this level to the top of the core.

Element count values for S are relatively low at the base of the core increasing to their maximum for the profile between 1.18mOD and 1.3mOD (Figure 6.6). At 1.3mOD values decrease and remain within noise levels throughout the rest of the core.

K, Ti, Fe and Br values between the base of the core and 1.14mOD are relatively low (Figure 6.6). They increase slightly and then remain constant to 1.47mOD. There is a sharp peak at 1.51mOD followed by a return to low values then a sharp trough at 1.63mOD and another peak at 1.64mOD. The trough at 1.63mOD can also be seen in the Zn, Zr and Rb profiles and also corresponds with the negatively correlated trough and peak in the Si and Al profiles. Above 1.64mOD low values return and then decrease slightly to the top of the core. Fe is the only profile to remain above 600 throughout.

Ca and Sr counts are close to zero for the majority of the core; however, there is a double peak between 1.77mOD and 1.83mOD where Ca values rise significantly above background noise levels; between is a trough to approximately noise level at 1.8mOD (Figure 6.6).

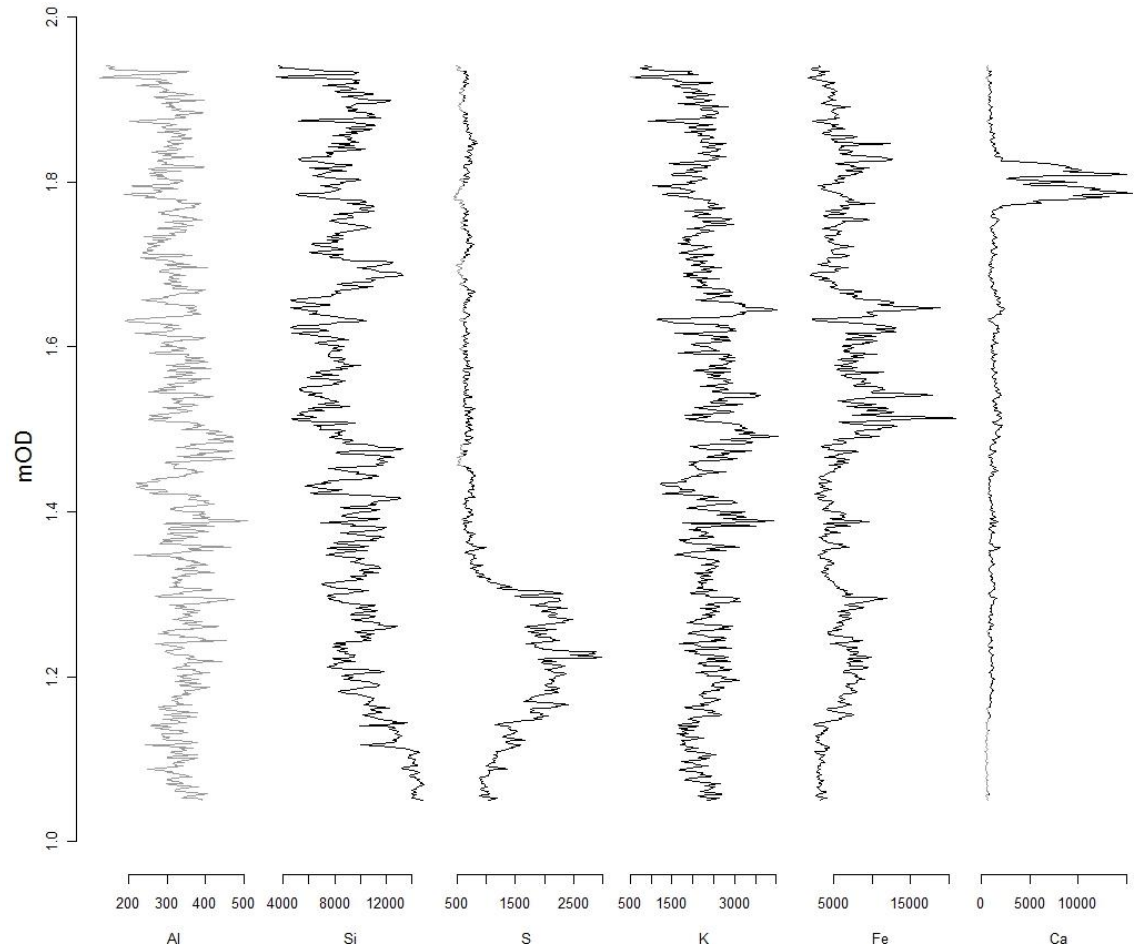

Figure 6.6 Examples from each of the downcore profile groups identified for DYN1. Values below 600cpa (corresponding to the threshold at which signal can be separated from noise) are plotted in grey.

6.2.5. DYN2

Al, K, Ti, Fe, Br and Rb are relatively low with little variability between the base of the core and 1.07mOD values are relatively low with little variability. Between 1.07mOD and 1.29mOD the overall trend is increasing but with high variability and numerous peaks and troughs. From 1.29mOD to the top of the core values decrease (Figure 6.7). K and Fe are the only elements those values are above 600cpa throughout the profile.

Si is maximum at the base of the core; there is a decreasing trend to 1.07mOD (Figure 6.7). Between 1.07mOD and 1.38mOD there is an overall decreasing trend however within this section there are numerous peaks and troughs. Count values then increase slightly to the top of the core.

Between the base of the core and 1.04mOD S values increase slightly (Figure 6.7). There is then a double peak at 1.05-1.07mOD above which are 2 smaller peaks at 1.12mOD and 1.15mOD. Above 1.15mOD values drop to below 600cpa remaining around this level to the top of the core.

These Ca and Sr profiles are again closely correlated. Overall the general trend is a slight increase from the base to the top of the core (Figure 6.7). However, there are several peaks within the profiles, notably at 1.07mOD, 1.14mOD, 1.3mOD and 1.38mOD and a deep broad trough at 1.39mOD. The Sr values range between 100-500cpa.

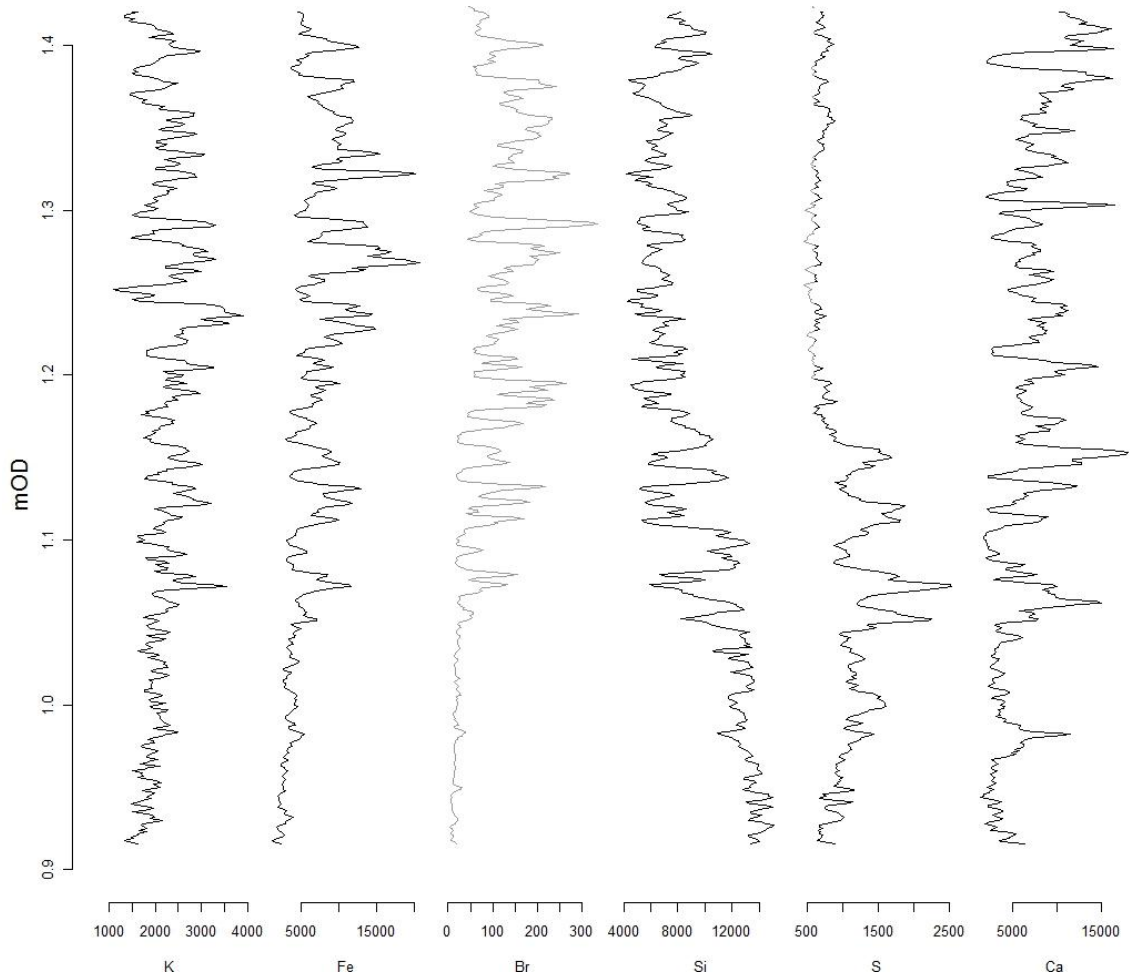

Figure 6.7 Examples from each of the downcore profile groups identified for DYN2. Values below 600cpa (corresponding to the threshold at which signal can be separated from noise) are plotted in grey.

6.2.6. Summary of core profiles

This initial exploratory examination of the downcore variations of element concentrations within the five cores identifies some relationships between both individual elements and element groups. Within all five cores a clear negative relationship can be seen between the elements associated with clay minerals (e.g. K, Ti, Al, Br, Zr) and the clastic, quartz sand, Si profiles. This is unsurprising as it has been seen that there are alternating layers of sand dominated and more organic rich units and therefore these profiles can be seen to alternate accordingly. Therefore it can be assumed that where there are peaks in the Si profile or troughs

in the clay element profiles this represents periods of fresh sand delivery to the sites. Within all the cores the Ca profile seems to show no significant relationships with any of the other elements apart from Sr. Assuming the primary source of the Ca is from $CaCO_3$ shell material this would suggest that shell material is not a consistent constituent of the wind blown sand deposited on the vegetated surfaces. The Ca profile of the SFD2, 3 and DYN1 cores are very similar to those identified in the previous carbonate analyses. Within the Sandfield core these would suggest a sudden cut-off of shell delivery to the machair surface whereas at Derryness the profile suggests two events occurring relatively closely in terms of time that delivered an increased supply of shell material to the vegetated surface. The sulphur profiles also often seem to vary independently of the other elements. The primary source of sulphur within these sediment sequences is likely to be from anoxic organic decay (Raven and Scrimgeour, 1997); therefore, peaks in these profiles potential indicate an increased organic content that was rapidly buried.

To enable further examination of the relationships between elements a correlation analysis was performed on the element data.

6.3. Correlation analysis

The distribution of elements in sediment sequences is primarily controlled by sediment texture and mineralogical composition. As a consequence of their bias towards a particular sediment source and/or sedimentology there are inherent auto-correlations between certain elements. For example, heavy metals show a strong affinity with silt and in particular clay as they are readily adsorbed onto its surface. Al, Ti, and K are all significant components of the clay fraction and therefore, in sediments with a silt and sand fraction, will behave inversely to Si, which is a major constituent of quartz particles (Cardoso *et al*., 2008).

Correlation matrices and significance tables provide additional visual interpretation and quantitative assessments of element relationships. Element vs. element scatter plots and correlograms (Friendly, 2002) were created for all element pair combinations in order to visually represent the statistical correlations (Figure 6.8). Pearson's correlation coefficient was applied to each element combination to quantify the strength, nature and significance of the associations.

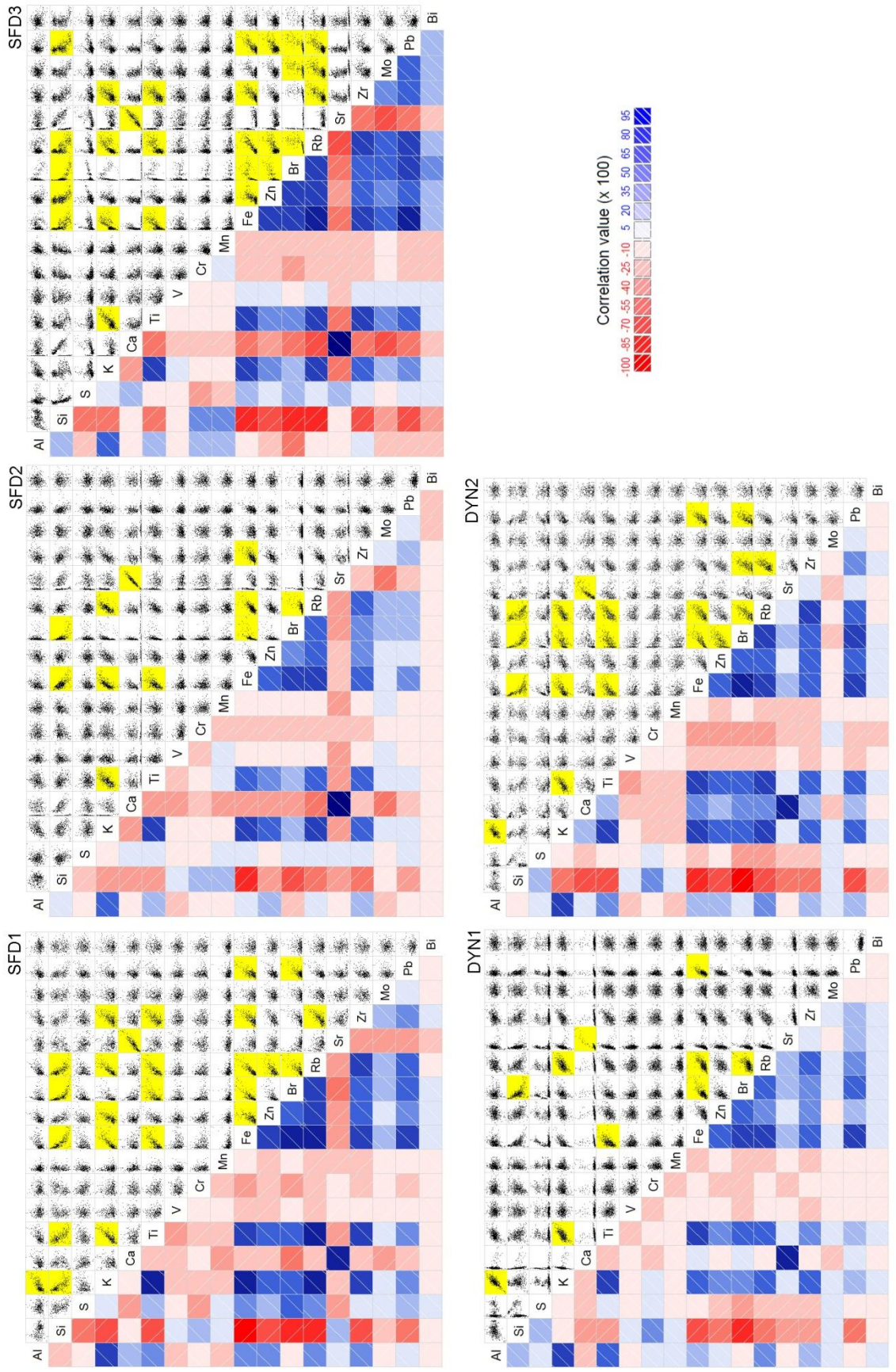

Figure 6.8 Element vs. element scatter plots (upper panels) and correlogram, indicating strength and characteristic of correlations, (lower panels). Correlations with a Pearson coefficient ≥ 0.6 or ≤ -0.6 highlighted in yellow.

6.3.1. SFD1

Within the SFD1 core Si is distinct as the only element to display significant negative correlations with other elements i.e. K, Ti, Fe, Br and Rb (Figure 6.8). K, Ti, Fe, Zn, Br, Zr and Pb are all strongly positively correlated with each other reflecting the similarities seen in their downcore profiles. However Al only correlates with K. Ca and Sr are again distinct from the other elements only positively correlating very strongly with each other.

6.3.2. SFD2

Figure 6.8 shows the element correlations present in the SFD2 core; however, due to the sharp decrease in the Ca and Sr values above 1.42mOD there appears to be 2 correlation groups in many of the element pairs. Therefore, in order to examine these correlations, the analysis considered core data above and below 1.42mOD as separate units.

Above 1.42mOD Si is distinct as the only element with significant negative correlations (Figure 6.9). Fe, Br and Rb all display positive correlations with each other and again Ca and Sr are strongly related with each other. Below 1.42mOD, Si shows distinct negative correlations. Sr and Ca are strongly positively correlated. K shows positive correlations with Al, Ti, Fe and Rb. Fe also correlates with Br and Rb (Figure 6.9).

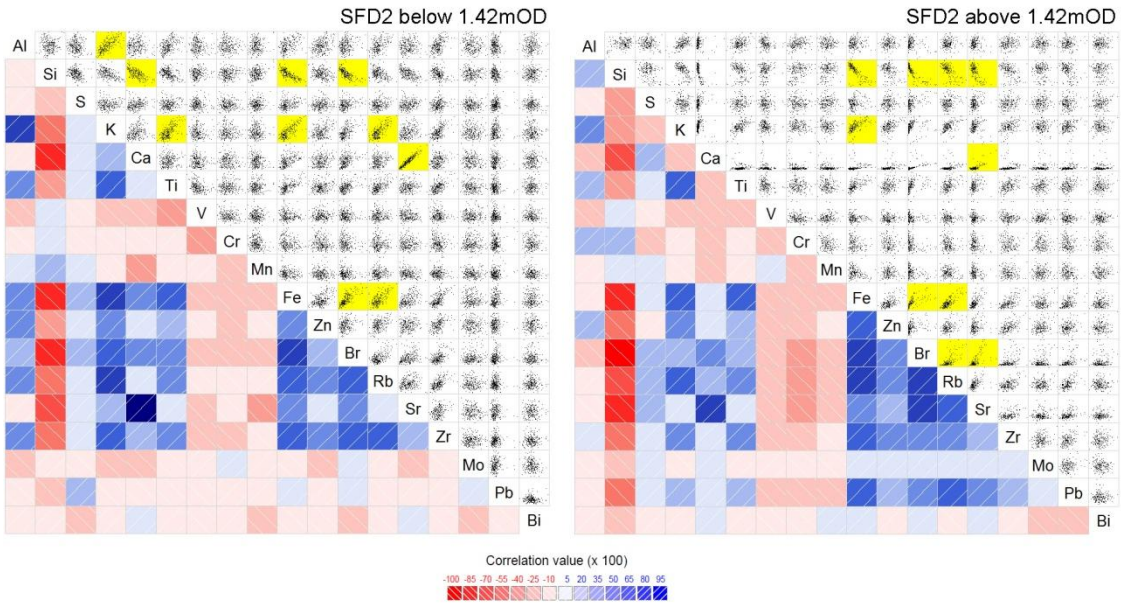

Figure 6.9 Separate correlograms for SFD2 above and below 1.42mOD.

6.3.3. SFD3

Figure 6.8 shows the correlations for the SFD3 core; again, due to the sharp decrease in the Ca and Sr values above 1.42mOD there appears to be 2 correlation groups in many of the element pairs. As with SFD2 the analysis was rerun on the data subsets above and below 1.42mOD.

Si is the only element to show negative correlations both above and below 1.42mOD. Ca and Sr are again strongly correlated; however above 1.42mOD, where their cpa values decrease, Ca also shows a positive correlation with Br and S and Sr with Rb, Br, Zn, S and negatively with Si. However, these correlations must be treated with caution due to the low count values of Ca in this section. Both above and below 1.42mOD Al, K, and Ti all show positive correlations. Above 1.42mOD Fe, Zn, Br, Rb, Mo and Pb form a correlation group as was seen and described for the individual element profiles (Figure 6.10).

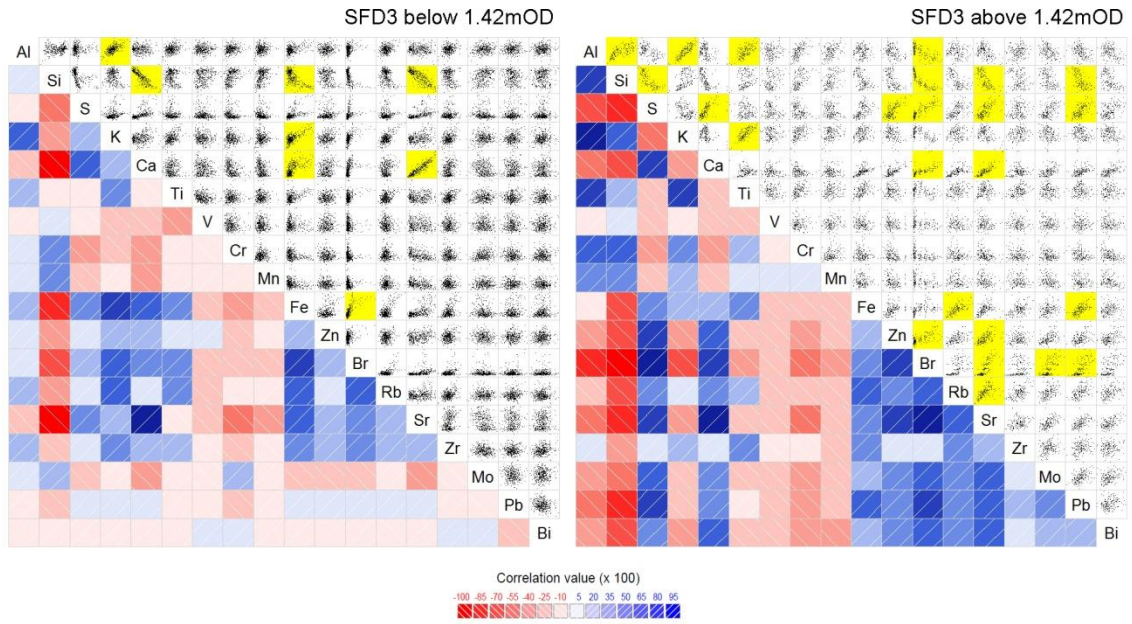

Figure 6.10 Separate correlograms for SFD3 above and below 1.42mOD.

6.3.4. DYN1

Within DYN1 Si is again the only element to display significant negative correlations, i.e. with Br, and Ca and Sr are strongly positively correlated with each other (Figure 6.8). The similarity of the Si and Al downcore profiles is not reflected by a significant correlation. Al, K and Ti show significant correlations with each other. Fe shows a number of positive correlations with Br, Rb, Pb and Ti reflecting the similarities identified in the downcore profiles.

6.3.5. DYN2

Si shows a number of negative correlations with Fe, Br and Rb. Again Ca and Sr are strongly positively correlated. The similarities identified in the downcore profiles of Al, K, Ti, Fe, Br, Rb and Pb are reflected in the correlations between these elements with the majority correlating positively with 3 or more elements from this group; the exception being Al which only correlates with K (Figure 6.8).

6.3.6. Summary of correlations

These correlation again highlight emphasises the presence of organic rich layers which are characterised by elements associated with clay particles and sand rich layers associated with silica quartz particles. The independence of Ca and Sr and their strong correlation with each other further confirms that the dominant source of Ca within the sediment is from shell material. This shell material does not correlate with either the clay or sand elements again highlighting the independence of its deposition.

Now that the relationship between these elements has been determined further analysis can be carried out to determine their potential as proxies of other environmental variables.

6.4. Element/element ratios and proxies

Ratios of element abundance are often used in geochemical analyses of sediments; in the marine and littoral environment previous studies have often focused on the presence and distribution of metal pollutants within the sediment (e.g. Ardelan and Steinnes, 2010; Vega *et al* 2009; Bouezmarni and Wollast, 2005). Element/element ratios are particularly important in analyses where effects of a constant sum in percentage data needs to be taken into account (Chayes, 1971). However, these ratios can provide useful additional information on the relationships between elements and their profiles on all geochemical data including count per area data.

6.4.1. Si/K

One major reason for normalising the data via ratios is to account for the effects of grain size (e.g. Bouezmarni and Wollast, 2005). Trace elements tend to be absorbed onto the surface of particles and therefore their concentrations increase as grain size decreases and total surface area increases (Daskalakis and O'Connor, 1995). Al, K, and Ti are all present in clay minerals (Deer *et al.*, 1992) and correlate strongly in the results. Of these, K has consistently the best signal (highest counts per area) throughout all the cores and was therefore used to normalise to correct for grain size. The Si/K ratio can be used to provide an indicator of sand-dominated layers.

All five cores show a marked repetition of peaks and troughs throughout the sequence (Figure 6.11). This reflects the light and dark banding described in the downcore profiles and peels associated with minerogenic rich and more organic layers. These peaks and trough occur fairly regularly throughout the profiles and are primarily 5mm or less in width. There are a number of individual features and groups of features that can be recognised in more than one core therefore allowing cross-correlation of the sequences (Figure 6.11). There are potentially two features correlating SFD2 and SFD3 with DYN1; a trough-peak-trough sequence occurring at approximately 1.3mOD in the Sandfield cores and at 1.65mOD in DYN1 and a drop in Si/K values and slight increase in the width of peaks and troughs at 1.18mOD and 1.47mOD in SFD 2/3 and DYN1 respectively (Figure 6.11).

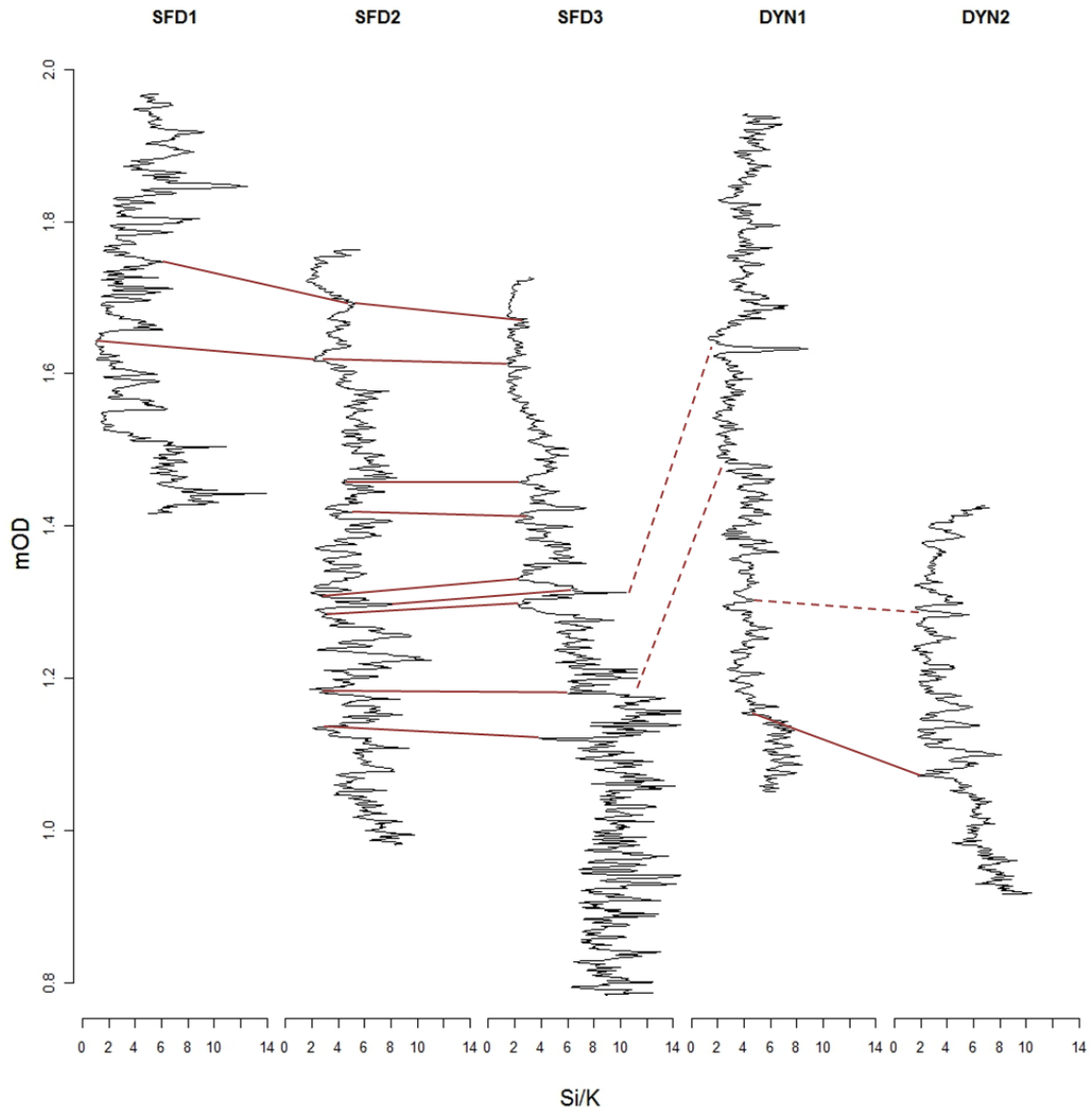

Figure 6.11 Downcore profiles of Si/K for all cores (red lines link similar features present in two or more cores, dashed lines indicate possible similarities).

The most similarities occur between SFD2 and SFD3. Both these cores show a decreasing trend from the base of the core upwards with Si/K values becoming less variable to the top of the cores. SFD1 is distinct from the other Sandfield cores in that it shows greater variability in Si/K values and more irregularity in the frequency of peaks and troughs particularly in the bottom half of the profile where two troughs of approximately 20cm occur. There is a decreasing trend to 1.76mOD (approximately the level of the top of SFD2) although above this Si/K values increase, indicating an increase in sand domination. Within this top section there are a number of sharp peaks most notably at 1.85mOD.

Between the Derryness cores there are few similarities, possibly due to the relatively small overlap in the elevations of the two cores. DYN1 shows no overall increasing or decreasing trend throughout the core and variability between the peaks and troughs is relatively small compared to the other cores.

6.4.2. Ca/K

Ca is also present within clay minerals; however it does not correlate with K. This suggests Ca within the sediment is likely to be due to the presence of calcium carbonate ($CaCO_3$), probably within shell material. This is corroborated by a significant similarity with the carbonate contents presented in Chapter 5.3 for cores SFD3 and DYN1 ($p=<0.001$, $R^2=0.935$ and $p=<0.001$, $R^2=0.7689$ respectively). The high correlation between Ca and Sr values is also indicative of the link to calcium carbonate as the Sr ion readily interchanges with Ca in the aragonite mineral structure (Deer *et al*, 1992). The Ca/K ratio was therefore used as an indicator of shell rich layers.

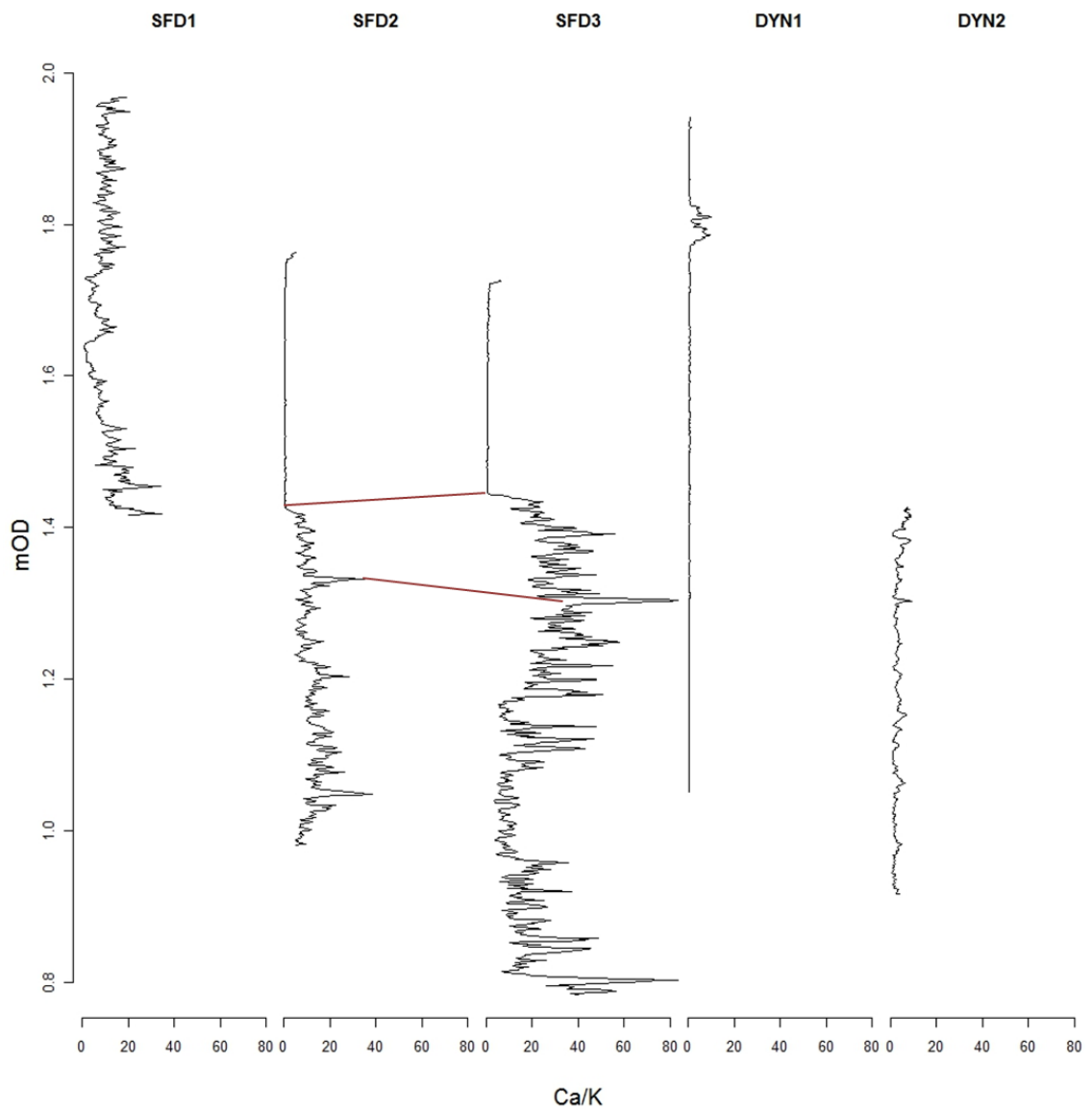

Figure 6.12 Downcore profiles of Ca/K for all cores (red lines link similar features present in two or more cores).

With the exception of SFD2 and SFD3 the Ca/K profiles are very different for each core (Figure 6.12). The SFD1 profile shows similar trends to its Si/K profile although less variable; i.e. a decreasing trend to ~1.76mOD with values increasing slightly above this. This would suggest the input of Ca (shell material) is via the same transport mechanism as the Si sand. The most dominant feature of SFD2 and 3 is the sharp drop in Ca/K values at ~1.42 - 1.45mOD. This is identical to that seen in the bulk carbonate results for SFD3 in chapter 5.3. Below this point SFD3 has significantly higher Ca/K values than at any point in any of the other cores indicating a greater carbonate content in this core.

Ca/K values for both the Derryness cores are at or around zero although there is slightly more variation in DYN2 with a slight increase to the top of the core. At 1.80mOD in DYN1 there is a small double peak indicating a short period when carbonate (likely shell material) was deposited onto this site.

6.4.3. Fe/K

Fe can be present within clay minerals but also in the Fe-precipitates (Deer *et al.*, 1992). Within the majority of correlations Fe is significantly positively correlated with K indicating its presence within the clay minerals; therefore, the Fe/K ratio was used to indicate discrete Fe-rich horizons. This can therefore be used to give an indication of the redox potential of the environment, i.e. Fe is soluble under anoxic conditions and precipitates when oxic. Mn and Pb, although noisy, show a similar pattern to Fe in many of the core profiles as they have a similar redox-behaviour. It would be expected that V and Mo would display the opposite profile. However they are too rare to show up in this analysis.

Within all three Sandfield cores there is a peak in Fe/K values at 1.62-1.63mOD (Figure 6.13); this coincides with the elevation of MHWS (1.63mOD). It is possible that mobile, soluble Fe is being transported though the sediment and its oxidation and precipitation are controlled by ground water saturation levels. However, a distinct peak at a similar level in DYN1 is not present; a peak of similar appearance is present at 1.50mOD. Within SFD3 there is an increasing trend towards the top of the core not present in any of the other cores. This may be due to the greater percentage of finer material in the SFD3 core providing a source from which Fe-precipitates may form. Also the more organic rich nature of the top of this core would suggest more biological oxidation of the sediment.

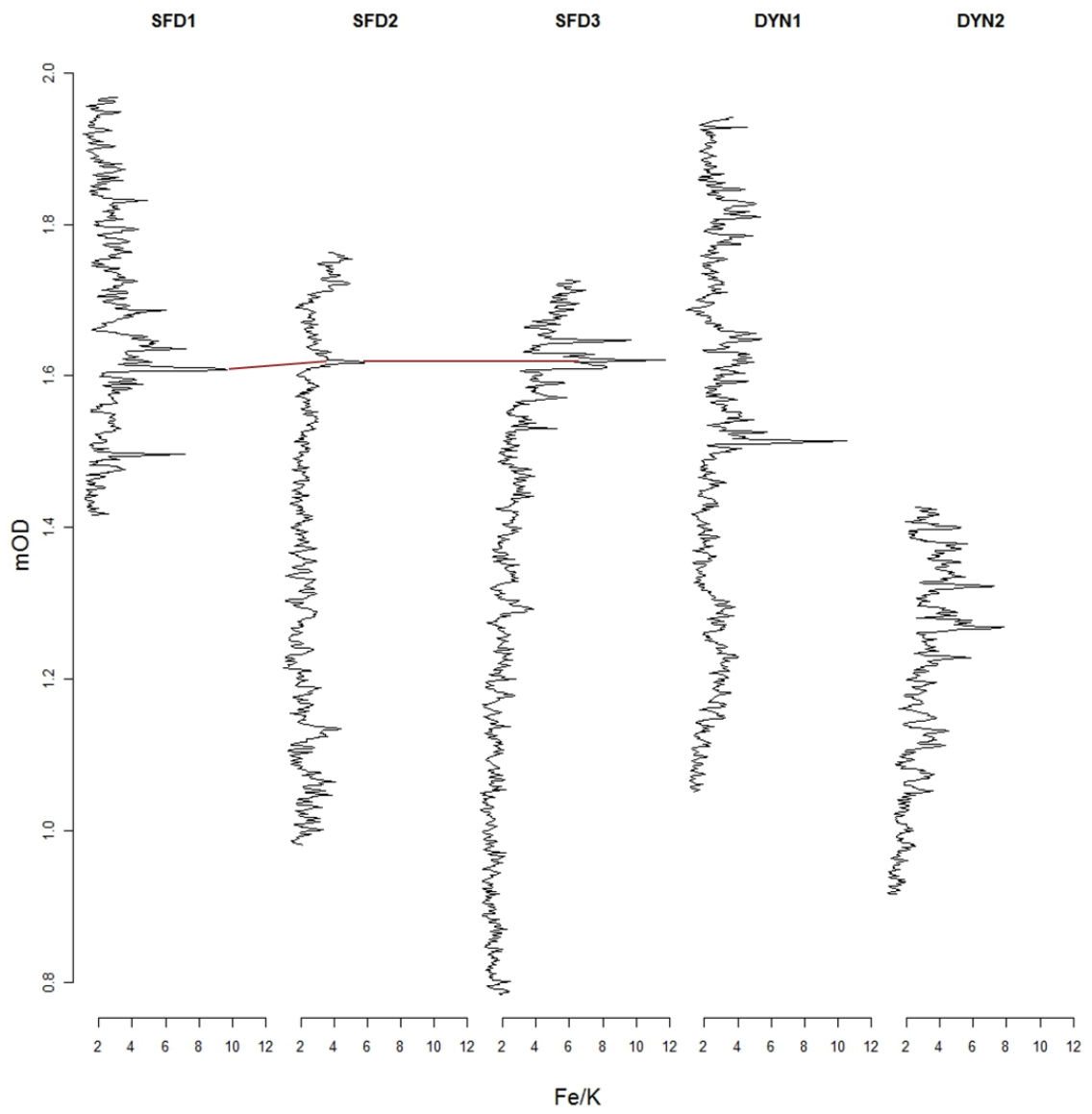

Figure 6.13 Downcore profiles of Fe/K for all cores (red lines link similar features present in two or more cores).

6.4.4. Br

When Br is available it absorbs onto organic matter (Gerritse and George, 1988); therefore Br was used as an indicator of organic material and validated against the organic content results (chapter 5.3) (SFD3: p=<0.001, R^2=0.9223, DYN1: p=<0.001, R^2= 0.5095).

There is a pronounced broad trough present at a similar level in SFD1, SFD3 and DYN1; either side of this the SFD1 and DYN1 profiles are very similar, i.e. a small peak followed by a decrease in Br values (Figure 6.14). Both SFD2 and 3 show an increasing trend in the top section of the core; this is likely due to the increase in finer material of organic origin. There is an increasing trend in SFD1 to the broad trough at approximately 1.68mOD above which Br

levels decrease suggesting decreasing in organic matter and therefore plant material from this point to the top of the core.

DYN1 and DYN2 have Br values of close to zero from the base of the core to 1.08mOD and 1.13mOD respectively. Above this point, Br increases slightly in DYN1 reaching a maximum immediately above the broad trough. Br then decreases to the top of the core. In DYN2, Br values are more variable but with no overall trend to the top of the core.

The decreasing trend in the upper sections of SFD1 and DYN1 suggest that at these locations either organic productivity has decreased and/or input of minerogenic material has increased. Conversely the increasing trends of SFD2 and SFD3 suggest an increase in organic productivity and/or a decrease in the input of minerogenic material.

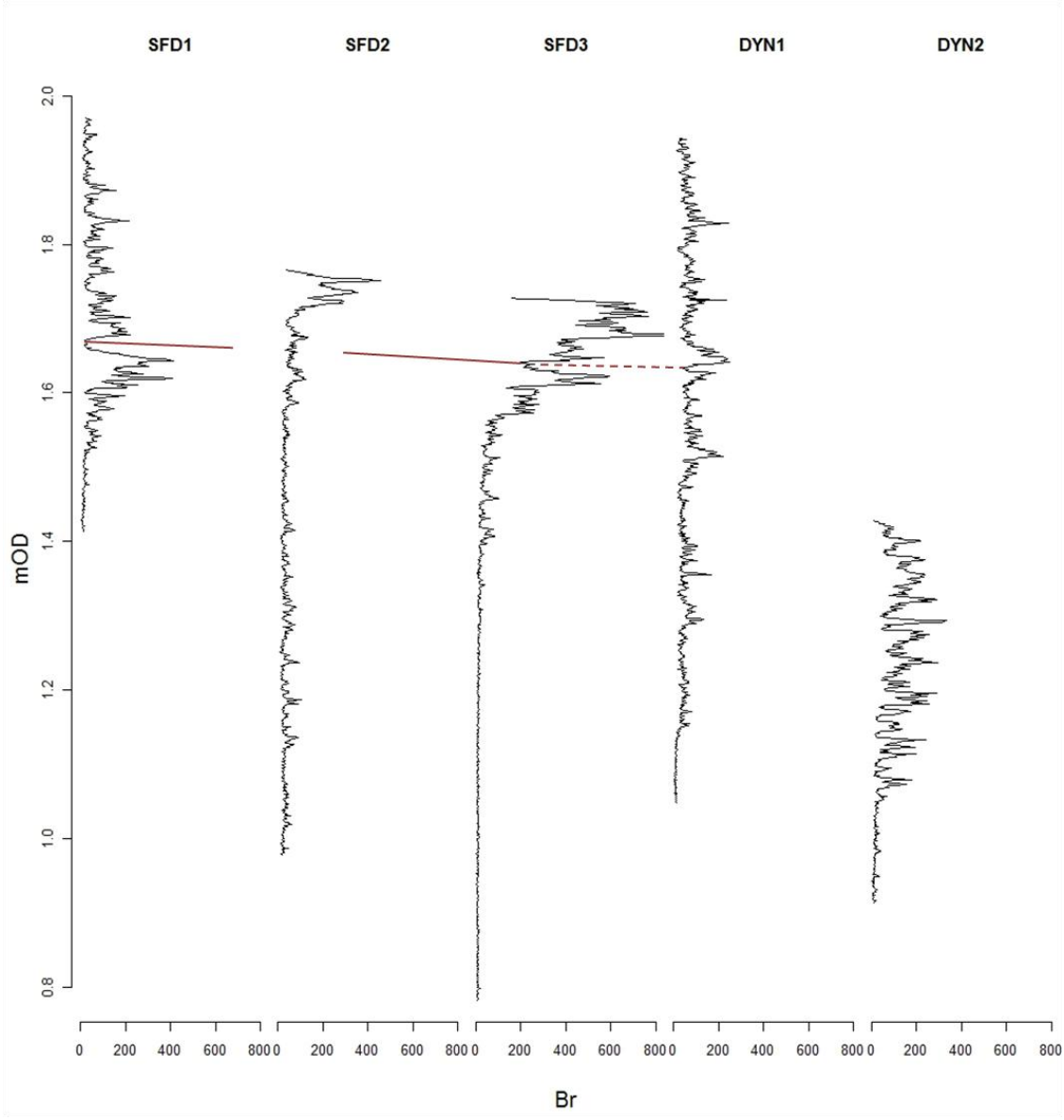

Figure 6.14 Downcore profiles of Br (counts per area) for all cores (red lines link similar features present in two or more cores, dashed lines indicate possible similarities).

6.4.5. Pb/K

Increases in the concentrations of lead within sediment sequences is has been used to indicate an increase as atmospheric pollution increased as a result of the industrial revolution. Therefore this has the potential to be used as a proxy for timing of deposition. Pb is a grain size controlled element as it readily absorbs onto particle surfaces therefore the Pb/K ratio has been used to take into account this grain size effect. SFD3 is the only core in which there is any overall trend in the Pb/K profile. Within this core Pb/K values are low with no overall increasing or decreasing trend for the majority of the core, there is a slight increase in values from approximately 1.6mOD to the top of the core (Figure 6.15). If this increase is implied to be indicative of increased pollution as a result of the industrial revolution from around 1800 this would indicate a deposition rate of approximately 0.5mm per year. This is significantly lower than the rate of 1.3±1mm calculated from ^{210}Pb and ^{137}Cs dating and would place the transition from tidal flat to vegetated marsh (i.e. 25cm depth) to approximately 1500. However, there is a large amount of uncertainty associated with using this ratio as a proxy for timing of deposition in this situation due to the very low concentrations of Pb within the SFD3 core (well below the inferred 600cpa threshold of repeatability).

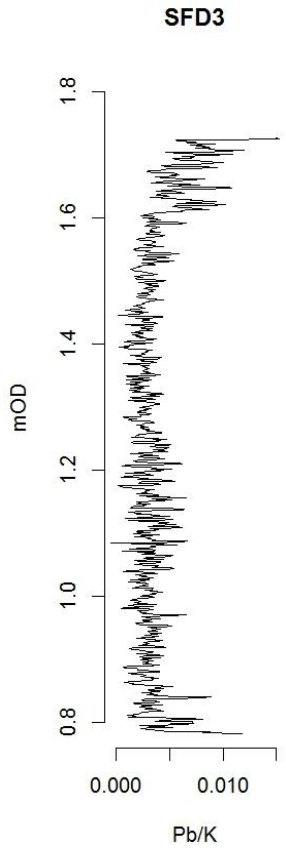

Figure 6.15 Downcore profile of Pb/K for SFD3

6.4.6. Summary of ratios and proxies

Using an element ratio approach enables the normalisation of results to take into account grain size effects both within and between cores and to allow analysis of elements as proxies for other environmental information. Here, this has enabled the correlation of features between cores and potentially between sites. This is significant as it implies that the factors influencing sediment deposition and controlling the development of the sedimentary record are operating on an estuary-wide scale rather than local to the individual sites.

The Si/K ratio is particularly important to these cores as it is the geochemical representation of the light and dark banding clearly visible within the sections. The ability to quantify this feature enables further analysis of the structure of the sedimentary sequences to be carried out. The Ca/K ratios are also significant as they confirm the $CaCO_3$ cut-off identified in previous analyses and at this higher resolution of sampling further emphasise the abrupt nature of the decrease. This provides further supporting evidence for the occurrence of a single short lived event resulting in the cessation of supply of shell material to the east of the Sandfield site. The ability to correlate this with the SFD2 core not only provides more information on the spatial extent of the reduction in shell content but also allows the limited chronology information for the SFD3 core to be applied to a certain extent to the SFD2 core. Based upon a deposition rate of 1.3mm/year the $CaCO_3$ cut-off in SFD3 can be dated to around 1790; therefore this date can also be applied to the SFD2 core for this downcore feature.

The following section examines in further detail the structure of downcore changes identified in the element ratios.

6.5. Downcore structure

Identification of formal groupings of downcore element trends within the individual cores was achieved through application of multivariate analysis (PCA and cluster analysis) to the scanning XRF data.

Both PCA and cluster analyses were performed on the data. To maintain the importance of the influence of the dominant elements in determining sediment characteristic scaling of element data to unit variance was not applied; this also allows the uncertainty associated with low values to be taken into account. The cluster analysis was carried out using Ward's method which forms clusters by maximising the within group similarities (Primpas *et al*, 2008). This method is generally regarded as being very efficient and produces a well-proportioned hierarchical structure (Swan and Sandilands, 1995).

Grouping based upon ordination of the PCA alone is insufficient to identify distinct clusters. Cluster analysis is useful in providing definitive groups and boundaries. The choice of the

position of the phenon line, i.e. the level at which to cut the dendrogram, was based on primarily on "natural solutions" where there are large gaps between linkage points. The combined use of PCA and Cluster analysis allowed a grouping approach to be taken (identifying samples with similar features) with a data reduction approach (reducing the number of variables to a smaller set of PCs). The result of which enables a systematic approach to the identification of groups. Further analysis of the resulting PC scores for the individual element provides additional information on the elements that typify or explain the most variation in the identified cluster groups.

6.5.1. SFD1

Cluster analysis of the SFD1 data forms 4 distinct clusters (Figure 6.16). Analysis of PC scores for the individual elements allows characterisation of the PCs and cluster groups (Figure 6.17). Repeated banding of the 4 groups and in particular groups 1-3 is present throughout the core. Group 1 is characterised by clay elements and associates, i.e. K, Ti, Mn and Zn; it becomes more common towards the top of the core although also occurs in two relatively thick bands between 1.55 and 1.60mOD. Group 2 is primarily associated with Si and occurs throughout the core but again becomes more dominant towards the top of the core. Group 3 is associated with Ca and can be seen to occur most frequently below 1.85mOD. Group 4 is primarily associated with Fe and occurs in a relatively thick band between 1.60 and 1.65mOD. As can be seen in the ratio profiles this unit is distinct from the rest of the core having low Si/k and Ca/K values but high Fe/K and Br values (Figure 6.16).

Overall the analysis of this core indicates an alternation of layers characterised by Si and clay elements throughout the core. Below 1.85mOD Ca is more common; the Fe dominated layers in the mid section of the section may be due to an increase organic content. These changes are indicative of the overall transition from unvegetated (sand dominated) tidal flat environment where shell material is more common to vertically accreting vegetated area where finer, more organic sediments are deposited.

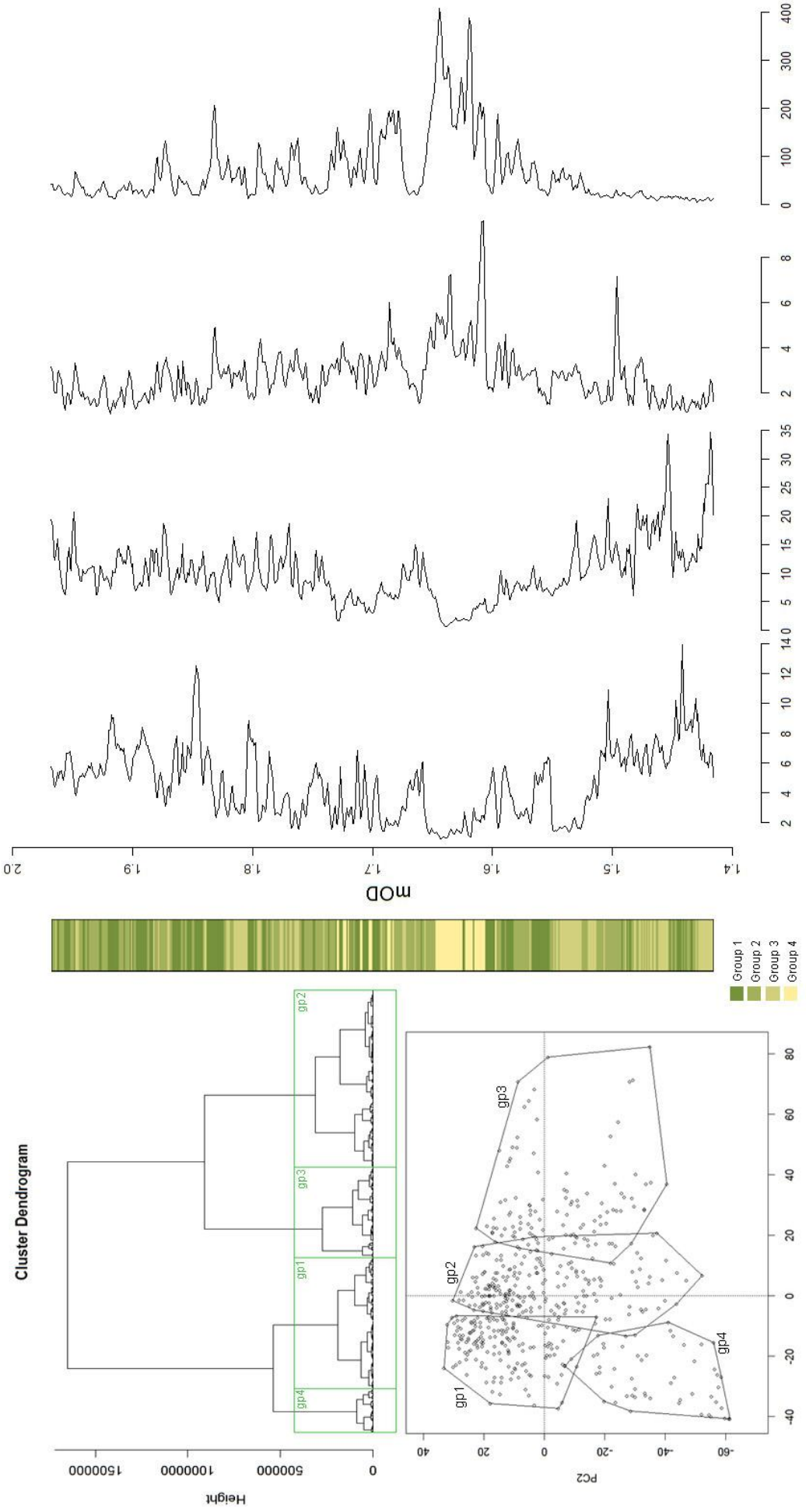

Figure 6.16 SFD1 PCA and cluster analysis. Top left: cluster analysis of scanning XRF data. Bottom left: PCA of scanning XRF data indicating cluster groups. Right: Representation of cluster groups downcore against the 4 ratio plots that best describe the downcore variations identified.

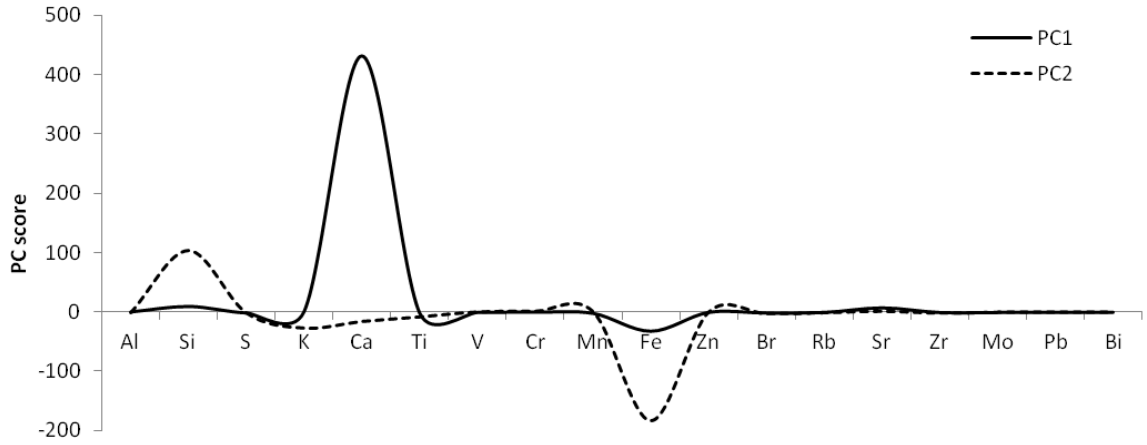

Figure 6.17 SFD1 Principal Component scores for individual elements.

6.5.2. SFD2

Due to the dramatic decrease in Ca and Sr values at 1.42mOD having a significant impact on the cluster and PCA analysis which potentially masks other downcore patterns and groupings the analyses were performed on the sections above and below 1.42mOD separately. Within the bottom section of the core the primary variable influencing cluster groupings is Ca (Figure 6.19). Group 1 is associated with Si and occurs in relatively thick bands at the base of the core and between 1.25 and 1.42mOD where the Si/K ratio is high (Figure 6.18). Group 2 is associated with the clay elements K and Ti and is relatively uncommon throughout this lower section of the core. Group 3 is primarily associated with Fe and is also relatively uncommon. Group 4 is associated with Ca and occurs frequently throughout the lower section of the core where Ca/K values rise. Within the top section of the core, i.e. above 1.42mOD, 3 cluster groups were identified (Figure 6.18). Group 1 is associated with Fe and to a lesser extent Ca (Figure 6.19); it occurs in the top ~8cm of the core and in an approximately 2cm band at about 1.63mOD. The association of Ca to group 1 is likely due its slight increase in the top 1cm of the core. Group 2 is associated with the clay elements K and Ti and also slightly with Mn and Zn. This group becomes more common towards the top of the core and is dominant between 1.60 and 1.72mOD. Group 3 is associated with Si and occurs where the Si/K ratio is at its highest for this top section of the core, i.e. 1.42 to 1.6mOD.

Overall the analysis of this core indicates an alternation of layers characterised by Si and Ca in the lower section of the core, below 1.42mOD. Above this, in the upper section, there is a transition up-core characterised by a decrease in Si with a corresponding increase in clay elements and an increase in Fe to the top of the core which as discussed previously is likely associated with an increase in organic material. These changes are indicative of the overall transition from unvegetated (sand dominated) tidal flat environment to vertically accreting vegetated area where finer, more organic sediments are deposited. The increase in Fe to the top is likely due to the greater organic content in this section of the core.

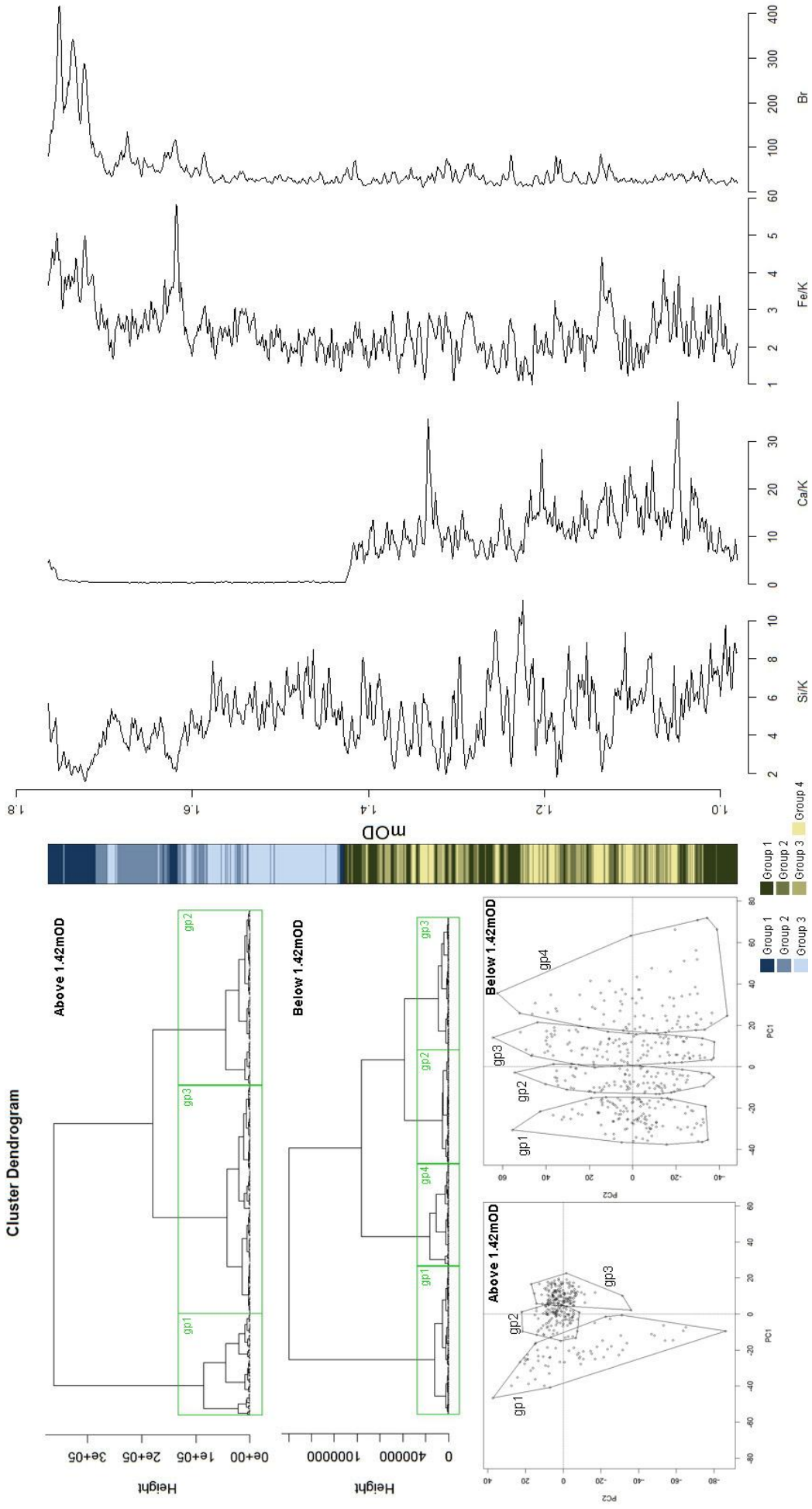

Figure 6.18 SFD2 PCA and cluster analysis. Top left: cluster analysis of scanning XRF data. Bottom left: PCA of scanning XRF data indicating cluster groups. Right: Representation of cluster groups downcore against the 4 ratio plots that best describe the downcore variations identified

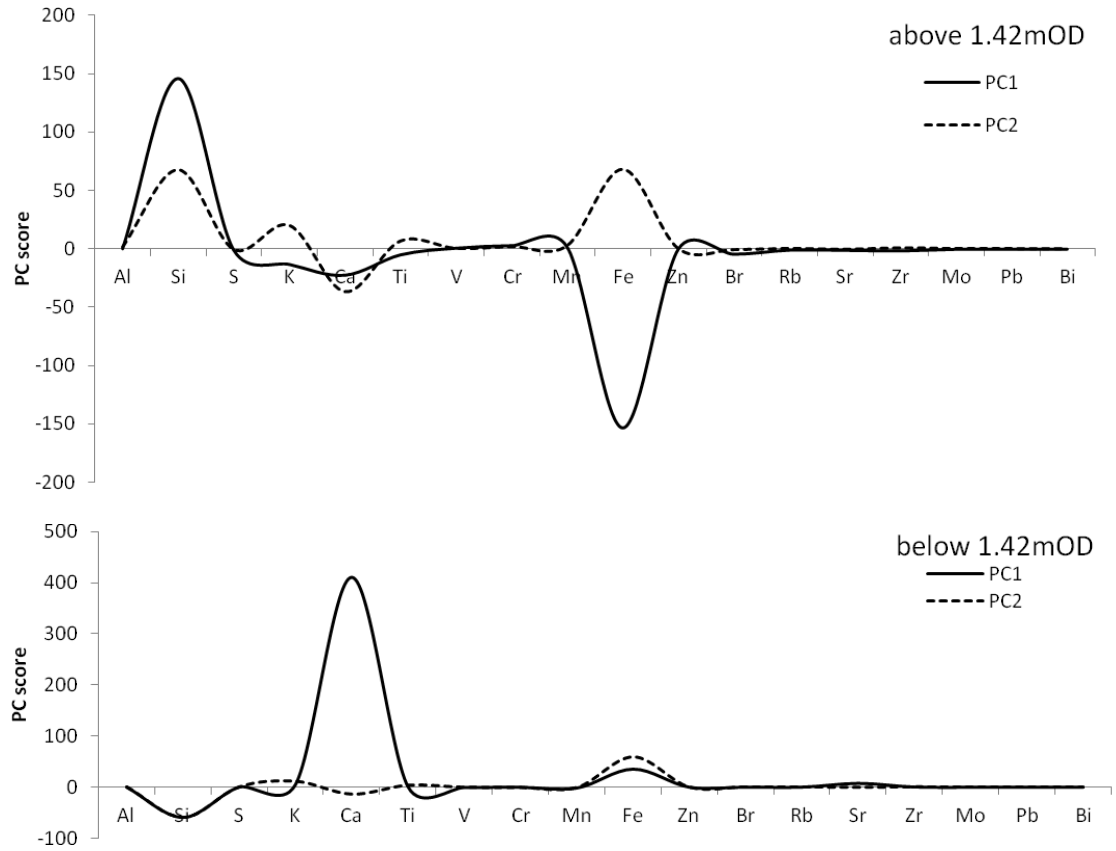

Figure 6.19 SFD2 Principal Component scores for individual elements

6.5.3. SFD3

Similarly to SFD2, for the reasons stated above, analyses were performed on the sections above and below 1.42mOD separately. Both the cluster groupings and principal component scores of individual elements for SFD3 are very similar to those of SFD2 (Figure 6.20, Figure 6.21). Below 1.42mOD the main variable influencing the groups is Ca. Group 1 is associated with Si and occurs predominately below 1.2mOD, becoming more intermittent towards the base. Group 2 is associated with the clay elements, K, Ti and Mn. It is the least common of the 4 groups in the bottom section occurring predominately in the base of the core below 1.0mOD. Group 3 is associated with Fe and Sr and occurs throughout the bottom section of the core although is more common above 1.2mOD. Group 4 is associated with Ca and occurs mainly above 1.2mOD where it is banded with predominantly Group 3 this is likely due to the significant correlations between Ca and Sr described earlier.

Above 1.42mOD 3 cluster groups were identified. Group 1 is associated with Ca and Br and occurs in the top 10cm of the core intermittent with Group 2. Group 2 is associated with Fe and occurs above 1.56mOD. As mentioned previously, the importance of Fe and Br in the top of the core is likely indicative of an increase in organic matter. Group 3 is associated with Si and occurs almost exclusively between 1.42 and 1.56mOD.

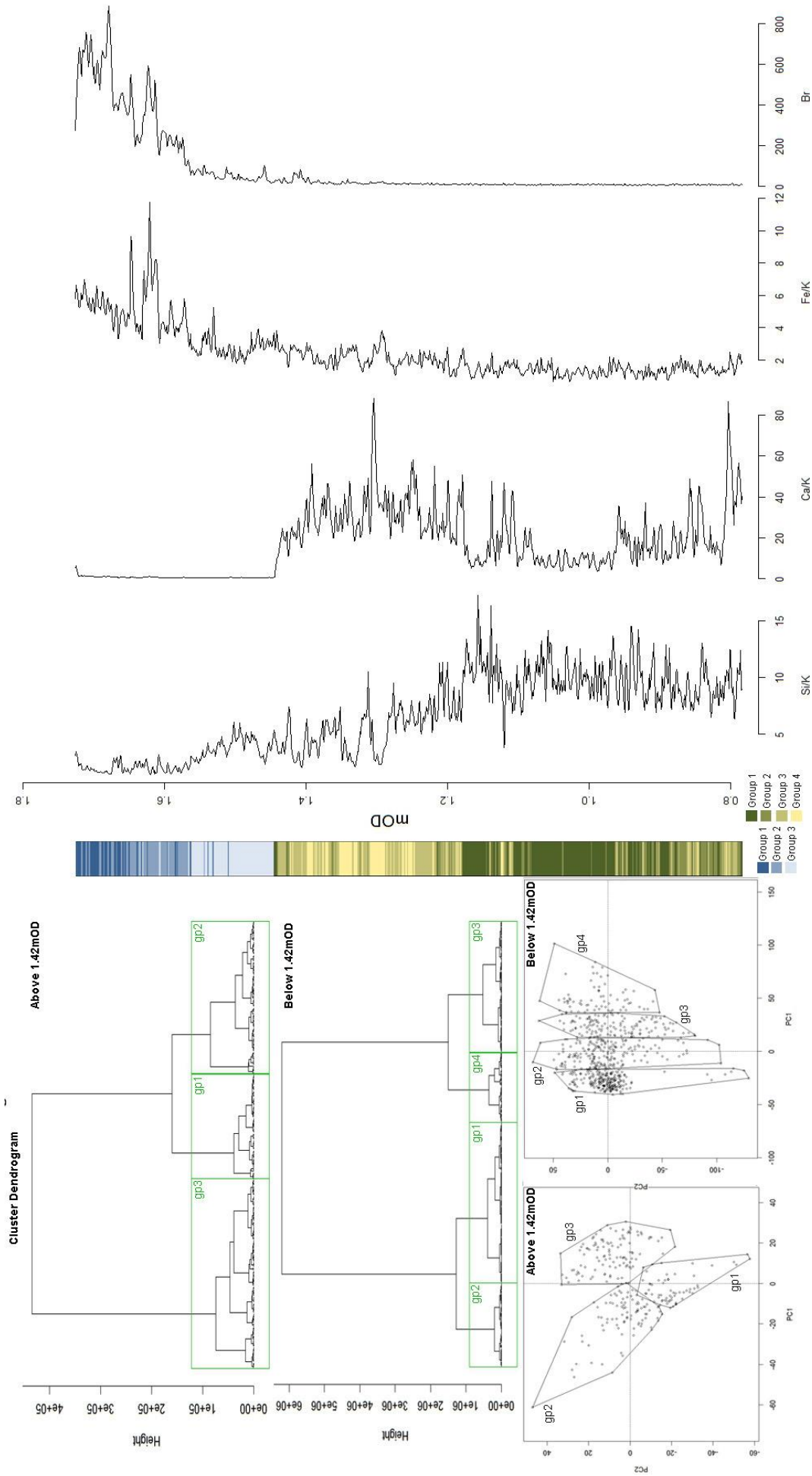

Figure 6.20 SFD3 PCA and cluster analysis. Top left: cluster analysis of scanning XRF data. Bottom left: PCA of scanning XRF data indicating cluster groups. Right: Representation of cluster groups downcore against the 4 ratio plots that best describe the downcore variations identified

Similar to SFD2 the overall the analysis of this core indicates an alternation of layers characterised by Si and Ca in the lower section of the core, below 1.42mOD. Above this, in the upper section, there is a transition up-core characterised alternation between two clay groups, i.e. one characterised by Ca and Br and one characterised by Fe. The presence of the Si group only within a limited section suggests organic deposition dominates in this upper section and inputs of fresh aeolian sand are rare. These changes are indicative of the overall transition from unvegetated (sand dominated) tidal flat environment to vertically accreting vegetated area where finer, more organic sediments are deposited.

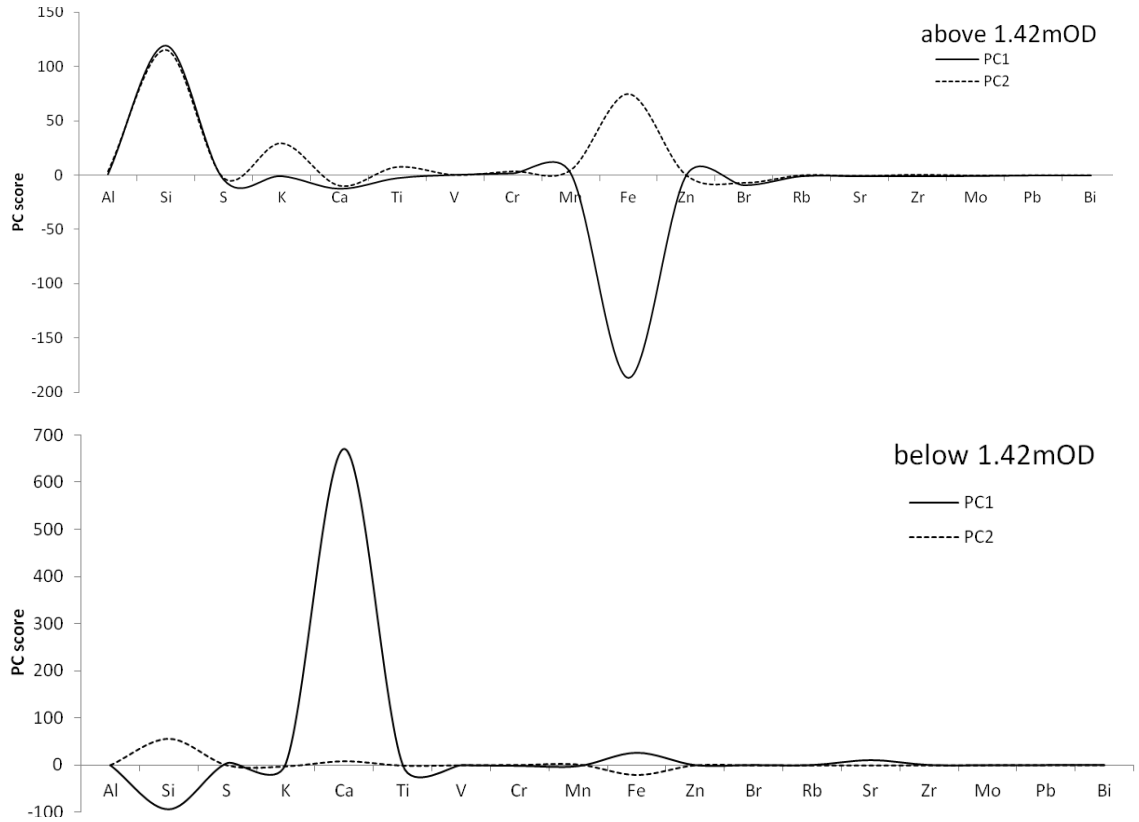

Figure 6.21 SFD3 Principal Component scores for individual elements.

6.5.4. DYN1

Five cluster groups were identified in the DYN1 core. The ordination plot shows little variation between groups 1, 2 and 3. Defining a higher phenon line would combine these 3 in to one or two groups, but when compared to the ratio profiles, the original clusters appear to represent significant features (Figure 6.22), so the original analysis was retained. Group 1 is associated with Mn, Zn and Br (Figure 6.23) it occurs throughout the core in bands of less than 1cm however there are two bands of approximately 5cm thickness at 1.35mOD and at the top of the core. Group 2 is associated with K (Figure 6.23) and occurs throughout the core again in bands predominantly less than 1cm thick. This group is indicative of finer material and consequently

occurs where the Si/K ratio value is lower. Group 3 is associated with Si (Figure 6.23) and occurs predominately in a thick band at the base of the core where the Si/K ratio is high. This group represents sections where there is a very high proportion of quartz sand. Group 4 is associated with Fe (Figure 6.23) and occurs in thin bands (less than 1cm) mostly between 1.50 and 1.65mOD (Figure 6.22). Within this group Si/K values are low and Fe/K and Br values are high, given the link between Fe and organic content discussed earlier, this suggests that this group represents sections of higher organic content. Group 5 is associated with Ca (Figure 6.23) and occurs in two relatively thick bands between 1.78 and 1.81mOD concurrent with the two peaks in the Ca/K profile and therefore identifying sections of greater shell content.

Overall the analysis of this core indicates an alternation of layers characterised by Si and clay elements throughout the core and is indicative of the light and dark banding clearly visible in the sections. These alternations are indicative of an overall relatively consistent environment of repeating depositions of sand and organic material. In contrast, the less regular occurrence of Fe and Ca dominated layers is suggestive of rare atypical events where higher proportions of shell or organic material are deposited on the surface.

6.5.5. DYN2

Within the DYN2 core 3 cluster groups were identified (Figure 6.24). Group 1 is the least common throughout the core and is associated with the clay mineral elements, i.e. K and Ti, and with the organic proxy Br (Figure 6.25). This group occurs in bands of up to 1cm thickness above 1.08mOD. Group 2 is associated with Ca and Fe (Figure 6.25). Given the relatively low Ca count per area and Ca/K values of this core, particularly compared to those of the Sandfield cores, it is possible that a greater percentage of Ca is present in the clay fraction rather than from shell material. This would account for the association between Fe and Ca and would therefore suggest that group 2 is indicative of sections of finer material and higher organic content. Group 3 is associated with Si (Figure 6.25) and occurs, predominately, between 1.1mOD and the base of the core where the Si/K ratio is highest (Figure 6.24). This group therefore represents a greater dominance of quartz sand in the sediment.

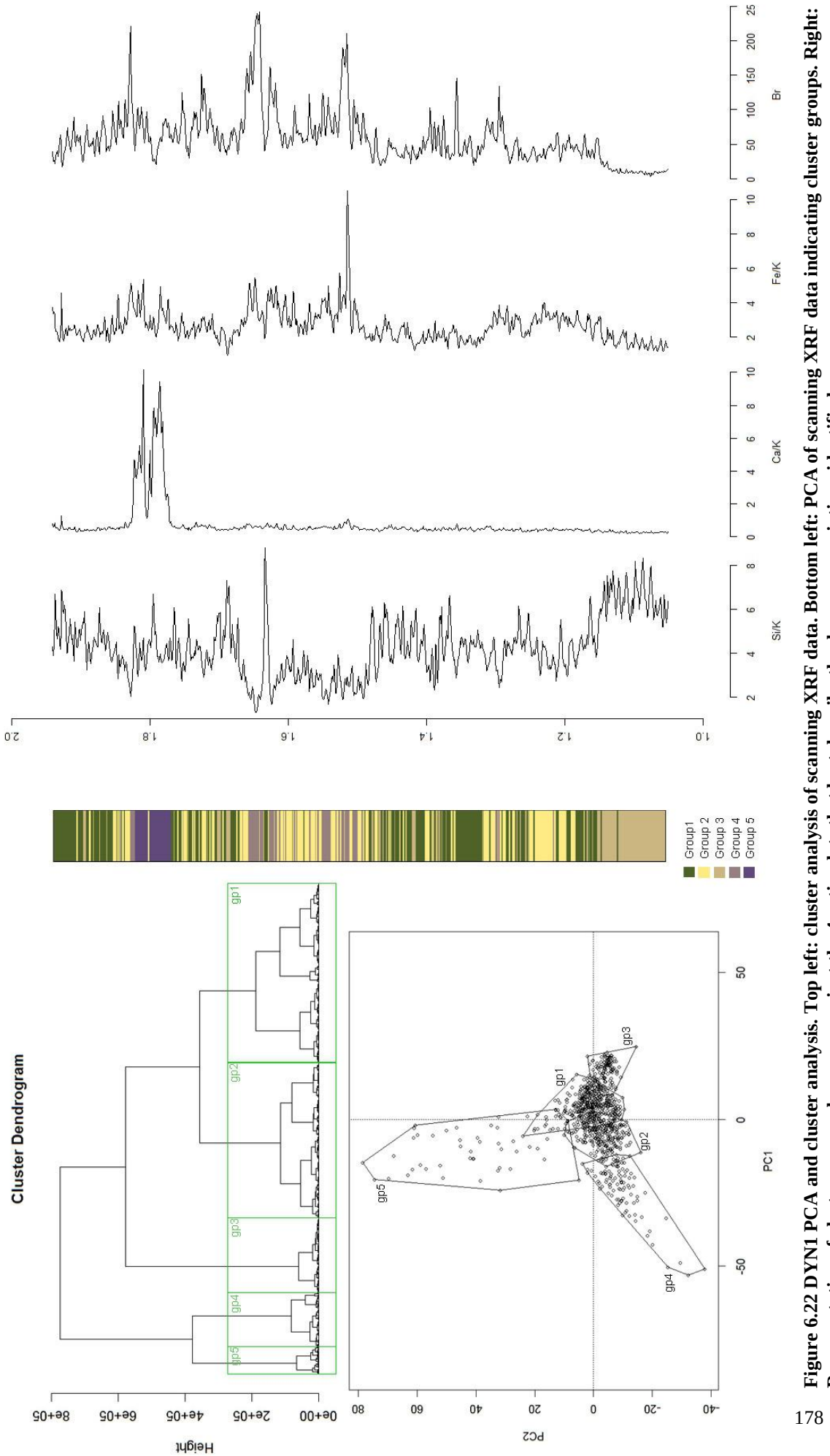

Figure 6.22 DYN1 PCA and cluster analysis. Top left: cluster analysis of scanning XRF data. Bottom left: PCA of scanning XRF data indicating cluster groups. Right: Representation of cluster groups downcore against the 4 ratio plots that best describe the downcore variations identified

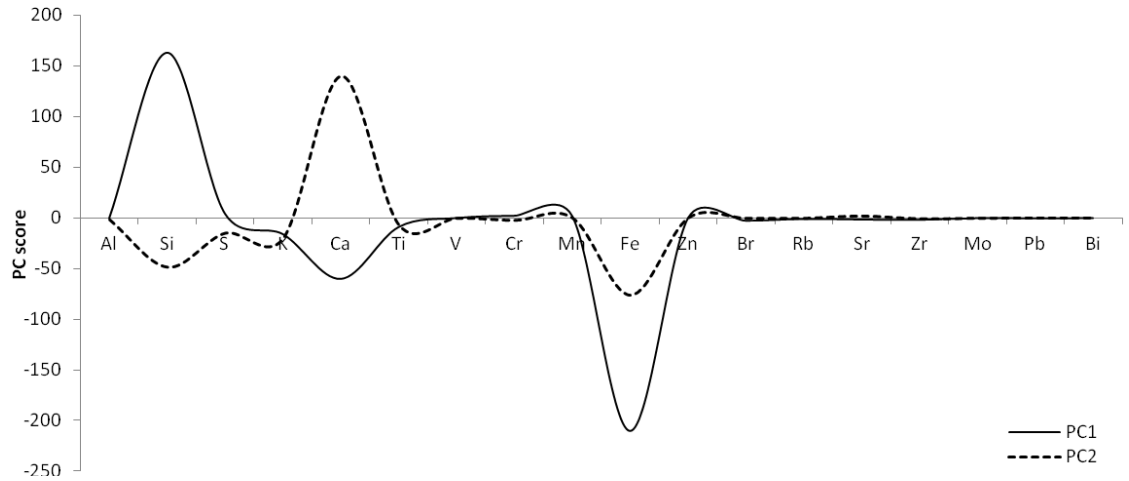

Figure 6.23 DYN1 Principal Component scores for individual elements.

There is less variation identified within the DYN2 core than the other 4 Sandfield and Derryness cores with only 3 groups identified. Overall the analysis of this core indicates a transition from a sand dominated lower section to finer sediment and greater organic content towards the top of the core. This transition is interpreted as sand dominated deposition on a tidal flat area with increased fine and organic material as vertical accretion raises the surface above the tidal flat and vegetation becomes established. The width of the layers of the individual groups is also significantly greater in this core than the other 4 Sandfield and Derryness cores. This reflects the wider alternating light and dark bands identified in the visual description of this core. There are two potential reasons for the layers being thicker in this core; 1) deposition rates are greater, 2) this area is not subject to the same degree of environmental change. Given the close proximity to the DYN1 core the possibility of this amount of variation in the environmental change is unlikely therefore a greater deposition rate would seem likely.

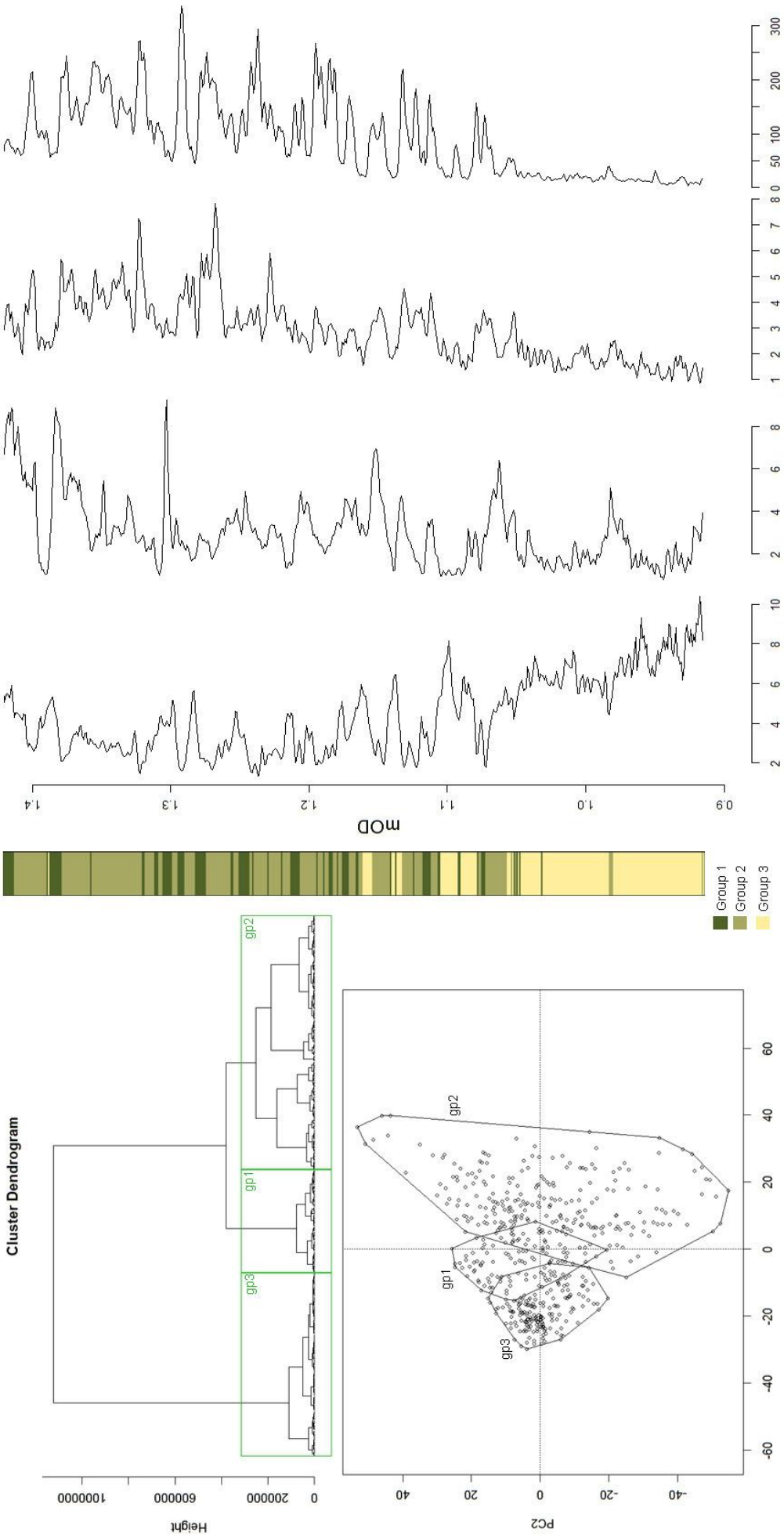

Figure 6.24 DYN2 PCA and cluster analysis. Top left: cluster analysis of scanning XRF data. Bottom left: PCA of scanning XRF data indicating cluster groups. Right: Representation of cluster groups downcore against the 4 ratio plots that best describe the downcore variations identified

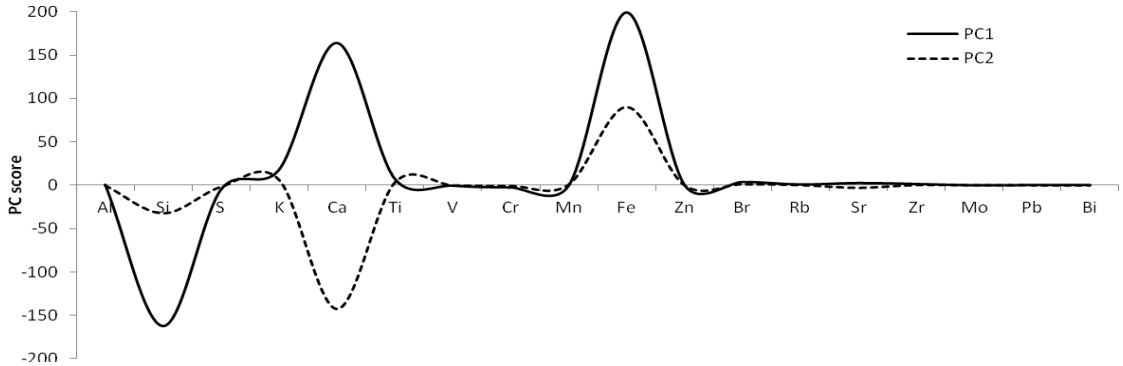

Figure 6.25 DYN2 Principal Component scores for individual elements.

6.6. Singular spectrum analysis

Singular spectrum analysis (SSA) is a time series analysis technique based on principal components analysis (Vautard and Ghil, 1989; Vautard *et al*, 1992). It enables the decomposition of a time series into the sum of a number of independent components such as trend, oscillation and noise (Hassani, 2007). Individual components can then be reconstructed; these reconstructed components (RCs) retain the amplitude, frequency and phase of the time series (Fagel *et al*, 2008). Typically, SSA will produce RCs that are approximately periodic with periods less than the window length of the analysis (M) and one or two RCs with periods greater than M (Schoellhamer, 2001). A particular advantage of this method is that it requires no prior knowledge of any periodicity or dynamics underlying the sequence (Fagel *et al*, 2008).

The use of this method in this study is significantly restricted due to the poor geochronology information. Within this further analysis variation of age with depth has been assumed to be constant to enable the analyses to be run. However, as shown previously where limited dating information has been able to be applied this has shown that a constant deposition rate is not present. Therefore the following the results from the following analyses cannot be used with any degree of certainty. It was still considered beneficial to apply these analyses to further explore the potential of scanning XRF data in the analysis of intertidal sediments. Therefore the following analyses are carried out assuming no major changes in sediment accumulation rate.

Singular spectrum analysis was run on individual Si, K, Ca and Fe element profiles. These elements are most representative of the geochemistry of the sequences and additionally count values are consistently above 600cpa for the entire core. The exception to this are the Ca profiles for SFD2 and SFD3 where the analysis was run on the lower section of the core below 1.42mOD and DYN1 where the analysis was run on the Ca profile below the peak at 1.77mOD. Given the benefits of using element/element ratios, discussed earlier, SSA was also run on the Si/K and Ca/K profiles for each core. The window length (M) used for each of the analyses was

half of the original series length. The reconstructed components were assessed and the trend and most significant signals/oscillations identified.

6.6.1. SFD1

The overall trends of the Si and K profiles are opposites of each other (Figure 6.26); this is to be expected with Si being associated with sand and K silts and clays. The Si profile contains two distinct periodicities however only one has a consistent wavelength, i.e. 42mm. Within the K profile there are again two distinct periodicities one with a consistent wavelength of 104mm and the other 50mm. The amplitude of these signals increases downcore possibly indicating an increased effect of the underlying influencing factor.

The SFD1 Ca profile has only a slight increasing trend towards the base of the core (Figure 6.27). Three periodicities are identified two of which have consistent wavelengths of 119mm and 68mm. As with the K profile these oscillations increase in amplitude downcore. There is a marked arched trend to the Fe profile and two distinct oscillations can be identified (Figure 6.27). Of these only one has a consistent periodicity, i.e. wavelength = 38mm. The remaining amplitude again increases downcore. The SSA results for the Si/K and Ca/K ratio profiles are shown in Figure 6.28. Both profiles have a similar trend i.e. a parabola with the lowest values in the lower third of the core. Examination of the RCs reveals 2 distinct periodicities in the Si/K profile with wavelengths of 48mm and 37mm. For the Ca/K profile again two distinct periodicities present of wavelengths 75mm and 103mm.

Within the SFD1 core the only similarities between the element profiles in terms of the periodicities are the oscillations of 104mm and 103mm in K and Ca/K and 38mm and 37mm in Fe and Si/K respectively. However the K and Ca/K oscillations are approximately a third of a wavelength out of phase. The Fe and Si/K 38mm and 37mm oscillations are approximately half a wavelength out of phase.

Although the individual profiles for K, Ca and Fe display increases in oscillation amplitude towards the bottom of the core this characteristic is not seen in either the Si/K or Ca/K periodicities. Therefore it is likely that this variation in amplitude is due to the effect of grain size.

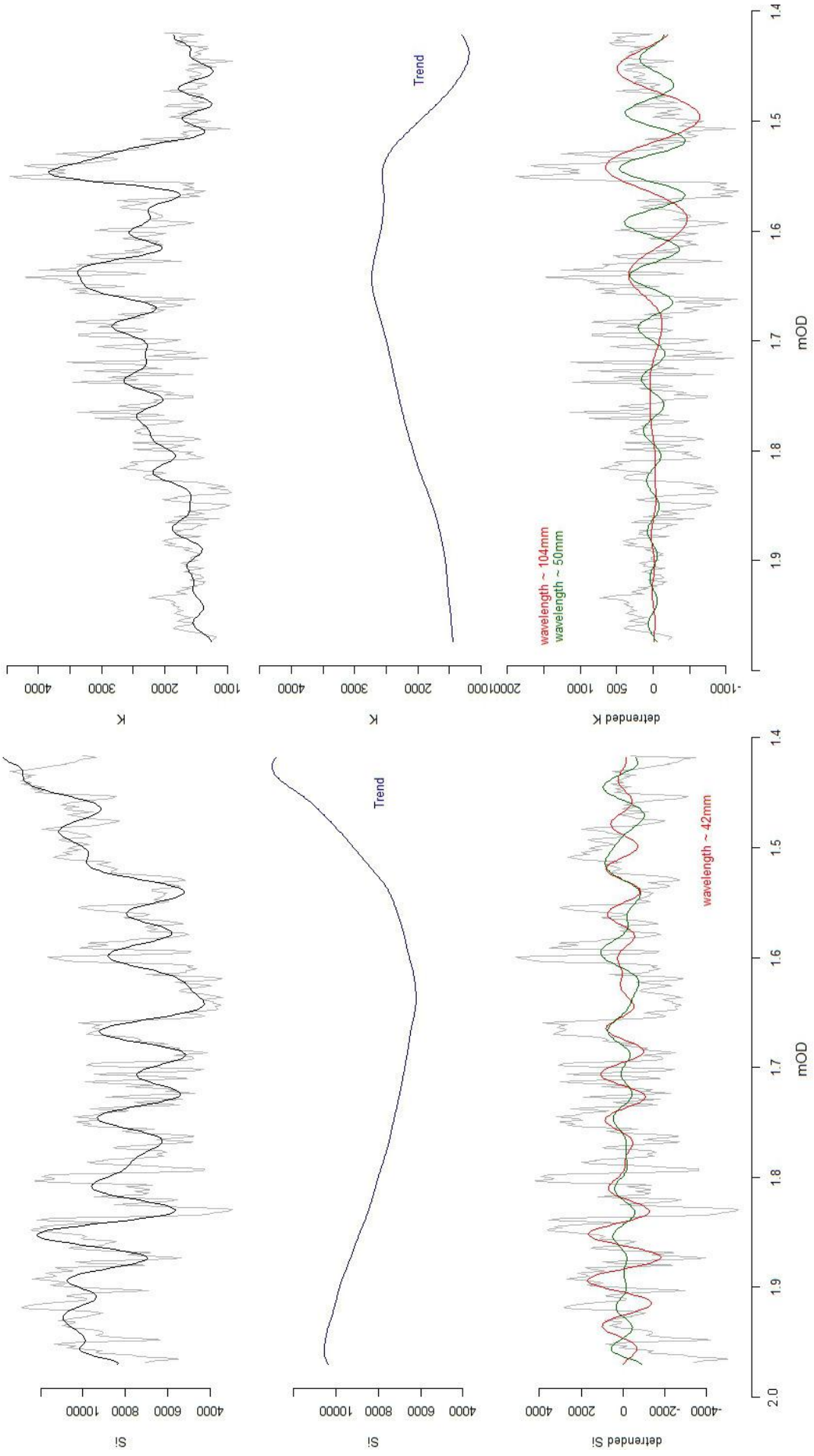

Figure 6.26 SFD1 SSA analysis for Si (left) and K (right). Top: de-noised signal; middle: trend; bottom: most significant oscillatory components.

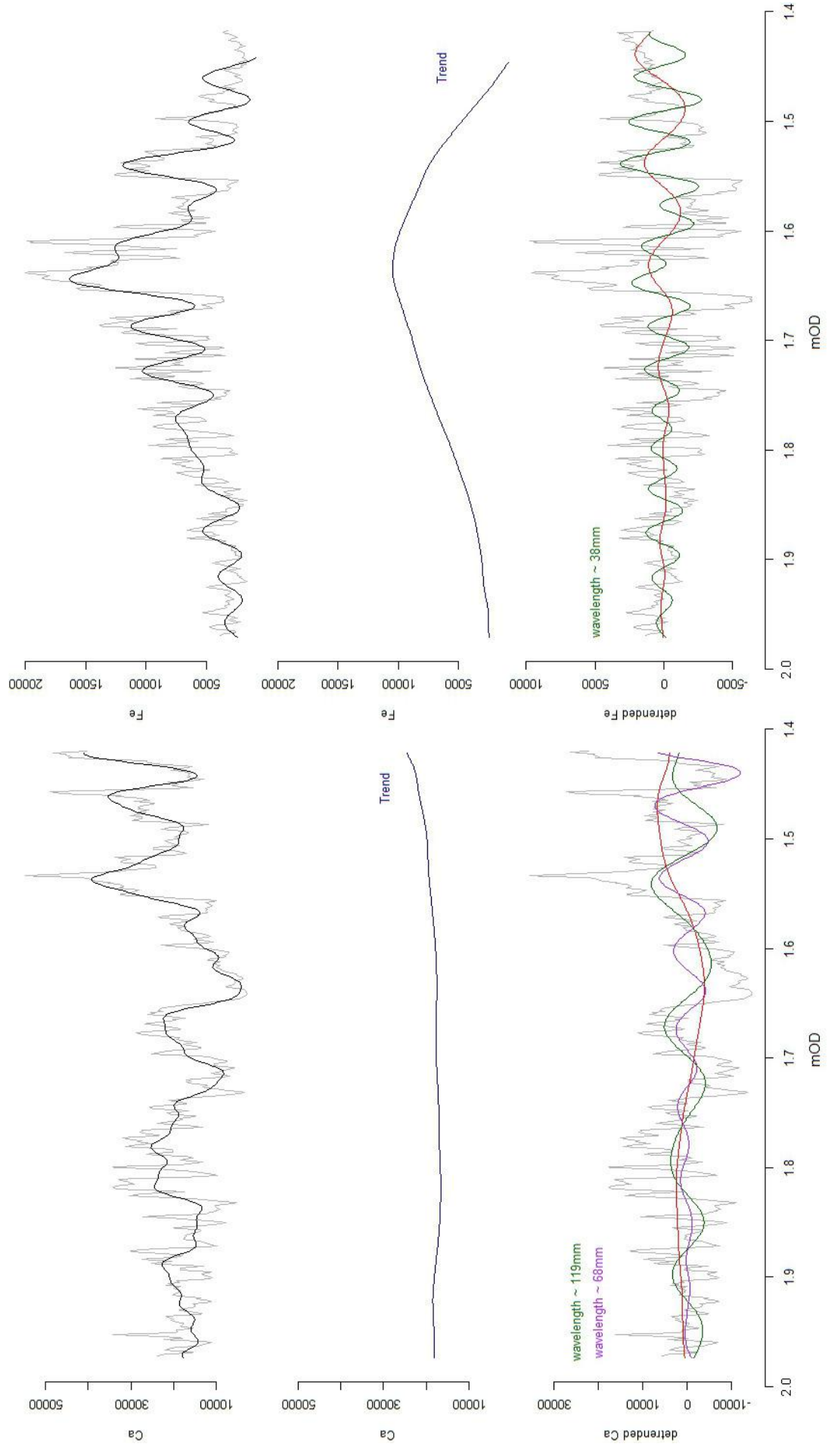

Figure 6.27 SFD1 SSA analysis for Ca (left) and Fe (right). Top: de-noised signal; middle: trend; bottom: most significant oscillatory components.

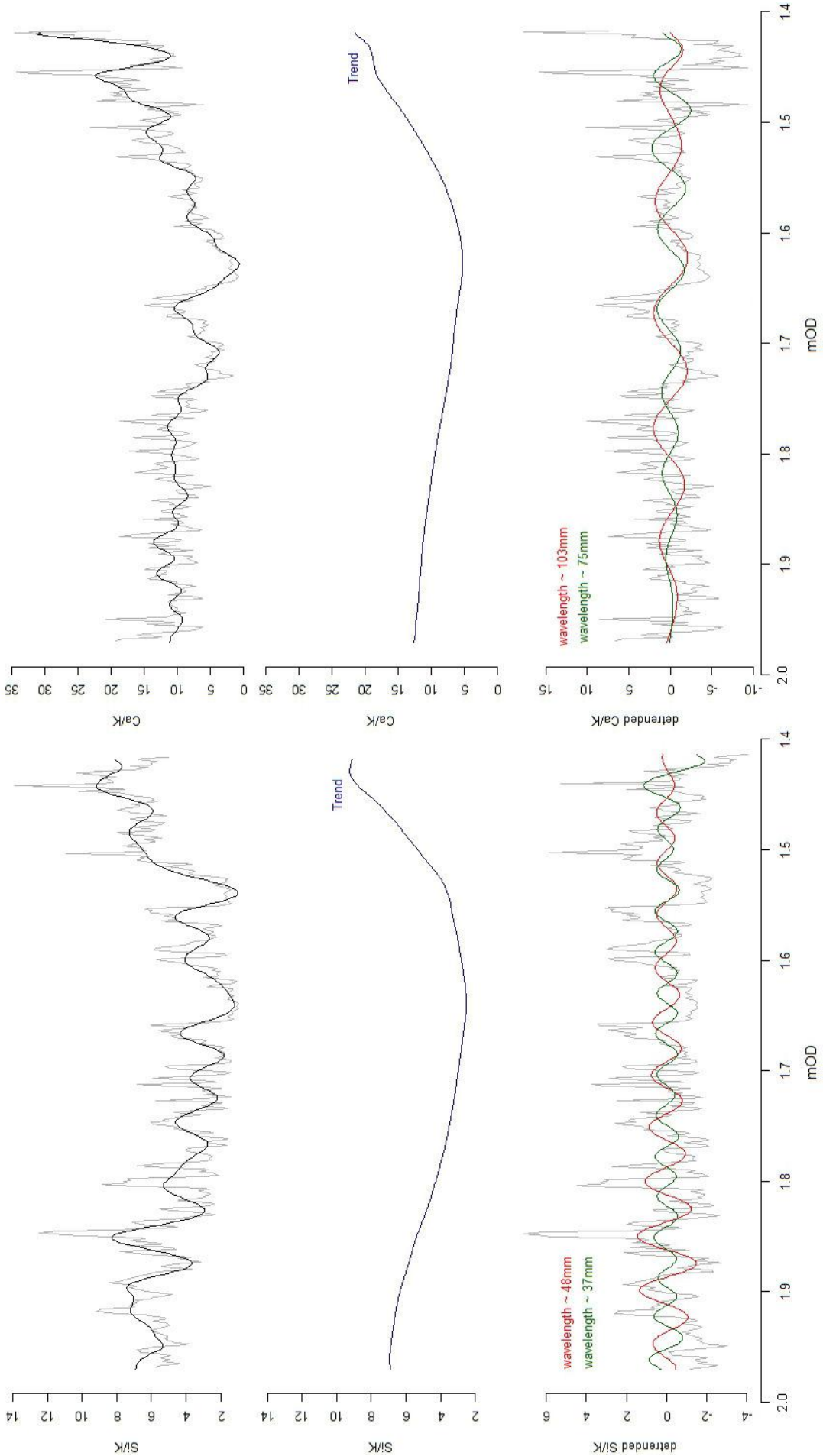

Figure 6.28 SFD1 SSA analysis for Si/K (left) and Ca/K (right). Top: de-noised signal; middle: trend; bottom: most significant oscillatory components.

6.6.2. SFD2

The overall trend for the SFD2 Si profile is an increase to 1.5mOD followed by a slight decrease to the base of the core (Figure 6.29). Three distinct periodicities are identified in the Si profile (Figure 6.29); of these two have consistent wavelengths of 272mm and 44mm. Within the K profile the overall trend is a decrease to the base of the core. Two oscillations can be identified however only one has a consistent wavelength, i.e. 36mm. This 36mm oscillation increases in amplitude towards the base of the core; above ~1.57mOD the amplitude is approximately 0 (Figure 6.29). SSA on the Ca profile below 1.42mOD shows a slight increasing trend to the base of the core and two periodicities of 136mm and 27mm (Figure 6.30). The Fe profile has a slight decreasing trend to the base of the core and two distinct oscillations only one of which has a consistent wavelength, i.e. 37mm. The second wavelength is dominated by the two notable peaks in the top section of the Fe profile and reduces to an amplitude of 0 below this. The trend of the Si/K profile is a very slight increase to the base of the core. Three significant periodicities are present although only two have consistent wavelengths (77mm and 36mm) (Figure 6.31). Both of these oscillations display an increase in amplitude to the base of the core. The overall trend of the Ca/K profile is a slight increase to the base of the core. Three periodicities are present with two having consistent wavelengths, 41mm and 27mm (Figure 6.31). Of these the oscillation of 41mm decreases in amplitude to the base of the core and the 27mm oscillation increases in amplitude to the base of the core.

There are some similarities between the individual element profiles for this core. K, Fe and Si/K contain periodicities with wavelengths of 36mm, 37mm and 36mm respectively; within the K and Fe profiles these oscillations are approximately in phase whereas the Si/K oscillation is approximately half a wavelength out of phase. As the Si/K profile would be expected to be the opposite of that of the K profile it would also be expected that any periodicity effecting both profiles would be a half wavelength out of phase. It is therefore likely that the influencing factor affecting this periodicity is acting on all three elements. The Ca and Ca/K profiles both contain a periodicity of a wavelength of 27mm which are approximately in phase with each other. This suggests an underlying dynamic effecting Ca concentration which is not influenced by the effects of grain size. Each of the K, Si, Ca, Si/K and Ca/K SSAs produce long period / wavelength oscillations although the wavelengths and phases of these periodicities are inconsistent they are indicative of underlying dynamics acting over a longer period than the other identified oscillations.

The profile for K contains an oscillation which increases in amplitude towards the base of the core; a similar trend is displayed in periodicities from both Si/K and Ca/K, this would suggest that here the change in amplitude is not due to the effects of grain size as suggested for SFD1.

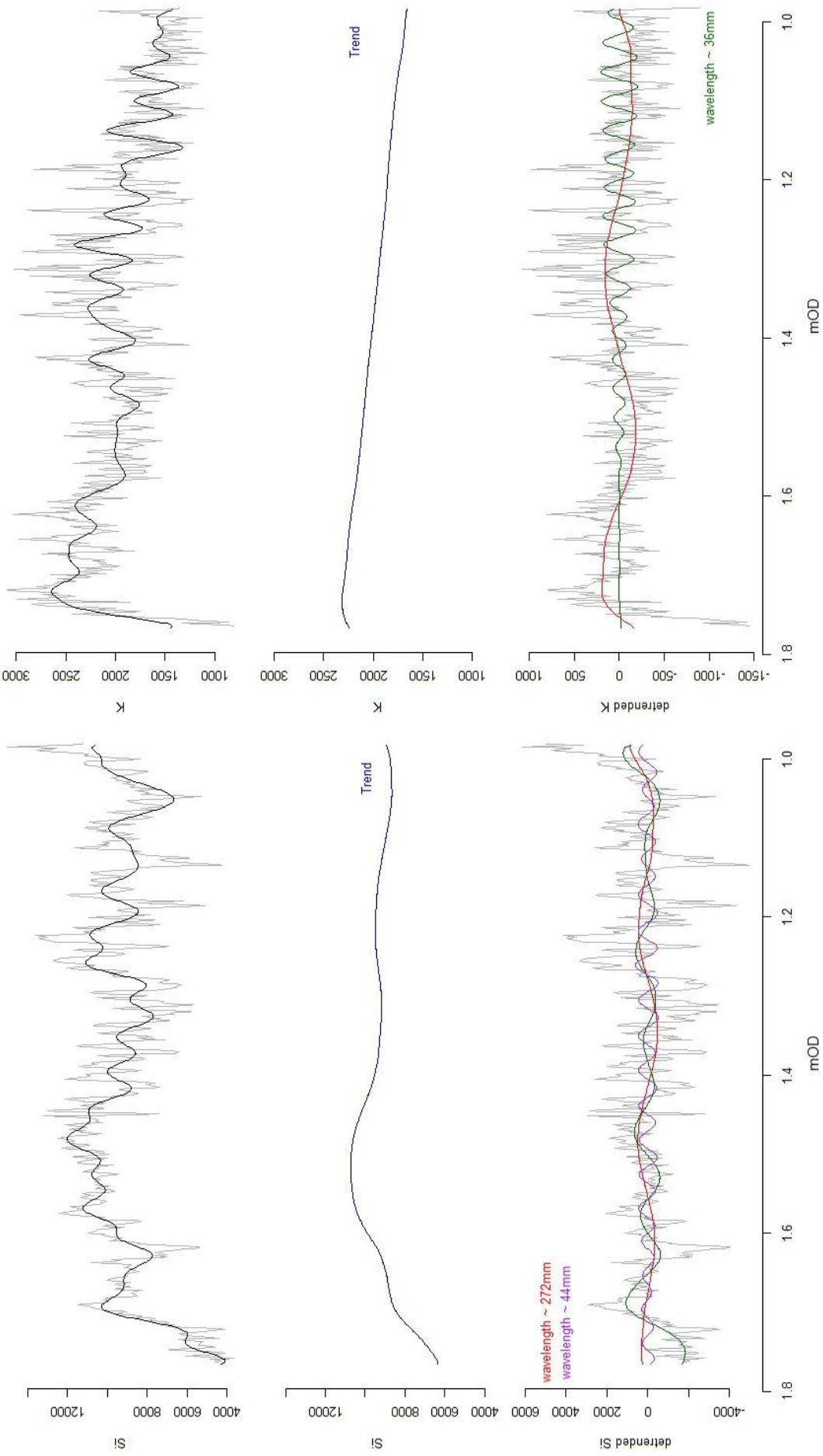

Figure 6.29 SFD2 SSA analysis for Si (left) and K (right). Top: de-noised signal; middle: trend; bottom: most significant oscillatory components.

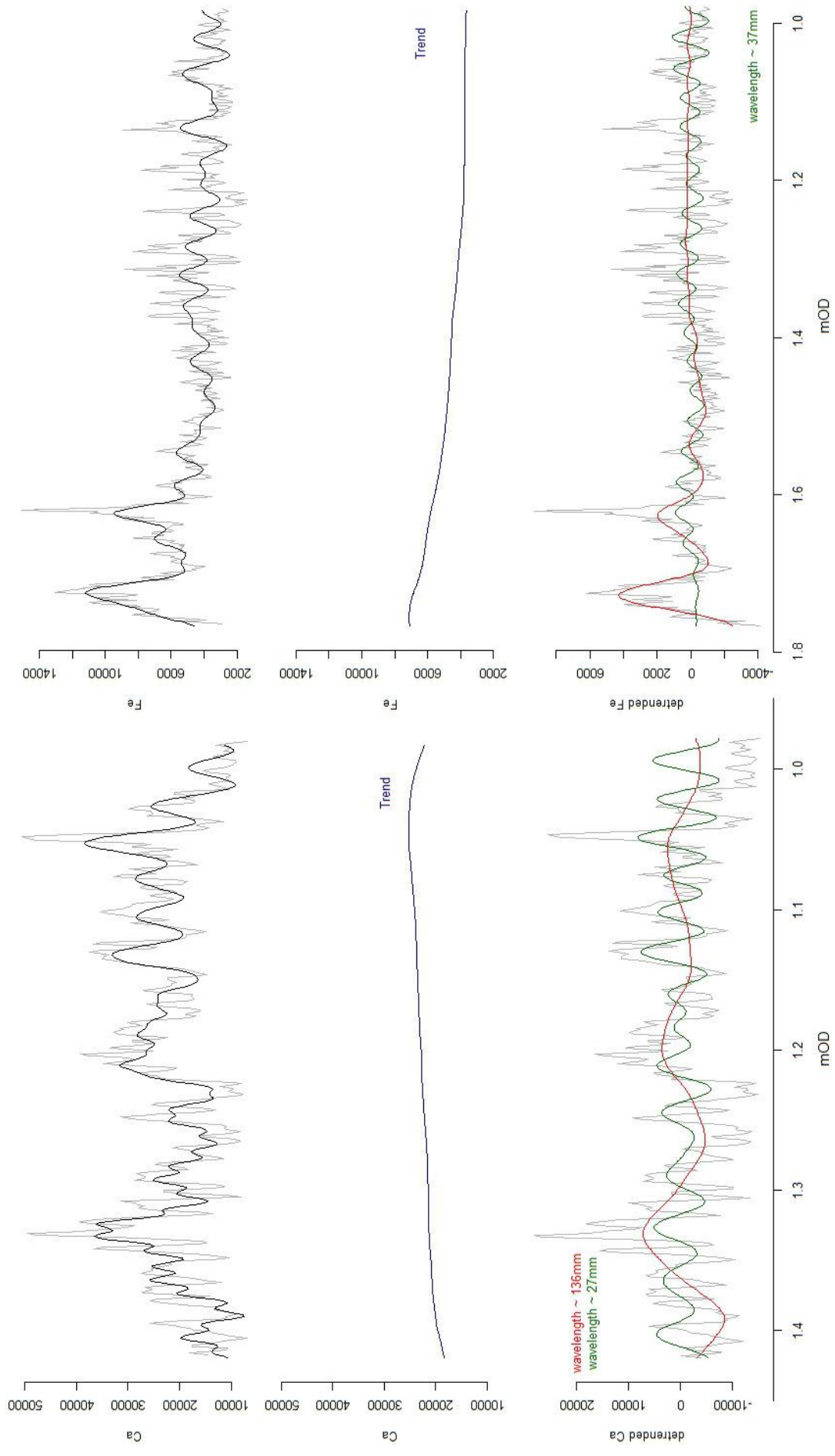

Figure 6.30 SFD2 SSA analysis for Ca (left) and Fe (right). Top: de-noised signal; middle: trend; bottom: most significant oscillatory components.

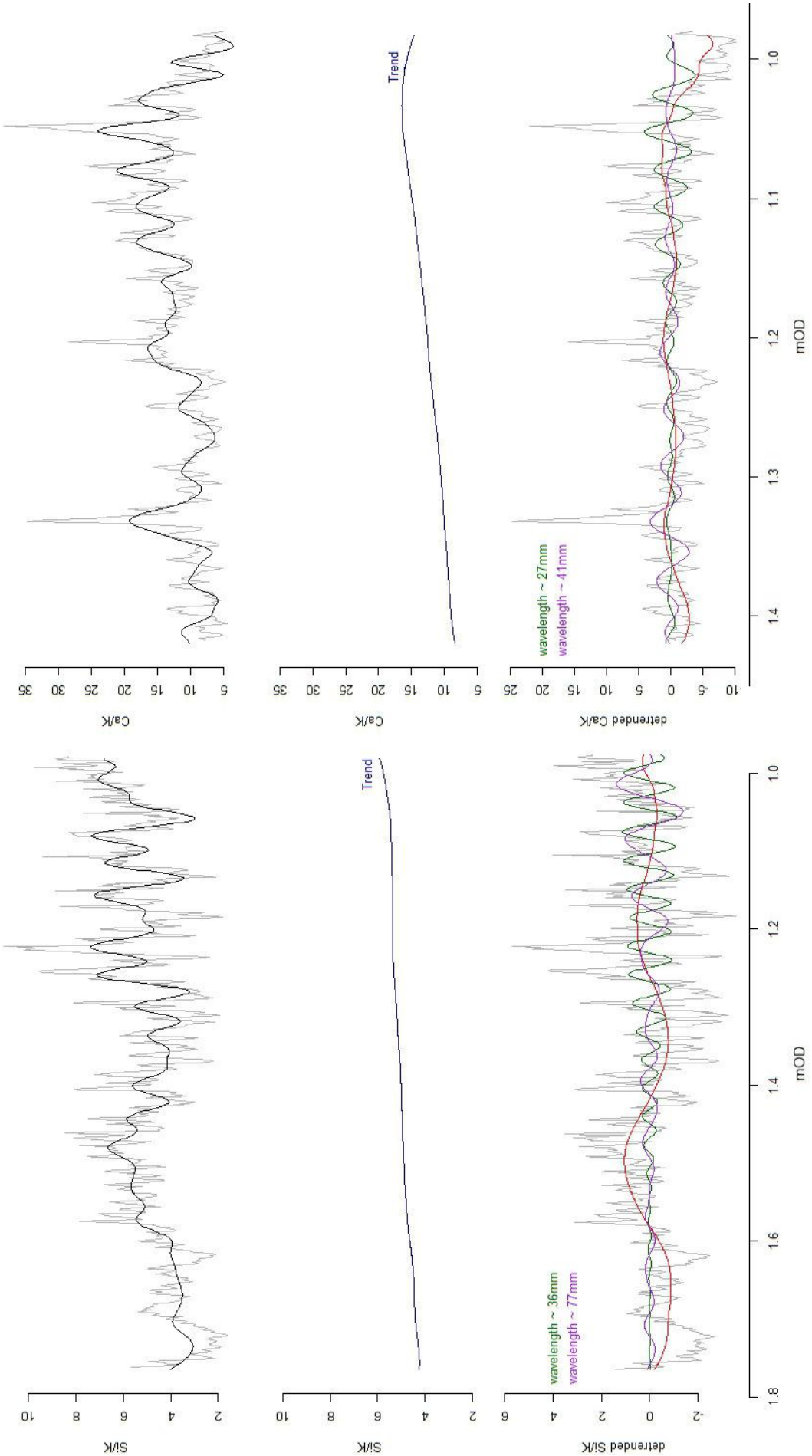

Figure 6.31 SFD2 SSA analysis for Si/K (left) and Ca/K (right). Top: de-noised signal; middle: trend; bottom: most significant oscillatory components.

6.6.3. SFD3

The overall trend of the Si profile is a steady increase to the base of the core. Four significant oscillations are identified in the SSA, three of which have consistent wavelengths, i.e. 94, 55 and 35mm (Figure 6.32). The K profile trend shows an increase from the top of the core to approximately1.6mOD followed by a steady decrease to the base of the core. Two periodicities are identified in the K profile of wavelengths of 61 and 44mm. Both of these oscillations display a decrease in amplitude to the base of the core (Figure 6.32). The overall trend of the Ca profile for the section below 1.42mOD is an increase to a maximum at approximately 1.3mOD followed by a parabola type trend below with the minimum values at approximately 1.05mOD. Two distinct periodicities are present within this profile although only one has a consistent wavelength (39mm) (Figure 6.33). The Fe profile has a decreasing trend towards the base of the core. Three oscillations are identified in the SSA two with regular wavelengths, i.e. 57 and 39mm, the remaining oscillation is dominated by the two peaks in the top section of the profile. All three oscillations show a decrease in amplitude to the base of the core (Figure 6.33). The Si/K profile shows and overall increase to approximately 1.05mOD followed by a levelling off and slight decrease in trend to the base of the core. Four distinct periodicities are identified for this profile three of which have regular wavelengths, i.e. 107mm, 55mm and 37mm (Figure 6.34). The overall trend of the Ca/K profile for the section below 1.42mOD is almost identical to that of the Ca profile. SSA identified two regular oscillations of 61mm and 32mm wavelength both of these display a decrease in amplitude towards the base of the core (Figure 6.34).

There are several similarities between the oscillations identified in the SSA of the SFD3 profiles. Each of the Ca, Fe, and Si/K profiles display periodicities with wavelengths of 39mm, 39 and 37mm respectively. Within the Ca and Fe profiles these oscillations are in phase. The Si and Ca/K profiles also contain oscillations of 35 and 32mm respectively it is possible that these are also related to those of the Ca, Fe and Ca/K profiles. Si, Fe and Si/K contain periodicities of wavelength 55, 57 and 55mm respectively the Si and Si/K oscillations being in phase. This indicates an underlying dynamic effecting the concentrations of Si. K and Ca/K both display a periodicity of 61mm; these oscillations are half a wavelength out of phase as would be expected.

Given the accumulation rates calculated for the SFD3 core from the ^{210}Pb and ^{137}Cs dating presented in chapter 5.4 (1.3±0.1mm/yr) oscillation cycle time periods can be estimated. The 39mm oscillations of Ca and Fe would therefore represent a cycle of period 30±2.5yrs; the Si and Si/K oscillations of 55mm a cycle period of 42±3.5yrs and the K and Ca/K oscillations of 61mm a cycle period of 47±4yrs. The Si and Si/K profiles also display long period / wavelength oscillations of less than two cycles within the core length; these are in phase with each other. Similarly to SFD2, this suggests an underlying dynamic acting over a much longer time period than the other periodicities identified.

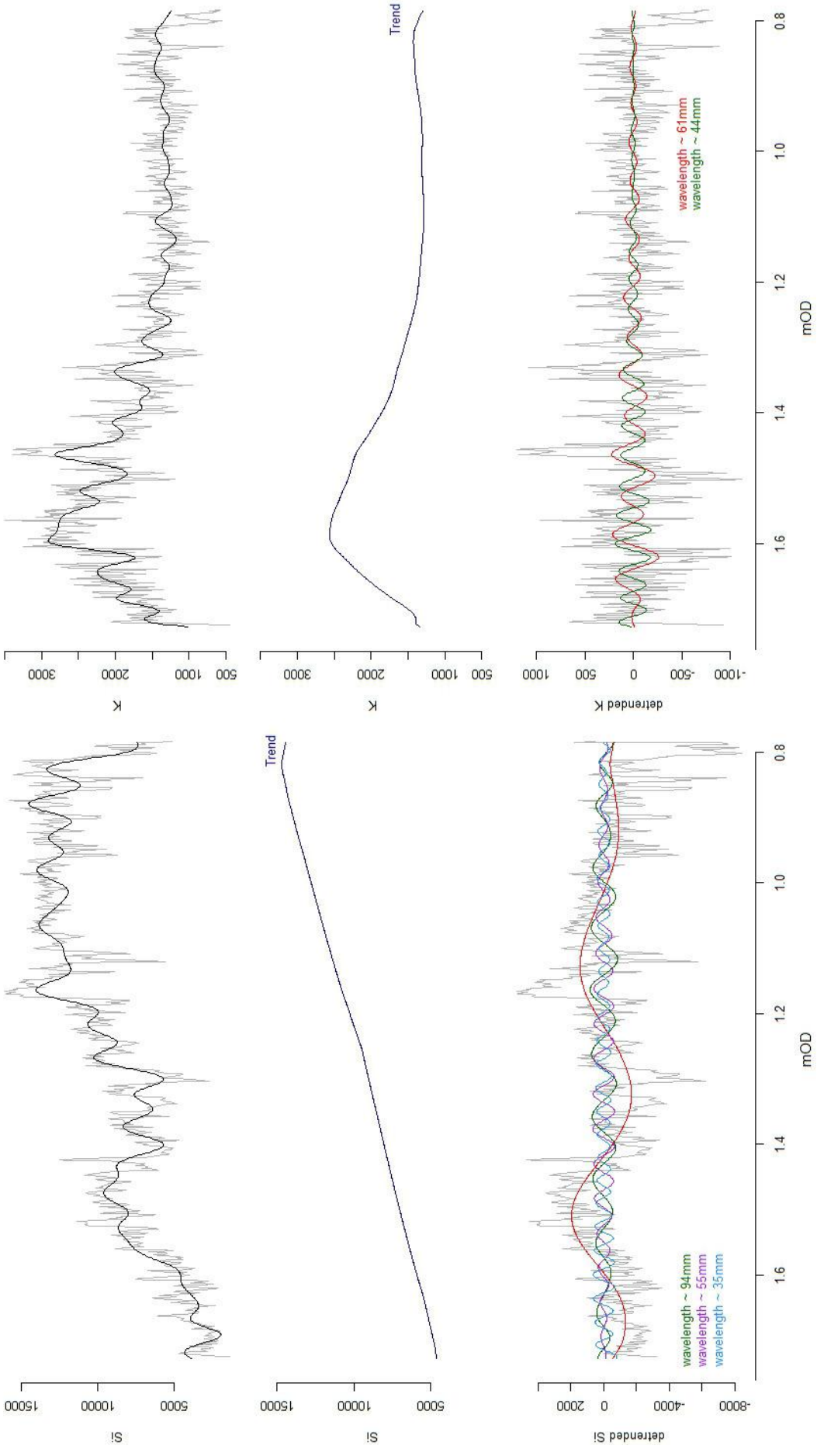

Figure 6.32 SFD3 SSA analysis for Si (left) and K (right). Top: de-noised signal; middle: trend; bottom: most significant oscillatory components.

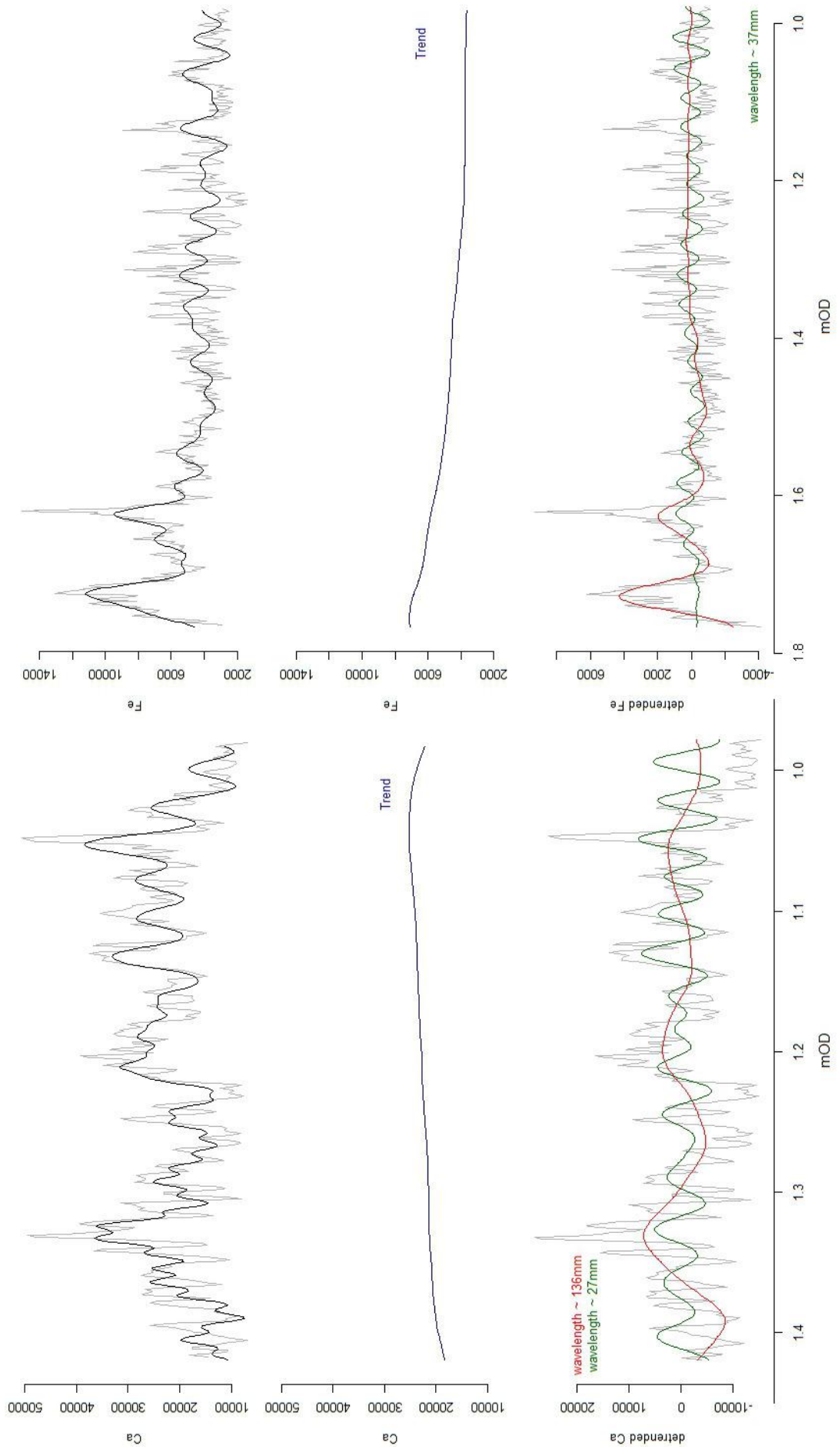

Figure 6.33 SFD3 SSA analysis for Ca (left) and Fe (right). Top: de-noised signal; middle: trend; bottom: most significant oscillatory components.

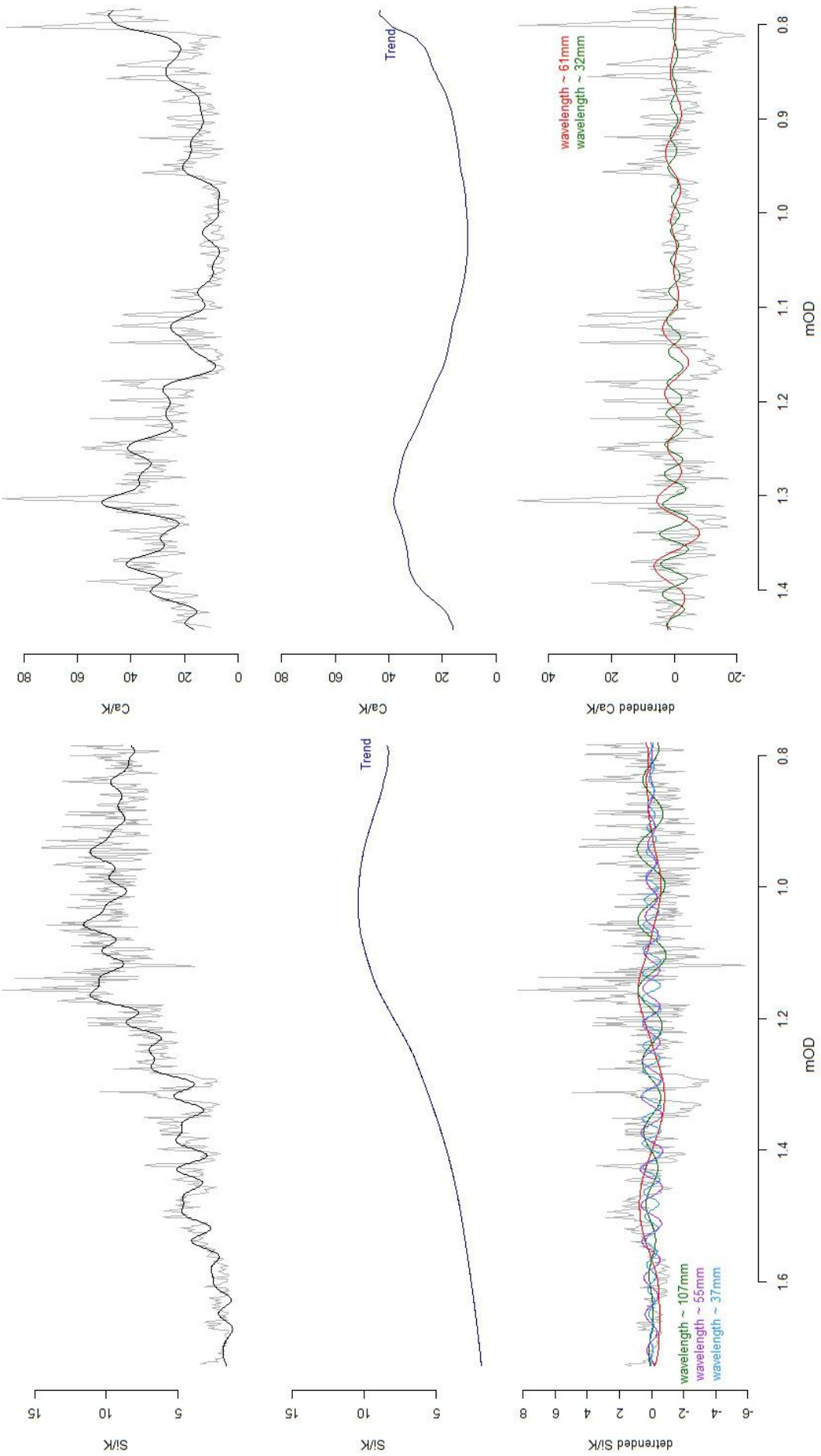

Figure 6.34 SFD3 SSA analysis for Si/K (left) and Ca/K (right). Top: de-noised signal; middle: trend; bottom: most significant oscillatory components.

6.6.4. DYN1

The overall trend of the DYN1 Si profile is a slight increase to the base of the core. SSA identifies three significant periodicities two with regular wavelengths (107mm and 71mm) (Figure 6.35). The K profile has a very slight arched trend with the highest values at approximately 1.6mOD. Two distinct periodicities are present within this profile of 90mm and 51mm (Figure 6.35). The Ca profile displays an overall decreasing trend to the base of the core. Three distinct oscillations can be identified although only one has a consistent wavelength (52mm). All three of the oscillations of this profile show a decrease in amplitude towards the base of the core (Figure 6.36). The Fe profile shows a very slight decreasing trend to the base of the core. SSA identifies three distinct periodicities two of which have regular wavelengths (123mm and 52mm) (Figure 6.36). The Si/K profile has a dish shaped trend with the lowest values occurring at approximately 1.6mOD. Three oscillations were identified for this profile only one of which has a regular wavelength (54mm) (Figure 6.37). The Ca/K profile displays a decreasing trend to the base of the core. Again three oscillations were identified only one of which has a consistent wavelength, i.e. 29mm; all these oscillations show a decrease in amplitude to the base of the core (Figure 6.37).

The only similarities between the periodicities present in this core are the 51mm, 52mm, 52mm and 54mm oscillations identified in the K, Ca, Fe and Si/K profiles respectively. Of these the K, Ca and Fe oscillations are approximately in phase. The Si, Ca, Fe and Si/K profiles all contain long period / wavelength oscillations of which the Si and Si/K are in phase and the Fe half a wavelength out of phase; similarly to SFD2 and 3 this suggests a longer timescale factor influencing the sediment sequence. Given the uncertainties associated with the ^{210}Pb and ^{137}Cs dating of the DYN1 core it is not possible to attribute time periods to the oscillations identified in these profiles.

The decrease in amplitude of the oscillations of Ca and Ca/K suggest this is not and effect of grain size but rather a feature of the underlying dynamic affecting the periodicity.

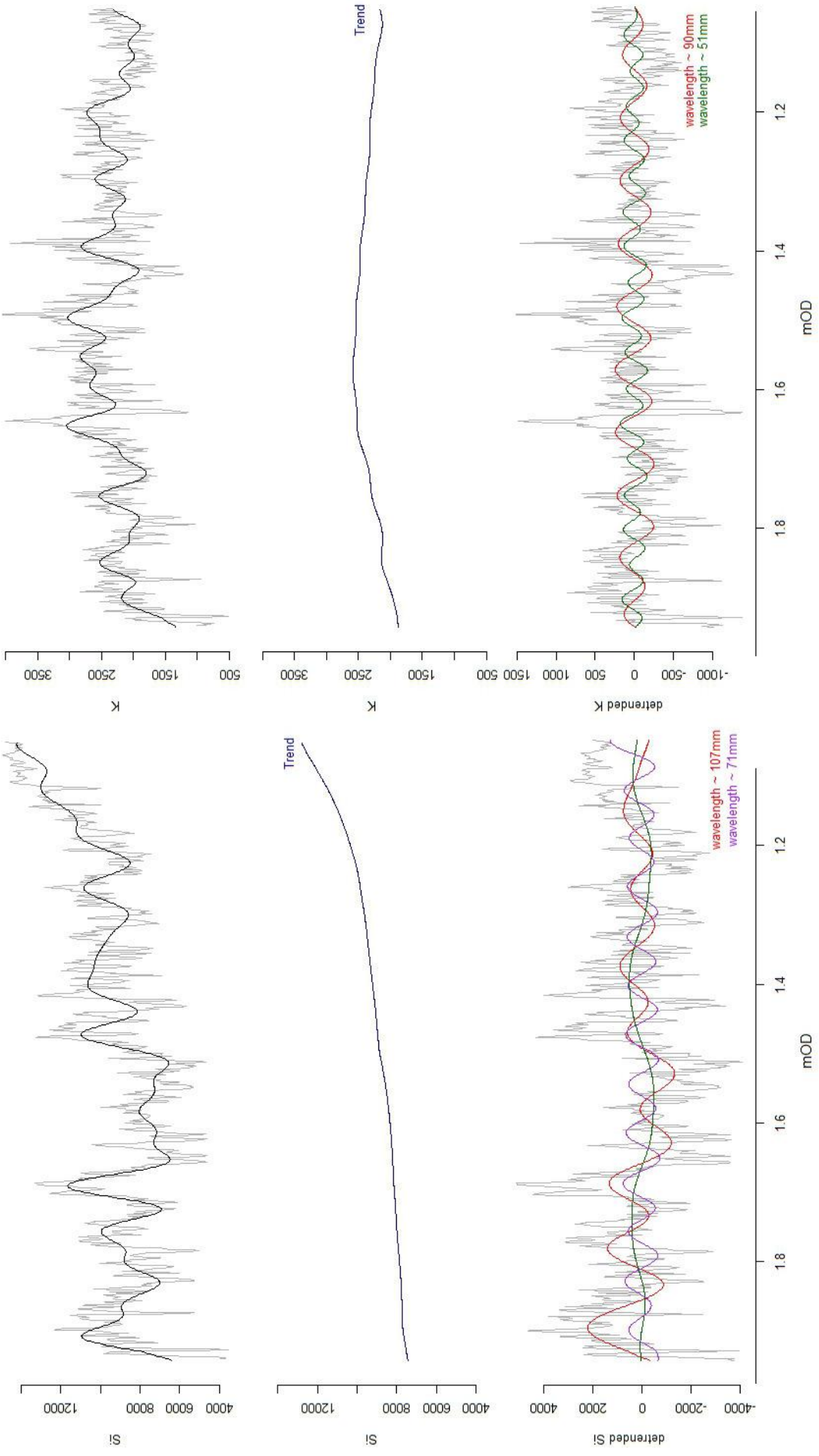

Figure 6.35 DYN1 SSA analysis for Si (left) and K (right). Top: de-noised signal; middle: trend; bottom: most significant oscillatory components.

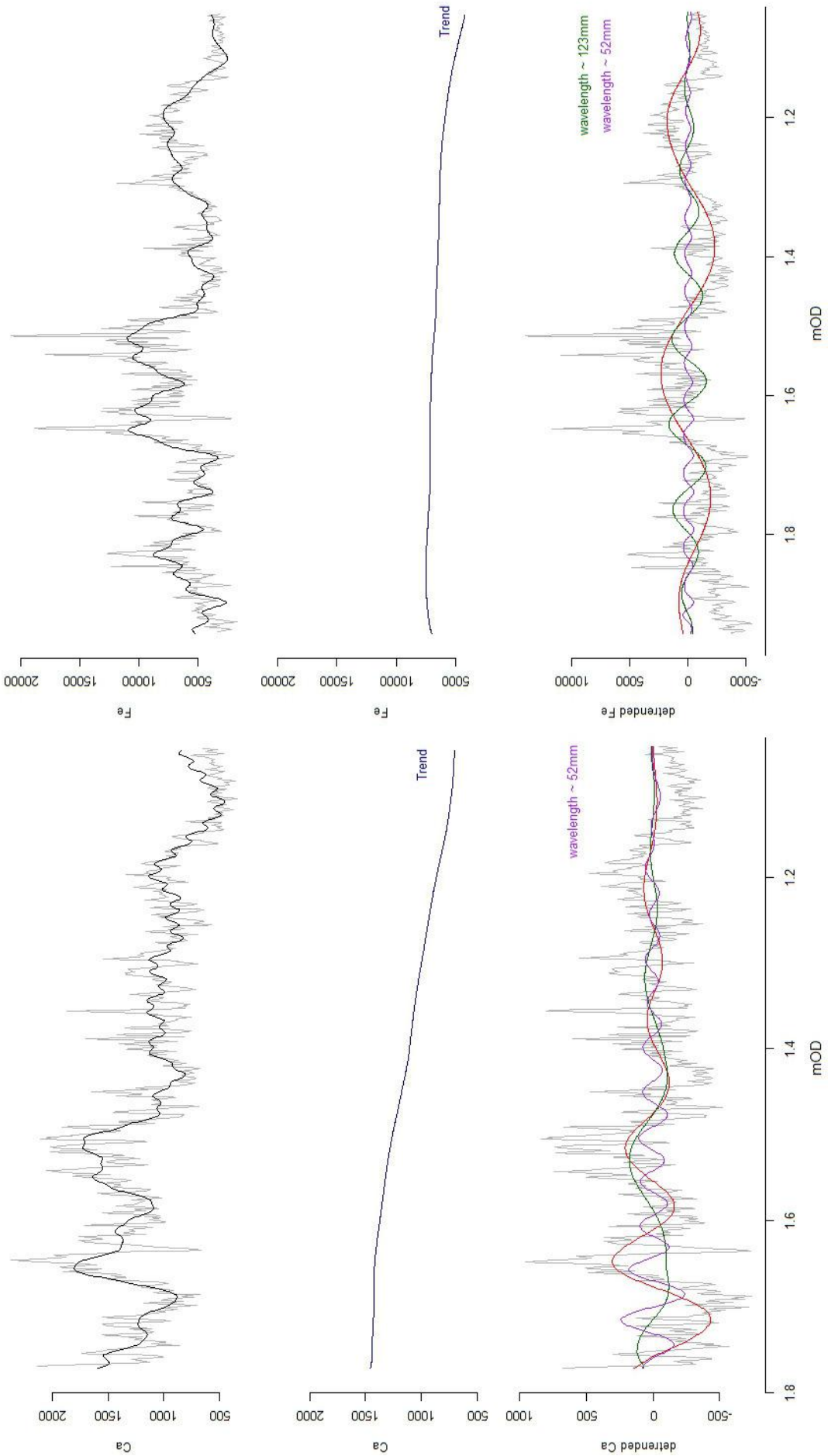

Figure 6.36 DYN1 SSA analysis for Ca (left) and Fe (right). Top: de-noised signal; middle: trend; bottom: most significant oscillatory components.

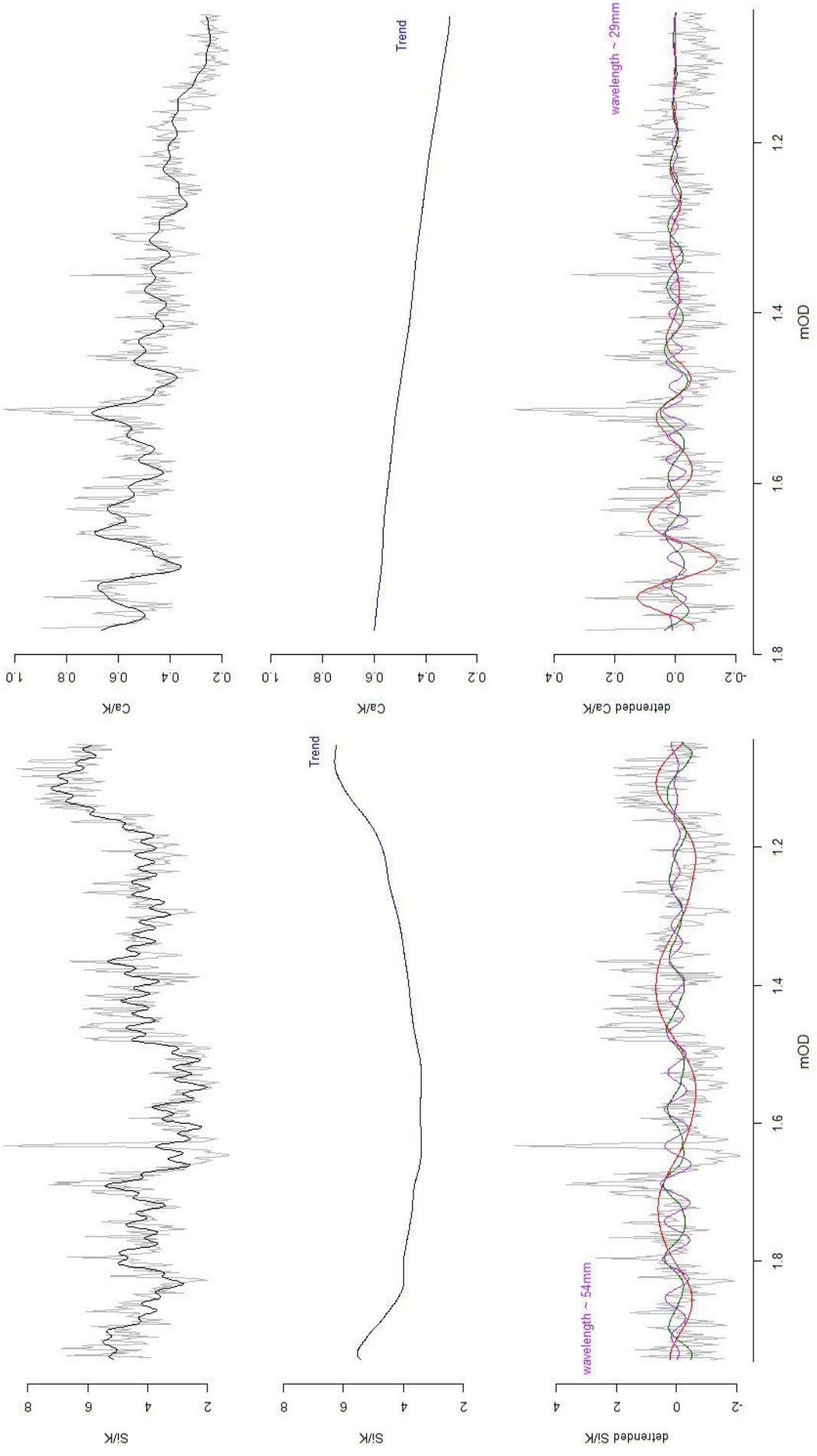

Figure 6.37 DYN1 SSA analysis for Si/K (left) and Ca/K (right). Top: de-noised signal; middle: trend; bottom: most significant oscillatory components.

6.6.5. DYN2

The overall trend of the Si profile is a decrease to approximately 1.3mOD followed by an increase to the base of the core. SSA identifies two significant periodicities of 65 and 20mm in wavelength. Both of these oscillations show an increase in amplitude from the top of the core to about 1.3mOD from this point the amplitude remains constant to the base of the core (Figure 6.38). The K profile has a very slight arched trend. Again two periodicities were identified of wavelengths 40 and 29mm; these decrease in amplitude to the base of the core (Figure 6.38). The overall trend of the Ca profile is a decrease to the base of the core. Two oscillations were identified both with regular wavelengths (87 and 26mm); the 87mm oscillation shows a decrease in amplitude to the top of the core (Figure 6.39). The Fe profile also shows a decreasing trend to the base of the core. Within this profile only one significant periodicity was identified (wavelength = 50mm) (Figure 6.39). The Si/K profile has an overall dish shaped trend similar to that of the Si profile. Three periodicities were identified two of which have consistent wavelengths, i.e. 67 and 18mm. All three of these oscillations display an increase in amplitude from the top of the core to approximately 1.3mOD from which it remains constant to the base of the core (Figure 6.40). The Ca/K profile trend decreases to the base of the core. Two periodicities were identified of wavelengths 90 and 24mm; of which the 90mm oscillation shows and increase in amplitude to the top of the core (Figure 6.40).

Within this core there are a few similarities between the periodicities of individual profiles. Si and Si/K contain periodicities of 65 and 67mm respectively these are approximately in phase with each other and also both show a decrease in amplitude to the top of the core. The Ca and Ca/K profiles contain periodicities of 87 and 90mm respectively again these are approximately in phase and display similar characteristics, i.e. a decrease in amplitude to the top of the core. Here, the Ca and Ca/K periodicities are thought to relate to changes in abundance of shell material within the sediment.

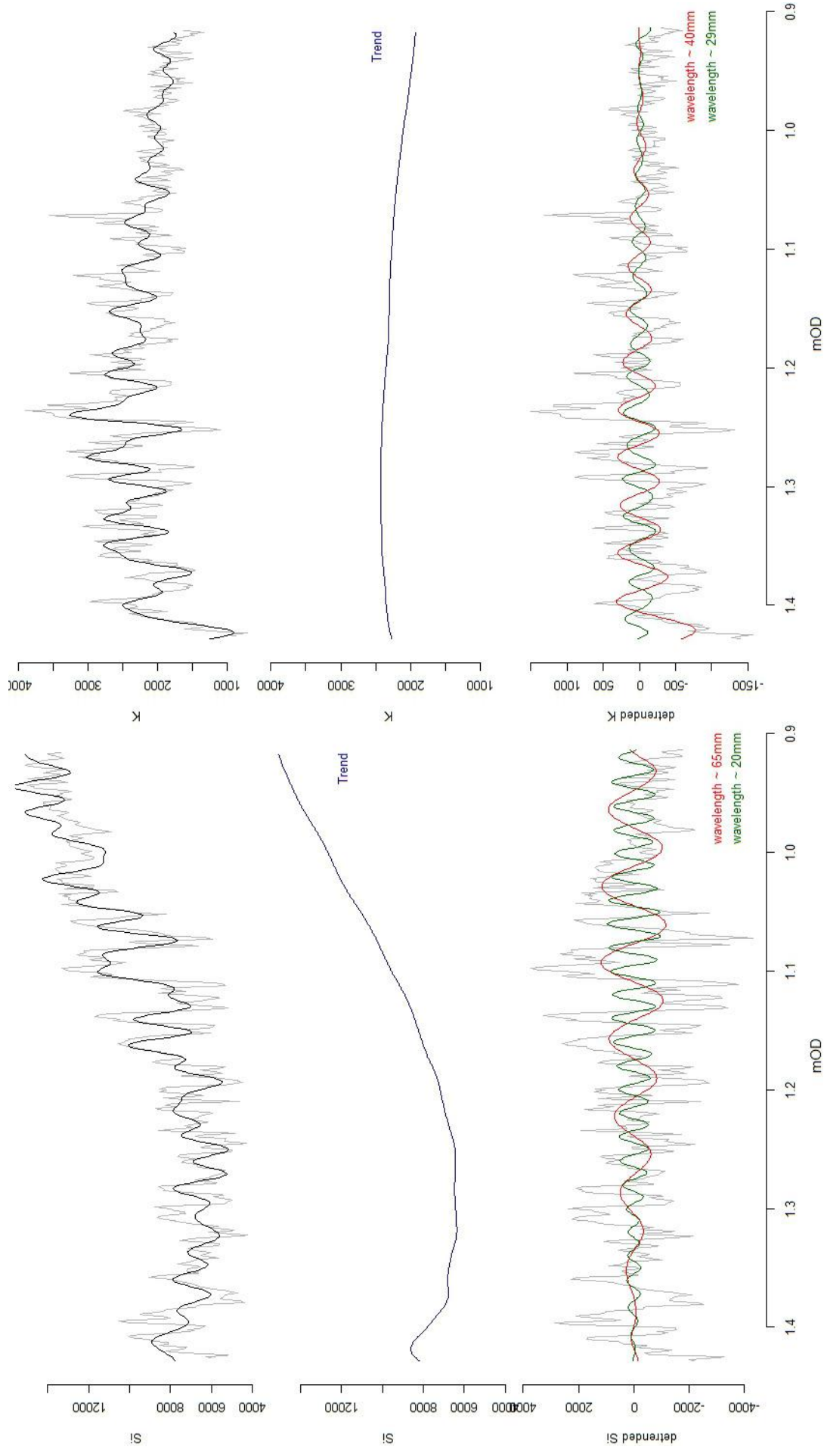

Figure 6.38 DYN2 SSA analysis for Si (left) and K (right). Top: de-noised signal; middle: trend; bottom: most significant oscillatory components.

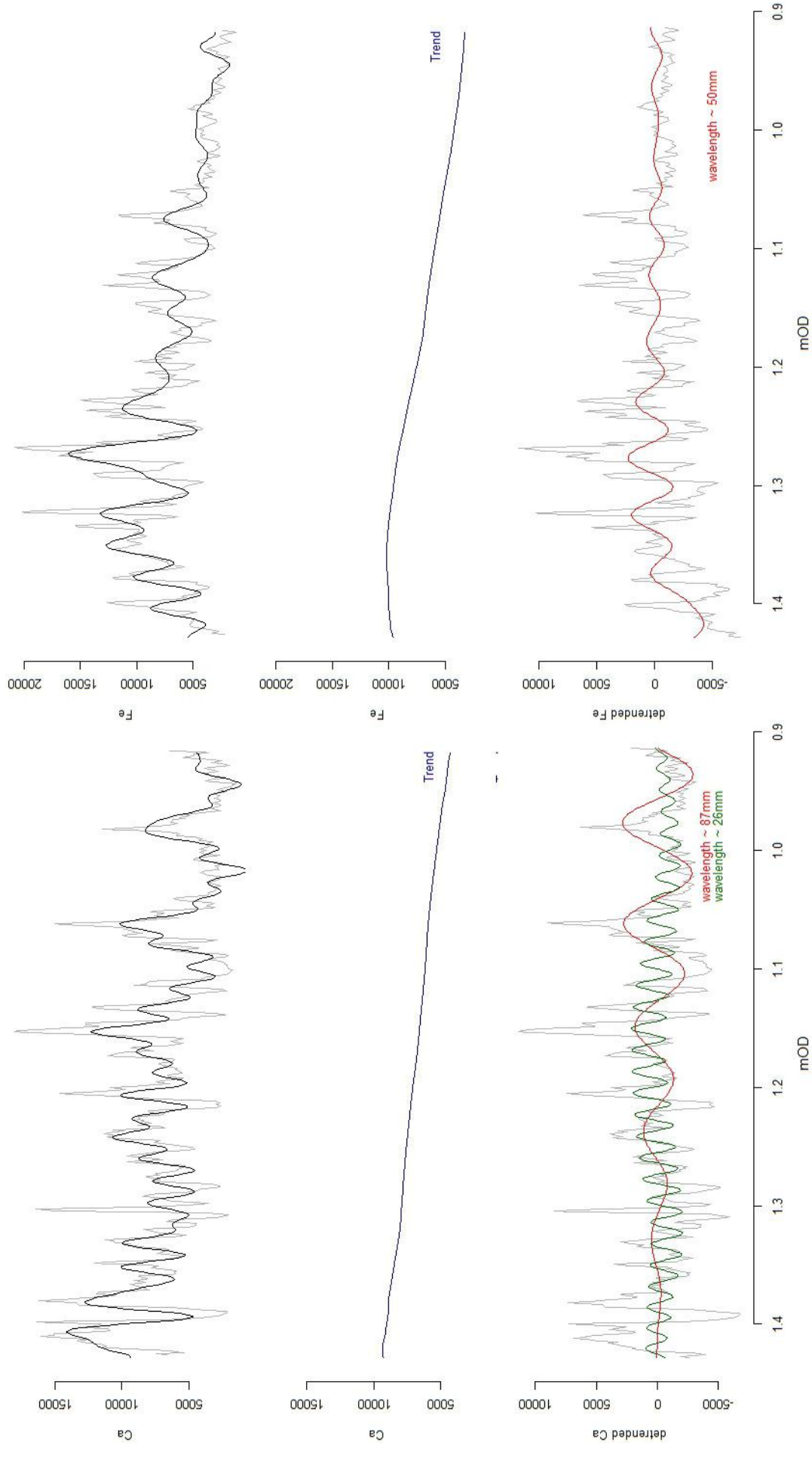

Figure 6.39 DYN2 SSA analysis for Ca (left) and Fe (right). Top: de-noised signal; middle: trend; bottom: most significant oscillatory components.

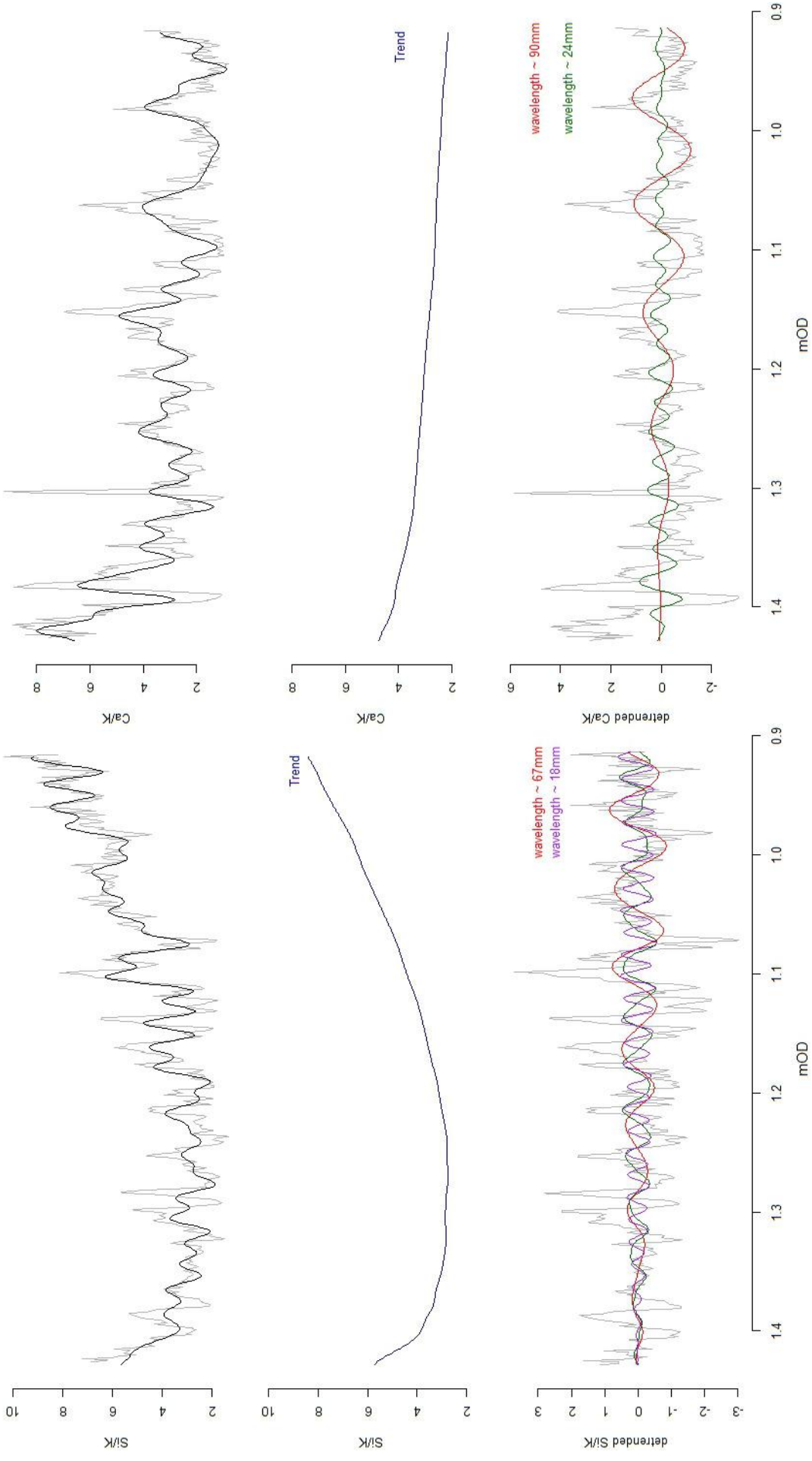

Figure 6.40 DYN2 SSA analysis for Si/K (left) and Ca/K (right). Top: de-noised signal; middle: trend; bottom: most significant oscillatory components.

6.6.6. SSA cross core comparison and summary

The periodicities identified above are based upon the assumption that there is no major change in sediment accumulation rate; however, it has been shown previously that this is unlikely to be true. These analyses have been carried out to examine the potential of the method and any conclusions drawn must be viewed with a great deal of caution and uncertainty.

A summary of the periodicities identified in the SSA of the five cores is given in Table 6.2. There are two periodicities which occur across multiple cores. Firstly a periodicity of wavelength 35-37mm is present in all 3 Sandfield cores (SFD1, 2 and 3) and across multiple element and ratio profiles. The phases of these oscillations vary between cores. However, comparing phases between cores is problematic due to uncertainties associated with variation in surface height at time of deposition and the application of an average value across the core when accounting for the effects of core compression. Additional periodicities of 32-39mm are also present and may also represent the same underlying dynamic. Given the similarities between the SFD3 and SFD2 cores in terms of their individual element and ratio profiles (discussed earlier in this chapter) it is reasonable to assume that the accumulation rate of 1.3±0.1mm given for SFD3 can also be applied to SFD2. It is not possible to assess whether this is also applicable to SFD1 due to the lack of overlap in elevation between this core and the other two Sandfield cores. Therefore an oscillation wavelength of 35-37mm is equivalent to a cycle period of 27.5±2.5yrs. As discussed previously (chapter 5.4) this accumulation rate can only be applied to the top section of the core and the rate is likely to be significantly different in the lower section of the core. This may explain the decrease in amplitude to the base of the core seen in many of the periodicities identified in the Sandfield cores. However, the oscillations of the 35-37mm wavelength often display little or no change in amplitude throughout the length of the core.

Table 6.2 Summary of oscillation wavelengths (in mm) identified for the 5 cores.

	SFD1	SFD2	SFD3	DYN1	DYN2
Si	42	272 44	94 55 35	107 71	65 20
K	104 50	36	61 44	90 51	40 29
Ca	119 68	136 27	39	52	87 26
Fe	38	37	57 39	123 52	50
Si/K	48 37	77 36	107 55 37	54	67 18
Ca/K	103 75	41 27	61 32	29	90 24

The second periodicity occurring across multiple cores is of wavelength 50-52mm and is present predominantly in the Derryness cores (DYN1 and 2) although there is a single occurrence of this wavelength in the K profile of SFD1. Again phases vary between cores and comparison is problematic. Additionally SFD3 displays two periodicities of 55mm. However, The uncertainty associated with the DYN1 accumulation rate makes it impossible to compare periodicities between the Sandfield and Derryness sites.

6.7. Assessment of the effectiveness of using scanning XRF on intertidal sediment sequences

Scanning XRF provides a non-destructive method of assessing the geochemistry of sediment core samples. The method is also less time and labour intensive than the destructive methods such as bulk pellet XRF and loss on ignition. The validation via comparison with non scanning XRF analysis and the more traditional loss on ignition techniques has shown the scanning XRF method to provide accurate results where the count per area is above 600 for these intertidal sediments. Scanning at 1mm intervals produces a large dataset for each core and provides a continuous high-resolution record of elemental composition. Scanning at a lower resolution would produce a less noisy but non-continuous profile; it is therefore more effective to apply a smoothing filter to the 1mm profiles.

The detailed profiles produced allow a thorough assessment of the individual element trends and characteristics and also comparison and correlation within and between cores. An understanding of the behaviour of individual elements allows individual elements or element ratios to be used as proxies for other sedimentary characteristics such as grain size or organic content. However in the intertidal environment this is complicated by the frequent change of conditions due to tidal inundation and bioturbation. These fluctuations will have an effect on the oxidation conditions of the sediment and also the mobility of elements.

The detailed datasets allow a variety of statistical analyses to be applied. This allows additional information to be extracted from the data. These methods are often affected significantly by dramatic changes in element profiles and therefore this needs to be taken into account when applying these analyses. It is therefore possible to examine the downcore structure of the core with multivariate analyses and identify periodicities of underlying dynamics with time series methods such as singular spectrum analysis. Combining this with other analyses, core dating information in particular, allows a better understanding of the dynamics effecting sediment deposition.

Overall this method is effective in providing a continuous record of the geochemistry of sediment cores from this environment. This can be used for detailed analyses and combined with other stratigraphic analysis methods to aid interpretation of the sediment sequence.

6.8. Summary of XRF analysis

Given that it has been established that scanning XRF can be a valuable tool in assessing the geochemistry of intertidal sediment sequences the following summaries can be made from the analysis of the Sandfield and Derryness cores. Four distinct element groupings are identified in the majority of the cores:

1. Clay mineral elements and their associates – K is the characteristic element of this group; other elements include Ti and Al although there values are frequently below certainty levels. This group is indicative of finer silt and clay material.
2. Silica – Si is the only element in this group. The sediment in these cores is dominated by quartz sand therefore high Si values are indicative sand rich layers within the sequence.
3. Carbonates – It has been established that the majority of Ca present within the cores is contained within carbonates of shell material. Sr also closely correlates. Therefore high values of Ca and Sr are indicative of shell rich layers
4. Organic indicators – Fe and Br are the characteristic elements of this group. They are often associated with organic matter and are therefore indicative of organic rich layers. However the correlations between these two elements are inconsistent and the conclusions to be made from the presence of these elements less certain.

The Sandfield cores show numerous similarities between the cores. Matching of the element ratio plots reveals several similarities in the characteristics of the profiles the most numerous of these are between the SFD2 and SFD3 Si/K plots. The dramatic reduction of $CaCO_3$ values identified in the SFD3 core in the previous chapter (5.2.3) is replicated in the Ca values of both the SFD3 and SFD2 cores. The PCA and cluster analysis also produces similar results for the SFD2 and 3 cores; i.e. alternating silica rich and shell rich layers in the lower section of the core below 1.42mOD and a gradation from silica rich to organic at the top of the core. The similar elevations of these matching characteristics in each plot suggest a similar environmental history and deposition rate for these two cores. Therefore it is reasonable to assume that the core dating results for SFD3 can also be applied to SFD2. The SFD1 core has significantly different Si/K and Ca/K profiles to the other Sandfield cores with very few points of correlation. It is therefore likely that SFD1 has had a significantly different depositional history. The singular spectrum analysis also reveals several similarities between the SFD2 and 3 cores and less with SFD1. It is difficult to attribute an accurate cycle period to the 35-37mm wavelength present in several

individual profiles and all three cores due to the uncertainties and likely changes in deposition rates. However this periodicity appears to be associated with a multi-decadal cycle.

Comparatively there are very few similarities between the two Derryness cores. This may partly be due to less elevation overlap between the two cores. The PCA and cluster analysis produce significantly different results for the two cores. DYN1 displays more variation in alternation and thickness of element groups downcore; this partly due to the greater number of cluster groups identified for this core. There are a couple of correlations between the periodicities identified in the SSA for DYN1 and 2. Both cores contain periods of 29 and 50-52mm. Due to the lack of dating evidence for these cores and the likely variations in deposition rates it is not possible to assess the cycle period for these oscillations.

No similarities were identified between the Sandfield and Derryness cores. In terms of Ca the two sites have very different depositional histories with almost a complete absence of shell material from the Derryness cores.

The multi-decadal scales of the suggested cycles could indicate several possible forcing factors in the deposition of these sediments. The previous analyses indicate episodic high energy events which result in the deposition of the sand layers seen throughout all the cores followed by periods of vegetation re-establishment and organic deposition. Therefore the cyclicity of storminess identified by several previous authors (e.g. Meeker and Mayewski, 2002; Dawson *et al.* 2007; Burningham and French, 2013) would seem the most likely controlling factor driving sediment deposition in these environments.

The implications of the analyses of the downcore stratigraphies, periodicities and cycles, and the historical environmental change identified in this and the previous two chapters are discussed further in the following chapter.

7. Discussion and summary

This chapter summarizes and draws together the results of the previous chapters. These results are discussed in terms of the wider estuary and regional dynamics and influencing factors. Ultimately this chapter seeks to describe how the overall aim and objectives of this study have been met.

7.1. Characterisation of present day environments

7.1.1. Physical environment

The Sandfield and Derryness sites occupy the high intertidal / low supratidal shoreline of the Loughros More estuary; however, both sites display complex and varying environmental characteristics. The present day morphology is that of a low lying, largely vegetated, surface that is raised above the tidal flat by approximately 1m and predominately at an elevation between MHWS and HAT. Surface features such as the ridge in the south of the Sandfield site and the channel running across the northern tip of the maritime grassland at Derryness indicate previous morphodynamic activity. Evidence from historical mapping and aerial photographs reveals significant localised morphological change over the last ~160yrs however the timing of phases of progradation and retreat vary both between and within sites.

The surface sediment from both sites is dominated by medium to fine sand. The sedimentology indicates that this sediment is sourced from reworked sands of the Magheramore dune system to the northwest. Across the tidal flat areas west of each site there is little variation in sediment sorting and mean grain size. However between the sites, the Sandfield tidal flat contains a significant proportion of coarse and very coarse sand whereas this fraction is virtually absent from the Derryness tidal flat. This coarse sediment comprises primarily shell fragments and their absence from Derryness is confirmed by the significantly lower $CaCO_3$ content. The reason for this difference in carbonate distribution is unclear and requires further work to aid understanding. The sediment source for the two sites is the same i.e. a combination of direct transport from the reworked dunes and via the tidal flat; however, the transport pathways and modes vary between sites. The spatial variation in $CaCO_3$ content may be due to local variation in mollusc productivity and/or the availability of suitable transport methods for these coarser grains. Shell material is often less susceptible to aeolian transportation (Jackson and Nordstrom, 2011); however here, it is clearly being transported by this mechanism as aeolian sediment deposits observed on the western edge of the Sandfield machair platform contain shell fragments and the $CaCO_3$ content is equivalent to that found on the adjacent tidal flat.

There appear to be significant differences in the transport of sediment at Sandfield and Derryness. The influence of the prevailing south westerly winds is highlighted at Sandfield by the presence of the aeolian deposits on the western margin of the vegetated surface and the

nature of the quartz grain microtextures. Although grain size trend analysis does not specify a transport mechanism, it too confirms a transport direction consistent with south westerly winds. At Derryness aeolian sediment transport appears to be less important; this is reflected with fewer occurrences of upturned cleavage plates within the quartz grain microtextures compared to Sandfield. This corresponds with Derryness's more sheltered position further up the estuary with no direct line of sight to the estuary mouth and therefore protected to a degree from the prevailing winds. The Sandfield and Derryness sites both comprise large vegetated areas that are almost wholly below HAT, which means that depositional processes are possible at high tide on these raised surfaces. The dominance of the aerophilous, littoral, diatom species *Diploneis interrupta* characterises the elevation and exposure of these surfaces on a regular basis. However, the presence of planktonic marine diatom species confirms the action of depositional processes at high tide. However, no significant differences in tidal deposition were identified between the sites, this further emphasises the importance of variable aeolian sediment transport and deposition in determining the character of the site. Consequently, position within the estuary and level of exposure to the prevailing winds can be expected to be a key factor controlling the morphological evolution of these sites.

7.1.2. Habitat definition

The ecological character of the sand flat areas is well defined by the diatom communities present, i.e. that of a clean, sandy shore. However the difficulty encountered in classifying the vegetated zones highlights the complexity of these areas. Prior to this work there had been disagreement in the literature over the definition of the vegetated habitats at Sandfield and Derryness. Sandfield has been described by Gaynor (2006) as machair or partially machair and Derryness as saltmarsh; whereas, Curtis and Sheehy Skeffington (1998) and McCorry and Ryle (2009) define both areas as saltmarsh.

This disagreement reflects the complexity of the sites and the need for a more integrated approach to describing habitats of this type that takes in to account the morphology, sedimentology and ecology of an area. Ritchie's (1976) definition of machair applies this integrated approach and is a good example of where characterisation of an environment as a whole has been used to define a habitat. However the majority of work on machair (Ritchie, 1976; 1979; Gimingham, 1974; Angus, 1994; 2006; Mate, 1992) is based upon the extensive and well established machair plains of northwest Scotland, and there is no current literature on less well established machair or those environments transitional to machair. Sandfield meets the criteria for machair defined by Ritchie (1979) and Angus (2006) with the exception of the core plant species, although this may be due to previous overgrazing of the site. Whereas, the Derryness vegetated areas appear to represent transitional phases towards the machair as described by Ritchie (1979). These sites have, to varying degrees, some of the characteristics of

machair; if deposition continues in these areas and they become sufficiently separated from the influence of tidal processes these characteristic are likely to become more developed. However it is unclear whether these sites will ever reach the full definition of machair and there further work is needed on both the differences between Scottish and Irish machair and also the ecological character of these smaller more transitional habitats. The position of these environments within the tidal frame within the context of a falling sea level in this region during the late Holocene (Wheeler *et al*., 1999) should also be considered. Under these conditions it is possible that the arrangement of the contemporary marginal coastal habitats here, in particular the two raised vegetated surface, represent the terrestrialisation of relict saltmarsh environments. This is a hitherto unrecognised and unexplored idea and further work is needed to establish its validity.

Based on the integrated approach employed in this research it is suggested that the Sandfield vegetated surface should be defined as machair, Derryness vegetated surface as maritime grassland and Derryness vegetated flat as saltmarsh.

7.1.3. Management implications

The definition of an environment can have significant implications for how it is managed for its conservation. For example, whether a habitat is described as machair or saltmarsh could influence the grazing regime employed on the site as a feature of machair is biotic interference caused by grazing or cultivation; this is not necessarily required for sustaining a saltmarsh environment. Recently the cattle stocking density at Sandfield has been reduced to relieve the grazing pressure on the habitat. This change in management will hopefully result the development of a stronger machair character it is able to recover from the effects of intensive grazing, surface disturbance and soil enrichment. Future monitoring of the morphology, sedimentology and ecology will be required to fine tune these management practices.

Recognition of temporal changes to these environments, both in the context of the localised site evolution but also in the wider estuary system, also has important management implications. It has been shown here that these marginal environments may vary significantly over century and decadal timescales. For example, it can be seen that the Sandfield site in particular has changed significantly in response varying tidal channel position within the estuary and resulting sediment supply. Management strategies are predominantly based upon a general interpretation of an environment taken at a fixed point in time. However, it should be recognised that management of marginal coastal environments, which are inherently dynamic, should be flexible to adapt to these natural changes.

7.2. Environmental reconstruction

7.2.1. Site evolution, timing and rates of deposition

Determining sediment deposition timing and rates has proven difficult in this sandy intertidal environment due to the paucity of datable material and the nature of sediment transport. At Sandfield a deposition rate of 1.3±0.1mm/yr would appear to be applicable for the top 25cm of the sequence in the east of the area where the finer, more organic, sediments top the sequence. However, this assumes a linear rate of deposition which would appear to be unlikely given the nature of the sediment sequence, i.e. alternating laminations suggesting rapid sand deposition followed by a period of slower more organic accumulation. It is therefore only possible to view this rate as an average for the top 25cm of the SFD3 core. Although there is potential to use the Pb/K ratio to provide additional information on timings of deposition and deposition rates the very low Pb values in these sediments cannot be relied upon to produce accurate results. Therefore, in this instance no further chronology can be inferred from this method. Furthermore, this organic upper unit decreases in thickness to the west and therefore the deposition rate calculated for the east of the site (SFD3) is not applicable to a similar depth in the sequences of the centre and west of the area. Below the finer organic unit deposition rates are less certain due to the limitations of the ^{210}Pb and ^{137}Cs methods i.e. the need for a sufficient proportion of fine material. At Derryness the lack of datable material and any supporting geochemical evidence makes determination of the deposition rates by Pb-based methods impossible.

The deposition rates calculated for Sandfield are less than half that reported by Wheeler *et al*. (1999) for the Bracky Bridge saltmarsh (i.e. 5mm/yr) at the head of the Loughros Beg estuary approximately 5km to the south of Loughros More. There are several potential reasons for the differences seen between these two sites. Firstly the sections dated by Wheeler *et al.* (1999) were taken from the cliffed western margin of the saltmarsh; whilst a similar method was employed in this study the core used for dating (SFD3) was taken from an internal creek cliffed margin. This area represents a longer record of deposition and, more recently, a more sheltered environment where slower biogenic deposition is more dominant. However, towards the more exposed southern and western margins of Sandfield where minerogenic deposition is more prominent, rate of deposition is likely to increase. Secondly, the elevation of the Bracky Bridge saltmarsh surface and in particular the sampling locations (1.5mOD) is lower than at both Sandfield (1.73mOD at SFD3) and Derryness zone B (1.95mOD at DYN1). This places the Bracky Bridge seaward margin below Mean High Water Springs (1.63mOD), a vertical position where tidal inundation and deposition would be more frequent. Wheeler *et al.* (1999) do not distinguish between tidal and aeolian deposition but it is likely that tidal deposition plays a more important role on the Bracky Bridge marsh than on the areas of machair and marsh at Sandfield and Derryness. Aeolian sediment supply to the Bracky Bridge marsh is unlikely due to its inner

estuary location. The sedimentology of the sections is also significantly different with the Bracky Bridge marsh being dominated by silt and clay sized sediment exhibiting a general coarsening upward through the core. Wheeler *et al.* (1999) suggest this is due to the decreasing importance of tidal deposition as the marsh becomes further elevated above the tidal flat and a consequent increasing importance of surge events and storm waves. Its position within the tidal frame and the relative importance of tidal deposition is similar to that of the Sandfield and Derryness raised surfaces earlier in their evolution. However, the difference in grain size is a marked difference which again is likely attributed to the inner estuary location of Bracky Bridge in comparison to the mid-estuary location of Sandfield and Derryness. Given these differences it is likely that the rates of deposition are determined by different controls with the Bracky Bridge site receiving additional input from frequent tidal deposition.

The overall evolutionary trend and characteristics of the Sandfield site are summarised in Figure 7.1. The initiation of the transition from a tidal flat environment to a more marginal accreting environment is marked by a change in the sediment characteristics from erosional to depositional, as highlighted by the log-hyperbolic distribution analyses. Once the site enters this depositional phase numerous changes are seen to occur. Firstly the organic content of the sediment begins to increase, likely due to the colonisation of pioneer plant species. At this time the area is likely to have been analogous to the present day saltmarsh area at Derryness with the presence of a high intertidal plant community akin to the species seen, e.g. *Glaux maritima* and *Triglochin maritima*. Subsequently the supply of aeolian sediment and shell material to the east of the site is significantly reduced or cut off. It is likely that the dunes identified on the 1850 map formed as a low barrier during this period, effectively blocking the supply of aeolian sediment transport (including carbonate shell material) by creating a topographic barrier for wind-blown sediment to the east of the site. This period is also consistent with the timing of the "Night of the Big Wind" in January 1839. During this hurricane scale storm event large amounts of wind-blown sand are reported to have been eroded, mobilised and deposited up to 2 miles inland along the Donegal coastline (O'Brien *et al*., 2013). The abrupt nature of the $CaCO_3$ cut off to the east of the Sandfield site, in particular, is suggestive of a significant short-term event rather than gradual barrier development. It is likely that this area was already shifting to vegetated conditions but this event represents the tipping point marking end of tidal flat conditions and a shift to an accreting environment sufficiently separated from the influence of tidal flat dynamics. Based upon these coincident lines of evidence it is tempting to link this significant 1839 storm event with major morphological changes in this area. If these assumptions are accepted it would then enable the timing of this event to be applied to the $CaCO_3$ cut off seen in the SFD2 core from the south of the site. However, applying the 1.3mm/yr rate to the SFD3 core, the transition to machair identified in the SFD3 sediment log, is dated to approximately 1805 ±15yrs in the east of the site. This occurs shortly after the

formation of the dune barrier in the west of the site, indicated by the calcium cut off (Figure 7.2). This timing would therefore imply that the dune barrier formed between 1790 and 1820, contradicting the suggestion of the 1839 storm initiating its formation. However, given the uncertainties with the ^{210}Pb and ^{137}Cs dating associated with the assumption of a linear deposition rate and given the additional geochemical and historical evidence, it may still be possible that this storm event led to the formation of the dune barrier and the cut off of $CaCO_3$ supply. But based on the evidence available these links are too tenuous to draw any direct conclusions.

Subsequent to dune formation the area behind the barrier would be sheltered from prevailing winds, storm events and rapid changes in sediment erosion and/or deposition. This would allow a greater variety of plant species to become established in this area further increasing the organic content of the sediment. At some point between the mid 1800s and early 1900s the bulk of the supratidal topography of this barrier was removed from the western edge of the area. The mechanism of this removal is unclear, although deflation and redistribution over the raised surface behind is possible as this feature remains here, though somewhat reworked and modified in extent. Burningham (2005) also notes a similar significant change in the morphological character of the dunes of the Loughros Beg estuary, to the south, during the same period. Here both historical maps and personal accounts indicate supra-tidal areas of the Maghera dune system underwent a period denudation and deflation resulting in a change to a topographically flat area at or just below MHWS.

Between 1907 and 1977 the environment continues to be depositional with progradation of the western margin. During this period the morphology and sedimentology are broadly similar to that of the present day environment. This includes a low lying surface raised above the tidal flat with sedimentary organics increasing to the east where minerogenic sediment supply is limited; and greater carbonate content in the west where linkage to the wider tidal flats and dunes, and aeolian processes, are enhanced. After 1977 the area enters a period of erosion and the western margin continues to retreat to the present day (2012).

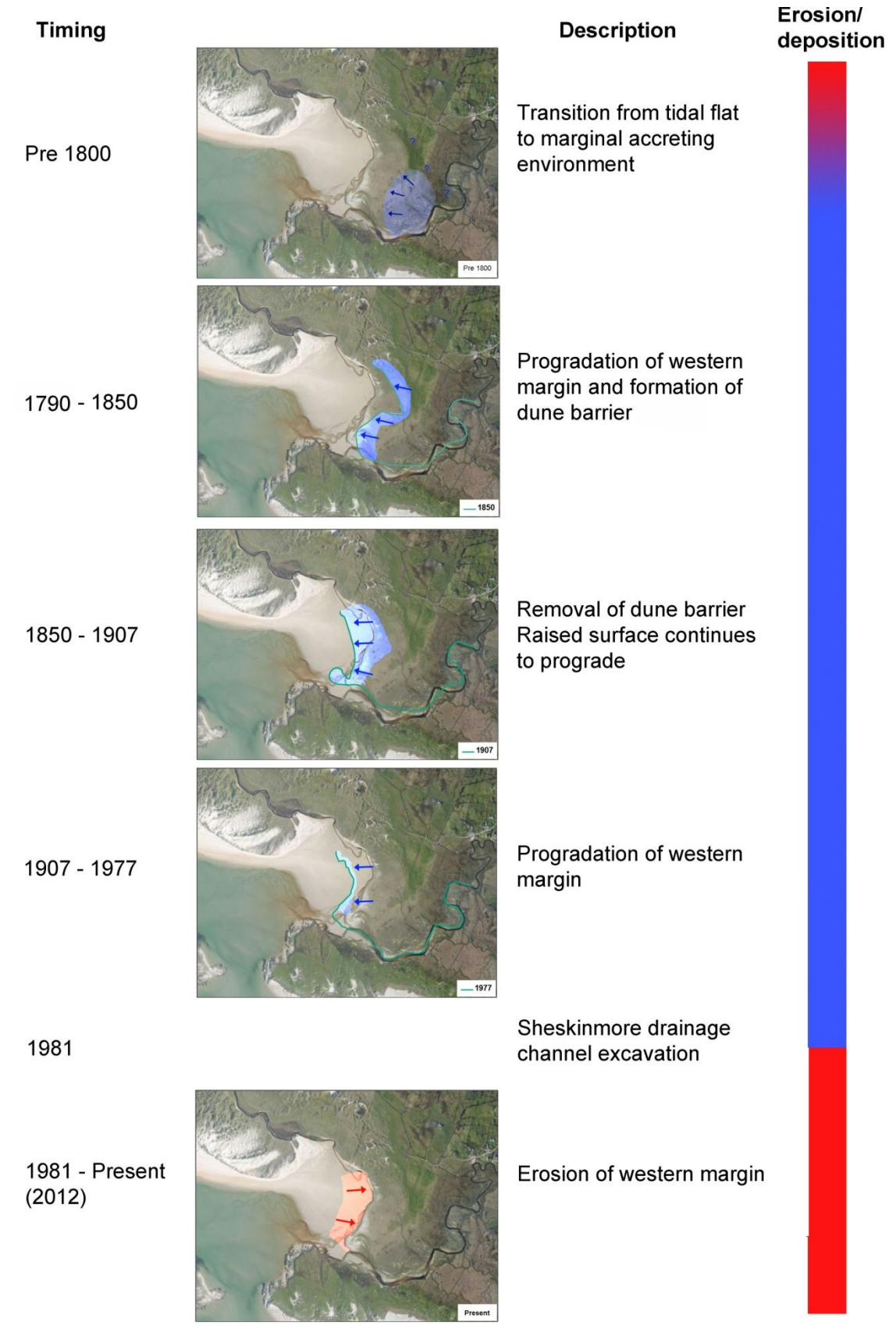

Figure 7.1 Summary of the major trends and features identified in the evolution of the Sandfield site and their approximate timings (blue indicates location and periods of accretion and red erosion and retreat).

The extent of the influence of the Bellanagoal River and Sheskinmore Lough outflow on the erosion/progradation of the western and southern margins of the Sandfield site is uncertain. However, evidence from the historical maps and aerial photographs suggest their positions relative to the vegetated area may be a contributory or controlling factor affecting both the retreat seen on the western margin and the formation of the historical morphological surface features. At the time when the dunes were present the 1850 map indicates the Bellanagoal River channel was at least 50m further north of its present day position. This alignment corresponds to the present day ridge identified on the Sandfield surface which is thought to be indicative of the northern most extent of this channel. The timing of the excavation of the drainage outflow channel from Sheskinmore Lough (1981) and the continued enhanced flow until the construction of an effective sluice in 2005 directly links with the change to an erosion-dominated shoreline. This intervention possibly initiated the erosion seen on the western margin of the Sandfield machair area and has had a significant effect on the evolution of the site subsequently.

A summary of the main trends and characteristics in the evolution of the Derryness site are shown in Figure 7.3. Due to a paucity of dateable material within the Derryness sedimentary sequence and the fact that the core sites show evidence of vegetated conditions for the complete recovered record of the site, determination of the timing and deposition rates of the upper sections of the sediment sequence is not possible.

The sedimentology indicates that for the majority of the evolution of the raised vegetated surface in the south of the site deposition has dominated. Evidence from historic maps and aerial photos shows that, although the northern tip of this area has been subjected to some erosion, the extent of the majority of the area has been relatively stable from 1850 to the present day. Currently (2012) some erosion is occurring along the western edge although at a significantly lower rate than that seen at Sandfield. Subsequent to the transition from tidal flat to vegetated surface (identified in the sediment logs at 42cm (1.53mOD) and 22cm (1.21mOD) in DYN1 and 2 respectively) the area receives a greater input of aeolian sediment, evidenced in the quartz grain microtextures, and organic contents increase. This additional input of aeolian sediment may have triggered the formation of this area by raising it sufficiently above the tidal flat for plants to become established. Sedimentation continues, raising the surface above MHWS, as evidenced in the changing diatom communities and increasing organic content.

Evidence for the evolution of the area of vegetated tidal flat fringing the rocky outcrop in the north of the Derryness site comes solely from the historic maps and aerial photographs. This shows the environment to already be established by 1850 and therefore examination of its initiation is not possible. It undergoes a period of retreat between 1850 and 1951 (Figure 7.3) followed by a progradation to the present day (2012).

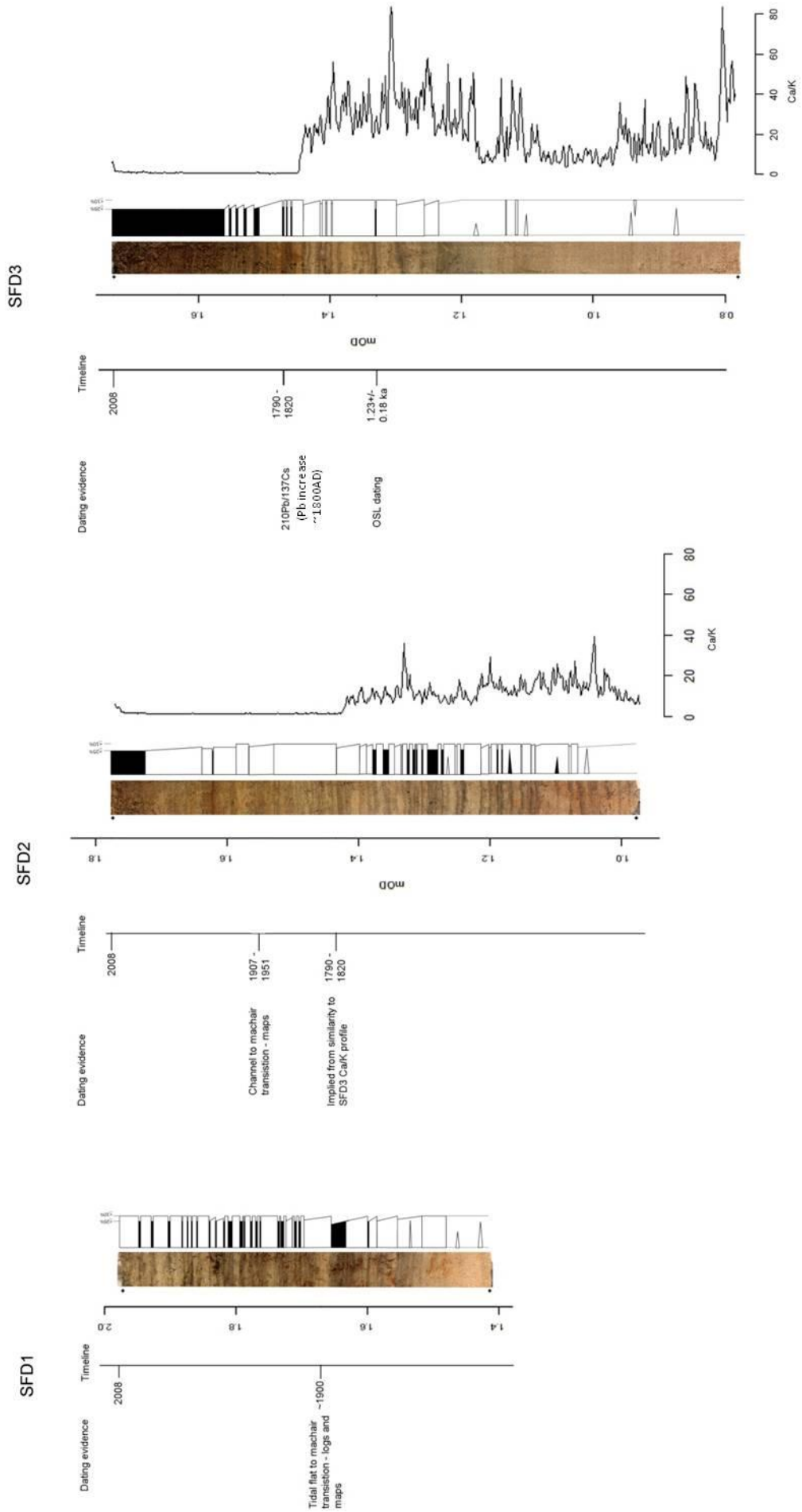

Figure 7.2 Summary of dating evidence for Sandfield (black bars indicate laminations with greater than 25% organic content, as identified in the sedimentary logs).

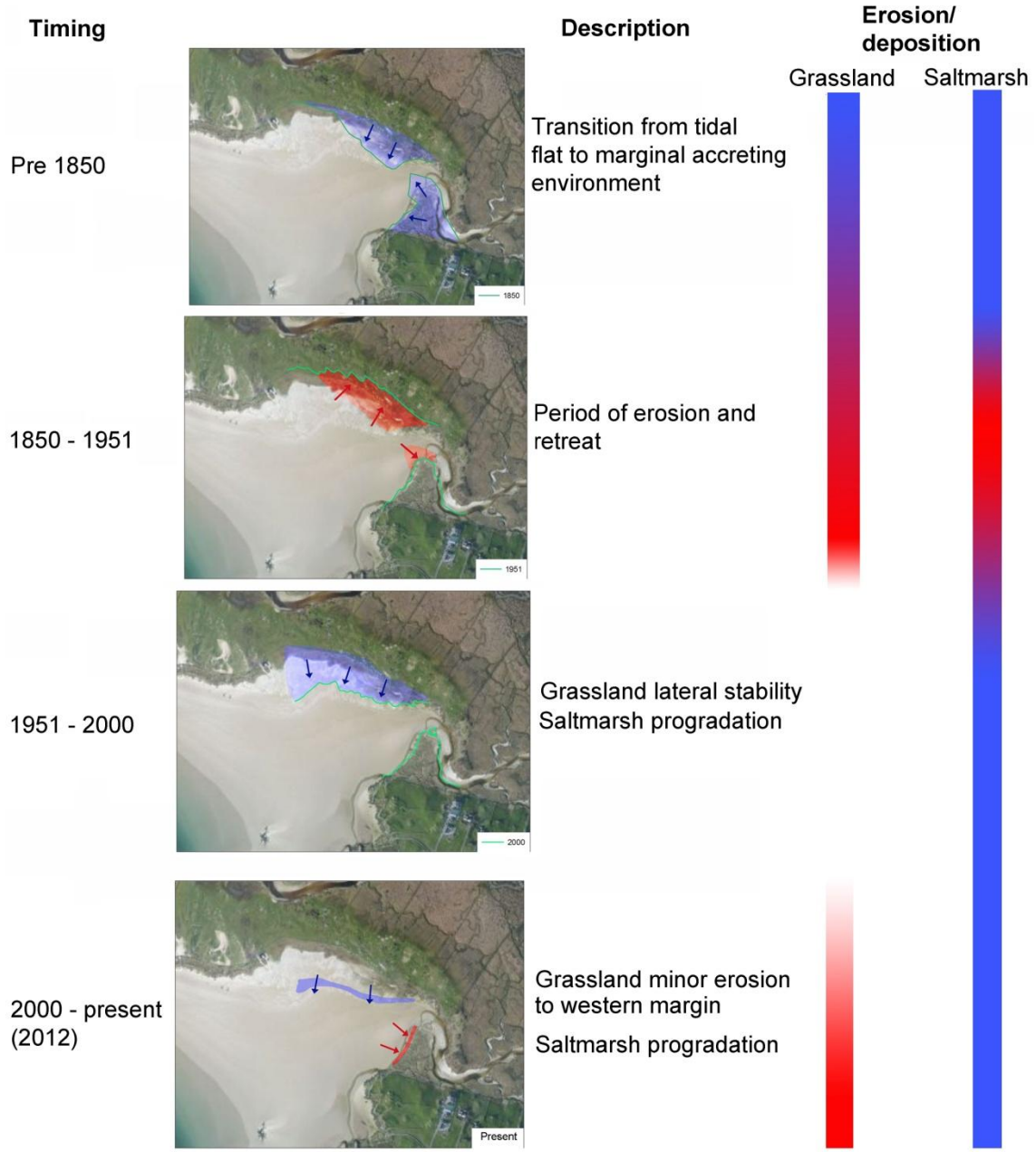

Figure 7.3 Summary of the major trends and features identified in the evolution of the Derryness site and their approximate timings (blue indicates location and periods of accretion and red erosion and retreat).

Optically Stimulated Luminescence (OSL) dating at both Sandfield and Derryness points to a period of sediment movement and accumulation between 1000 and 2000 years ago. Although the accuracy of this dating is uncertain due to the possibility of partial bleaching of the quartz grains, this timing is consistent with the period of the instability and large scale movement of the Magheramore dune system inferred in wetland sediments associated with Sheskinmore Lough to the north (Shaw and Carter, 1994). Additional, later, sand accumulations prior to the transition from tidal flat to vegetated surface may in part be related to a period of increased storminess around 1400AD as identified by Dawson *et al.* (2007). However further dating and stratigraphic analyses of the machair and wider dune environment would need to be undertaken to investigate these ideas.

In summary, the overall trends in the evolution of the Sandfield and Derryness sites are distinctly different. This indicates significant local variation in sediment transport and erosion. This is important as it suggests that the factors controlling sediment transport and erosion are significantly variable on a local scale.

7.2.2. Cyclicity

In addition to the broad overall trends in the evolution there is also evidence of repeating or cyclic events acting over smaller timescales. The most dominant visual feature of the sediment sequences from Sandfield and Derryness is the light and dark banding identifiable in both the sediment cores and field sections (Figure 7.4). These often form thin layers as fine as 1mm but on average not more than 5mm in thickness. Closer examination of these alternating bands in the sediment peels reveals frequent fining upward sequences which become more common in the upper more organic sections of the cores. These alternations are not picked up in the majority of the analyses due to the need for 1cm sub-sampling. However the 1mm resolution scanning XRF has enabled the identification of a high level of geochemical detail in the sediment cores.

Cluster analysis of this data has enabled description and characterisation of these layers. Within the base of the Sandfield sections, alternations between layers of sand with high and low calcium contents are common. Further up the sequence the light and dark banding becomes more prominent with alternations between sandier clastic and finer organic layers. These regular alternations suggest a repeating deposition of fresh sand onto the surface which is deposited quickly resulting in plant burial and little or no addition of organic material to the substrate at that time. Subsequently plants become re-established, the surface stabilises and organic material is deposited until the next fresh supply of sand. This is confirmed by the identification of fining upwards sequences identified in several of the sediment logs. This sequence is interpreted as the repeated deposition of estuarine and/or dune sands by wind and/or wave action over the established machair platform. A similar pattern of repeating sand and organic layers is also

found in the Derryness sequences. To the top of the sections within the east of Sandfield site, organic content increases and very sandy layers are less common. This is likely to be indicative of a slowing of the deposition rates in this area as it is separated from the aeolian sediment source.

Figure 7.4 Example of the light and dark layers visible in field sections (DYN1)

This detailed analysis of the sedimentology of the layers is further evidence of the non-linear nature of sediment deposition within these sequences. The abrupt lower boundaries and fining up sequences are more suggestive of episodic deposition. Therefore, although the deposition rate of 1.3mm/yr calculated for SFD3 may represent the average deposition over the top 25cm of the core it is likely that within this there were periods of significantly higher and lower rates of deposition.

Via singular spectrum analysis of the scanning XRF data two distinct periodicities in element and ratio downcore variation are identified; one within the Sandfield cores and one within the Derryness cores. The occurrence of these periodicities in multiple cores is significant as it indicates processes influencing the whole area. Within the Sandfield cores a periodicity of 35-37mm is approximately equivalent to a cycle of 27.5±2.5yrs based upon the 1.3mm/yr accumulation rate calculated for SFD3. As highlighted earlier the deposition rate varies spatially

across the machair at Sandfield. However, it is possible that this variation may be accounted for in the range of both the period length (i.e. 35-37mm) and cycle duration (27.5±2.5yrs) meaning it may be possible to apply this cycle duration to the similar periodicity seen across the Sandfield cores. Further analysis of the variation in deposition rates across the machair would need to be done to confirm this. A periodicity of 50-52mm is identified within the Derryness cores; however, due to the lack of any accurate dating information for these cores it is not possible to attribute a time interval to this. Given that it appears likely that the Derryness accumulation rate is greater than that of Sandfield, based upon the presence of ^{137}Cs throughout the DYN1 core, it is possible that this 50-52mm periodicity is equivalent to the 35-37mm seen at Sandfield. However, this assumption is made without any degree of certainty. As a result of all these uncertainties it would only seem safe to say that these periodicities identified at Sandfield and Derryness are associated with a multi-decadal cycle(s).

Similar cyclic depositional sequences have been observed in numerous equivalent marginal coastal deposits in the northwest of Britain and Ireland (e.g. Ritchie and Whittington, 1994; Delany and Devoy, 1995; Wheeler *et al*, 1999). Wheeler *et al*. (1999) identify similar alternating laminations within the Bracky Bridge saltmarsh sequences in Loughros Beg with the coarsest sediment layers fining upwards. They encounter similar problems in attributing any timings or periodicities to these alternations due to the varying deposition rates associated with these sequences. However, using Markov Chain analysis they are able to identify three longer term cycle durations of 11yrs, 15yrs and decadal-plus (20-25yrs). The potential decadal-plus (20-25yrs) cycle identified in their results is of particular interest due to its similarity to the 27.5±2.5yrs cycle identified at Sandfield. This implies inter-estuary forcing of sediment transport and deposition processes. However, Wheeler *et al.* (1999) are unsure of the significance of this multi-decadal cycle due to the length of the time window used in the analysis and the variation in deposition rate between laminations. Each of these three longer term cycle durations Wheeler *et al*. (1999) attribute to rhythmicity in storm surge generation. However, comparison of these results with any potential cyclicity at Sandfield and Derryness must be made with caution as the laminations identified at Bracky Bridge represent alternations of silt and clay sized sediment with no discrete sand layers and as stated previous likely represent different depositional controls. The alternating laminated deposits of clastic and more organic layers identified by Ritchie and Whittington (1994) in the machair sites of northwest Scotland are far more similar in terms of their sedimentology to the laminations identified here. Ritchie and Whittington (1994) attribute the alternations seen in the northwest Scotland machair to repeated cycles of sand blowing and surface stabilisation. They suggest that more recently this is due to human intervention (i.e. since human occupation of the Uists); however, there is evidence for previous natural stability/instability cycles driven by sea-level rise, coastal erosion and possibly modified by climate changes. Other than identifying a first sand blowing period at

around 7810BP they are unable to draw any further conclusions on the timings and frequency of these sand blow events. Delaney and Devoy (1995) also identify a similar repeating trend in the dune/machair/marsh sequences of County Mayo, western Ireland. Here, they attribute these depositional cycles to sudden inputs of energy from an external source such as the passage of storms.

The fine alternating light and dark layers are clearly picked out in analyses of image intensity of the photographs of the individual cores (Figure 6.1). The more sandy layers are clearly identifiable in the core photographs and visual comparison with the Si content reveals a very similar downcore profile (Figure 7.5). The layers can be explicitly linked with peaks and troughs in the Si/K content through the majority of the length of the cores; the inset in Figure 7.5 clearly illustrates this relationship. However, the presence of any periodicity of repeating sequences is not clearly identifiable rather inputs of sand appear to occur episodically. A simple count of the numbers of layers per distance downcore in the SFD3 core suggests on average an alternation every 3years; however this was not regular and the actual timings between alternations is likely to vary significantly. The non-repeating and episodic nature of these layers means lamination analysis, for example Markov Chains analysis, cannot be applied to these deposits.

7.2.3. Forcing factors and drivers of morphological change

There are several processes described in the literature by which alternating layers in a depositional sedimentary sequence may be produced within the intertidal environment. These include tidal rhythmites and tidalites (e.g. Allen and Duffy, 1998; Stupples, 2002), sea level change, human intervention (e.g. Ritchie and Whittington, 1994) and the impact of storms (e.g. Allen, 2004).

The factors behind the production of tidal rhythmites and tidalites are not applicable to the layered sedimentary sequences identified in this study. The chronology presented here implies process timescales longer than those associated with rhythmic tidal forcing, and the relatively high energy environment is not conducive to the production and preservation of this type of deposit. The influence of sea-level change over the last 2000 years is relatively unclear in the northwest of Ireland. Sea level has unlikely been static over this period, and complicated relationships between eustatic sea level rise and isostatic land adjustments may have resulted in impacts on the high intertidal / low supratidal zone, but as yet no significant overall trend has been identified (Delany and Devoy, 1995; Wheeler *et al*., 1999). However it can be said that over the last 200 years, i.e. the period of recent morphological evolution at the Sandfield and Derryness sites, there is no evidence for significant, repeating sea level events that would result in the deposition of alternating sedimentary sequences.

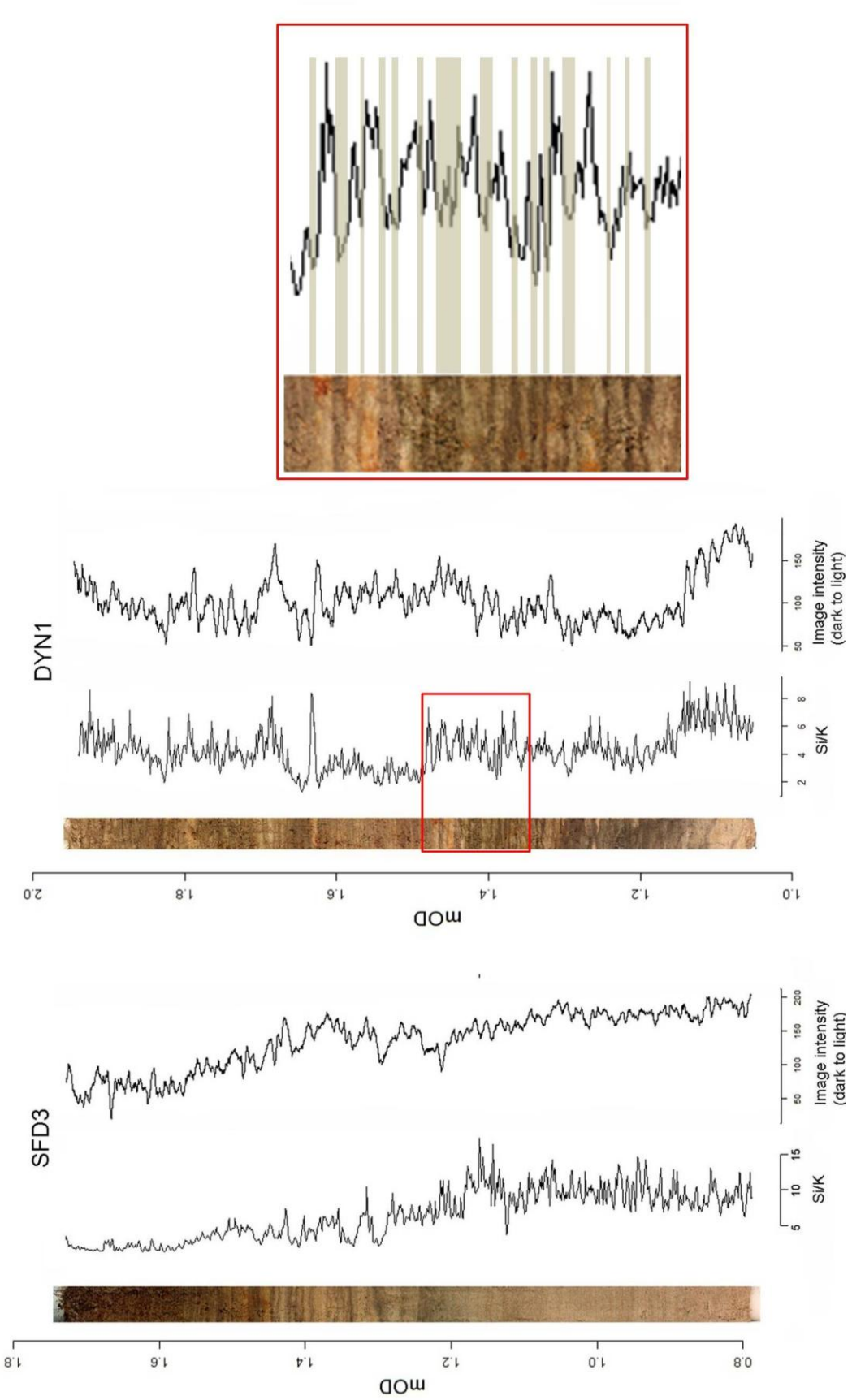

Figure 7.5 Visual comparison of image intensity with Si/K profile for DYN1 and SFD3. Inset shown by red box highlights the correspondence between Si content and stratigraphic layering

The role of multi-year astronomical cycles (i.e. lunar nodal cycle – 18.6yrs) has the potential to influence sediment deposition within the study sites where large areas of the estuarine sedimentary shoreline occupy the high intertidal zone between Mean High Water Springs (MHWS) and Highest Astronomical Tide (HAT). However, the evidence here presented based on sedimentological analyses suggests sedimentation comprises periods of high energy sand deposition followed by a period of slower, organic-based accumulation. High energy deposition is unlikely to be driven simply by extreme tide levels (around HAT) unless combined with a storm event. The evidence for rapid burial of vegetated surfaces, the relative abundance of aeolian deposits and the subsequent re-stabilisation of the surface suggest episodic, high energy – low frequency events storm events are likely to be the most dominant factor influencing the depositional cycles in these sequences.

Several authors have described the century and decadal scale changes in storminess in the northeast Atlantic region (e.g. Dawson *et al*. 2004; Lozano *et al*. 2004; Hanna *et al.* 2008). Several of these authors have found apparent links between the changes in storminess over the past 150years and the North Atlantic Oscillation (NAO) (e.g. Dawson *et al.* 2004). The NAO is the primary mode of inter-annual atmospheric variation and climate variability across the north Atlantic region (Hurrell, 1995). Whilst the NAO winter index is often used as a proxy for storminess, its actual association with winter wind climate in northwest Europe is more complex and evidence for its association with event-scale storm frequency is weak (Burningham and French, 2013). Hickey (2003) provides a summary of the record of storminess in Northern Ireland from 1796 – 1999 based upon observations from the Amargh Observatory. Although located approximately 80miles east of the study sites this provides the earliest near complete record for the region. The 1796 – 1844 period of this record is purely descriptional with no instrumental observations recorded. During this earlier period of the record Hickey (2003) identifies two periods of relatively high storminess between 1796 to 1825 and 1835 to 1844. The timing of this is of interest as it is consistent with the period of barrier building in the west of the Sandfield site, evidenced here in the sedimentary and map records.

Dawson *et al.* (2002) identify a subsequent period of increased storminess between 1870 and 1900. Although this period of increased storminess is identified across both northwest Ireland and Scotland it is not represented by a significant positive phase in the NAO highlighting the complexity of the relationship between atmospheric circulation and storminess. Based on historic maps and aerial images, the period 1850 to 1907 seems to be characterised by erosion across the vegetated areas of Derryness and dune barrier deflation and sediment redistribution at Sandfield. It is therefore likely that much of this morphological change occurred as a result of storm events during this period of increased storm frequency. Progradation of the western margin of Sandfield was possibly facilitated by the release of sediment from the dune barrier and persistent westerlies.

The most recent period of increased storminess occurs between 1980 and the early twenty first century. This period corresponds with a distinctly positive phase of the NAO and occurrence of gale events at Malin Head can been seen to increase during this time (Figure 7.6). During this period the raised vegetated surfaces at both Sandfield and Derryness begin to erode. At Sandfield this is thought to be at least partly due to the anthropogenic alteration of the Sheskinmore Lough outflow; however, the period of increased storminess could have accelerated this erosion.

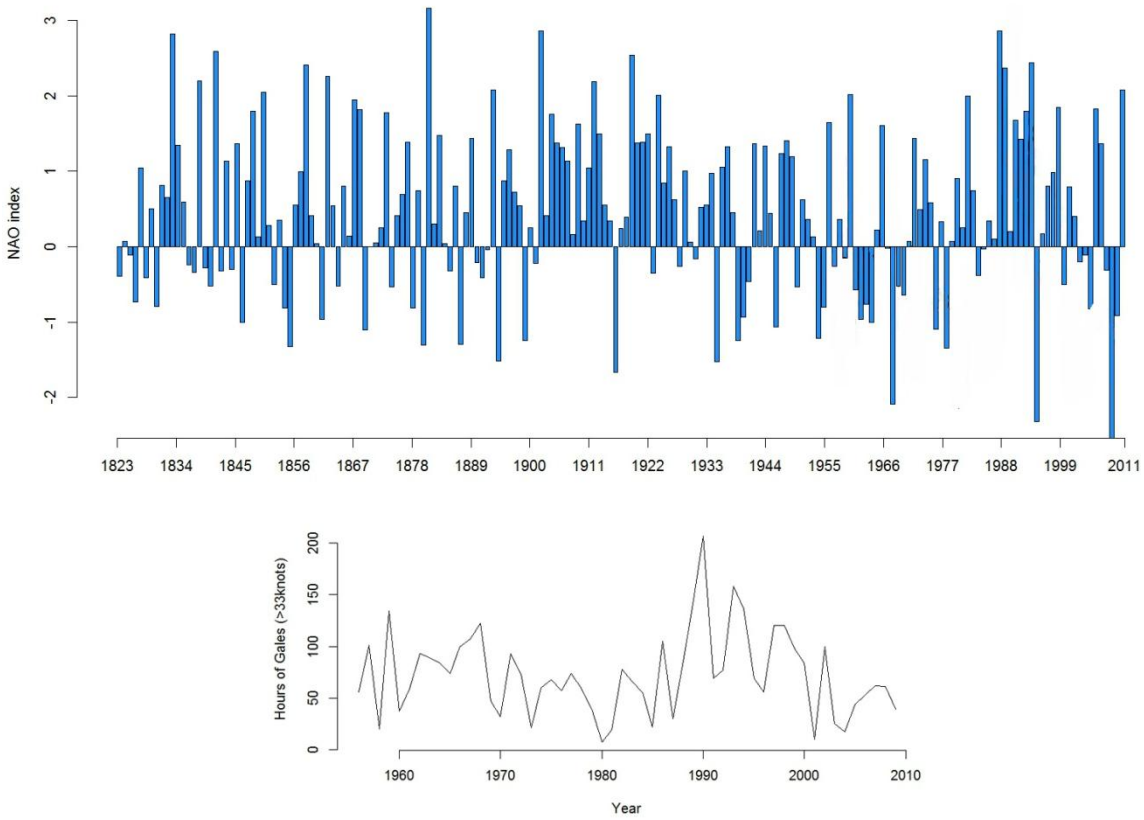

Figure 7.6 NAO winter index (DJFM) for the period 1823-2010 (above) and number of hours of gales (>33knots) per year at Malin Head 1956-2009 (below).

Due to the lack of dating evidence it is not possible to attribute any of these periods of increased storminess to individual layers or groups of layers in the sedimentary sequences. However, the scenario of periods of increased winter storminess, when significant amounts of wind-blown sand may be deposited on the vegetated surfaces, followed by intervening periods of quiescence when plants re-establish and organic deposition dominates as soil development resumes corresponds with the evidence identified in the stratigraphy.

It is clear from both this study and previous works that storms play an important role in controlling the depositional characteristics and consequently morphological evolution of the high intertidal marginal sedimentary environments of northwest Ireland and Britain. The

creation of a dune barrier along the western margin of Sandfield was a morphological milestone in the evolution of the site and was likely the result of a storm event in the early 1800s (potentially the "Night of the Big Wind" in 1839). This highlights the importance of storms in driving morphological change and their potential to be the tipping point between alternating stability domains (e.g. Stallins, 2005). Cooper et al. (2004) recognise that on high energy coastlines, such as northwest Ireland, the difference between the "normal" conditions and a storm event is comparatively lower than on low energy coasts and therefore larger storms may be required for significant morphological change to occur. This is important as it implies that on these higher energy coasts, whilst overall storminess is important in defining the character of the environment, individual storm events could be key in driving morphological change. At Malin Head, during the period 1957 – 2010, there have been 11 extreme storm events (i.e. wind speeds >60knots) (MacClenhan et al. 2001) (Table 7.1). Of these, none can be explicitly linked to changes seen in the morphology or sediment sequences of the Sandfield and Derryness sites due to the paucity of dating evidence and the fact that historical maps and aerial images only represent a snapshot in time. It is likely, however, that many of these events are responsible for the more distinct and discrete sand layers present within the sediment sequences (Figure 7.4).

The fact that these more recent extreme events have not resulted in the same extent of morphological adjustment as the early 1800s storm event may be due to several factors. Firstly, the early 1800s storm event may have between even more exceptional than that of recent decades; however, due to a lack of accurate local wind speed records for this period this is not able to be confirmed. Secondly, the morphological adjustment to the early 1800s storm event may have attuned the system to a higher energy regime (as suggested by Cooper *et al.* 2004) therefore resulting in less morphological adjustment in later, similar magnitude, events. To explore this idea further, research on the role of storm events on the future morphological evolution of high intertidal environments is required.

This study also presents evidence of the significance of storm events on the geochemistry of the sedimentary environment, seen here in the abrupt stop in supply and deposition of shell material ($CaCO_{3)}$. Although not evidenced here this has the potential to significantly alter the ecology of an environment. For example, as shelly sand and a relatively high pH value are characteristic of machair environments, a reduction in $CaCO_3$ supply to an area could prompt a habitat shift response.

Table 7.1 Extreme storm events (wind speeds >60knots) at Malin Head 1957 – 2010 (after MacClenhan *et al.* 2001)

Date	Duration (hours)	Peak Speed (knots)	Mean Speed (knots)	Mean Direction (degrees)
31/01/1957	1	62	62	209
05/02/1957	1	60	60	219
16/09/1961	3	68	65	203
15/01/1968	2	62	61	229
28/01/1974	1	61	61	189
04/09/1983	1	60	60	259
11/01/1984	1	60	60	269
20/03/1986	1	62	62	269
13/02/1989	1	60	60	269
26/12/1998	3	61	60	249
09/01/2008	1	61	61	250

7.3. The potential of scanning XRF in the analysis of high intertidal sedimentary sequences

The scanning XRF method enables an efficient, non-destructive, high-resolution analysis of the structure of marginal intertidal sediment sequences. It produces extensive, detailed, data which allows various statistical analyses to be applied. From this, not only the analysis of individual elements can be undertaken, but calculations of their ratios and proxies generate further insights. The application of XRF methods to coastal sediment sequences is uncommon and where they are used it is more often the pellet sample XRF method that has been employed (e.g. Tsompanoglou *et al*., 2011). The advantages of the scanning method over the pellet method are: i) the non-destructive nature of the method, ii) the ability to analyse geochemical variations over smaller distances (it is not necessary to homogenise the sample as in the pellet method) and iii) the relative efficiency of the method in terms of both time and labour. However, the scanning method does not produce quantitative percentage values for individual elements and therefore in this study it was necessary to run a sub-sample of pellet XRF samples to obtain an estimation of the element concentrations.

Although the scanning XRF method provides a high-resolution analysis of down core geochemical variation it is debatable whether such a high level of detail is needed. The 1mm resolution data analysed here, in the pre-processed form, comprise highly fluctuating (noise-signal ratio) data series that required a certain amount of processing (numerical smoothing) before analysis. In their study of intertidal saltmarsh sediment sequences Tsompanoglou *et al*. (2011) produced detailed downcore records of geochemical change with 1cm subsamples. However, Boning *et al*. (2007) report on the usefulness of the recent advances in micron-scale scanning XRF in tracing the extent and timing of chemical, mineralogical and sedimentological transitions. The ability to analyse sequences at the micron-scale is particularly useful in slow deposition environments where annual and intra-annual variations are of interest (Shanahan *et*

al., 2008). It is clear therefore that the resolution requirements for XRF analysis are significantly dependent on the scale of the depositional structures or features within the environment being examined. In this study similar results would have been achieved using a 5mm scanning resolution.

The high-resolution data produced by the scanning XRF method, at 1-5mm resolution, allows the structure of sequences to be examined and statistical methods such as cluster analysis and singular spectrum analysis applied. This allows an additional level of information to be extracted from the sequences that would not be possible from other standard methods (e.g. LOIs, sedimentology and palaeoecology). Combining this with these other analyses and chronological information where available facilitates a multiproxy, multivariate investigation that can draw from a range of evidence to deliver a greater understanding of the sedimentary evolution.

The potential of the scanning XRF data was limited to a certain extent in this study by the lack of datable material in the cores. Had the sedimentary sequences been dated accurately time series analyses of the XRF profiles could have been tied to specific dates and temporal periodicities. The results of such analyses on high intertidal sequences could have significant implications for the understanding of the timing, cyclicity or periodicity of forcing factors such as the NAO, storminess or tidal cycles and their influence on marginal sedimentary coastal environments.

7.4. Conclusions

The present day definition of the vegetated high-intertidal sedimentary environments identified at Sandfield and Derryness have been determined as a range of machair, maritime grassland and saltmarsh. However it has been seen that high intertidal marginal habitats, co-located within the same estuary, may display significant morphological, ecological and sedimentological differences although their initial physical appearance is similar. These differences are highly influential in determining the resultant characteristics of the habitat. The clarification of habitat types should enable appropriate management techniques to be applied; however, it is also noted that these should be flexible to adapt to the natural morphological evolution of the sites.

The occurrence of individual storm events is considered to be the key driver of morphological change in these environments. Isolated extreme events may represent the tipping point resulting in the switch from one stable state to another. Subsequent storm events may not be as significant in effecting morphological change due to the geomorphological adjustments of the system. It is possible to link periods of morphological evolution here to periods of increased storminess in the northeast Atlantic region and analyses of the stratigraphy suggest primary forcing on a

multi-decadal timescale. However links to the North Atlantic Oscillation (NAO) are less clear. In addition to extreme storm events driving significant morphological change, more regular winter storm events are seen to impart distinctive layered bedding to the stratigraphy indicative of repeating, but independent, depositional sequences.

Within intertidal environments analysis of morphological and environmental change can often be restricted due to incomplete or poorly preserved environmental records. Therefore there is significant value in using a multi-proxy approach as has been shown in this study. Due to the sedimentary characteristics of the environments studied here, palaeo-ecological records are either not present or poorly preserved. However both XRF and sedimentology analyses can fill the gap left, both as direct indicators (e.g. quartz grain micro textures) and as proxies (e.g. bromine content as a proxy for organic content).

There is still some uncertainty associated with the timing of the evolution and the deposition rates of the sites investigated. This has meant that although the chronological sequence of events can be broadly determined linking them to explicit external forcing factors, with known timing and/or periodicity, can be difficult. However, supporting evidence from historical sources, i.e. maps and photographs, and geochemical analyses, i.e. carbonate content, are especially valuable and have helped elucidate and reduce the uncertainty of the dating results alone.

Scanning XRF can be a valuable tool in the examination of marginal intertidal sediment sequences. It can provide an additional line of evidence which, when combined with more traditional methods and dating information, can establish a more complete record of downcore changes. With appropriate chronological control, scanning XRF data can be explored through time series analysis. This may then enable direct links between sediment dynamics and forcing, such as sea level change, NAO and storminess, to be drawn.

This study provides a significant contribution to the hitherto relatively unstudied marginal paraglacial coastal environments of northwest Ireland. It has been shown that the main internal system controls on the formation of these environments are the deposition of aeolian sand during storm events and the subsequent deposition of more organic material associated with plant establishment. These alternations are clearly recorded in the layering of the sediment sequences. These sequences, therefore, provide a clear visual signal of the environmental history of the area. The external driving factor of this deposition would appear to be the variation in the storminess of the region. Individual storm events have been shown to result in significant morphological change events switching the marginal environments from one stable state to another. This greater understanding of the functioning of these environments in response to these factors will be of significant importance to potential future studies aiming to further the currently limited understanding of relative sea level change in this region. The geochronology analysis was only partly successful and this compromised the effectiveness of the single

spectrum analysis and the ability to attribute time periods and absolute dates to events identified in the cores. Significant contributions have also been made to the habitat classification of these marginal intertidal environments. Clearly further work needs to be done on the characteristics of Irish machair however confirming the presence of machair enables appropriate management strategies to be employed.

References

Allen, J.R.L. 1989. Evolution of salt-marsh cliffs in muddy and sandy systems: A qualative comparison of British west-coast estuaries. *Earth surface processes and landforms*, 14, 85-92.

Allen, J.R.L. 1997. Simulation models of salt-marsh morphodynamics: some implications for high-intertidal sediment couplets related to sea-level change. *Sedimentary Geology,* 113, 211-223.

Allen, J.R.L. 2000. Morphodynamics of Holocene salt marshes: A review sketch from the Atlantic and southern North Sea coasts of Europe. *Quaternary Science Reviews,* 19, 1155-1231.

Allen, J.R.L. 2004. Annual textural bending in Holocene estuarine silts, Severn Estuary Levels (SW Britain): patterns, cause and implications. *The Holocene*, 14 (4), 536-552.

Allen, J.R.L. and Duffy, M.J. 1998. Temporal ans spatial depositional patterns in the Severn Estuary, southwestern Britain; intertidal studes at spring-neap and seasonal scales, 1991-1993. *Marine Geology*, 146, 147-171.

Anfuso, G., Dominguez, L. and Garcia, F.J. 2007. Short and medium-term evolution of a coastal sector in Cadiz, SW Spain. *Catena*, 70, 229-242.

Angus, S. 1994, The conservation importance of the machair systems of the Scottish islands, with particular reference to the Outer Hebrides, *In:* J. M. Baxter & M. B. Usher, eds., *The islands of Scotland: a living marine hertiage*, Edinburgh: HMSO, pp. 95-120.

Angus, S. 2006, De tha machair? Towards a machair definition, *In:* S. Angus & W. Ritchie, eds., *Sand Dune Machair 4*, Aberdeen: Aberdeen Institute for Coastal Science & Management, pp. 7-22.

Angus, S. and Hansom, J.D. 2006. Tir a'mhachair, tir nan loch? Climate change senarios for Scottish machair systems: a wet future? *In:* S. Angus & W. Ritchie, eds., *Sand Dune Machair 4*, Aberdeen: Aberdeen Institute for Coastal Science & Management, pp. 29-36.

Ardelan, M.V. and Steinnes, E. 2010. Changes in mobility and solubility of the redox sensitive metals Fe, Mn and Co at the sewater-sediment interface following CO_2 seepage. *Biogeosciences*, 7, 569-583.

Arnaud-Fassetta, G., Bertrand, F., Costa, S. and Davidson, R. 2006. The western lagoon marshes of the Ria Formosa (Southern Portugal): Sediment-vegetation dynamics, long-term to short-term changes and perspective. *Continental Shelf Research*, 26, 363-384.

Arroyo, J. and Bolger, T. 2010. The mite (Arachnida: Acari) fauna inhabiting Irish machair: a European Union priority coastal habitat. *Journal of Coastal Conservation*, 15, 181-194.

Bacon, S. and Carter, D.J.T. 1991. Wave climate changes in the North Atlantic and North Sea. *International Journal of Climatology*, 11, 545-558.

Baldini, L.M., McDermott, F., Baldini, J.U.L., Fischer, M.J. and Möllhoff, M. 2010. An investigation of the controls on Irish precipitation $\delta^{18}O$ values on monthly and event timescales. *Climate Dynamics*, 35, 977-993.

Ballantyne, C.K. 2002a. Paraglacial geomorphology. *Quaternary Science Reviews*, 21, 1935-2017.

Ballantyne, C.K. 2002b. A general model of paraglacial landscape response. *The Holocene*, 12, 371-376.

Barndorff-Nielsen, O. 1977. Exponentially decreasing distributions for the logarithm of particle size. *Proceedings of the Royal Society A*, 353, 401-419.

Barndorff-Nielsen, O. And Christiansen, C. 1988. Erosion, deposition and size distributions of sand. *Proceedings of the Royal Society A*, 417, 335-352.

Barrett-Mold, C. and Burningham, H. 2010. Contrasting ecology of prograding coastal dunes on the northwest coast of Ireland. *Journal of Coastal Conservation*, 14, 81-90.

Barrett-Mold, C., Burningham, H. and French, J. R. Stratigraphic insights from sedimentary peels of littoral estuarine depositional systems. *Journal of Coastal Research*, SI56, 584-588.

Bassett, J.A. & Curtis, T.G.F. 1985. The Nature and Occurrence of Sand-Dune Machair in Ireland. *Proceedings of the Royal Irish Academy Section B-Biological Geological and Chemical Science*, 85, (1) 1-17.

Bateman, M.D. and Catt, J.A. 1996. An absolute chronology for the raised beach deposits at Sewerby, E. Yorkshire, UK. *Journal of Quaternary Science*, 11, 389-395.

Bateman, M.D., Frederick, C.D., Jaiswal, M.K. and Singhvi, A.K. 2003. Investigations into the potential effects of pedoturbation on luminescence dating. *Quaternary Science Reviews*, 22, 1169-1176.

Battarbee, R.W., Jones, V.J., Flower, R.J., Cameron, N.G., Bennion, H., Carvalho, L. and Juggins, S. 2001. Diatoms. *In:* Smol, J.P., Birks, H.J.B. and Last, W.M. 2001. *Tracking environmental change using lake sediments. Volume 3: Terrestrial, Algal, and Siliceous indicators*. Kluwer Academic Publishers, Dordrecht, The Netherlands pp 155-202.

Berendse, F., Lammerts, E.J. and Olff, H. 1998. Soil organic matter accumulation and its implications for nitrogen mineralization and plant species composition during succession in coastal dune slacks. *Plant ecology*, **137**, 71-78.

BirdLife International. 2007. *BirdLife's online World Bird Database: the site for bird conservation* Version 2.1. Cambridge, UK: BirdLife International. [http://www.birdlife.org/datazone/sites/index.html?action=SitHTMDetails.asp&sid=554&m=0#]. Accessed on 13/08/09.

Blackmore, R. and Reddish, A. 1996. *Global Environmental Issues*. Hodder and Stoughton, 354pp.

Blamely, M., Fitter, R. & Fitter, A. 2003. *The Wild Flowers of Britain and Ireland: The Complete Guide to the British and Irish Flora*. A & C Black, pp 512.

Blott, S.J. & Pye, K. 2001. GRADISTAT: a grain size distribution and statistics package for the analysis of unconsolidated sediments. *Earth Surface Processes and Landforms*, 26, 1237-1248.

Boggs, S. 1987. *Principles of Sedimentology and Stratigraphy*. Merril, pp 784.

Boning, P., Bard, E. and Rose, J. 2007. Toward direct, micron-scale XRF elemental maps and quantitative profiles of wet marine sediments. *Geochemistry, Geophysics, Geosystems*, 8, doi:10.1029/2006GC001480.

Boorman, L.A. 2003. *Saltmarsh Review. An overview of coastal saltmarshes, their dynamic and sensitivity characteristics for conservation and management*. JNCC Report No. 334, JNCC Peterborough.

Bouezmarni, M. and Wollast, R. 2005. Geochemical composition of sediments in the Scheldt estuary with emphasis on trace metals. *Hydrobiologia*, 540, 155-168.

Bowen, D.Q., Phillips, F.M., McCabe, A.M., Knutz, P.C. and Sykes G.A. 2002. New data for the Last Glacial Maximum in Great Britain and Ireland. *Quaternary Science Reviews*, 21, 89-101.

Boyle, J.F. 2000. Rapid elemental analysis of sediment samples by isotope source XRF. *Journal of Paleolimnology* 23, 213–221.

Brayshay, B.A., Gilbertson, D.D., Kent, M., Edwards, K.J., Wathern, P. and Weaver, R.E. 2000. Surface pollen-vegetation relationships on the Atlantic seaboard: South Uist, Scotland. *Journal of Biogeography*, 27, 359-378.

Brooks, A.J., Bradley, S.L., Edwards, R.J., Milne, G.A., Horton, B. and Shennan, I. 2008, Postglacial relative sea level observations from Ireland and their role in glacial rebound modelling. *Journal of Quaternary Science*, 23(2), 175-192.

Brown, S.L., Warman, E.A., McGrorty, S., Yates, M., Pakeman, R.J., Boorman, L.A., Goss-Custard, J.D. and Gray, A.J. 1998. Sediment influxes in intertidal biotopes: BIOTA II. *Marine Pollution Bulletin*, 37, 173-181.

Bui, E.N., Mazullo, J. and Wilding, L.P. 1990. Using quartz grain size and shape analysis to distinguish between aeolian and fluvial deposits in the Dallol Bosso of Niger (West Africa). *Earth Surface Processes and Landforms*, 14, 157-166.

Buller, A.T. and McManus, J. 1972. Simple metric sedimentary statistics used to recognize different environments. *Sedimentology*, 18, 1-100.

Burger, J.A.; Klein, G. De V., and Sanders, J.E., 1969. A field technique for making epoxy relief-peels in sandy sediments saturated with saltwater. *Journal of Sedimentary Research*. 39 (1), 338-341.

Burningham, H. 2002. Meso-scale morphological changes in the Loughros More estuary. *Proceedings of Littoral 2002: The Changing Coast*, 3, 265-270.

Burningham, H. 2005, Morphodynamic Behaviour of a High-Energy Coastal Inlet: Loughros Beg, Donegal, Ireland. *In:* Fitzgerald, D.M. and Knight, J. 2005. *High Resolution Morphodynamics and Sedimentary Evolution of Estuaries*. Springer pp. 215-242.

Burningham, H. 2008. Contrasting geomorphic response to structural control: The Loughros estuaries, northwest Ireland. *Geomorphology*, 97, 300-320.

Burningham, H. & Cooper, J.A.G. 2003. Morphology and historical evolution of north-east Atlantic coastal deposits: the west Donegal estuaries, north-west Ireland. *Journal of Coastal Research*, SI 41, 148-159.

Buringham, H. and French, J. 2013. Is the NAO winter index a reliable proxy for wind climate and storminess in northwest Europe? *International Journal of Climatology*, doi: 10.1002/joc.3571

Cahoon, D.R., French, J.R., Spencer, T., Reed, D. and Moller, I. 2000. Vertical accretion verus elevation adjustment in UK saltmarshes: an evaluation of alternative methodologies. *Coastal and estuarine environments: Sedimentology, geomorphology and geoarchaeology*, Geological society special publication, 175, pp 223-238.

Callaway, J.C., DeLaune, R.D. and Patrick, Jr, W.H. 1996. Chernobyl ^{137}Cs used to determine sediment accretion rates at selected northern European coastal wetlands. *Limnology and Oceanography*, 41 (3), 444-450.

Campbell, J.R. 2003. Limitations in the laser particle sizing of soils. In: Roach, I.C. (ed) 2003. *Advances in Regolith*, pp 38-42.

Cardoso, R., Araujo, M.F., Freitas, M.C. and Fatela, F. 2008. Geochemical characterisation of sediments from marginal environments of Lima Estuary (NW Portugal). *e-Terra* Geosciences Online Journal, 5, http://e-terra.geopor.pt/artigos/cong_geoq/cardoso.pdf .

Carter, R.W.G. 1991. Near-future sea level impacts on coastal dune landscapes. *Landscape Ecology*, 6, 29-39.

Carter, R.W.G., Devoy, R.J.N. and Shaw, J. 1989. Late Holocene sea levels in Ireland. *Journal of Quaternary Science*, 4 (1), 7-24.

Carter, R.W.G., Orford, J.D., Forbes, D.L. and Taylor, R.B. 1990. Morphosedimentary development of drumlin-flank barriers with rapidly rising sea level, Story Head, Nova Scotia. *Sedimentary Geology*, 69, 117-138.

Chao, R.B., Casais, M.C., Cortizas, A.M., Alberti, A.P. and Paz, M.V. 2002. Holocene evolution on Galician coast (NW Spain): an example of paraglacial dynamics. *Quaternary International*, 93-94, 149-159.

Chanton, J.P., Martens, C.S. and Kipphut, G.W. 1983. Lead-210 sediment geochronology in a changing coastal environment. *Geochimica et Cosmochimica Acta*, 47, 1791-1804.

Chmura, G.L., Helmer, L.L., Beecher, C.B. and Sutherland, E.M. 2001. Historical rates of salt marsh accretion on the outer Bay of Fundy. *Canadian Journal of Earth Sciences*, 38, 1081-1092.

Chayes, F. 1971. Ratio *Correlation: A Manual for Students of Petrology and Geochemistry*. University of Chicago Press, pp 99.

Clark, P.U., McCabe, A.M., Mix, A.C. and Weaver, A.J. 2004. Rapid rise of sea level 19,000 years ago and its global implications. *Science*, 304, 1141-1144.

Clarke, M.L. and Rendell, H.M. 2006. Effects of storminess, sand supply and the North Atlantic Oscillation on sand invasion and coastal dune accretion in Western Portugal. *The Holocene*, 16, 341-355.

Coch, N.K. and Krinsley, D.H. 1971. Comparison of Stratigraphic and Electron Microscopic Studies in Virginia Pleistocene Coastal Sediments. *The Journal of Geology*, 79 (4), 426-437.

Cooper, A., McCann, T., & Ballard, E. 2005. The effects of livestock grazing and recreation on Irish machair grassland vegetation. *Plant Ecology*, 181, (2) 255-267.

Cooper, J.A.G., Jackson, D.W.T., Dawson, A.G., Dawson, S., Bates, C.R. and Ritchie, W. 2012. Barrier islands on bedrock: A new landform type demonstrationg the role of antecedent topography on barrier form and evolution. *Geology*, 40 (10), 923-926.

Cooper, J.A.G., McKenna, J., Jackson, D.W.T. and O'Connor, M. 2007. Mesoscale coastal behavior related to morphological self-adjustment. *Geology*, 35 (1), 187-190.

Coughenour, C.L., Archer, A. W. and Lacovara, K.J. 2009. Tides, tidalites, and secular changes in the Earth-Moon system. *Earth Science Reviews*, 97, 59-79.

Cundy A.B., Croudace I.W., Cearreta A. and Irabien M.J. 2003. Reconstructing historical trends in metal input in heavily-disturbed, contaminated estuaries: studies from Bilbao, Southampton Water and Sicily. *Applied Geochemistry*, 18, 311-325.

Cundy, A.B. and Croudace, I.W. 1996. Sediment accumulation and recent sea-level rise in the Solent, southern England: Inferences from radiometric and geochemical studies. *Estuarine, Coastal and Shelf Science*, 43, 449-467.

Curray, J.R. 1964. Transgressions and regressions. *In*: Miller, R.L. eds. 1964. *Papers in Marine Geology, Shepard Commemorative Volume*. Macmillian, New York, pp 175-203.

Curtis, T.G.F. and Sheehy Skeffington, M.J. 1998. The salt marshes of Ireland: An inventory and account of their geographical variation. *Proceedings of the Royal Irish Academy: Biology and Environment*, 98B (2), 87-104.

Daskalakis, K.D. and O'Connor, T.P. 1995. Normalization and elemental sediment contamination in the coastal United States. *Environmental Science and Technology*, 29, 470-477.

Davis, R. and Fitzgerald, D. 2004. *Beaches and Coasts*. Blackwell Science, pp 419.

Davis, R.A. and Hayes, M.O. 1984. What is a wave-dominated coast? *Marine Geology*, 60, 313-329.

Dawson, A., Elliott, L., Noone, S., Hickey, K., Holt, T., Wadhams, P. and Foster, I. 2004. Historical storminess and climate 'see-saws' in the North Atlantic region. *Marine Geology*, 210, 247-259.

Dawson, A.G., Hickey, K., Holt, T., Elliott, L., Dawson, S., Foster, I.D.L., Wadhams, P., Jonsdttir, I., Wilkinson, J., McKenna, J., Davis, N.R. and Smith, D.E. 2002. Complex North Atlantic Oscillation (NAO) Index signal of historic North Atlantic storm-track changes. *The Holocene*, 12, 363-369.

Dawson, A.G., Hickey, K., Mayewski, P.A. and Nesje, A. 2007. Greenland (GISP2) ice core and historical indicators of complex North Atlantic climate changes during the fourteenth century. *The Holocene*, 17 (4), 427-434.

De Boer, P.L. and Alexandre, J.T. 2012. Orbitally forced sedimentary rhythms in the stratigraphic record: is there room for tidal forcing? *Sedimentology*, 59, 379-392.

Dech, J.P., Maun, M.A. and Pazner, M.I. 2005. Blowout dynamics on Lake Huron sand dune: analysis of digital multispectral data from colour air photos. *Catena*, **60**, 165-180.

Deer, W.A., Howie, R.A. and Zussman, J. 1992. *An Introduction to the rock forming minerals (2nd edition)*. Prentice Hall, pp 696.

Delaney, C. and Devoy, R. 1995. Evidence from sites in Western Ireland of late Holocene changes in coastal environments. *Marine Geology*, 124, 273-287.

Denys, L. 1994. Diatom assemblages along a former intertidal gradient: A palaeoecological study of a subboreal clay layer (Western coastal plain, Belgium). *Netherlands Journal of Aquatic Ecology*, 28 (1), 85-96.

Devoy, R.J.N. 2008. Coastal Vulnerability and the Implications of Sea-Level Rise for Ireland. *Journal of Coastal Research*, 24, (2), 325-341.

Duffy, M.J. and Devoy, R.J.N. 1999. Contemporary process controls on the evolution of sedimentary coasts under low to high energy regimes: western Ireland. *Geologie en Mijnbouw*, 77, 333-349.

Edwards, K.J., Whittington, G. and Ritchie, W. 2005. The possible role of humans in the early stages of machair evolution: palaeoenvironmental investigations in the Outer Hebrides, Scotland. *Journal of Archaeological Science*, 32, 435-449.

Eliot, M. 2012. Sea level variability influencing coastal flooding in the Swan River region, Western Australia. *Continental Shelf Research*, 33, 14-28.

Emery, N.C., Ewanchuk, P.J. and Bertness, M.D. 2001. Competition and salt-marsh zonation: stress tolerators may be dominant competitors. *Ecology*, 82 (9), 2471-2485.

European Commission. 1979. *Council directive 79/409/EEC on the conservation of Wild Birds*. EC. Brussels.

European Commission. 1992. *Council directive 92/43/EEC on the conservation of natural habitats and of wild fauna and flora*. EC. Brussels.

European Environment Agency. 2010. Sheskinmore Lough SPA Natura 2000 factsheet. http://eunis.eea.europa.eu/sites/IE0004090/general. accessed on 2/09/2011.

Fagel, N., Boës, X and Loutre, M.F. 2008. Climate oscillations evidenced by spectral analysis of Southern Chilean lacustrine sediments: the assessment of ENSO over the last 600 years. *Journal of Palaeoliminology*, 39, 253-266.

Fieller, N.R.J., Flenley, E.C. and Olbricht, W. 1992. Statistics of particle size data. *Applied Statistics*, 41 (1), 127-146.

Fitter, R., Fitter, A. and Farrer, A. 1984. *Grasses, Sedges, Rushes and Ferns of Britain and Northern Europe*. Collins, 256pp.

Fitzgerald, D.M. and van Heteren, S. 1999. Classification of paraglacial barrier systems: coastal New England, USA. *Sedimentology*, 46, 1083-1108.

Folk, R.L. and Ward, W.C. 1957. Brazos River bar: a study in the significance of grain size parameters. *Journal of Sedimentary Petrology*, 27, 3-26.

Forbes, D.L., Orford, J.D., Carter, R.W.G., Shaw, J. and Jennings, S.C. 1995. Morphodynamic evolution, self-organisation, and instability of coarse-clastic barriers on paraglacial coasts. *Marine Geology*, 126, 63-85.

Forbes, D.L. and Syvitski, J.P.M., 1994. Paraglacial coasts. *In*: Carter, R.W.G., and Woodroffe, C.D. eds., *Coastal Evolution. Late Quaternary Shoreline Morphodynamics*. Cambridge University Press, Cambridge, pp. 373–424.

Fossitt, J.A. 1994. Late-glacial and Holocene vegetation history of western Donegal, Ireland. *Proceedings of the Royal Irish Academy: Biology and Environment*, 94B, 1-31.

Foster, I.D.L., Mighall, T.M., Proffitt, H., Walling, D.E. and Owens P.N. 2006. Post-depositional ^{137}Cs mobility in the sediments of three shallow coastal lagoons, SW England. *Journal of Paleolimnology*, 35, 881-895.

French, J. 2006. Tidal marsh sedimentation and resilience to environmental change: Exploratory modelling of tidal sea-level and sediment supply forcing in predominantly allochthonous systems. *Marine Geology*, 235, 119-136.

French, J.R., Spencer, T., Murray, A.L. and Arnold, N.S. 1995. Geostatistical analysis of sediment deposition in two small tidal wetalnds, Norfolk, U.K. *Journal of Coastal Research*, 11(2), 308-321.

French, P.W., Allen, J.R.L. and Appleby, P.G. 1994. 210-Lead dating of a modern period saltmarsh deposit from the Severn Estuary (Southwest Britain), and its implications. *Marine Geology*, 118, 327-334.

Freund, H., Gerdes, G., Streif, H., Dellwig, O. and Watermann, F. 2004. The indicative meaning of diatoms, pollen and botanical macro fossils for reconstruction of palaeoenvironments and sea-level fluctuations along the coast of Lower Saxony; Germany. *Quaternary International*, 112, 71-87.

Friendly, M. 2002. Corrgrams. *The American Statistician*, 56 (4), 316-324.

Galbraith, R.F. and Green, P.F. 1990. Estimating the component ages in a finite mixture. *Radiation Measurements*, 17,197-206.

Gallagher, K.A., Wheeler, A.J. and Orford, J.D. 1996. An assessment of the heavy metal pollution of two tidal marshes on the north-west coast of Ireland. *Proceedings of the Royal Irish Academy: Biology and Environment*, 96B (3), 177-188.

Gao, S. and Collins, M. 1992. Net sediment transport patterns inferred from grain-size trends, based upon defintion of "transport vectors". *Sedimentary Geology*, 80, 47-60.

Gaynor, K. 2006. The vegetation of Irish machair. *Biology and Environment*, 106B, (3) 311-321.

Gerritse, R.G. and George, R.J. 1988. The role of soil organic matter in the geochemical cycling of chloride and bromide. *Journal of Hydrology*, 101, 83-95.

Gilbertson, D. D., Kent, M., Schwenninger, J. L., Wathern, P. A., & Brayshay, B. A. 1995, The Machair vegetation of South Uist and Barra in the Outer Hebrides of Scotland: its interacting ecological geomorphic and historical dimensions, *In:* R. A. Butlin & N. Roberts, eds., *Ecological relations in historical times: Human impact and adaption*, Oxford: Blackwell, pp. 17-44.

Gilbertson, D.D., Schwenninger, J.L., Kemp, R.A., & Rhodes, E.J. 1999. Sand-drift and soil formation along an exposed North Atlantic coastline: 14,000 years of diverse geomorphological, climatic and human impacts. *Journal of Archaeological Science*, 26, (4) 439-469.

Gimingham, C.H. 1974. Plant communities of the machair and floristic relationships with non-dune vegetation. *In*: Ranwell, D.S. 1974. *Sand Dune Machair*. NERC Institute of Terrestrial Ecology, London, pp13-14.

Goldberg, P.S., 1974. Sediment peels from prehistoric sites. *Journal of Field Archaeology*. 1 (3/4), 323-328.

Goodman, J.E., Wood, M.E. and Gehrels, W.R. 2007. A 17-yr ercord of sediment accretion in the salt marshes of Maine (USA). *Marine Geology*, 242, 109-121.

Greaver, T.L. and Sternberg, L.L. 2006. Fluctuating deposition of ocean water drives plant function on coastal sand dunes. *Global Change Biology*, **12**, 1-8.

Grootjans, A.P., Adema, E.B., Bekker, R.M. and Lammerts, E.J. 2004. Why young coastal dune slacks sustain a high biodiversity. *In:* Martinez, M.L. and Psuty, N.P. (Eds). 2004. *Coastal Dunes, Ecology and Conservation*. Springer-Verlag Berlin Heidelberg.

Grunewald, R. and Schubert, H. 2007. The definition of a new plant diversity index "H'_{dune}" for assessing human damage on coastal dunes – Derived from the Shannon index of entropy *H'*. *Ecological Indicators*, **7**, 1-21.

Gupta, B.K. 2002. *Modern Foraminifera*. Springer, pp 384.

Hansom, J.D. & Angus, S. 2005. Machair nan Eilean Siar (Machair of the Western Isles). *Scottish Geographical Journal*, 121, (4) 401-411.

Hanna, E., Cappelen, J., Allan, R., Jonsson, T., Le Blanco, F., Lillington, T. and Hickey, K. 2008. New insights into North European and North Atlantic surface pressure variability, storminess, and related climatic change since 1830. *Journal of Climate*, 21, 6739-6766.

Hartmann, D. and Christiansen, C. 1992. The hyperbolic shape triangle as a tool for discriminating populations of sediment samples of closely connected origin. *Sedimentology*, 39, 697-708.

Harvey, M.M., Hansom, J.D. and MacKenzie, A.B. 2007. Constraints on the use of anthropogenic radionuclide-derived chronologies for saltmarsh sediments. *Journal of Environmental Radioactivity*, 95, 126-148.

Hassani, H. 2007. Singular spectrum analysis: Methodology and comparison. *Journal of Data Science*, 5, 239-257.

Hayes, M.O. 1979. Barrier island morphology as a function of tidal and wave regime. *In:* Leatherman, S.P. eds. *Barrier islands from the Gulf of St. Lawrence to the Gulf of Mexico*, Academic Press, New York, pp 1-27.

Hemphill-Haley, E. 1995. Intertidal diatoms from Willapa Bay, Washington: Application to studies of small-scale sea-level changes. *Northwest Science*, 69, 29-45.

Hendey, N.I. 1964. *An Introductory Account of the Smaller Algae of British Coastal Waters. Part V: Bacillariophyceae*. Ministry of Agriculture, Fisheries and Food, Fishery Investigations Series IV, HMSO, London pp 317.

Hesp, P. 2002. Foredunes and blowouts: initiation, geomorphology and dynamics. *Geomorphology*, 48, 245-268.

Hickey, K.R. 2003. The storminess record from Armagh Observatory, Northern Ireland, 1796-1999. *Weather*, 58, 28-25.

Hill, M.O. 1996. *TABLEFIT version 1.0, for identification of vegetation types*. Huntington: Institute of Terrestrial Ecology.

Hobson, R.D. 1979. *Definition and use of the phi grade scale*. US Army Corps of Engineers pp18.

Houser, C., Hapke, C. and Hamilton, S. 2008. Controls on coastal dune morphology, shoreline erosion and barrier island response to extreme storms. *Geomorphology*, 100, 223-240.

Hurrell, J.W. 1995. Decadal trends in the North Atlantic Oscillation: Regional temperatures and precipitation. *Science*, 269, 676-679.

Inman, D.L. and Nordstrom, C.E. 1971. On the tectonic and morphological classification of coasts. *Journal of Geology*, 79, 1-21.

IPCC. 2007. *Climate Change 2007: The Physical Science Basis. Summary for Policymakers*. IPCC, Geneva.

Jackson, N.L. and Nordstrom, K.F. 2011. Aeolian sediment transport and landforms in managed coastal systems: A review. *Aeolian Research*, 3, 181-196.

Jansen, J.H.F., Van der Gaast, S.J., Koster, B., & Vaars, A.J. 1998. CORTEX, a shipboard XRF-scanner for element analyses in split sediment cores. *Marine geology*, 151, (1-4) 143-153.

Julia, O. and Vives-Rego, J. 2008. A microbiology application of the skew-Laplace distribution. *SORT*, 32(2), 141-150.

Keddy, P.A. 2000. *Wetland Ecology. Principles and Conservation*. Cambridge University Press, pp 614.

Kent, M., Owen, N.W. and Dale, M.P. 2005. Photosynthetic responses of plant communities to sand burial on the machair dune systems of the Outer Hebrides, Scotland. *Annals of Botany*, 95, 869-877.

Keough, J.R., Thompson, T.A., Guntenspergen, G.R. and Wilcox, D.A. 1999. Hydrogeomorphic factors and ecosystems in coastal wetlands of the Great Lakes. *Wetlands*, 19, 821-834.

Kidwell, S.M.; Moore, J.A., and Moore, J.R., 1985. Inexpensive field technique for polyester resin peels of structures in unconsolidated sediments. *Marine Geology*. 64, 351-359.

King, T.J. 1989. *Ecology*. Nelson, pp 181.

Kirchner, G. and Ehlers, H. 1998. Sediment geochronology in changing coastal environments: Potentials and limitations of the ^{137}Cs and ^{210}Pb methods. *Journal of Coastal Research*, 14 (2), 483-492.

Kirwan, M. and Temmerman, S. 2009. Coastal marsh response to historical and future sea-level acceleration. *Quaternary Science Reviews*, 28, 1801-1808.

Knox, A.J. 1974. Agricultural use of machair. *In*: Ranwell, D.S. 1974. *Sand Dune Machair*. NERC Institute of Terrestrial Ecology, London, pg 19.

Komar, P.D. 1998. *Beach Processes and Sedimentation, second edition*. Prentice Hall, pp 544.

Krammer, K. and Lange-Bertalot, H. 1986. Bacillariophyceae. 1. Teil. In Süsswasserflora von Mitteleropa 2/1. In Ettl, H., Gerloff, J., Heynig, H. and Mollenhauer, D. (eds), Fischer Verlag, G., Stuttgart: 876 pp.

Krammer, K. and Lange-Bertalot, H. 1988. Bacillariophyceae. 2. Teil. In Süsswasserflora von Mitteleropa 2/2. In Ettl, H., Gerloff, J., Heynig, H. and Mollenhauer, D. (eds), Fischer Verlag, G., Stuttgart: 596 pp.

Krammer, K. and Lange-Bertalot, H. 1991a. Bacillariophyceae. 3. Teil. In Süsswasserflora von Mitteleropa 2/3. In Ettl, H., Gerloff, J., Heynig, H. and Mollenhauer, D. (eds), Fischer Verlag, G., Stuttgart: 576 pp.

Krammer, K. and Lange-Bertalot, H. 1991b. Bacillariophyceae. 4. Teil. In Süsswasserflora von Mitteleropa 2/4. In Ettl, H., Gerloff, J., Heynig, H. and Mollenhauer, D. (eds), Fischer Verlag, G., Stuttgart: 437 pp.

Krinsley, D.H. and Donahue, J. 1968. Environmental interpretation of sand grain surface textures by electron microscopy. *Geological Society of America Bulletin*, 79, 743-748.

Krinsley, D.H. and Funnell, B.M. 1965. Environmental histroy of quartz sand grains from the Lower and Middle Pleistocene of Norfolk, England. *Quarterly Journal of the Geological Society*, 121, 435-456.

Krinsley, D.H. and Takahashi, T. 1962a. Surface textures of sand grains: an application of electron microscopy. *Science*, 135, 923-925.

Krinsley, D.H. and Takahashi, T. 1962b. Surface textures of sand grains – an application of electron microscopy: glaciation. *Science*, 138, 1262-1264.

Krinsley, D.H. and Takahashi, T. 1964. A technique for the study of surface textures of sand grains with electron microscopy. *Journal of Sedimentary Petrology*, 34, 423-426.

Krinsley, D.H., Takahashi, T., Silberman, M.L. and Newman, W.S. 1964. Transportation of sand grains along the Atlantic shore of Long Island, New York: an application of electron microscopy. *Marine Geology*, 2 100-120.

Łabuz, T.A. 2005. Present-day dune environment dynamics on the coast of the Swina Gate Sandbar (Polish West coast). *Estuarine, Coastal and Shelf Science*, 62, 507-520.

Lambeck, K. 1996. Glaciation and sea level change for Ireland and the Irish Sea since late Devensian/Midlandian times. *Journal of the Geological Society, London*, 153, 853-872.

Long, A.J.; Innes, J.B.; Shennan, I., and Tooley, M.J., 1999. Coastal stratigraphy: A case study from Johns River, Washington, U.S.A. *In:* Jones, A.P.; Tucker, M.E., and Hart, J.K. (eds), 1999. *The description and analysis of quaternary stratigraphic field sections*. Technical guide 7. Quaternary Research Association, London, pp. 267-286.

Lozano, I., Devoy, R.J.N., May, W. and Andersen, U. 2004. Storminess and vulnerability along the Atlantic coastlines of Europe: analysis of storm records and of a greenhouse gases induced climate scenario. *Marine Geology*, 210, 205-225.

MacClenahan, P., McKenna, J., Cooper, J.A.G. and O'Kane, B. 2001. Identification of the highest magnitude coastal storm events over western Ireland on the basis of wind speed and duration thresholds. *International Journal of Climatology*, 21, 829-842.

Madhavaraju, J., García y Barragán, J.C., Hussain, S.M., and Mohan, S.P. 2009. Microtextures on quartz grains in the beach sediments of Puerto Peñasco and Bahia Kino, Gulf of California, Sonora, Mexico. *Revista Mexicana de Ciencias Geológicas*, 26 (2), 367-379.

Madsen, A.T., Murray, A.S., Andersen, T.J. Pejrup, M. And Breuning-Madsen, H. 2005. Optically stimulated luminsense dating of young estuarine sediments: a comparison with ^{210}Pb and ^{137}Cs dating. *Marine Geology*, 214, 251-268.

Margolis S.V. and Krinsley, D.H. 1971. Submicroscopic frosting on eolian and subaquaeous quartz sand grains. *Geological Society of America Bulletin*, 82, 3395-3406.

Marion, C., Anthony, E.J. and Trentesaux, A. 2009. Short-term (≤2 yrs) estuarine mudflat and saltmarsh sedimentation: High-resolution data from ultrasonic altimetry, rod surface-elevation table, and filter traps. *Estuarine, Coastal and Shelf Science*, 83, 475-484.

Mate, I.D. 1992. The Theoretical Development of Machair in the Hebrides. *Scottish Geographical Magazine*, 108, (1) 35-38.

Maun, M.A. 1998. Adaptations of plants to burial in coastal sand dunes. *Canadian Journal of Botany*, 76 (5), 713-738.

Mazda, Y., Magi, M., Ikeda, Y., Kurokawa, T. and Asano, T. 2006. Wave reduction in a mangrove forest dominated by *Sonneratia* sp. *Wetlands Ecology and Management*, 14, 365-378.

Mazumder, R. and Arima, M. 2005. Tidal rhythmites and their implications. Earth-Science Reviews, 69, 70-95.

McCabe, A.M., Clark, P.U., and Clark, J. 2007. Radiocarbon constraints on the history of the western Irish ice sheet prior to the Last Glacial Maximum. *Geology*, 35 (2), 147-150.

McCorry, M. and Ryle, T. 2009. *Saltmarsh monitoring project*. Report for National Parks and Wildlife Service.

McLaren, P. 1981. An interpretation of trends in grain size measurements. *Journal of Sedimentary Petrology*, 51, 611-624.

McLaren, P. and Bowles, D. 1985. The effects of sediment transport on grain-size distributions. *Journal of Sedimentary Petrology*, 55 (4), 457-470.

Meeker, L.D. and Mayewski, P.A. 2002. A 1400-year high-resolution record of atmospheric circulation over the North Atlantic and Asia. *The Holocene*, 12, 257-266.

Mercier, D. 2008a. Paraglacial geomorphology: Conceptual and methodological revival. *Géomorphologie : relief, processus, environnement, 4, 219-222.*

Mercier, D. 2008b. Paraglacial and paraperiglacial landsystems: concepts, temporal scales and spatial distribution. *Géomorphologie : relief, processus, environnement, 4, 223-233.*

Milan, C.S., Swenson, E.M., Turner, R.E. and Lee, J.M. 1995. Assessment of the ^{137}Cs method for estimating sediment accumulation rates: Louisiana Salt Marshes. *Journal of Coastal Research*, 11, 296-307.

Mitsch, W.J. and Gosselink, J.G. 1993. *Wetlands (Second Edition).* Van Nostrand Reinhold, New York, pp 154.

Möller, I., Spencer, T., French, J.R., Leggett, D.J. and Dixon, M. 1999. Wave transformation over salt marshes: A field and numerical modelling study from north Norfolk, England. *Estuarine, Coastal and Shelf Science*, 49, 411-426.

Moreno-Casasola, P. 1986. Sand movement as a factor in the distribution of plant communities in a coastal dune system. *Vegetatio*, 65, 67-76.

Murray, A.S. and Olley, J.M. 2002. Precision and accuracy in the optically stimulated luminescence dating of sedimentary quartz: A status review. *Geochronometria*, 21, 1-16.

Murray, A.S. and Wintle, A.G. 2000. Luminescence dating of quartz using an improved single-aliquot regenerative-dose protocol. *Radiation Measurements* 32, 57-73.

Murray, A.S. and Wintle, A.G. 2003. The single aliquot regenerative dose protocol: potential for improvements in reliability. *Radiation Measurements* 37: 377-381.

National Parks and Wildlife Service. 2005. *West of Ardara/Maas Road SAC Site synposis*. [http://www.npws.ie/en/media/Media,3889,en.pdf]. Accessed on 13/08/09.

National Parks and Wildlife Service. 2011. *Sheskinmore Lough Management Plan*.

Nelson, A.R. and Kashima, K. 1993. Diatom zonation in southern Oregon tidal marshes relative to vascular plants, foraminifera, and sea level. *Journal of Coastal Research*, 9 (3), 673-697.

Neumeier, U. and Amos, C.L. 2006. The influence of vegetation on turbulence and flow velocities in European salt-marshes. *Sedimentology*, 53, 259-277.

O'Brien, L; Dudley, J.M. and Dias, F. 2013. Extreme wave events in Ireland: 14 680 BP – 2012. *Natural Hazards and Earth System Sciences*, 13, 625-648.

Oost, A.P., de Haas, H., Ijensen, F., van den Boogert, J.M. and de Boer, P.L. 1993. The 18.6yr nodal cycle and its impact on tidal sedimentation. *Sedimentary Geology*, 87, 1-11.

Orford, J.D., Murdy, J. and Freel, R. 2006. Developing constraints on the relative sea-level curve for the north-east of Ireland from the mid-Holocene to the present day. *Philosophical Transactions of the Royal Society A*, 364, 857-866.

OSi (2013) Irish Grid Reference System http://www.osi.ie/Services/GPS-Services/Reference-Information/Irish-Grid-Reference-System.aspx

Owen, N.W., Kent, M. and Dale, M.P. 2001. Spatial and temporal variability in seed dynamics of machair sand dune plant communities, the Outer Hebrides, Scotland. *Journal of Biogeography*, 28, 565-588.

Owen, N.W., Kent, M. and Dale, M.P. 2004. Plant species and community responses to sand burial on the machair of the Outer Hebrides, Scotland. *Journal of Vegetation Science*, 15, 669-678.

Pacheco, A., Vila-Concejo, A., Ferreira, O. and Dias, J.A. 2008. Assessment of tidal inlet evolution and stability using sediment budget computations and hydraulic parameter analysis. *Marine Geology*, 247, 104-127.

Palike, H., Shackleton, N.J., & Rohl, U. 2001. Astronomical forcing in Late Eocene marine sediments. *Earth and Planetary Science Letters*, 193 (3-4), 589-602.

Pennings, S.C. and Callaway, R.M. 1992. Salt marsh plant zonation: the relative importance of competition and physical factors. *Ecology*, 73 (2), 681-690.

Pethick, J. 2001. Coastal management and sea-level rise. *Catena*. 42. 307-322.

Phillips, J.D. 2009. Landscape evolution space and the relative importance of geomorphic processes and controls. *Geomorphology*, 109, 79-85.

Pirrie, D., Camm, G.S., Sear, L.G., & Hughes, S.H. 1997. Mineralogical and geochemical signature of mine waste contamination, Tresillian River, Fal Estuary, Cornwall, UK. *Environmental Geology*, 29 (1), 58-65.

Pitcher, W.S. and Berger, A.R. 1972. *The Geology of Donegal: A Study of Granite Emplacement and Unroofing*. Wiley-Interscience, pp 435.

Plater, A.J. and Shennan, I. 1992. Evidence of Holocene sea-level change from the Northumberland coast, eastern England. *Proceedings of the Geologists Association*, 103, 201-216.

Plater, A.J., Stupples, P. and Roberts, H.M. 2009. Evidence of episodic coastal change during the Late Holocene: The Dungeness barrier complex, SE England. *Geomorphology*, 104, 47-58.

Primpas, I., Karydis, M. and Tsirtsis, G. 2008. Assessment of clustering algorithms in discriminating eutrophic levels in coastal waters. *Global NEST Journal*, 10, 359-365.

Rae, J.E. 1989. Copper, lead and zinc in salt marsh sediments of the Severn Estuary, UK: The potential for their early diagnetic mobility. *Environmental Geochemistry and Health*, 11 (3), 121-126.

Raven, J.A. and Scrimgeour, C.M. 1997. The influence of anoxia on plants of saline habitats with special reference to the sulphur cycle. *Annals of Botany*, 79, 79-86.

Reed, D.J. 2002. Sea-level rise and coastal marsh sustainability: geological and ecological factors in the Mississippi delta plain. *Geomorphology*, 48, 233-243.

Reed, D.J., Spencer, T., Murray, A.L., French, J.R. and Leonard, L. 1999. Marsh surface sediment deposition and the role of tidal creeks: Implications for created and managed coastal marshes. *Journal of Coastal Conservation*, 5, 81-90.

Rhodes, E.J. 2011. Optically stimualted luminesense dating of sediments over the past 200,000 years. *Annual Review of Earth and Planetary Sciences*, 39, 461-488.

Richards, J.A., Mokrech, M., Berry, P.M. and Nicholls, R.J. 2008. Regional assessment of climate change impacts on coastal and fluvial ecosystems and the scope for adaptation. *Climate Change*, 90, 141-167.

Ritchie, W. 1976. The meaning and definition of machair. *Transactions of the Botanical Society of Edinburgh*, 42, 431-440.

Ritchie, W. 1979. Machair development and chronology in the Uists and adjacent islands. *Proceedings of the Royal Society of Edinburgh*, 77, (B) 107-122

Ritchie, W. 2006, Historical changes in the water table and drainage in the machair of the Uists - An introduction, *In:* S. Angus & W. Ritchie, (eds.), *Sand Dune Machair 4,* Aberdeen: Aberdeen Institute for Coastal Science & Management, pp. 23-28.

Ritchie, W. and Mather, A.S. 1974. The machair landform and its regional variation. *In*: Randwell, D.S. (ed.), *Sand Dune Machair*. NERC Insitute of Terrestrial Ecology, London, pp. 6-7.

Ritchie, W., Whittington, G. and Edwards, K.J. 2001. Holocene changes in the physiography and vegetation of the Atlantic littoral of the Uists, Outer Hebrides, Scotland. *Transactions of the Royal Society of Edinburgh, Earth Sciences*, 92, 121-136.

Robbins J.A. 1978. Geochemical and geophysical applications of radioactive lead. *In:* Nriagu J.O. (Ed). 1978. *The Biogeochemistry of Lead in the Environment Part A*. Elsevier/North Holland Biomedical Press, pp 285-293.

Robson, D., Fieller, N. and Stillman, E. 1997. *Shefsize*.

Rodwell, J.S. (ed) 2000. *British plant communities. Volume 5. Maritime communities and vegetation of open habitats*. Cambridge University Press.

Roe, H.M., Doherty, C.T., Patterson, R.T. and Swindles, G.T. 2009. Contemporary distributions of saltmarsh diatoms in the Seymour-Belize Inlet Complex, British Columbia, Canada: Implications for studies of sea-level change. *Marine Micropaleontology*, 70, 134-150.

Roman, C.T., Peck, J.A., Allen, J.R., King, J.W. and Appleby, P.G. 1997. Accretion of a New England (U.S.A.) salt marsh in response to inlet migration, storms, and sea-level rise. *Estuarine, Coastal and Shelf Science*, 45, 717-727.

Rose, F. 1981. *The Wild Flower Key: A Guide to Plant Identification in the Field*. Frederick Warne, 480pp.

Rothwell, R. G., Hoogakker, B., Thomson, J., Croudace, I. W., & Frenz, M. 2006, Turbidite emplacement on the southern Balearic Abyssal Plain (western Mediterranean Sea) during Marine Isotope Stages 1-3: an application of ITRAX XRF scanning of sediment cores to lithostratigraphic analysis, *In:* R. G. Rothwell, ed., *New techniques in sediment core analysis*, vol. 267 London: Geological Society, pp. 79-98.

Ryle, T., Murray, A., Connolly, C. 2009. *Coastal Monitoring Project 2004-2006*. Unpublished Report to the National Parks & Wildlife Service.

Schettler, G., Romer, R.L., O.Connell, M. and Molloy, K. 2006. Holocene climatic variations and postglacial sea-level rise geochemically recorded in the sediments of the brackish karst lake An Loch Mór, western Ireland. *Boreas*, 35, 674-693.

Schoellhamer, D.H. 2001. Singular spectrum analysis for time series with missing data. *Geophysical Research Letters*, 28 (16), 3187-3190.

Sejrup, H.P., Hjelstuen, B.O., Dahlgren, K.I.T., Haflidason, H., Kuijpers, A., Nygard, A., Praeg, D., Stoker, M.S. and Vorren, T.O. 2005. Pleistocene glacial history of the NW European continental margin. *Marine and Petroleum Geology*, 22, 1111-1129.

Shanahan, T.M., Overpeck, J.T., Hubeny, J.B., King, J., Hu, F.S., Hughen, K., Miller, G. and Black J. 2008. Scanning micro- X-ray fluorescence elemental mapping: A new tool for the study of laminated sediment records, *Geochemistry Geophysics Geosystems*, 9, Q02016, doi:10.1029/2007GC001800.

Shaw, J. and Carter, R.W.G. 1994, Coastal peats from northwest Ireland: implications for late-Holocene relative sea-level change and shoreline evolution. *Boreas*, 23, 74-91.

Shennan, I., Long, A.J., Rutherford, M.M., Green, F.M., Innes, J.B., Lloyd, J.M., Zong, Y. and Walker, K.J. 1999. Tidal marsh stratigraphy, sea-level change and large earthquakes, I: A 5000 year record in Washington, U.S.A. *Quaternary Science Reviews*, 15, 1023-1059.

Shennan, I., Innes, J.B., Long, A.J. and Zong, Y. 1995. Holocene relative sea-level changes and coastal vegetation history at Kentra Moss, Argyll, northwest Scotland. *Marine Geology*, 124, 43-59.

Shennan, I., Tooley, M., Green, F., Innes, J., Kennington, K., Lloyd, J. and Rutherford, M. 1999. Sea level, climate change and coastal evolution in Morar, northwest Scotland. *Geologie en Mijnbouw*, 77, 247-262.

Shepard, F.P. 1976. Coastal classification and changing coastlines. *Geoscience and Man*, 14, 53-64.

Short, A. D. and Hesp, P. 1982. Wave, beach and dune interaction in southeast Australia. *Marine Geology,* 48, 259-284.

Skipper, J.A.; Ward, D.J., and Johnson, R., 1998. A rapid, lightweight sediment peel technique using polyurethane foam. *Journal of Sedimentary Research*. 68 (3), 516-518.

Slingsby, D. and Cook, C. 1986. *Practical Ecology*. Macmillan, 213pp.

Spofforth, D.J.A., Palike, H. and Green, D. 2008. Paleogene record of elemental concentrations in sediments from the Arctic Ocean obtained by XRF analyses. *Paleoceanography* , 23, pp 13.

Stallins, J.A. 2005. Stability domains in barrier island dune systems. *Ecological Complexity*, 2, 410-430.

Stephens, N. and Synge, F.M. 1965. Late Pleistocene shorelines and drift limits in north Donegal. *Proceedings of the Royal Irish Academy*, 64B, 131-151.

Stumpf, R.P. 1983. The process of sedimentation on the surface of a salt marsh. *Estuarine and Coastal Science*, 17 (5), 495-508.

Stupples, P. 2002. Tidal cycles preserved in late Holocene tidal rhythmites, the Wainway Channel, Romney Marsh, southeast England. *Marine Geology*, 182, 231-246.

Sutherland, R.A. and Lee, C.T. 1994. Discrimation between coastal subenvironments using textural characteristics. *Sedimentology*, 41, 1133-1145.

Swan, A.R.H. and Sandilands, M. 1995. *Introduction to geological data analysis*. Blackwell Science, Oxford, pp 446.

Sykes, M.T. and Bastow, W.J. 1991. Vegetation of a coastal sand dune system in southern New Zealand. *Journal of Vegetation Science*, **2**, 531-538.

Thomas, D.S.G. 1987. Discrimination of depositional environments using sedimentary characteristics in the Mega Kalahari, central southern Africa. *In:* Frostick, L and Reid, I. (eds) 1987. *Desert Sediments: Ancient and Modern*, Geological Society Special Publication No. 35, pp 293-306.

Thomas, T., Phillips, M.R., Williams, A.T. and Jenkins R.E. 2012. Medium timescale behaviour of adjacent embayed beaches: Influence of low energy external forcing. *Applied Geography*, 32, 265-280.

Thompson, D.W.J. and Wallace, J.M. 1998. The Arctic Oscillation signature in the wintertime geopotential height and temperature fields. *Geophysical Research Letters*, 25 (9), 1297-1300.

Tomas. C.R. (Eds) 1996. *Identifying marine diatoms and dinoflagellates*. Academic Press, pp 598.

Tsompanoglou, K., Croudace, I., Birch, H. and Collins, M. 2011. Geochemical and radiochronological evidence of North Sea storm surges in salt marsh cores from The Wash embayment (UK). *The Holocene*, 21, 225-236.

Udayaganesan, P., Angusamy, N., Gujar, A.R. and Rajamanickam, G.V. 2011. Surface microtextures of quartz grains from the central coast of Tamil Nadu. *Journal of the Geological Society of India*, 77, 26-34.

USACE. 2002. *Coastal Engineering Manual*. Coastal and Hydrulics laboratory, US Army Corps of Engineers, [http://chl.erdc.usace.army.mil/cemtoc] Accessed on 12/10/09.

Vautard, R and Ghil, M. 1989. Singular spectrum analysis in nonlinear dynamics, with applications to paleoclimatic time series. *Physica D*, 35, 395-424.

Vautard, R., Pascal, Y. and Ghil, M. 1992. Singular-spectrum analysis: A toolkit for short, noisy chaotic signals. *Physica D*, 58, 95-126.

Vega, F.A., Covelo, E.F., Cerqueira, B. and Andrade, M.L. 2009. Enrichment of marsh soils with heavy metals by effect of anthopic pollution. *Journal of Hazardous Materials*, 170, 1056-1063.

Vega Leinert, A.C. de la, Keen, D.H., Jones, R.L., Wells, J.M. and Smith, D.E. 2000. Mid-Holocene environmental changes in the Bay of Skaill, Mainland Orkney, Scotland: an integrated geomorphological, sedimentological and stratigraphical study. *Journal of Quaternary Science*, 15 (5), 509-528.

Vos, P.C. and de Wolf, H. 1993a. Diatoms as a tool for reconstructing sedimentary environments in coastal wetlands; methodological aspects. *Hydrobiologia*, 269, 285-296.

Vos, P.C. and de Wolf, H. 1993b. Reconstruction of sedimentary environments in Holocene coastal deposits of the southwest Netherlands; the Poortvliet boring, a case study of palaeoenvironmental diatom research. *Hydrobiologia,* 269, 297-306.

Vos, P.C. and de Wolf, H. 1994. Palaeoenvironmental research on diatoms in early and middle Holocene deposits in central north Holland (The Netherlands). *Netherlands Journal of Aquatic Ecology*, 28 (1), 97-115.

Walker, M. 2005. *Quaternary dating methods*, John Wiley & Sons, Ltd, pp 286.

Walker, M.J.C., Bohncke, S.J.P., Coope, G.R., O'Connell, M., Usinger, H. and Verbruggen, C. 1994. The Devensian/weichselian Late-glacial in northwest Europe (Ireland, Britain, north Belgium, The Netherlands, northwest Germany). *Journal of Quaternary Science*, 9, 109-118.

Waugh, D. 1995. *Geography an integrated approach*. Nelson, pp 593.

Wedd, M.W. 2003. Determination of particle size distributions using laser diffraction. *Educational Resources for Particle Technology*, 32, 1-16.

Wheeler, A.J., Orford, J.D. and Dardis, O. 1999a. Saltmarsh deposition and its relationship to coastal forcing over the last century on the north-west coast of Ireland. *Geologie en Mijnbouw*, 77, 295-310.

Wheeler A.J., Oldfield F. and Orford J.D. 1999b. Depositional and post-depositional controls on magnetic signals from saltmarshes on the north-west coast of Ireland. *Sedimentology*, 46, 545-558.

Whittington, G. and Edwards, K.J. 1997. Evolution of a machair landscape: pollen and related studies from Benbecula, Outer Hebrides, Scotland. *Transactions of the Royal Society of Edinburgh: Earth Sciences*, 87, 515-531.

Williams, A.T. and Thomas, M.C. 1989. Analysis of barrier island surface sediments by scanning electron microscopy. *Marine Geology*, 86, 101-118.

Wilson, P. 2002. Holocene coastal dune development on the South Erradale peninsula Wester Ross, Scotland. *Scottish Journal of Geology*, 38 (1), 5-13.

Wilson, J.B. and Sykes, M.T. 1999. Is zonation on coastal sand dunes determined primarily by sand burial or by salt spray? A test in New Zealand dunes. *Ecology Letters*, **2**, 233-236.

Wilson, P. and Sellier, D. 1995. Active patterned ground and cryoturbation on Muckish Mountian, Co. Donegal, Ireland. *Permafrost and Periglacial Processes*, 6, 15-25.

Witkowski, A. 1991. Diatoms of the Puck Bay coastal shallows (Poland, Southern Baltic). Nordic Journal of Botany, 11, 689-701.

Witon, E., Malmgren, B., Witkowski, A. and Kuijpers, A. 2006. Holocene marine diatoms from the Faeroe Islands and their paleoceanographic implications. *Palaeogeography, Palaeoclimatology, Palaeoecology*, 239, 487-509.

Woodcock, N. and Strachan, R. 2002. *Geological History of Britain and Ireland*. Oxford, Blackwell Science, 423p

Yasso, W.E., and Hartman Jr, E.M., 1972. Rapid field technique using spray adhesive to obtain peels of unconsolidated sediment. *Sedimentology*. 19, 295-298.

Zong, Y. 1997. Mid-late Holocene sea-level changes in Roudsea Marsh, northwest England: A diatom biostratigraphical investigation. *The Holocene*, 7, 309-321.

Zong, Y. 1998. Diatom records and sedimentary responses to sea-level change during the last 8000 years in Roudsea Wood, northwest England. *The Holocene*, 8 (2), 219-228.

Zong, Y. and Horton, B.P. 1999. Diatom-based tidal-level transfer functions as an aid in reconstructing Quaternary history of sea-level movements in the UK. *Journal of Quaternary Science*, 14 (2), 153-167.

Appendix 1 – Additional data sources

Map, aerial photography and satellite imagery

Year	Source
1850	Map: Ordnance Survey
1907	Map: Ordnance Survey (1:10560)
1951	Black and white aerial photography: Irish Air Corps (flight elevation: 400ft)
1977	Black and white aerial photography: Ordnance Survey (flight elevation: 4750m)
1995	Black and white aerial photography: Ordnance Survey
2000	Colour aerial photography: Ordnance Survey
2005	Colour aerial photography: Ordnance Survey
2009	Google Earth Digital Globe Imagery
2011	Bing 2011-2012 World Imagery (http://www.arcgis.com/home/item.html?id=10df2279f9684e4a9f6a7f08febac2a9)

Wind magnitude and direction

Year	Data	Source
1956 - 2009	Hourly magnitude and direction data from Belmullet and Malin Head	Met Éireann (www.met.ie)

Tide

Year	Data	Source
Jan 2009 – Jun 2011	6 minutely tide level and hourly pressure from Killybegs and Malin head tide gauges	Marine Institute (www.marine.ie)

Appendix 2 – Location of surface sample and core points

NB: All X and Y coordinates refer to the Irish National Grid (Transverse Mercator 1965).

Surface sample locations

Code	x_tm65	y_tm65	Sediment	Vegetation	Diatom	Code	x_tm65	y_tm65	Sediment	Vegetation	Diatom
DS001	171295.042	393322.524	x			SS024	170184.600	394511.570	x		
DS002	171267.353	393315.492	x			SS025	170278.180	394481.830	x		
DS003	171251.280	393342.880	x			SS026	170367.230	394447.560	x		
DS004	171210.966	393344.593	x			SS027	170465.510	394409.260	x		
DS005	171213.242	393383.383	x			SS028	170569.330	394421.390	x		
DS006	171197.822	393459.676	x			SS029	170647.760	394402.010	x		
DS007	171174.121	393566.061	x			SS030	170726.360	394381.280	x		
DS008	171166.482	393652.668	x			SS031	170800.600	394355.560	x		
DS009	171077.176	393639.222	x			SS032	170873.670	394324.890	x		
DS010	170959.196	393695.520	x			SS033	170945.660	394287.690	x		
DS011	170920.151	393712.514	x			SS034	170968.470	394319.220	x		
DS012	170900.289	393633.221	x			SS035	170955.910	394384.830	x		
DS013	170977.193	393603.193	x			SS036	170939.509	394445.198	x		
DS014	171299.386	393590.338	x			SS037	170888.192	394444.014	x		
DS015	171393.731	393614.458	x			SS038	170821.396	394504.154	x		
DS016	171439.407	393601.617	x			SS039	170702.887	394512.845	x		
DS017	171349.764	393546.493	x			SS040	170639.753	394474.100	x		
DS018	171305.196	393499.977	x			SS041	170723.497	394437.857	x		
DS019	171263.757	393462.011	x			SS042	170823.732	394425.732	x		
DS020	171261.994	393405.355	x		x	SS043	170887.627	394370.763	x		
DQ001	171321.95	393310.71	x	x		SS044	170930.319	394333.543	x		
DQ002	171307.74	393314.07	x	x		SS045	170767.215	394118.002	x		
DQ003	171301.11	393308.62	x	x		SS046	170629.000	394126.685	x		
DQ004	171292.69	393309.96	x	x		SS047	170823.960	394070.719	x		
DQ005	171277.54	393296.18	x	x		SS048	170855.925	394043.746	x		x
DQ006	171368.43	393502.25	x	x	x	SS049	170922.305	394037.440	x		
DQ007	171382.03	393522.81	x	x	x	SS050	171050.213	393944.207	x		
DQ008	171402.35	393539.83	x	x		SS051	171200.859	393957.379	x		
DQ009	171435.33	393525.86	x	x	x	SS052	171346.162	394081.014	x		
DQ010	171381.06	393652.39	x	x		SS053	171323.133	394126.916	x		x
DQ011	171357	393676.6	x	x		SQ003	171189.08	394084.07	x	x	
DQ012	171327.58	393663.99	x	x		SQ007	170943.88	394177.34	x	x	
DQ013	171310.24	393664.47	x	x		SQ013	171155.3	394471.54	x	x	
DQ014	171284.37	393675.82	x	x	x	SQ030	170951.43	394167.06	x	x	
DQ015	171204.83	393683.99	x	x		SQ033	170937.96	394202.95	x	x	
DQ016	171219.6	393693.07	x	x		SQ034	171231.9	394121.67	x	x	
DQ017	171247.94	393705.68	x	x		SQ035	170993.22	394226.91	x	x	
DQ018	171324.93	393705.78	x	x		SQ044	171136.36	394046.51	x	x	
SS001	170895.600	394178.810	x			SQ047	171082.12	394139.89	x	x	
SS002	170847.910	394211.500	x			SQ048	171157.79	394180.5	x	x	x
SS003	170786.530	394196.890	x			SQ050	170882.32	394144.61	x	x	x
SS004	170721.570	394192.930	x			SQ068	171039.62	394181.55	x	x	
SS005	170659.320	394219.800	x			SQ070	171045.64	394190.28	x	x	
SS006	170621.580	394268.990	x			SQ071	171016.62	394348.61	x	x	
SS007	170688.710	394266.410	x			SQ072	170952.86	394244.32	x	x	
SS008	170750.610	394258.090	x			SQ084	171039.57	394212.06	x	x	
SS009	170812.080	394246.850	x			SQ085	171014.2	394053.31	x	x	
SS010	170893.580	394222.640	x			SQ087	171046.34	394203.53	x	x	
SS011	170932.010	394243.830	x			SQ092	171048.41	394349.36	x	x	
SS012	170870.000	394269.320	x			SQ098	170992.29	394189.59	x	x	
SS013	170802.260	394288.160	x			SQ101	170870.75	394120.11	x	x	x
SS014	170729.020	394309.510	x			SQ102	171066.29	394024.78	x	x	x
SS015	170659.020	394329.260	x			SQ103	171054.04	393975.74	x	x	
SS016	170586.930	394350.940	x			SQ104	171127.99	393971.45	x	x	x
SS017	170506.610	394368.420	x			SQ105	171133.93	393975.38	x	x	
SS018	170413.970	394381.190	x			SQ106	171134.48	394000.47	x	x	
SS019	170318.570	394415.150	x			SQ107	171203.21	393973.2	x	x	
SS020	170195.750	394451.880	x			SQ108	171228.07	394007.56	x	x	
SS021	170171.240	394357.930	x			SQ109	171224.62	394048.28	x	x	x
SS022	170060.330	394583.680	x			SQ110	171256.61	394074.78	x	x	
SS023	170116.580	394553.400	x			SQ111	171229	394203.74	x	x	

Core sample locations

	X	Y
DYN1	171379.779	393523.914
DYN2	171420.836	393588.398
SFD1	170858.861	394113.453
SFD2	171027.610	393984.080
SFD3	171136.590	393995.950

Appendix 3 – Availability of Data

The data used in this thesis are held at:

https://dl.dropboxusercontent.com/u/6268963/CBMPhDData.xlsx

and can be obtained on request.